BULLETIN OF THE EARTHQUAKE RESEARCH INSTITUTE,
UNIVERSITY OF TOKYO. Vol. 39, Part 3. September, 1961.

東京大学
地震研究所彙報

第 39 号　第 3 冊

昭和 36 年 9 月

目　次

論文及報告

			頁
12.	表面波に関する一つの問題（序報）（英文）	金井　清	359
13.	波型の境界面における弾性波の反射，屈折 第2報（英文）	浅野周三	367
14.	伊豆大島熔岩による古地磁気学（英文）	行武　毅	467
15.	実在建物の周期と減衰（英文）	金井　清，吉沢静代	477
16.	江の島津波観測所における IGY 期間中の観測（英文）	高橋龍太郎，平能金太郎，相田　勇，羽鳥徳太郎，清水静子	491
17.	津波スペクトルの研究		
	1. ウェーブアナライザーの製作		
	2. 江の島津波観測所で観測された津波及び常時長波の周期分析		
	3. 日本各地で観測されたチリ津波の周期分析（邦文）	高橋龍太郎，相田　勇	523
18.	長岡地震による地盤変動（邦文）	岡田　惇	537
19.	昭和36年2月2日 長岡地震の家屋被害について（邦文）	大沢　胖，山本正勝	549
20.	1961年2月27日 日向灘地震に伴なつた津波について（邦文）	高橋龍太郎，羽鳥徳太郎	561

(The titles in occidental languages are given on the back cover.)

地震研究所彙報は，年4回定期に（ただし，第1号より第6号までは不定期に，第7号は3冊として刊行された），彙報別冊は不定期に刊行される．

この彙報に載せられた論文及び報告についての責任は，すべてその著者のみにある．

この彙報についての照会通信は，すべて東京大学地震研究所長にあてられたい．

The Bulletin is published quarterly. (Vols. 1-6 were published at irregular intervals and Vol. 7 consisted of three parts.)
Supplementary Volume is published at irregular interval.

The authors of the papers alone are responsible for the statements and opinions contained in their respective papers.

All communications relating to this Bulletin should be addressed to the Director of the Earthquake Research Institute, University of Tokyo, Japan.

Earthquake Research Institute, University of Tokyo
Address:
No. 1, Motofuji-cho, Bunkyo-ku,
Tokyo Metropolis, Japan.
Telephone: 921-3161-Extension 6506
Cable address: ZISINKEN, TOKYO.

東京大学地震研究所
所在地
東京都文京区本富士町一番地
電話 小石川 921—3161 (代) 構内 6506
電略 ブンケウ トウダイ ヂシン

BULLETIN OF THE EARTHQUAKE
RESEARCH INSTITUTE
Vol. 39 (1961), pp. 359-366

12. *A New Problem Concerning Surface Waves.*

(Preliminary Notes)

By Kiyoshi KANAI,

Earthquake Research Institute.

(Read Mar. 28 and May 23, 1961.—Received June 30, 1961.)

The features of seismic waves are usually influenced to a large extent by the discontinuity surfaces in the earth, and the mathematical treatment of them is carried out on the assumption that boundary conditions, as adjacent media, are undoubtedly fixed in relation to each other,—that is, displacements as well as stresses at the boundary surface of two media have perfect continuity. As a matter of fact, in general, such treatment has been adopted in order to simplify the problem, and pays slight consideration to the actual conditions of the earth. Nevertheless the results of mathematical studies on seismic waves by means of the treatment mentioned above agree with the results of analytical studies of actual seismograms. It is, however, uncertain whether or not the conditions at the discontinuity surfaces in the earth are correctly determined fixed. In order to clear the uncertainties just mentioned, the problem of waves, under the conditions of surfaces of discontinuity in which the normal components of stress and displacement are continuous, on the other hand, the transversal components of stress and displacement are not, were solved.[1] Furthermore, it is assumed that, at the same surface, there is a tangential resistance that is proportional to the relative tangential velocity.[2] In the previous paper, it has been ascertained that if a discontinuity surface in the earth's crust has a frictional resistance of a dissipative nature, the input energy of the waves is partly absorbed by the discontinuity surface in question, even were there no damping resistance in the media through which the waves are transmitted.

1) G. NISHIMURA and K. KANAI, "On the Effects of Discontinuity Surfaces upon the Propagation of Elastic Waves," *Bull. Earthq. Res. Inst.*, **11** (1933), 123-186, 595-631: **12** (1934), 277-316, 331-367, (in Japanese),

S. NATSUME, *Monthly Meeting of the Earthquake Research Institute*, (Oct. 1953).

2) K. SEZAWA and K. KANAI, "A Fault Surface or a Block Absorbs Seismic Wave Energy," *Bull. Earthq. Res. Inst.*, **18** (1940), 465-482.

In this paper, the case will be discussed in which Love-type waves are transmitted in a singly stratified visco-elastic layer residing on the semi-infinite visco-elastic body under the same above-mentioned conditions at the surface of discontinuity.

Let ρ, μ, ν, u and H be the density, elastic constant, coefficient of solid viscosity, displacement and thickness of layer. Suffix 1 and 2 represent the layer and the subjacent medium, respectively. Then the equation of the SH-type wave motion of each medium may be written as follows:

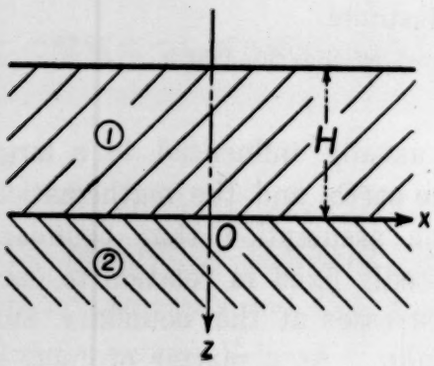

Fig. 1.

$$\left.\begin{aligned}\left(\mu_1+\nu_1\frac{\partial}{\partial t}\right)\left(\frac{\partial^2 u_1}{\partial z^2}+\frac{\partial^2 u_1}{\partial x^2}\right)&=\rho_1\frac{\partial^2 u_1}{\partial t^2}\,,\\ \left(\mu_2+\nu_2\frac{\partial}{\partial t}\right)\left(\frac{\partial^2 u_2}{\partial z^2}+\frac{\partial^2 u_2}{\partial x^2}\right)&=\rho_2\frac{\partial^2 u_2}{\partial t^2}\,.\end{aligned}\right\} \tag{1}$$

The resulting displacements of the layer and the subjacent medium are expressed by

$$\left.\begin{aligned}u_1&=(A\cos s_1 z+B\sin s_1 z)\exp\left[i(p_0 t-fx)\right]\,,\\ u_2&=C\exp\left[-s_2 z+i(p_0 t-fx)\right]\,,\end{aligned}\right\} \tag{2}$$

where A, B and C are arbitrary constants determined by boundary conditions and

$$s_1^2=\frac{\rho_1 p_0^2}{\mu_1+ip_0\nu_1}-f^2\,,\qquad s_2^2=f^2-\frac{\rho_2 p_0^2}{\mu_2+ip_0\nu_2}\,. \tag{3}$$

Let the tangential resistance at the discontinuity surface $z=0$ be

$$F\frac{\partial}{\partial t}\,(\text{relative displacement}), \tag{4}$$

then the boundary conditions at the discontinuity, $z=0$, are

$$z=0\,;\qquad \left(\mu_1+\nu_1\frac{\partial}{\partial t}\right)\frac{\partial u_1}{\partial z}=-F\frac{\partial}{\partial t}\,(u_1-u_2)\,, \tag{5}$$

$$\left(\mu_2+\nu_2\frac{\partial}{\partial t}\right)\frac{\partial u_2}{\partial z}=-F\frac{\partial}{\partial t}\,(u_1-u_2) \tag{6}$$

and the boundary condition at the free surface, $z=-H$, is

$$z=-H\ ;\qquad \left(\mu_1+\nu_1\frac{\partial}{\partial t}\right)\frac{\partial u_1}{\partial z}=0\ . \tag{7}$$

Substituting (2) in (5)–(7), we get

$$\cot s_1H-\frac{(\mu_1+ip_0\nu_1)s_1}{(\mu_2+ip_0\nu_2)s_2}+\frac{i(\mu_1+ip_0\nu_1)s_1}{p_0F}=0\ . \tag{8}$$

When $\nu_1=\nu_2=0$ and $F=\infty$, we get

$$\cot s_1H-\frac{\mu_1s_1}{\mu_2s_2}=0\ . \tag{8'}$$

This is of the same form as the usual velocity equation for Love-waves.

Now, we write

$$p_0=p+iq\ , \tag{9}$$

in which $2\pi/p$ and q are the period and damping coefficient of waves, respectively. (8) is transformed finally into the two expressions

$$\left.\begin{aligned} a\cos\alpha-b\cos\beta+c\cos\gamma&=0\ ,\\ a\sin\alpha-b\sin\beta-c\sin\gamma&=0\ ,\end{aligned}\right\} \tag{10}$$

where

$$a=(E_2^2+E_1^2)^{1/2}(F_1^2+F_2^2)^{1/4}\ ,$$

$$b=v\phi(G_1^2+G_2^2)^{1/2}(H_1^2+H_2^2)^{-1/4}(F_1^2+F_2^2)^{1/4}\ ,$$

$$c=v\phi(Y_1^2+Y_2^2)^{1/2}\ ,$$

$$\alpha=\tan^{-1}\left(\frac{E_1}{E_2}\right)+\frac{1}{2}\tan^{-1}\left(\frac{F_2}{F_1}\right),$$

$$\beta=\tan^{-1}\left(\frac{G_2}{G_1}\right)+\frac{1}{2}\tan^{-1}\left(\frac{F_2}{F_1}\right)-\frac{1}{2}\tan^{-1}\left(\frac{H_2}{H_1}\right),$$

$$\gamma=\tan^{-1}\left(\frac{Y_2}{Y_1}\right),$$

$$Y_1=\frac{\cos X_1\sin X_1}{\cos^2X_1\,\mathrm{sh}^2X_2+\sin^2X_1\,\mathrm{ch}^2X_2}\ ,$$

$$Y_2=\frac{\mathrm{ch}\,X_2\,\mathrm{sh}\,X_2}{\cos^2X_1\,\mathrm{sh}^2X_2+\sin^2X_1\,\mathrm{ch}^2X_2}\ ,$$

$$X_1=fH(F_1^2+F_2^2)^{1/4}\cos\left\{\frac{1}{2}\tan^{-1}\left(\frac{F_2}{F_1}\right)\right\},$$

$$X_2=fH(F_1^2+F_2^2)^{1/4}\sin\left\{\frac{1}{2}\tan^{-1}\left(\frac{F_2}{F_1}\right)\right\},$$

$$E_1=\frac{1}{1+\kappa_2}, \qquad E_2=\frac{\kappa-\xi_1-\xi_1\kappa^2}{1+\kappa^2},$$

$$F_1=\frac{v^2\{(1-\kappa^2)(1-\xi_1\kappa)+2\xi_1\kappa\}}{(1-\xi_1\kappa)^2+\xi_1^2}-1,$$

$$F_2=\frac{v^2\{2\kappa(1-\xi_1\kappa)-\xi_1(1-\kappa^2)\}}{(1-\xi_1\kappa)^2+\xi_1^2},$$

$$G_1=\frac{m\{(1-\xi_1\kappa)(1-\xi_2\kappa)+\xi_1\xi_2\}}{(1-\xi_2\kappa)^2+\xi_2^2},$$

$$G_2=\frac{m\{\xi_1(1-\xi_2\kappa)-\xi_2(1-\xi_1\kappa)\}}{(1-\xi_2\kappa)^2+\xi_2^2},$$

$$H_1=1-\frac{mrv^2\{(1-\kappa^2)(1-\xi_2\kappa)+2\xi_2\kappa\}}{(1-\xi_2\kappa)^2+\xi_2^2},$$

$$H_2=\frac{mrv^2\{2\kappa(1-\xi_2\kappa)-\xi_2(1-\kappa^2)\}}{(1-\xi_2\kappa)^2+\xi_2^2}, \tag{11}$$

and

$$\left.\begin{aligned} &m=\frac{\mu_1}{\mu_2}, \quad r=\frac{\rho_2}{\rho_1}, \quad v=\frac{p}{f}\sqrt{\frac{\rho_1}{\mu_1}}, \quad \kappa=\frac{q}{p}, \\ &\xi_1=\frac{\nu_1 p}{\mu_1}, \quad \xi_2=\frac{\nu_2 p}{\mu_2}, \quad \phi=\frac{F}{\sqrt{\mu_1\rho_1}}. \end{aligned}\right\} \tag{12}$$

From (10) it is possible to get the velocity and damping coefficient of Love-type waves for any ratios of μ_2/μ_1, ρ_2/ρ_1, $\nu_1 p/\mu_1$, $\nu_2 p/\mu_2$, $F/\sqrt{\mu_1\rho_1}$ and fH.

In the present case, however, there are a number of quantities for determining the velocity and damping coefficient, the problem then being extremely complex. Whereupon, we tried various special methods of numerical calculation. For example, in some cases, the values of κ as well as ϕ were obtained, which satisfied the assumed values of v and fH, in other cases, higher orders of κ were neglected.

The results of calculating the various ratios of $F/\sqrt{\mu_1\rho_1}$ and fH in the case where $\rho_2/\rho_1=1$, $\mu_2/\mu_1=5$, as well as the conditions where $\nu_1 p/\mu_1=\nu_2 p/\mu_2=0$, are shown in Table 1 and in Figs. 2, 3.

Fig. 3 tells us that the relation between the attenuation factor and the period of Love-type waves is not so simple, and neither the attenua-

tion factor varies as the square of the frequency[3] nor the first power of it[4] then the attenuation factor takes a maximum values in the appropriate frequency of such waves.

Table 1.

$\frac{p}{f}\sqrt{\frac{\rho_1}{\mu_1}}$	$\frac{L}{H}$	$\frac{F}{\sqrt{\rho_1\mu_1}}$	$\frac{q}{p}$
2.15	10.47	1.1	0.2
	12.39	1.2	0.1
	15.09	1.4	0.05
	18.80	4.3	0.01
2.00	10.03	1.2	0.2
	10.90	1.8	0.1
	11.58	3.1	0.05
	11.70	6.9	0.02
	11.85	47.8	0.003
	12.70	0.74	0.866
1.732	7.62	47.8	0.005
	7.74	11.9	0.02
	7.79	2.5	0.1
	8.16	1.2	0.25
	8.61	0.94	0.4
	10.40	0.79	0.816
1.414	4.765	40.4	0.005
	4.775	8.1	0.025
	4.78	6.8	0.03
	5.02	3.2	0.07
	5.76	1.3	0.2
	6.34	0.93	0.3
	9.40	0.80	0.707
1.30	3.81	10.0	0.016
1.20	4.36	0.90	0.2
	8.32	0.75	0.6
1.10	1.97	10.0	0.005
	7.50	0.65	0.408

It is a noteworthy fact that the tendency of the relation between the attenuation factor to the period obtained in the present investigation agrees qualitatively with the results[5] of the observational studies

3) K. SEZAWA, "On the Decay of Waves in Visco-Elastic Solid Bodies," *Bull. Earthq. Res. Inst.*, **3** (1927), 43-53.

4) L. KNOPOFF, "The Seismic Pulse in Materials Possessing Solid Friction," *Bull. Seism. Soc. Amer.*, **46** (1956), 175-183, **49** (1959), 403-413.

5) M. EWING and F. PRESS, "An Investigation of Mantle Rayleigh Waves," *Bull. Seism. Soc. Amer.*, **44** (1954), 127-147.
ditto, "Mantle Rayleigh Waves from the Kamchatka Earthquake of November 4, 1952," *ditto*, 471-479.
Y. SATO, "Attenuation, Dispersion and the Wave Guide of the G Wave," *Bull. Seism. Soc. Amer.*, **48** (1958), 231-268.

of long period surface waves.

On the other hand, it should however be borne in mind that the

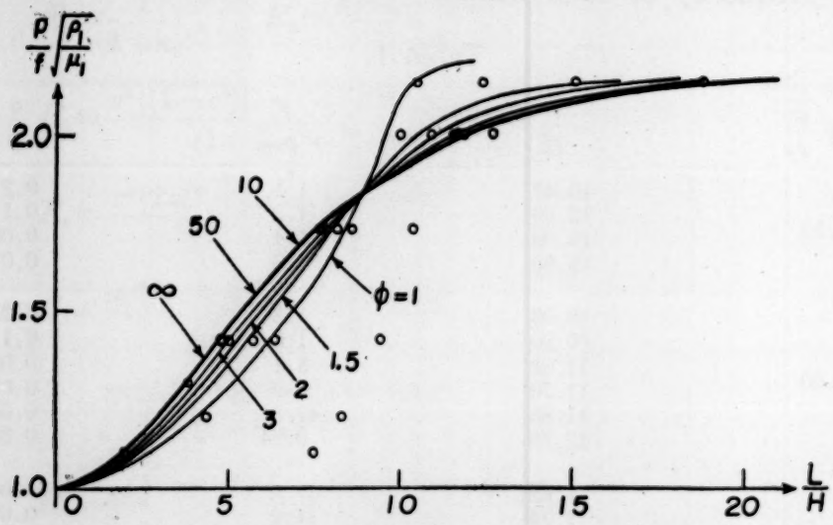

Fig. 2. Relation between the velocity and the period of Love-type waves. ($\rho_2/\rho_1=1$, $\mu_2/\mu_1=5$.)

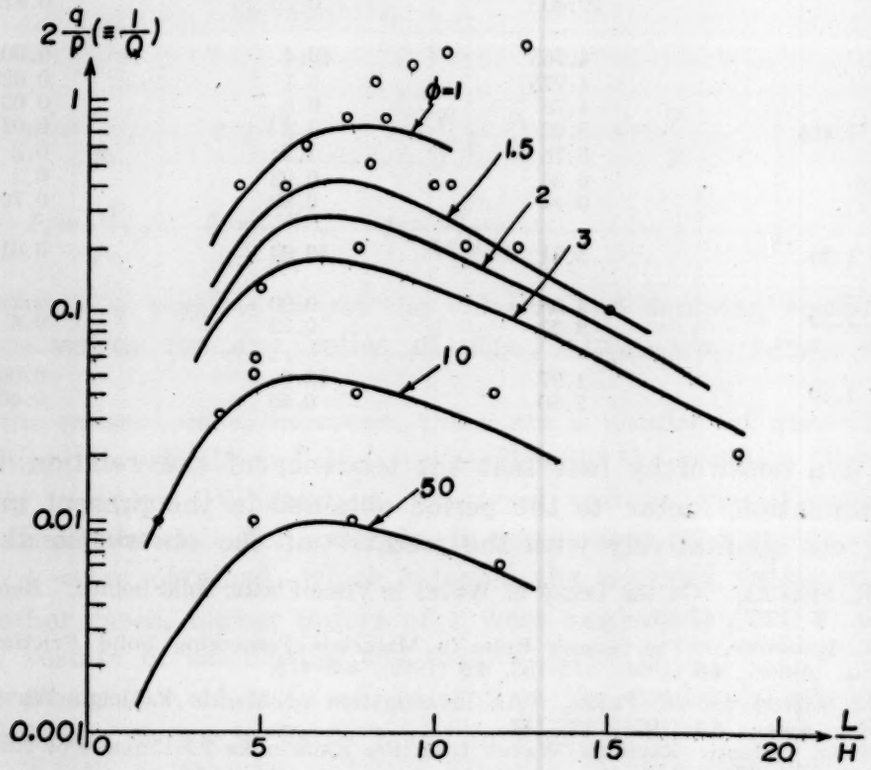

Fig. 3. Relation between the attenuation factor and the period of Love-type waves. ($\rho_2/\rho_1=1$, $\mu_2/\mu_1=5$.)

dispersion curve in the present case, except in the case of extremely small resistance at the discontinuity surface, coincides considerably with that of usual Love-waves.

In the case of Rayleigh-type waves, the boundary conditions at the discontinuity surface may be taken as follows:

$$\widehat{zz}_{1p}+\widehat{zz}_{1s}=\widehat{zz}_{2p}+\widehat{zz}_{2s}\ , \tag{13}$$

$$w_{1p}+w_{1s}=w_{2p}+w_{2s}\ , \tag{14}$$

$$\widehat{xz}_{1p}+\widehat{xz}_{1s}=-F\frac{\partial}{\partial t}\{(u_{1p}+u_{1s})-(u_{2p}+u_{2s})\}\ , \tag{15}$$

$$\widehat{xz}_{2p}+\widehat{xz}_{2s}=-F\frac{\partial}{\partial t}\{(u_{1p}+u_{1s})-(u_{2p}+u_{2s})\}\ , \tag{16}$$

in which $\widehat{zz}$, w, $\widehat{xz}$ and u represent normal stress, vertical displacement, tangential stress and horizontal displacement, respectively and suffixes 1, 2, p, and s represent the layer, the subjacent medium, P-waves and S-waves, respectively.

It is natural to consider that the influence of resistant phenomena at the discontinuity surface on Reyleigh-type waves is less than that on Love-type waves, because, in the former case, two of the four boundary conditions at the discontinuity surface have a bearing on the problem, in the latter case, nevertheless it is so with all the boundary conditions.

When the boundary conditions adopted here exist and also the above contentions are true, the amplitude relation between Rayleigh-type waves and Love-type waves is considered as follows:

$$\frac{L_c}{M_c}>\frac{L_m}{M_m}\ , \tag{17}$$

in which L, M, c and m represent Love-type waves, Rayleigh-type waves, earthquakes occurred in the crust and earthquakes occurred in the mantle.

In conclusion the author wishes to convey his thanks to Miss. S. Yoshizawa without whose help this work could not have been done.

12. 表面波に関する一つの問題 (序報)

地震研究所 金 井 清

地球内部には，いくつかの不連続面がある．その不連続面を地震波が通過するときの，境界条件としては，変位ならびに応力が連続という仮定が，一般に採用されてきた．しかし，ひるがえつて考えてみると，この仮定の是非は，よく吟味されたというものではなさそうである．

本研究は，上に述べた仮定を変えると，はたして，どんな結果が生れるかということを，しらべてみたものである．ここでは，不連続面で有限の大きさの，“すべり抵抗”のようなものを考えてみた．取扱つた地震波は SH 型表面波である．数値計算の結果，“すべり抵抗”の値が非常に小さい場合を別にすると，分散曲線は従来のものと大して変らないことがわかつた．しかし，減衰の性質としては，従来の理論的研究結果では見られないものが得られた．即ち，減衰は周期の 1 乗とか 2 乗とかに逆比例するというようなものではなく，ある周期に極大があることになつた．この結果は，最近，長周期の表面波に関する験震的研究結果と定性的には，よく合うものである．

Bulletin of the Earthquake Research Institute
Vol. 39 (1961). pp. 367-466

13. *Reflection and Refraction of Elastic Waves at a Corrugated Boundary Surface. Part II.*[1)]

By Shuzo Asano,

Earthquake Research Institute.

(Read Nov. 22, 1960; Feb. 28 and April 25, 1961.—Received June 30, 1961.)

Contents

Chapter 1. Introduction 367
Chapter 2. Fundamental Equations 370
§ 1. Equation of Boundary Surface 370
§ 2. Equations of Motion and Boundary Conditions 371
Chapter 3. Cases of the Incidence of P and SV Waves 373
§ 1. Incident, Reflected and Refracted Waves 373
§ 2. Boundary Conditions 375
§ 3. The Solutions of the First Approximation.....378
§ 4. The Solutions of the Second Approximation.....380
§ 5. The Case of Normal Incidence on the Mean Surface of the Boundary $\zeta=c\cos px$.....389
§ 5.1. The Case of Incidence of the P Wave 389
§ 5.2. The Case of Incidence of the SV Wave.....410
Chapter 4. Discussions and Conclusions 433
§ 1. Discussions 433
§ 2. Conclusions.....439
Acknowledgement 465

Chapter 1. Introduction

The pioneering seismological studies of Lord Rayleigh in 1885 and C. G. Knott in 1888 on the theory of elastic surface waves and reflection and refraction of the same body waves respectively, which in themselves were directed along the way laid by Navier, Poisson, Cauchy, Green and Stokes with a view to optical application, gave profound stimulus to many theoretical investigators with the results that in-

1) The study of the case of a SH wave, which is appropriately included as a chapter in this paper, has already been published as Part I in this Bulletin (Vol. 38 (1960), pp. 177). Therefore in the present Part II, a general review is made from the broader point of view of all the subjects including those in Part I.

numerable papers on the theory of elastic waves were written and great progress has now been made thereby towards an understanding of earthquake phenomena.

However, there still remains many points to be clarified for a full understanding of the complicated nature of seismic waves. The problems, as it seems to the writer, are rooted in part in the complexities of the mechanism of an earthquake and in part in the structure of the earth in which earthquake waves are propagated. In fact, if the structure of the earth were very simple, for example uniform and homogeneous, we would be able to grasp the nature of the earthquake motion much more easily because the seismic wave propagated from the origin to the surface would have no chance to be modified by reflection and refraction at the boundaries of different media. We may therefore say that the voluminous existent seismograms of natural earthquakes and artificial seismic shootings pile up vainly barren of important further information which could be drawn if there were more data or some theoretical clues could be found. Thus theoretical studies of the propagation of elastic waves are deemed to occupy a very important position in seismology.

One of the most important problems on elastic waves is the study of the reflection and refraction of elastic waves at a boundary surface or surfaces. With regard to cases of a plane boundary surface or surfaces, there have been many studies by senior authorities, but an important and interesting problem in this field which has not yet been studied in detail, is the effect on the propagation of seismic waves of corrugation or roughness of a boundary surface.

It is well-known in geophysics and geology that there are many strata which are not bounded by planes but by corrugated interfaces especially in mountainous regions. Many of the geophysical exploration methods such as seismic, gravity and other prospecting and also geodetic measurement on a larger scale have revealed such evidences in various parts of the world.

We may also count many other phenomena supporting the above inference, amongst which those cited below seem to the writer to deserve notice.

(1) The distribution of earthquake intensity in north-eastern Japan through Hokkaido in the case of an earthquake originating under the sea off the Pacific coast of Hokkaido. In these earthquakes the seismic intensity attenuates more rapidly in a direction perpendicular to the

island arc from Hokkaido to the Kwanto District than in a direction parallel to the same arc. It is to be remarked in most of the above mentioned regions that the former direction is across the central mountain range while the latter is parallel to it[2].

There are many other regions in Japan which display abnormally high or low seismic intensities in comparison to those in the neighbourhood of like epicentral distances.

(2) A remarkably similar situation, found by H. E. Tatel and others in the Andes, South America, although it cannot yet be claimed to be fully established. In the course of seismic explorations by these investigators in the area, they found the fact that the seismic waves across the mountain range could not be observed clearly at a distance while on a similar spread along the Andes they succeeded in their work, which fact was ascribed by them to the difference in dissipation of the energy in the two directions[3].

(3) The smallness of the reflected waves from the Mohorovičić discontinuity (' Moho ') in western California as reported by Tatel and others[4]. Needless to say, the observation of reflected waves from the ' Moho ' is one of the powerful methods of elucidating the crustal structure, and the difficulty in one region and no difficulty in the other in the above inference is a very interesting fact in need of explanation, although the above fact mentioned by Tatel and others was not found during another exploration made by G. G. Shor in the vicinity[5]. According to the Japanese experiences, though meagre, the success or failure in getting good reflected waves from the ' Moho ' seems to depend on the crustal conditions under the observing point[6].

In view of these circumstances, it is desirable to obtain some clue

2) For example, H. KAWASUMI, *Publ. Bureau Central Séism. Intern., Série A, Trav. Sci., Fasc.* No. **19** (1956), 99.

K. WADATI and T. HIRONO, *Publ. Bureau Central Séism. Intern., Série A, Trav. Sci., Fasc.* No. **20** (1959), 221.

3) H. E. TATEL, M. A. TUVE and COLLEAGUES, "Abstract of paper presented at 39th Annual Meeting of American Geophysical Union held in 1958", *Trans. Amer. Geophys. Un.*, **39** (1958), 533.

4) H. E. TATEL, L. H. ADAMS and M. A. TUVE, *Proc. Amer. Phil. Soc.*, **97** (1953), 658.

5) G. G. SHOR, *Trans. Amer. Geophys. Un.*, **36** (1955), 133.

6) THE RESEARCH GROUP FOR EXPLOSION SEISMOLOGY, *Bull. Earthq. Res. Inst.*, **33** (1955), 699; **37** (1959), 89; **37** (1959), 495.

T. MATUZAWA, *Bull. Earthq. Res. Inst.*, **37** (1959), 123.

T. MATUZAWA, T. MATUMOTO and S. ASANO, *Bull. Earthq. Res. Inst.*, **37** (1959), 509.

from theoretical knowledge of the effects of corrugation on the propagation of elastic waves. This is one of the geophysical significances of the writer's attempt in this paper.

It was Lord Rayleigh who opened the gate of study on the present problem, and introduced an ingeneous method towards this purpose although his problem was confined to sound and light waves[7]. Recently considerations concerning the reflection of a sound wave at the sea surface have been examined by many investigators and various methods have been attempted in these studies[8]. With respect to seismic waves, S. Homma considered the problem of their reflection at a corrugated free surface for the first time[9], and R. Sato solved the same problem by Rayleigh's method[10].

The present writer has been studying the case of the reflection of elastic waves at a corrugated boundary surface between two different media, using the same method as Lord Rayleigh, and part of the results obtained will be reported in this paper.

Chapter 2. Fundamental Equations

§ 1. Equation of Boundary Surface

The coordinate axes are taken as shown in Fig. 1. That is, the x- and y-axis are on the mean horizontal surface of the boundary of the two media and z-axis is taken vertically downwards.

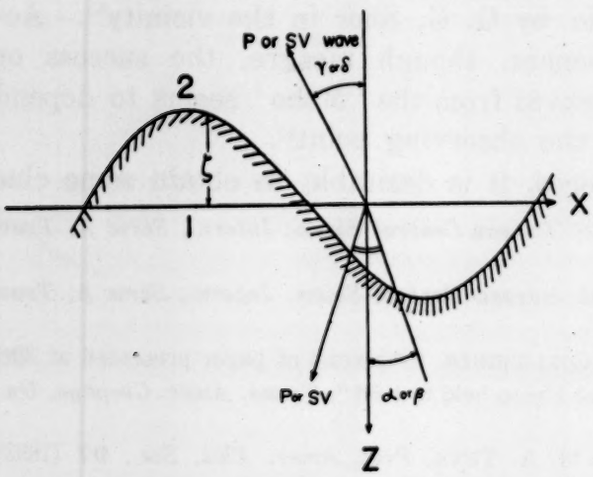

Fig. 1.

The equation of the boundary surface is given as $z=\zeta$, where ζ is assumed to be a periodic function of x but independent of y, the mean value of which being zero by assumption. Taking the origin of coordinates suit-

7) LORD RAYLEIGH, *Proc. Roy. Soc. Lond.*, **A 79** (1907), 399.
8) For example, CARL ECKART, *Journ. Acoust. Soc. Amer.*, **25** (1953), 566.
E. O. LACASCE and P. TAMARKIN, *Journ. Appl. Phys.*, **27** (1956), 138.
9) S. HOMMA, *Quart. Journ. Seism.*, **11** (1940-41), 349; **12** (1942), 17 (in Japanese).
10) R. SATO, *Zisin*, [ii], **8** (1955), 8 (in Japanese).

ably, we can represent ζ by Fourier's series without a loss of generality as follows:

$$\zeta=\sum_{n=1}^{\infty}(\zeta_n e^{inpx}+\zeta_{-n}e^{-inpx})$$
$$=c_1\cos px+c_2\cos 2px+s_2\sin 2px+\cdots+c_n\cos npx+s_n\sin npx+\cdots, \tag{1}$$

where

$$\zeta_1=\zeta_{-1}=c_1/2\ , \qquad \zeta_{\pm n}=(c_n\mp is_n)/2\ .$$

When the boundary surface is expressible by one cosine term, i.e. $\zeta=c\cos px$, the wave length of the corrugation is $2\pi/p$.

§ 2. Equations of Motion and Boundary Conditions

We will consider the case, in the following, where a plane wave with a period of $2\pi/\omega$ is incident with an angle of incidence α in the case of a dilatational wave or β in the case of a distorsional wave to the boundary from the lower medium to the upper one. The quantities concerning the lower medium will be shown by suffix 1 and those of the upper medium, by suffix 2.

Equations of motion in the case of the incidence of P or SV waves are given by using displacement potentials ϕ and ψ as follows:

$$(\nabla^2+h_i^2)\phi_i=0\ , \qquad (\nabla^2+\sigma_i h_i^2)\psi_i=0\ , \tag{2}$$

where

∇^2=Laplacian, λ_i, μ_i=Lamé's constants,
$h_i^2=\rho_i\omega^2/(\lambda_i+2\mu_i)$, ρ_i=density,
$\sigma_i=(\lambda_i+2\mu_i)/\mu_i$, i =1 or 2.

The displacement $(u, 0, w)$ is to be obtained from the potentials by the following formulae

$$u=\partial\phi/\partial x+\partial\psi/\partial z \quad \text{and} \quad w=\partial\phi/\partial z-\partial\psi/\partial y\ .$$

In the case of the incidence of SH waves, if the displacement v is parallel to the y-axis, the equations of motion are given as follows:

$$(\nabla^2+\sigma_i h_i^2)v_i=0\ . \tag{3}$$

Now let us deduce the conditions concerning the stress on a corrugated boundary surface in terms of displacement potentials ϕ and ψ or displacement v. Since the direction cosines of normal ν to the surface $z=\zeta(x)$ are $(1/\sqrt{1+\zeta'^2},\ 0,\ \zeta'/\sqrt{1+\zeta'^2})$ and those of tangent t, $(-\zeta'/\sqrt{1+\zeta'^2},\ 0,\ 1/\sqrt{1+\zeta'^2})$ where $\zeta'=d\zeta/dx$, normal and tangential stresses N_ν, T_ν, Y_ν in the νyt-system are connected to those X_x, Z_x, Z_z in the xyz-system by the following formulae,

$$\begin{aligned} N_\nu&=[(Z_z-X_x)\zeta'+Z_x(1-\zeta'^2)]/(1+\zeta'^2)\\ T_\nu&=[Z_z+X_x\cdot\zeta'^2-2Z_x\cdot\zeta']/(1+\zeta'^2)\\ Y_\nu&=[Y_z-Y_x\cdot\zeta']/\sqrt{1+\zeta'^2} \end{aligned} \tag{4}$$

Substituting the following well-known relations between displacement, stress component and displacement potentials into (4),

$$X_x=\lambda\Delta+2\mu\frac{\partial u}{\partial x}=-\lambda h^2\phi+2\mu\frac{\partial^2\phi}{\partial x^2}+2\mu\frac{\partial^2\psi}{\partial x\partial z}\ ,$$

$$Z_x=\mu\left(\frac{\partial u}{\partial z}+\frac{\partial w}{\partial x}\right)=\mu\left(2\frac{\partial^2\phi}{\partial x\partial z}-\sigma h^2\psi-2\frac{\partial^2\psi}{\partial x^2}\right),$$

$$Z_z=\lambda\Delta+2\mu\frac{\partial w}{\partial z}=-\lambda h^2\phi+2\mu\frac{\partial^2\phi}{\partial z^2}-2\mu\frac{\partial^2\psi}{\partial x\partial z}\ ,$$

$$Y_z=\mu\left(\frac{\partial v}{\partial z}+\frac{\partial w}{\partial y}\right)=\mu\frac{\partial v}{\partial z}\ ,\qquad Y_x=\mu\left(\frac{\partial u}{\partial y}+\frac{\partial v}{\partial x}\right)=\mu\frac{\partial v}{\partial x}\ .$$

the representation of stress by displacement potentials or displacement is obtained as follows:

$$\begin{aligned} N_\nu=&\Big[-2\mu\left(h^2\phi+2\frac{\partial^2\phi}{\partial x^2}+2\frac{\partial^2\psi}{\partial x\partial z}\right)\zeta'\\ &+\mu\left(2\frac{\partial^2\phi}{\partial x\partial z}-\sigma h^2\psi-2\frac{\partial^2\psi}{\partial x^2}\right)(1-\zeta'^2)\Big]\Big/(1+\zeta'^2)\ ,\\ T_\nu=&\Big[-\lambda h^2\phi+2\mu\frac{\partial^2\phi}{\partial z^2}-2\mu\frac{\partial^2\psi}{\partial x\partial z}+\left(-\lambda h^2\phi+2\mu\frac{\partial^2\phi}{\partial x^2}+2\mu\frac{\partial^2\psi}{\partial x\partial z}\right)\zeta'^2\\ &-2\mu\left(2\frac{\partial^2\phi}{\partial x\partial z}-\sigma h^2\psi-2\frac{\partial^2\psi}{\partial x^2}\right)\zeta'\Big]\Big/(1+\zeta'^2)\ ,\\ Y_\nu=&\mu\left(\frac{\partial v}{\partial z}-\frac{\partial v}{\partial x}\zeta'\right)\Big/\sqrt{1+\zeta'^2}\ . \end{aligned} \tag{5}$$

At the gradient of ζ, i.e. ζ' is common to both media, the condition of continuity of N_ν is equivalent to that of $(1+\zeta'^2)N_\nu$ and so forth. Thus, in the case of incidence of P or SV waves, the conditions of the continuity of stresses are equivalent to those of the continuity of $(1+\zeta'^2)N_\nu$ and $(1+\zeta'^2)T_\nu$ at $z=\zeta$ and in the case of incidence of SH waves, the condition is equivalent to the continuity of $\sqrt{1+\zeta'^2}Y_\nu$ at $z=\zeta$.

Chapter 3. Cases of the Incidence of P and SV Waves

§ 1. Incident, Reflected and Refracted Waves

Next, the both cases of the incidence of P and SV waves are considered together, because the treatment for them is similar. The coordinate system used is shown in Fig. 1.

In regard to the incident, regularly reflected and regularly refracted waves, the following displacement potentials were adopted.

For the incidence of the P wave,

Displacement potential of the incident wave:

$$\phi_{10}=e^{ik_1(V_{p1}t+z\cos\alpha+x\sin\alpha)},$$

For the incidence of the SV wave,

Displacement potential of the incident wave:

$$\psi_{10}=e^{i\sqrt{\sigma_1}k_1(V_{s1}t+z\cos\beta+x\sin\beta)},$$

For both cases,

Displacement potential of regularly reflected wave:

$$\phi_1^{(0)}=A_0e^{ik_1(V_{p1}t-z\cos\alpha+x\sin\alpha)},$$

$$\psi_1^{(0)}=B_0e^{i\sqrt{\sigma_1}k_1(V_{s1}t-z\cos\beta+x\sin\beta)},$$

Displacement potential of a regularly refracted wave:

$$\phi_2^{(0)}=C_0e^{ik_2(V_{p2}t+z\cos\gamma+x\sin\gamma)},$$

$$\psi_2^{(0)}=D_0e^{i\sqrt{\sigma_2}k_2(V_{s2}t+z\cos\delta+x\sin\delta)},$$

where V_{p1}, V_{s1}, V_{p2} and V_{s2} are the velocities of P and S waves in the lower and the upper medium respectively. By Snell's law, the angle of

reflection of the P wave, α, that of the S wave, β, the angle of refraction of the P wave, γ, and that of the S wave, δ, are connected as follows:

$$h_1 \sin\alpha = \sqrt{\sigma_1} h_1 \sin\beta = h_2 \sin\gamma = \sqrt{\sigma_2} h_2 \sin\delta \ .$$

Besides these regular waves, it is necessary to take into consideration the effect of the corrugation on reflections and refractions and to introduce the following displacement potentials of irregular waves:

(1) Displacement potentials of irregularly reflected waves with whose spectrum of the nth order being:

$$\phi_1^{(n)} = A_n e^{ih_1(V_{p1}t - z\cos\alpha_n + x\sin\alpha_n)} + A_n' e^{ih_1(V_{p1}t - z\cos\alpha_n' + x\sin\alpha_n')} \ ,$$

$$\psi_1^{(n)} = B_n e^{i\sqrt{\sigma_1}h_1(V_{s1}t - z\cos\beta_n + x\sin\beta_n)} + B_n' e^{i\sqrt{\sigma_1}h_1(V_{s1}t - z\cos\beta_n' + x\sin\beta_n')} \ .$$

(2) Displacement potentials of irregularly refracted waves whose spectrum of the nth order being:

$$\phi_2^{(n)} = C_n e^{ih_2(V_{p2}t + z\cos\gamma_n + x\sin\gamma_n)} + C_n' e^{ih_2(V_{p2}t + z\cos\gamma_n' + x\sin\gamma_n')} \ ,$$

$$\psi_2^{(n)} = D_n e^{i\sqrt{\sigma_2}h_2(V_{s2}t + z\cos\delta_n + x\sin\delta_n)} + D_n' e^{i\sqrt{\sigma_2}h_2(V_{s2}t + z\cos\delta_n' + x\sin\delta_n')} \ ,$$

where α_n, α_n', β_n, β_n', etc. are connected by the following relations:

$$\sin\alpha_n - \sin\alpha = np/h_1 \ , \qquad \sin\alpha_n' - \sin\alpha = -np/h_1 \ ,$$

$$\sin\beta_n - \sin\beta = np/(\sqrt{\sigma_1}h_1) \ , \qquad \sin\beta_n' - \sin\beta = -np/(\sqrt{\sigma_1}h_1) \ ,$$

$$\sin\gamma_n - \sin\gamma = np/h_2 \ , \qquad \sin\gamma_n' - \sin\gamma = -np/h_2 \ ,$$

$$\sin\delta_n - \sin\delta = np/(\sqrt{\sigma_2}h_2) \ , \qquad \sin\delta_n' - \sin\delta = -np/(\sqrt{\sigma_2}h_2) \ ,$$

$$h_1 \sin\alpha_n = \sqrt{\sigma_1} h_1 \sin\beta_n = h_2 \sin\gamma_n = \sqrt{\sigma_2} h_2 \sin\delta_n \ .$$

Superposing above displacement potentials, the resultant displacement potentials are obtained in the lower and in the upper medium respectively.

In the lower medium:

$$\phi_1 = e^{ih_1 x\sin\alpha}\left[ae^{ih_1 z\cos\alpha} + A_0 e^{-ih_1 z\cos\alpha} + \sum_{n=1}^{\infty}\{A_n e^{i(npx - h_1 z\cos\alpha_n)} + A_n' e^{-i(npx + h_1 z\cos\alpha_n')}\}\right] , \qquad (6)$$

$$\psi_1=e^{ih_1x\sin\alpha}\left[be^{i\sqrt{\sigma_1}h_1z\cos\beta}+B_0e^{-i\sqrt{\sigma_1}h_1z\cos\beta}\right.$$
$$\left.+\sum_{n=1}^{\infty}\{B_ne^{i(npx-\sqrt{\sigma_1}h_1z\cos\beta_n)}+B_n'e^{-i(npx+\sqrt{\sigma_1}h_1z\cos\beta_n')}\}\right], \qquad (7)$$

where $a=1$ and $b=0$ in the case of incidence of the P wave and $a=0$ and $b=1$ in the case of incidence of the SV wave.
In the upper medium:

$$\phi_2=e^{ih_1x\sin\alpha}\left[C_0e^{ih_2z\cos\gamma}\right.$$
$$\left.+\sum_{n=1}^{\infty}\{C_ne^{i(h_2z\cos\gamma_n+npx)}+C_n'e^{i(h_2z\cos\gamma_n'-npx)}\}\right], \qquad (8)$$

$$\psi_2=e^{ih_1x\sin\alpha}\left[D_0e^{i\sqrt{\sigma_2}h_2z\cos\delta}\right.$$
$$\left.+\sum_{n=1}^{\infty}\{D_ne^{i(\sqrt{\sigma_2}h_2z\cos\delta_n+npx)}+D_n'e^{i(\sqrt{\sigma_2}h_2z\cos\delta_n'-npx)}\}\right]. \qquad (9)$$

In the above formulae, the common time factor $e^{i\omega t}$ is overlooked.

§ 2. Boundary Conditions

The boundary conditions are given by the conditions of the continuity of stress and displacement on the boundary surface $z=\zeta$.

Substituting ϕ_i, ψ_i, and their derivatives into $(1+\zeta'^2)N_\nu^{(1)}=(1+\zeta'^2)N_\nu^{(2)}$ or $(1+\zeta'^2)T_\nu^{(1)}=(1+\zeta'^2)T_\nu^{(2)}$, we can get the following relations between A_0, B_0, C_0, D_0, A_n, B_n, etc.

$$-2\mu_1h_1^2\{(1-2\sin^2\alpha)\zeta'+(1-\zeta'^2)\sin\alpha\cos\alpha\}ae^{ih_1\zeta\cos\alpha}$$
$$-2\mu_1h_1^2\{(1-2\sin^2\alpha)\zeta'-(1-\zeta'^2)\sin\alpha\cos\alpha\}A_0e^{-ih_1\zeta\cos\alpha}$$
$$+2\mu_1\sum_{n=1}^{\infty}\{-h_1^2\zeta'+2\zeta'(h_1\sin\alpha+np)^2$$
$$+h_1(h_1\sin\alpha+np)(1-\zeta'^2)\cos\alpha_n\}A_ne^{i(npx-h_1\zeta\cos\alpha_n)}$$
$$+2\mu_1\sum_{n=1}^{\infty}\{-h_1^2\zeta'+2\zeta'(h_1\sin\alpha-np)^2$$
$$+h_1(h_1\sin\alpha-np)(1-\zeta'^2)\cos\alpha_n'\}A_n'e^{-i(npx+h_1\zeta\cos\alpha_n')}$$
$$+\mu_1h_1^2\{4\sqrt{\sigma_1}\zeta'\sin\alpha\cos\beta-(\sigma_1-2\sin^2\alpha)(1-\zeta'^2)\}be^{i\sqrt{\sigma_1}h_1\zeta\cos\beta}$$
$$-\mu_1h_1^2\{4\sqrt{\sigma_1}\zeta'\sin\alpha\cos\beta+(\sigma_1-2\sin^2\alpha)(1-\zeta'^2)\}B_0e^{-i\sqrt{\sigma_1}h_1\zeta\cos\beta}$$

$$
\begin{aligned}
&-\mu_1\sum_{n=1}^{\infty}[4\sqrt{\sigma_1}h_1\zeta'(h_1\sin\alpha+np)\cos\beta_n \\
&\quad+\{\sigma_1h_1^2-2(h_1\sin\alpha+np)^2\}(1-\zeta'^2)]B_ne^{i(npx-\sqrt{\sigma_1}h_1\zeta\cos\beta_n)} \\
&-\mu_1\sum_{n=1}^{\infty}[4\sqrt{\sigma_1}h_1\zeta'(h_1\sin\alpha-np)\cos\beta_n' \\
&\quad+\{\sigma_1h_1^2-2(h_1\sin\alpha-np)^2\}(1-\zeta'^2)]B_n'e^{-i(npx+\sqrt{\sigma_1}h_1\zeta\cos\beta_n')} \\
&=-2\mu_2\{(h_2^2-2h_1^2\sin^2\alpha)\zeta'+(1-\zeta'^2)h_1h_2\sin\alpha\cos\gamma\}C_0e^{ih_2\zeta\cos\gamma} \\
&+\mu_2\{4\sqrt{\sigma_2}h_1h_2\zeta'\sin\alpha\cos\delta-(\sigma_2h_2^2-2h_1^2\sin^2\alpha)(1-\zeta'^2)\}D_0e^{i\sqrt{\sigma_2}h_2\zeta\cos\delta} \\
&-2\mu_2\sum_{n=1}^{\infty}[\{h_2^2-2(h_1\sin\alpha+np)^2\}\zeta' \\
&\quad+(1-\zeta'^2)(h_1\sin\alpha+np)h_2\cos\gamma_n]C_ne^{i(npx+h_2\zeta\cos\gamma_n)} \\
&-2\mu_2\sum_{n=1}^{\infty}[\{h_2^2-2(h_1\sin\alpha-np)^2\}\zeta' \\
&\quad+(1-\zeta'^2)(h_1\sin\alpha-np)h_2\cos\gamma_n']C_n'e^{-i(npx-h_2\zeta\cos\gamma_n')} \\
&+\mu_2\sum_{n=1}^{\infty}[4\sqrt{\sigma_2}h_2\zeta'(h_1\sin\alpha+np)^2\cos\delta_n \\
&\quad-(1-\zeta'^2)\{\sigma_2h_2^2-2(h_1\sin\alpha+np)^2\}]D_ne^{i(npx+\sqrt{\sigma_2}h_2\zeta\cos\delta_n)} \\
&+\mu_2\sum_{n=1}^{\infty}[4\sqrt{\sigma_2}h_2\zeta'(h_1\sin\alpha-np)^2\cos\delta_n' \\
&\quad-(1-\zeta'^2)\{\sigma_2h_2^2-2(h_1\sin\alpha-np)^2\}]D_n'e^{-i(npx-\sqrt{\sigma_2}h_2\zeta\cos\delta_n')}, \qquad (10) \\
&-h_1^2\{\lambda_1+2\mu_1\cos^2\alpha-4\mu_1\zeta'\sin\alpha\cos\alpha+\zeta'^2(\lambda_1+2\mu_1\sin^2\alpha)\}ae^{ih_1\zeta\cos\alpha} \\
&-h_1^2\{\lambda_1+2\mu_1\cos^2\alpha+4\mu_1\zeta'\sin\alpha\cos\alpha+\zeta'^2(\lambda_1+2\mu_1\sin^2\alpha)\}A_0e^{-ih_1\zeta\cos\alpha} \\
&-\sum_{n=1}^{\infty}[h_1^2(\lambda_1+2\mu_1\cos^2\alpha_n')+4\mu_1\zeta'h_1(h_1\sin\alpha-np)\cos\alpha_n' \\
&\quad+\zeta'^2\{\lambda_1h_1^2+2\mu_1(h_1\sin\alpha+np)^2\}]A_ne^{i(npx-h_1\zeta\cos\alpha_n)} \\
&-\sum_{n=1}^{\infty}[h_1^2(\lambda_1+2\mu_1\cos^2\alpha_n')+4\mu_1\zeta'h_1(h_1\sin\alpha-np)\cos\alpha_n' \\
&\quad+\zeta'^2\{\lambda_1h_1^2+2\mu_1(h_1\sin\alpha-np)^2\}]A_n'e^{-i(npx+h_1\zeta\cos\alpha_n')} \\
&+2\mu_1h_1^2\{\sqrt{\sigma_1}\sin\alpha\cos\beta+\zeta'(\sigma_1-2\sin^2\alpha) \\
&\quad-\zeta'^2\sqrt{\sigma_1}\sin\alpha\cos\beta\}be^{i\sqrt{\sigma_1}h_1\zeta\cos\beta} \\
&+2\mu_1h_1^2\{-\sqrt{\sigma_1}\sin\alpha\cos\beta+\zeta'(\sigma_1-2\sin^2\alpha) \\
&\quad+\zeta'^2\sqrt{\sigma_1}\sin\alpha\cos\beta\}B_0e^{-i\sqrt{\sigma_1}h_1\zeta\cos\beta}
\end{aligned}
$$

$$
\begin{aligned}
&+2\mu_1\sum_{n=1}^{\infty}[-\sqrt{\sigma_1}h_1(h_1\sin\alpha+np)\cos\beta_n+\zeta'\{\sigma_1h_1^2-2(h_1\sin\alpha+np)^2\}\\
&\quad+\zeta'^2\sqrt{\sigma_1}h_1(h_1\sin\alpha+np)\cos\beta_n]B_ne^{i(npx-\sqrt{\sigma_1}h_1\zeta\cos\beta_n)}\\
&+2\mu_1\sum_{n=1}^{\infty}[-\sqrt{\sigma_1}h_1(h_1\sin\alpha-np)\cos\beta_n'+\zeta'\{\sigma_1h_1^2-2(h_1\sin\alpha-np)^2\}\\
&\quad+\zeta'^2\sqrt{\sigma_1}h_1(h_1\sin\alpha-np)\cos\beta_n']B_n'e^{i(npx+\sqrt{\sigma_1}h_1\zeta\cos\beta_n')}\\
&=\{-h_2^2(\lambda_2+2\mu_2\cos^2\gamma)+4\mu_2\zeta'h_1h_2\sin\alpha\cos\gamma\\
&\quad-\zeta'^2(\lambda_2h_2^2+2\mu_2h_1^2\sin^2\alpha)\}C_0e^{ih_2\zeta\cos\gamma}\\
&-\sum_{n=1}^{\infty}[h_2^2(\lambda_2+2\mu_2\cos^2\gamma_n)-4\mu_2h_2\zeta'(h_1\sin\alpha+np)\cos\gamma_n\\
&\quad+\zeta'^2\{\lambda_2h_2^2+2\mu_2(h_1\sin\alpha+np)^2\}]C_ne^{i(npx+h_2\zeta\cos\gamma_n)}\\
&-\sum_{n=1}^{\infty}[h_2^2(\lambda_2+2\mu_2\cos^2\gamma_n')-4\mu_2h_2\zeta'(h_1\sin\alpha-np)\cos\gamma_n'\\
&\quad+\zeta'^2\{\lambda_2h_2^2+2\mu_2(h_1\sin\alpha-np)^2\}]C_n'e^{-i(npx-h_2\zeta\cos\gamma_n')}\\
&+2\mu_2\{\sqrt{\sigma_2}h_1h_2\sin\alpha\cos\delta+\zeta'(\sigma_2h_2^2-2h_1^2\sin^2\alpha)\\
&\quad-\zeta'^2\sqrt{\sigma_2}h_1h_2\sin\alpha\cos\delta\}D_0e^{i\sqrt{\sigma_2}h_2\zeta\cos\delta}\\
&+2\mu_2\sum_{n=1}^{\infty}[\sqrt{\sigma_2}h_2(h_1\sin\alpha+np)\cos\delta_n+\zeta'\{\sigma_2h_2^2-2(h_1\sin\alpha+np)^2\}\\
&\quad-\zeta'^2\sqrt{\sigma_2}h_2(h_1\sin\alpha+np)\cos\delta_n]D_ne^{i(npx+\sqrt{\sigma_2}h_2\zeta\cos\delta_n)}\\
&+2\mu_2\sum_{n=1}^{\infty}[\sqrt{\sigma_2}h_2(h_1\sin\alpha-np)\cos\delta_n'+\zeta'\{\sigma_2h_2^2-2(h_1\sin\alpha-np)^2\}\\
&\quad-\zeta'^2\sqrt{\sigma_2}h_2(h_1\sin\alpha-np)\cos\delta_n']D_n'e^{-i(npx-\sqrt{\sigma_2}h_2\zeta\cos\delta_n')} \qquad (11)
\end{aligned}
$$

From the condition of the continuity of displacement u and w, we have

$$
\begin{aligned}
&h_1(ae^{ih_1\zeta\cos\alpha}+A_0e^{-ih_1\zeta\cos\alpha})\sin\alpha\\
&\quad+\sum_{n=1}^{\infty}\{(h_1\sin\alpha+np)A_ne^{i(npx-h_1\zeta\cos\alpha_n)}\\
&\quad+(h_1\sin\alpha-np)A_n'e^{-i(npx+h_1\zeta\cos\alpha_n')}\}\\
&+\sqrt{\sigma_1}h_1(be^{i\sqrt{\sigma_1}h_1\zeta\cos\beta}-B_0e^{-i\sqrt{\sigma_1}h_1\zeta\cos\beta})\cos\beta\\
&\quad-\sqrt{\sigma_1}h_1\sum_{n=1}^{\infty}\{B_ne^{i(npx-\sqrt{\sigma_1}h_1\zeta\cos\beta_n)}\cos\beta_n+B_n'e^{-i(npx+\sqrt{\sigma_1}h_1\zeta\cos\beta_n')}\cos\beta_n'\}\\
&=h_1C_0e^{ih_2\zeta\cos\gamma}\sin\alpha\\
&\quad+\sum_{n=1}^{\infty}\{(h_1\sin\alpha+np)C_ne^{i(npx+h_2\zeta\cos\gamma_n)}+(h_1\sin\alpha-np)C_n'e^{-i(npx-h_2\zeta\cos\gamma_n')}\}
\end{aligned}
$$

$$+\sqrt{\sigma_2}h_2D_0e^{i\sqrt{\sigma_2}h_2\zeta\cos\delta}\cos\delta$$
$$+\sum_{n=1}^{\infty}\sqrt{\sigma_2}h_2\{D_ne^{i(npx+\sqrt{\sigma_2}h_2\zeta\cos\delta_n)}\cos\delta_n+D_n'e^{-i(npx-\sqrt{\sigma_2}h_2\zeta\cos\delta_n')}\cos\delta_n'\}\ ,$$
(12)

$$h_1(ae^{ih_1\zeta\cos\alpha}-A_0e^{-ih_1\zeta\cos\alpha})\cos\alpha$$
$$-h_1\sum_{n=1}^{\infty}\{A_ne^{i(npx-h_1\zeta\cos\alpha_n)}\cos\alpha_n+A_n'e^{-i(npx+h_1\zeta\cos\alpha_n')}\cos\alpha_n'\}$$
$$-h_1(be^{i\sqrt{\sigma_1}h_1\zeta\cos\beta}+B_0e^{-i\sqrt{\sigma_1}h_1\zeta\cos\beta})\sin\alpha$$
$$-\sum_{n=1}^{\infty}\{(h_1\sin\alpha+np)B_ne^{i(npx-\sqrt{\sigma_1}h_1\zeta\cos\beta_n)}$$
$$+(h_1\sin\alpha-np)B_n'e^{-i(npx+\sqrt{\sigma_1}h_1\zeta\cos\beta_n')}\}$$
$$=h_2C_0e^{ih_2\zeta\cos\gamma}\cos\gamma+h_2\sum_{n=1}^{\infty}\{C_ne^{i(npx+h_2\zeta\cos\gamma_n)}\cos\gamma_n+C_n'e^{-i(npx-h_2\zeta\cos\gamma_n')}\cos\gamma_n'\}$$
$$-h_1D_0e^{i\sqrt{\sigma_2}h_2\zeta\cos\delta}\sin\alpha$$
$$-\sum_{n=1}^{\infty}\{(h_1\sin\alpha+np)D_ne^{i(npx+\sqrt{\sigma_2}h_2\zeta\cos\delta_n)}$$
$$+(h_1\sin\alpha-np)D_n'e^{-i(npx-\sqrt{\sigma_2}h_2\zeta\cos\delta_n')}\}\ .$$
(13)

§ 3. The Solutions of the First Approximation

As in the case of incidence of the SH wave, the amplitude of corrugation, ζ, is assumed to be very small so that the terms of an order higher than ζ are neglected.

First the solutions of the first approximation will be obtained by picking up the term independent of x and ζ in (10) through (13).

$$-2\mu_1h_1^2(a-A_0)\sin\alpha\cos\alpha+\mu_1h_1^2(2\sin^2\alpha-\sigma_1)(b+B_0)$$
$$+2\mu_2h_1h_2C_0\sin\alpha\cos\gamma-\mu_2D_0(2h_1^2\sin^2\alpha-\sigma_2h_2^2)=0\ ,$$
$$-h_1^2(\lambda_1+2\mu_1\cos^2\alpha)(a+A_0)+2\mu_1h_1^2\sqrt{\sigma_1}(b-B_0)\sin\alpha\cos\beta$$
$$+h_2^2(\lambda_2+2\mu_2\cos^2\gamma)C_0-2\mu_2\sqrt{\sigma_2}h_1h_2D_0\sin\alpha\cos\delta=0\ ,$$
(14)
$$h_1(a+A_0)\sin\alpha+\sqrt{\sigma_1}h_1(b-B_0)\cos\beta-h_1C_0\sin\alpha-\sqrt{\sigma_2}h_2D_0\cos\delta=0\ ,$$
$$h_1(a-A_0)\cos\alpha-h_1(b+B_0)\sin\alpha-h_2C_0\cos\gamma+h_1D_0\sin\alpha=0$$

These equations are the same as those obtained in the case of the reflection and refraction of elastic waves at a plane boundary surface.

From the coefficients of e^{inpx} in (10) through (13), the following

formulae determining the first approximation of A_n, B_n, C_n and D_n are obtained.

$$
\begin{aligned}
&2\mu_1 h_1 A_n(h_1\sin\alpha+np)\cos\alpha_n-\mu_1 B_n\{\sigma_1 h_1^2-2(h_1\sin\alpha+np)^2\}\\
&\quad+2\mu_2 h_2 C_n(h_1\sin\alpha+np)\cos\gamma_n-\mu_2 D_n\{-\sigma_2 h_2^2+2(h_1\sin\alpha+np)^2\}\\
&=2i\mu_1\zeta_n h_1^2(a+A_0)\{np(1-2\sin^2\alpha)+h_1\sin\alpha\cos^2\alpha\}\\
&\quad-i\mu_1\sqrt{\sigma_1}h_1^2\zeta_n(b-B_0)\{4np\sin\alpha+h_1(2\sin^2\alpha-\sigma_1)\}\cos\beta\\
&\quad-2i\mu_2 C_0\zeta_n\{np(h_2^2-2h_1^2\sin^2\alpha)+h_1h_2^2\sin\alpha\cos^2\gamma\}\\
&\quad+i\mu_2 D_0\sqrt{\sigma_2}h_2\zeta_n\{4nph_1\sin\alpha-(\sigma_2h_2^2-2h_1^2\sin^2\alpha)\}\cos\delta\ ,\\
&-h_1^2A_n(\lambda_1+2\mu_1\cos^2\alpha_n)-2\mu_1\sqrt{\sigma_1}h_1B_n(h_1\sin\alpha+np)\cos\beta_n\\
&\quad+h_2^2C_n(\lambda_2+2\mu_2\cos^2\gamma_n)-2\mu_2\sqrt{\sigma_2}h_2D_n(h_1\sin\alpha+np)\cos\delta_n\\
&=ih_1^2\zeta_n(a-A_0)[h_1(\lambda_1+2\mu_1\cos^2\alpha)-4\mu_1np\sin\alpha]\cos\alpha\\
&\quad-2i\mu_1h_1^2\zeta_n(b+B_0)\{np(\sigma_1-2\sin^2\alpha)+\sigma_1h_1\sin\alpha\cos^2\beta\}\\
&\quad+iC_0h_2\zeta_n\{-(\lambda_2+2\mu_2\cos^2\gamma)h_2^2+4np\mu_2h_1\sin\alpha\}\cos\gamma\\
&\quad+2i\mu_2\zeta_nD_0\{\sigma_2h_1h_2^2\sin\alpha\cos^2\delta+np(\sigma_2h_2^2-2h_1^2\sin^2\alpha)\}\ ,
\end{aligned}
\tag{15}
$$

$$
\begin{aligned}
&(h_1\sin\alpha+np)A_n-\sqrt{\sigma_1}h_1B_n\cos\beta_n-(h_1\sin\alpha+np)C_n-\sqrt{\sigma_2}h_2D_n\cos\delta_n\\
&\quad=-ih_1^2\zeta_n(a-A_0)\sin\alpha\cos\alpha-i\sigma_1h_1^2\zeta_n(b+B_0)\cos^2\beta\\
&\quad+ih_1h_2C_0\zeta_n\sin\alpha\cos\gamma+i\sigma_2h_2^2\zeta_nD_0\cos^2\delta\ ,\\
&-h_1A_n\cos\alpha_n-(h_1\sin\alpha+np)B_n-h_2C_n\cos\gamma_n+(h_1\sin\alpha+np)D_n\\
&\quad=-ih_1^2\zeta_n(a+A_0)\cos^2\alpha+i\sqrt{\sigma_1}h_1^2\zeta_n(b-B_0)\sin\alpha\cos\beta\\
&\quad+ih_2^2\zeta_nC_0\cos^2\gamma-i\sqrt{\sigma_2}h_1h_2\zeta_nD_0\sin\alpha\cos\delta
\end{aligned}
\tag{16}
$$

From the coefficients of e^{-inpx} in (10) through (13), the following formulae concerning the first approximation of A'_n, B'_n, C'_n and D'_n are derived.

$$
\begin{aligned}
&2\mu_1h_1A'_n(h_1\sin\alpha-np)\cos\alpha'_n-\mu_1B'_n\{\sigma_1h_1^2-2(h_1\sin\alpha-np)^2\}\\
&\quad+2\mu_2h_2C'_n(h_1\sin\alpha-np)\cos\gamma'_n+\mu_2D'_n\{\sigma_2h_2^2-2(h_1\sin\alpha-np)^2\}\\
&=2i\mu_1h_1^2\zeta_{-n}(a+A_0)\{-np(1-2\sin^2\alpha)+h_1\sin\alpha\cos^2\alpha\}\\
&\quad+i\mu_1h_1^2\sqrt{\sigma_1}\zeta_{-n}(b-B_0)[4np\sin\alpha+(\sigma_1-2\sin^2\alpha)h_1]\cos\beta\\
&\quad-2i\mu_2C_0\zeta_{-n}\{-np(h_2^2-2h_1^2\sin^2\alpha)+h_1h_2^2\sin\alpha\cos^2\gamma\}\\
&\quad-i\mu_2\sqrt{\sigma_2}h_2D_0\zeta_{-n}\{4nph_1\sin\alpha+(\sigma_2h_2^2-2h_1^2\sin^2\alpha)\}\cos\delta
\end{aligned}
$$

$$
\begin{aligned}
&-h_1^2A'_n(\lambda_1+2\mu_1\cos^2\alpha'_n)-2\mu_1\sqrt{\sigma_1}\,h_1B'_n(h_1\sin\alpha-np)\cos\beta'_n\\
&\quad+h_2^2C'_n(\lambda_2+2\mu_2\cos^2\gamma'_n)-2\mu_2\sqrt{\sigma_2}\,h_2D'_n(h_1\sin\alpha-np)\cos\delta'_n\\
&\quad=ih_1^2\zeta_{-n}(a-A_0)\{h_1(\lambda_1+2\mu_1\cos^2\alpha)+4\mu_1np\sin\alpha\}\cos\alpha \qquad (17)\\
&\quad-2i\mu_1h_1^2\zeta_{-n}(b+B_0)\{-np(\sigma_1-2\sin^2\alpha)+\sigma_1h_1\sin\alpha\cos^2\beta\}\\
&\quad-iC_0h_2\zeta_{-n}\{(\lambda_2+2\mu_2\cos^2\gamma)h_2^2+4np\mu_2h_1\sin\alpha\}\cos\gamma\\
&\quad+2i\mu_2\zeta_{-n}D_0\{\sigma_2h_1h_2^2\sin\alpha\cos^2\delta-(\sigma_2h_2^2-2h_1^2\sin^2\alpha)np\}\ ,\\
&(h_1\sin\alpha-np)A'_n-\sqrt{\sigma_1}\,h_1B'_n\cos\beta'_n-(h_1\sin\alpha-np)C'_n-\sqrt{\sigma_2}\,h_2D'_n\cos\delta'_n\\
&\quad=-ih_1^3\zeta_{-n}(a-A_0)\sin\alpha\cos\alpha-i\sigma_1h_1^2\zeta_{-n}(b+B_0)\cos^2\beta\\
&\quad+ih_1h_2C_0\zeta_{-n}\sin\alpha\cos\gamma+i\sigma_2h_2^2\zeta_{-n}D_0\cos^2\delta\ ,\\
&-h_1A'_n\cos\alpha'_n-(h_1\sin\alpha-np)B'_n-h_2C'_n\cos\gamma'_n+(h_1\sin\alpha-np)D'_n\\
&\quad=-ih_1^2\zeta_{-n}(a+A_0)\cos^2\alpha+i\sqrt{\sigma_1}\,h_1^2\zeta_{-n}(b-B_0)\sin\alpha\cos\beta\\
&\quad+ih_2^2C_0\zeta_{-n}\cos^2\gamma-i\sqrt{\sigma_2}\,h_1h_2\zeta_{-n}D_0\sin\alpha\cos\delta\ .
\end{aligned}
$$

§ 4. The Solutions of the Second Approximations

If the terms, of an order higher than ζ^3, are omitted in the equations of boundary conditions (10), (11), (12) and (13),

$$
\begin{aligned}
&-2\mu_1h_1^2(a-A_0)\sin\alpha\cos\alpha-2\mu_1h_1^2(a+A_0)\{(1-2\sin^2\alpha)\zeta'+ih_1\zeta\sin\alpha\cos^2\alpha\}\\
&\quad+2\mu_1\sum[-\zeta'\{h_1^2-2(h_1\sin\alpha+np)^2\}\\
&\qquad+h_1(1-ih_1\zeta\cos\alpha_n)(h_1\sin\alpha+np)\cos\alpha_n]A_ne^{inpx}\\
&\quad+2\mu_1\sum[-\zeta'\{h_1^2-2(h_1\sin\alpha-np)^2\}\\
&\qquad+h_1(1-ih_1\zeta\cos\alpha'_n)(h_1\sin\alpha-np)\cos\alpha'_n]A'_ne^{-inpx}\\
&\quad-\mu_1h_1^2(b+B_0)(\sigma_1-2\sin^2\alpha)\\
&\qquad+\mu_1h_1^2(b-B_0)\{4\sqrt{\sigma_1}\,\zeta'\sin\alpha\cos\beta-i\sqrt{\sigma_1}\,h_1\zeta(\sigma_1-2\sin^2\alpha)\cos\beta\}\\
&\quad-\mu_1\sum[4\sqrt{\sigma_1}\,h_1\zeta'(h_1\sin\alpha+np)\cos\beta_n\\
&\qquad+\{\sigma_1h_1^2-2(h_1\sin\alpha+np)^2\}(1-i\sqrt{\sigma_1}\,h_1\zeta\cos\beta_n)]B_ne^{inpx}\\
&\quad-\mu_1\sum[4\sqrt{\sigma_1}\,h_1\zeta'(h_1\sin\alpha-np)\cos\beta'_n\\
&\qquad+\{\sigma_1h_1^2-2(h_1\sin\alpha-np)^2\}(1-i\sqrt{\sigma_1}\,h_1\zeta\cos\beta'_n)]B'_ne^{-inpx}\\
&\quad=-2\mu_2C_0\{(h_2^2-2h_1^2\sin^2\alpha)\zeta'+h_1h_2(1+ih_2\zeta\cos\gamma)\sin\alpha\cos\gamma\}\\
&\quad+\mu_2D_0\{4\sqrt{\sigma_2}\,h_1h_2\zeta'\sin\alpha\cos\delta-(\sigma_2h_2^2-2h_1^2\sin^2\alpha)(1+i\sqrt{\sigma_2}\,h_2\zeta\cos\delta)\}
\end{aligned}
$$

$$
\begin{aligned}
&-2\mu_2\sum[\{h_2^2-2(h_1\sin\alpha+np)^2\}\zeta' \\
&\quad+(h_1\sin\alpha+np)(1+ih_2\zeta\cos\gamma_n)h_2\cos\gamma_n]C_ne^{inpx} \\
&-2\mu_2\sum[\{h_2^2-2(h_1\sin\alpha-np)^2\}\zeta' \\
&\quad+(h_1\sin\alpha-np)(1+ih_2\zeta\cos\gamma'_n)h_2\cos\gamma'_n]C'_ne^{-inpx} \\
&+\mu_2\sum[4\sqrt{\sigma_2}h_2(h_1\sin\alpha+np)\zeta'\cos\delta_n \\
&\quad-\{\sigma_2h_2^2-2(h_1\sin\alpha+np)^2\}(1+i\sqrt{\sigma_2}h_2\zeta\cos\delta_n)]D_ne^{inpx} \\
&+\mu_2\sum[4\sqrt{\sigma_2}h_2(h_1\sin\alpha-np)\zeta'\cos\delta'_n \\
&\quad-\{\sigma_2h_2^2-2(h_1\sin\alpha-np)^2\}(1+i\sqrt{\sigma_2}h_2\zeta\cos\delta'_n)]D'_ne^{-inpx} \qquad (18)
\end{aligned}
$$

$$
\begin{aligned}
&-h_1^2(a+A_0)(\lambda_1+2\mu_1\cos^2\alpha) \\
&-h_1^2(a-A_0)\{ih_1(\lambda_1+2\mu_1^2\cos^2\alpha)\zeta\cos\alpha-4\mu_1\zeta'\sin\alpha\cos\alpha\} \\
&-h_1\sum\{h_1(\lambda_1+2\mu_1\cos^2\alpha_n)(1-ih_1\zeta\cos\alpha_n) \\
&\quad+4\mu_1\zeta'(h_1\sin\alpha+np)\cos\alpha_n\}A_ne^{inpx} \\
&-h_1\sum\{h_1(\lambda_1+2\mu_1\cos^2\alpha'_n)(1-ih_1\zeta\cos\alpha'_n) \\
&\quad+4\mu_1\zeta'(h_1\sin\alpha-np)\cos\alpha'_n\}A'_ne^{-inpx} \\
&+2\mu_1h_1^2\sqrt{\sigma_1}(b-B_0)\sin\alpha\cos\beta \\
&\quad+2\mu_1h_1^2(b+B_0)\{(\sigma_1-2\sin^2\alpha)\zeta'+i\sigma_1h_1\zeta\sin\alpha\cos^2\beta\} \\
&+2\mu_1\sum[-\sqrt{\sigma_1}h_1(h_1\sin\alpha+np)(1-i\sqrt{\sigma_1}h_1\zeta\cos\beta_n)\cos\beta_n \\
&\quad+\zeta'\{\sigma_1h_1^2-2(h_1\sin\alpha+np)^2\}]B_ne^{inpx} \\
&+2\mu_1\sum[-\sqrt{\sigma_1}h_1(h_1\sin\alpha-np)(1-i\sqrt{\sigma_1}h_1\zeta\cos\beta'_n)\cos\beta'_n \\
&\quad+\zeta'\{\sigma_1h_1^2-2(h_1\sin\alpha-np)^2\}]B'_ne^{-inpx} \\
&=C_0\{-h_2^2(\lambda_2+2\mu_2\cos^2\gamma)(1+ih_2\zeta\cos\gamma)+4\mu_2\zeta'h_1h_2\sin\alpha\cos\gamma\} \\
&-\sum\{h_2^2(\lambda_2+2\mu_2\cos^2\gamma_n)(1+ih_2\zeta\cos\gamma_n) \\
&\quad-4\mu_2\zeta'(h_1\sin\alpha+np)h_2\cos\gamma_n\}C_ne^{inpx} \\
&-\sum\{h_2^2(\lambda_2+2\mu_2\cos^2\gamma'_n)(1+ih_2\zeta\cos\gamma'_n) \\
&\quad-4\mu_2\zeta'(h_1\sin\alpha-np)h_2\cos\gamma'_n\}C'_ne^{-inpx} \\
&+2\mu_2D_0\{\sqrt{\sigma_2}h_1h_2(1+i\sqrt{\sigma_2}h_2\zeta\cos\delta)\sin\alpha\cos\delta+\zeta'(\sigma_2h_2^2-2h_1^2\sin^2\alpha)\} \\
&+2\mu_2\sum[\sqrt{\sigma_2}h_2(h_1\sin\alpha+np)(1+i\sqrt{\sigma_2}h_2\zeta\cos\delta_n)\cos\delta_n \\
&\quad+\zeta'\{\sigma_2h_2^2-2(h_1\sin\alpha+np)^2\}]D_ne^{inpx}
\end{aligned}
$$

$$+2\mu_2\sum[\sqrt{\sigma_2}h_2(h_1\sin\alpha-np)(1+i\sqrt{\sigma_2}h_2\zeta\cos\delta'_n)\cos\delta'_n$$
$$+\zeta'\{\sigma_2h_2^2-2(h_1\sin\alpha-np)^2\}]D'_ne^{-inpx} \tag{19}$$

$$h_1(a+A_0)\sin\alpha+ih_1\zeta(a-A_0)\sin\alpha\cos\alpha$$
$$+\sum\{(h_1\sin\alpha+np)(1-ih_1\zeta\cos\alpha_n)A_ne^{inpx}$$
$$+(h_1\sin\alpha-np)(1-ih_1\zeta\cos\alpha'_n)A'_ne^{-inpx}\}$$
$$+\sqrt{\sigma_1}h_1(b-B_0)\cos\beta+i\sigma_1h_1^2\zeta(b+B_0)\cos^2\beta$$
$$-\sqrt{\sigma_1}h_1\sum\{(1-i\sqrt{\sigma_1}h_1\zeta\cos\beta_n)B_ne^{inpx}\cos\beta_n$$
$$+(1-i\sqrt{\sigma_1}h_1\zeta\cos\beta'_n)B'_ne^{-inpx}\cos\beta'_n\}$$
$$=C_0h_1(1+ih_2\zeta\cos\gamma)\sin\alpha$$
$$+\sum\{(h_1\sin\alpha+np)(1+ih_2\zeta\cos\gamma_n)C_ne^{inpx}$$
$$+(h_1\sin\alpha-np)(1+ih_2\zeta\cos\gamma'_n)C'_ne^{-inpx}\}$$
$$+\sqrt{\sigma_2}h_2D_0(1+i\sqrt{\sigma_2}h_2\zeta\cos\delta)\cos\delta$$
$$+\sqrt{\sigma_2}h_2\sum\{D_ne^{inpx}(1+i\sqrt{\sigma_2}h_2\zeta\cos\delta_n)\cos\delta_n$$
$$+D'_ne^{-inpx}(1+i\sqrt{\sigma_2}h_2\zeta\cos\delta'_n)\cos\delta'_n\} \tag{20}$$

$$h_1(a-A_0)\cos\alpha+ih_1^2\zeta(a+A_0)\cos^2\alpha$$
$$-h_1\sum\{A_ne^{inpx}(1-ih_1\zeta\cos\alpha_n)\cos\alpha_n+A'_ne^{-inpx}(1-ih_1\zeta\cos\delta'_n)\cos\delta'_n\}$$
$$-h_1(b+B_0)\sin\alpha-ih_1^2\sqrt{\sigma_1}\zeta(b-B_0)\sin\alpha\cos\beta$$
$$-\sum[(h_1\sin\alpha+np)(1-i\sqrt{\sigma_1}h_1\zeta\cos\beta_n)B_ne^{inpx}$$
$$+(h_1\sin\alpha-np)(1-i\sqrt{\sigma_1}h_1\zeta\cos\beta'_n)B'_ne^{-inpx}]$$
$$=h_2C_0(1+ih_2\zeta\cos\gamma)\cos\gamma$$
$$+h_2\sum\{C_ne^{inpx}(1+ih_2\zeta\cos\gamma_n)\cos\gamma_n+C'_ne^{-inpx}(1+ih_2\zeta\cos\gamma'_n)\cos\gamma'_n\}$$
$$-h_1D_0(1+i\sqrt{\sigma_2}h_2\zeta\cos\delta)\sin\alpha$$
$$-\sum\{(h_1\sin\alpha+np)(1+i\sqrt{\sigma_2}h_2\zeta\cos\delta_n)D_ne^{inpx}$$
$$+(h_1\sin\alpha-np)(1+i\sqrt{\sigma_2}h_2\zeta\cos\delta'_n)D'_ne^{-inpx}\}\ . \tag{21}$$

From the above four equations we can obtain linear simultaneous equations determining the solutions of the second approximation for A_0, B_0, C_0 and D_0 by picking up the terms independent of x. They are as follows:

$$
\begin{aligned}
&-2\mu_1 h_1^2(a-A_0)\sin\alpha\cos\alpha-\mu_1 h_1^2(\sigma_1-2\sin^2\alpha)(b+B_0)\\
&\quad+2\mu_2 C_0 h_1 h_2\sin\alpha\cos\gamma+\mu_2 D_0(\sigma_2 h_2^2-2h_1^2\sin^2\alpha)\\
&=-2i\mu_1\zeta_{-n}A_n[np\{h_1^2-2(h_1\sin\alpha+np)^2\}-h_1^2(h_1\sin\alpha+np)\cos^2\alpha_n]\\
&\quad+2i\mu_1\zeta_n A'_n[np\{h_1^2-2(h_1\sin\alpha-np)^2\}+h_1^2(h_1\sin\alpha-np)\cos^2\alpha'_n]\\
&\quad-i\mu_1\sqrt{\sigma_1}h_1\zeta_{-n}B_n[4np(h_1\sin\alpha+np)+\{\sigma_1 h_1^2-2(h_1\sin\alpha+np)^2\}]\cos\beta_n\\
&\quad+i\mu_1\sqrt{\sigma_1}h_1\zeta_n B'_n[4np(h_1\sin\alpha-np)-\{\sigma_1 h_1^2-2(h_1\sin\alpha-np)^2\}]\cos\beta'_n\\
&\quad-2i\mu_2\zeta_{-n}C_n[-np\{h_2^2-2(h_1\sin\alpha+np)^2\}+h_2^2(h_1\sin\alpha+np)\cos^2\gamma_n]\\
&\quad-2i\mu_2\zeta_n C'_n[np\{h_2^2-2(h_1\sin\alpha-np)^2\}+h_2^2\cos^2\gamma'_n(h_1\sin\alpha-np)]\\
&\quad-i\mu_2\sqrt{\sigma_2}h_2\zeta_{-n}D_n[4np(h_1\sin\alpha+np)+\{\sigma_2 h_2^2-2(h_1\sin\alpha+np)^2\}]\cos\delta_n\\
&\quad+i\mu_2\sqrt{\sigma_2}h_2\zeta_n D'_n[4np(h_1\sin\alpha-np)-\{\sigma_2 h_2^2-2(h_1\sin\alpha-np)^2\}]\cos\delta'_n,
\end{aligned}
$$

$$
\begin{aligned}
&-h_1^2(\lambda_1+2\mu_1\cos^2\alpha)(a+A_0)+2\mu_1 h_1^2\sqrt{\sigma_1}(b-B_0)\sin\alpha\cos\beta\\
&\quad+C_0 h_2^2(\lambda_2+2\mu_2\cos^2\gamma)-2\mu_2\sqrt{\sigma_2}h_1 h_2 D_0\sin\alpha\cos\delta\\
&=-ih_1\zeta_{-n}A_n\{h_1^2(\lambda_1+2\mu_1\cos^2\alpha_n)+4\mu_1 np(h_1\sin\alpha+np)\}\cos\alpha_n\\
&\quad+ih_1\zeta_n A'_n\{-h_1^2(\lambda_1+2\mu_1\cos^2\alpha'_n)+4\mu_1 np(h_1\sin\alpha-np)\}\cos\alpha'_n\\
&\quad-2i\mu_1\zeta_{-n}B_n[\sigma_1 h_1^2(h_1\sin\alpha+np)\cos^2\beta_n-np\{\sigma_1 h_1^2-2(h_1\sin\alpha+np)^2\}]\\
&\quad-2i\mu_1\zeta_n B'_n[\sigma_1 h_1^2(h_1\sin\alpha-np)\cos^2\beta'_n+np\{\sigma_1 h_1^2-2(h_1\sin\alpha-np)^2\}]\\
&\quad-ih_2\zeta_{-n}C_n[h_2^2(\lambda_2+2\mu_2\cos^2\gamma_n)+4np\mu_2(h_1\sin\alpha+np)]\cos\gamma_n\\
&\quad-ih_2\zeta_n C'_n[h_2^2(\lambda_2+2\mu_2\cos^2\gamma'_n)-4np\mu_2(h_1\sin\alpha-np)]\cos\gamma'_n\\
&\quad+2i\mu_2\zeta_{-n}D_n[\sigma_2 h_2^2(h_1\sin\alpha+np)\cos^2\delta_n-np\{\sigma_2 h_2^2-2(h_1\sin\alpha+np)^2\}]\\
&\quad+2i\mu_2\zeta_n D'_n[\sigma_2 h_2^2(h_1\sin\alpha-np)\cos^2\delta'_n+np\{\sigma_2 h_2^2-2(h_1\sin\alpha-np)^2\}],
\end{aligned}
$$

$$
\begin{aligned}
&(a+A_0)h_1\sin\alpha+\sqrt{\sigma_1}h_1(b-B_0)\cos\beta-C_0 h_1\sin\alpha-\sqrt{\sigma_2}h_2 D_0\cos\delta\\
&=ih_1\zeta_{-n}A_n(h_1\sin\alpha+np)\cos\alpha_n+ih_1\zeta_n A'_n(h_1\sin\alpha-np)\cos\alpha'_n\\
&\quad-i\sigma_1 h_1^2\zeta_{-n}B_n\cos^2\beta_n-i\sigma_1 h_1^2\zeta_n B'_n\cos^2\beta'_n+ih_2\zeta_{-n}C_n(h_1\sin\alpha+np)\cos\gamma_n\\
&\quad+ih_2\zeta_n C'_n(h_1\sin\alpha-np)\cos\gamma'_n+i\sigma_2 h_2^2\zeta_{-n}D_n\cos^2\delta_n+i\sigma_2 h_2^2\zeta_n D'_n\cos^2\delta'_n,
\end{aligned}
$$

$$
\begin{aligned}
&(a-A_0)h_1\cos\alpha-(b+B_0)h_1\sin\alpha-h_2 C_0\cos\gamma+h_1 D_0\sin\alpha\\
&=-ih_1^2\zeta_{-n}A_n\cos^2\alpha_n-ih_1^2 A'_n\zeta_n\cos^2\alpha'_n-i\sqrt{\sigma_1}h_1\zeta_{-n}B_n(h_1\sin\alpha+np)\cos\beta_n\\
&\quad-i\sqrt{\sigma_1}h_1\zeta_n B'_n(h_1\sin\alpha-np)\cos\beta'_n+ih_2^2\zeta_{-n}C_n\cos^2\gamma_n+ih_2^2\zeta_n C'_n\cos^2\gamma'_n\\
&\quad-i\sqrt{\sigma_2}h_2\zeta_{-n}D_n(h_1\sin\alpha+np)\cos\delta_n-i\sqrt{\sigma_2}h_2\zeta_n D'_n(h_1\sin\alpha-np)\cos\delta'_n
\end{aligned}
$$

where for A_n, B_n, A'_n, B'_n, etc. those of the first approximation are used. Since A_n, A'_n, B_n, B'_n, etc. are of the order of ζ_n or ζ_{-n} as shown in the preceding section, A_0, B_0, C_0 and D_0 are of the order of ζ^2.

From the coefficients of e^{inpx} in (18) through (21) linear simultaneous equations determining A_n, B_n, C_n and D_n can be obtained as follows:

$$
\begin{aligned}
&-2i\mu_1 h_1^2\zeta_n(a+A_0)\{np(1-2\sin^2\alpha)+h_1\sin\alpha\cos^2\alpha\}\\
&\quad+2\mu_1[-\sum_{j\neq n} iA_j(n-j)p\zeta_{n-j}\{h_1^2-2(h_1\sin\alpha+jp)^2\}\\
&\qquad+h_1A_n(h_1\sin\alpha+np)\cos\alpha_n-\sum_{j\neq n} ih_1^2A_j\zeta_{n-j}(h_1\sin\alpha+jp)\cos^2\alpha_j]\\
&\quad-2i\mu_1\sum_{k=n+1}^{\infty} A'_{k-n}\zeta_k(kp[h_1^2-2\{h_1\sin\alpha-(k-n)p\}^2]\\
&\qquad+h_1^2\{h_1\sin\alpha-(k-n)p\}\cos^2\alpha'_{k-n})\\
&\quad+i\mu_1h_1^2\sqrt{\sigma_1}\zeta_n(b-B_0)\{4np\sin\alpha-h_1(\sigma_1-2\sin^2\alpha)\}\cos\beta\\
&\quad-\mu_1[4\sqrt{\sigma_1}h_1\sum_{j\neq n} i(n-j)pB_j\zeta_{n-j}(h_1\sin\alpha+jp)\cos\beta_j\\
&\qquad+\{\sigma_1h_1^2-2(h_1\sin\alpha+np)^2\}B_n\\
&\qquad-i\sqrt{\sigma_1}h_1\sum_{j\neq n}\zeta_{n-j}B_j\{\sigma_1h_1^2-2(h_1\sin\alpha+jp)^2\}\cos\beta_j]\\
&\quad-i\sqrt{\sigma_1}h_1\mu_1\sum_{k=n+1}^{\infty}(4kp\{h_1\sin\alpha-(k-n)p\}\\
&\qquad-[\sigma_1h_1^2-2\{h_1\sin\alpha-(k-n)p\}^2])\zeta_kB'_{k-n}\cos\beta'_{k-n}\\
&=-2i\zeta_n\mu_2C_0\{(h_2^2-2h_1^2\sin^2\alpha)np+h_1h_2^2\sin\alpha\cos^2\gamma\}\\
&\qquad+i\mu_2D_0\zeta_n\sqrt{\sigma_2}h_2\{4nph_1\sin\alpha-(\sigma_2h_2^2-2h_1^2\sin^2\alpha)\}\cos\delta\\
&\quad-2\mu_2[\sum_{j\neq n} i(n-j)pC_j\zeta_{n-j}\{h_2^2-2(h_1\sin\alpha+jp)^2\}+C_n(h_1\sin\alpha+np)h_2\cos\gamma_n\\
&\qquad+\sum_{j\neq n} ih_2^2C_j\zeta_{n-j}(h_1\sin\alpha+jp)\cos^2\gamma_j]\\
&\quad-2i\mu_2\sum_{k=n+1}^{\infty}\zeta_kC'_{k-n}[kp\{h_2^2-2(h_1\sin\alpha-(k-n)p)^2\}\\
&\qquad+h_2^2\{h_1\sin\alpha-(k-n)p\}\cos^2\gamma'_{k-n}]\\
&\quad+\mu_2[4\sqrt{\sigma_2}h_2\sum_{j\neq n} ip\zeta_{n-j}D_j(h_1\sin\alpha+jp)(n-j)\cos\delta_j\\
&\qquad-\{\sigma_2h_2^2-2(h_1\sin\alpha+np)^2\}D_n\\
&\qquad-i\sqrt{\sigma_2}h_2\sum_{j\neq n}\zeta_{n-j}D_j\{\sigma_2h_2^2-2(h_1\sin\alpha+jp)^2\}\cos\delta_j]\\
&\quad+i\mu_2\sqrt{\sigma_2}h_2\sum_{k=n+1}^{\infty}D'_{k-n}\zeta_k(4kp\{h_1\sin\alpha-(k-n)p\}\\
&\qquad-[\sigma_2h_2^2-2\{h_1\sin\alpha-(k-n)p\}^2])\cos\delta'_{k-n}\ ,
\end{aligned}
$$

$$
\begin{aligned}
&-ih_1^2\zeta_n(a-A_0)\{h_1(\lambda_1+2\mu_1\cos^2\alpha)-4\mu_1 np\sin\alpha\}\cos\alpha\\
&\quad+2i\mu_1h_1^2\zeta_n\{np(\sigma_1-2\sin^2\alpha)+\sigma_1h_1\sin\alpha\cos^2\beta\}(b+B_0)\\
&\quad-h_1[h_1A_n(\lambda_1+2\mu_1\cos^2\alpha_n)-\sum_{j\neq n}ih_1^2\zeta_{n-j}A_j(\lambda_1+2\mu_1\cos^2\alpha_j)\cos\alpha_j\\
&\qquad+\sum_{j\neq n}4i\mu_1pA_j\zeta_{n-j}(n-j)(h_1\sin\alpha+jp)\cos\alpha_j]\\
&\quad+h_1\sum_{k=n+1}^{\infty}i\zeta_kA'_{k-n}[h_1^2(\lambda_1+2\mu_1\cos^2\alpha'_{k-n})\\
&\qquad-4kp\mu_1\{h_1\sin\alpha-(k-n)p\}]\cos\alpha'_{k-n}\\
&\quad+2\mu_1[-\sqrt{\sigma_1}h_1B_n(h_1\sin\alpha+np)\cos\beta_n\\
&\qquad+\sum_{j\neq n}i\sigma_1h_1^2\zeta_{n-j}B_j(h_1\sin\alpha+jp)\cos^2\beta_j\\
&\qquad+\sum_{j\neq n}ip\zeta_{n-j}B_j(n-j)\{\sigma_1h_1^2-2(h_1\sin\alpha+jp)^2\}]\\
&\quad+2i\mu_1\sum_{k=n+1}^{\infty}B'_{k-n}\zeta_k(\sigma_1h_1^2\{h_1\sin\alpha-(k-n)p\}\cos^2\beta'_{k-n}\\
&\qquad+kp[\sigma_1h_1^2-2\{h_1\sin\alpha-(k-n)p\}^2])\\
&=ih_2\zeta_nC_0\{-h_2^2(\lambda_2+2\mu_2\cos^2\gamma)+4np\mu_2h_1\sin\alpha\}\cos\gamma\\
&\qquad+2i\mu_2D_0\zeta_n\{\sigma_2h_1h_2^2\sin\alpha\cos^2\delta+np(\sigma_2h_2^2-2h_1^2\sin^2\alpha)\}\\
&\quad-[h_2^2C_n(\lambda_2+2\mu_2\cos^2\gamma_n)+\sum_{j\neq n}ih_2^2C_j\zeta_{n-j}(\lambda_2+2\mu_2\cos^2\gamma_j)\cos\gamma_j\\
&\qquad-\sum_{j\neq n}4i\mu_2h_2pC_j\zeta_{n-j}(n-j)(h_1\sin\alpha+jp)\cos\gamma_j]\\
&\quad-\sum_{k=n+1}^{\infty}ih_2\zeta_kC'_{k-n}[h_2^2(\lambda_2+2\mu_2\cos^2\gamma'_{k-n})-4\mu_2kp\{h_1\sin\alpha-(k-n)p\}]\cos\gamma'_{k-n}\\
&\quad+2\mu_2[\sqrt{\sigma_2}h_2D_n(h_1\sin\alpha+np)\cos\delta_n+\sum_{j\neq n}i\sigma_2h_2^2D_j\zeta_{n-j}(h_1\sin\alpha+jp)\cos^2\delta_j\\
&\qquad+\sum_{j\neq n}ipD_j\zeta_{n-j}(n-j)\{\sigma_2h_2^2-2(h_1\sin\alpha+jp)^2\}]\\
&\quad+2\mu_2\sum_{k=n+1}^{\infty}i\zeta_kD'_{k-n}(\sigma_2h_2^2\{h_1\sin\alpha-(k-n)p\}\cos^2\delta'_{k-n}\\
&\qquad+kp[\sigma_2h_2^2-2\{h_1\sin\alpha-(k-n)p\}^2]),
\end{aligned}
$$

$$
\begin{aligned}
&ih_1^2\zeta_n(a-A_0)\sin\alpha\cos\alpha+A_n(h_1\sin\alpha+np)-\sum_{j\neq n}ih_1A_j\zeta_{n-j}(h_1\sin\alpha+jp)\cos\alpha_j\\
&\quad-\sum_{k=n+1}^{\infty}ih_1\zeta_kA'_{k-n}\{h_1\sin\alpha-(k-n)p\}\cos\alpha'_{k-n}+i\sigma_1h_1^2\zeta_n(b+B_0)\cos^2\beta\\
&\quad-\sqrt{\sigma_1}h_1[B_n\cos\beta_n-i\sqrt{\sigma_1}h_1\sum_{j\neq n}\zeta_{n-j}B_j\cos^2\beta_j]+i\sigma_1h_1^2\sum_{k=n+1}^{\infty}\zeta_kB'_{k-n}\cos^2\beta'_{k-n}\\
&=iC_0h_1h_2\zeta_n\sin\alpha\cos\gamma+C_n(h_1\sin\alpha+np)+ih_2\sum_{j\neq n}\zeta_{n-j}C_j(h_1\sin\alpha+jp)\cos\gamma_j
\end{aligned}
$$

$$+\sum_{k=n+1}^{\infty} ih_2\zeta_k C'_{k-n}\{h_1\sin\alpha-(k-n)p\}\cos\gamma'_{k-n}+i\sigma_2 h_2^2 D_0\zeta_n\cos^2\delta$$

$$+\sqrt{\sigma_2}h_2[D_n\cos\delta_n+\sum_{j\neq n} i\sqrt{\sigma_2}h_2 D_j\zeta_{n-j}\cos^2\delta_j]+\sum_{k=n+1}^{\infty} i\sigma_2 h_2^2 D'_{k-n}\zeta_k\cos^2\delta'_j\ ,$$

$$(a+A_0)ih_1^2\zeta_n\cos^2\alpha-h_1\{A_n\cos\alpha_n-ih_1\sum_{j\neq n}A_j\zeta_{n-j}\cos^2\alpha_j\}$$

$$+ih_1^2\sum_{k=n+1}^{\infty}A'_{k-n}\zeta_k\cos^2\alpha'_{k-n}-(b-B_0)i\sqrt{\sigma_1}h_1^2\zeta_n\sin\alpha\cos\beta$$

$$-(h_1\sin\alpha+np)B_n+i\sqrt{\sigma_1}h_1\sum_{j\neq n}\zeta_{n-j}B_j(h_1\sin\alpha+jp)\cos\beta_j$$

$$+i\sqrt{\sigma_1}h_1\sum_{k=n+1}^{\infty}B'_{k-n}\zeta_k\{h_1\sin\alpha-(k-n)p\}\cos\beta'_{k-n}$$

$$=ih_2^2C_0\zeta_n\cos^2\gamma+h_2\{C_n\cos\gamma_n+ih_2\sum_{j\neq n}C_j\zeta_{n-j}\cos^2\gamma_j\}$$

$$+ih_2^2\sum_{k=n+1}^{\infty}C'_{k-n}\zeta_k\cos^2\gamma'_{k-n}-i\sqrt{\sigma_2}h_1h_2D_0\zeta_n\sin\alpha\cos\delta$$

$$-(h_1\sin\alpha+np)D_n-i\sqrt{\sigma_2}h_2\sum_{j\neq n}D_j\zeta_{n-j}(h_1\sin\alpha+jp)\cos\delta_j$$

$$-i\sqrt{\sigma_2}h_2\sum_{k=n+1}^{\infty}D'_{k-n}\zeta_k\{h_1\sin\alpha-(k-n)p\}\cos\delta'_{k-n}$$

From the coefficients of e^{-inpx} in (18) through (21), the following equations to determine A'_n, B'_n, C'_n and D'_n of the second approximation are obtained.

$$-2i\mu_1h_1^2\zeta_{-n}(a+A_0)\{-np(1-2\sin^2\alpha)+h_1\sin\alpha\cos^2\alpha\}$$

$$+2i\mu_1\sum_{k=n+1}^{\infty}\zeta_{-k}A_{k-n}(kp[h_1^2-2\{h_1\sin\alpha+(k-n)p\}^2]$$

$$-h_1^2\{h_1\sin\alpha+(k-n)p\}\cos^2\alpha_{k-n})$$

$$+2\mu_1[i\sum_{j\neq n}(n-j)p\zeta_{j-n}A'_j\{h_1^2-2(h_1\sin\alpha-jp)^2\}$$

$$+h_1A'_n(h_1\sin\alpha-np)\cos\alpha'_n-i\sum_{j\neq n}h_1^2\zeta_{j-n}A'_j(h_1\sin\alpha-jp)\cos^2\alpha'_j]$$

$$-i\mu_1\sqrt{\sigma_1}h_1^2\zeta_{-n}(b-B_0)\{4np\sin\alpha+h_1(\sigma_1-2\sin^2\alpha)\}\cos\beta$$

$$+i\mu_1\sqrt{\sigma_1}h_1\sum_{k=n+1}^{\infty}\zeta_{-k}B_{k-n}[4kp\{h_1\sin\alpha+(k-n)p\}$$

$$+(\sigma_1h_1^2-2\{h_1\sin\alpha+(k-n)p\}^2)]\cos\beta_{k-n}$$

$$-\mu_1[4\sqrt{\sigma_1}h_1\sum_{j\neq n}i(j-n)p\zeta_{j-n}B'_j(h_1\sin\alpha-jp)\cos\beta'_j$$

$$+\{\sigma_1h_1^2-2(h_1\sin\alpha-np)^2\}B'_n$$

$$-i\sqrt{\sigma_1}h_1\sum_{j\neq n}\{\sigma_1h_1^2-2(h_1\sin\alpha-jp)^2\}\zeta_{j-n}B'_j\cos\beta'_j]$$

$$
\begin{aligned}
&=-2i\mu_2\zeta_{-n}C_0\{-np(h_2^2-2h_1^2\sin^2\alpha)+h_1h_2^2\sin\alpha\cos^2\gamma\}\\
&\quad-i\mu_2\sqrt{\sigma_2}\,h_2\zeta_{-n}D_0\{4nph_1\sin\alpha+\sigma_2h_2^2-2h_1^2\sin^2\alpha\}\cos\delta\\
&\quad-2i\mu_2\sum_{k=n+1}^{\infty}\zeta_{-k}C_{k-n}(-[h_2^2-2\{h_1\sin\alpha+(k-n)p\}^2]kp\\
&\qquad+h_2^2\{h_1\sin\alpha+(k-n)p\}\cos^2\gamma_{k-n})\\
&\quad-2\mu_2[\sum_{j\neq n}ip\zeta_{j-n}C_j'(j-n)\{h_2^2-2(h_1\sin\alpha-jp)^2\}\\
&\qquad+(h_1\sin\alpha-np)h_2C_n'\cos\gamma_n'+\sum_{j\neq n}ih_2^2C_j'\zeta_{j-n}(h_1\sin\alpha-jp)\cos^2\gamma_j']\\
&\quad-i\mu_2\sqrt{\sigma_2}\,h_2\sum_{k=n+1}^{\infty}D_{k-n}\zeta_{-k}(4kp\{h_1\sin\alpha+(k-n)p\}\\
&\qquad+[\sigma_2h_2^2-2\{h_1\sin\alpha+(k-n)p\}^2]\cos\delta_{k-n})\\
&\quad+\mu_2[\sum_{j\neq n}4i\sqrt{\sigma_2}\,h_2p\zeta_{j-n}D_j'(j-n)(h_1\sin\alpha-jp)\cos\delta_j'\\
&\qquad-\{\sigma_2h_2^2-2(h_1\sin\alpha-np)^2\}D_n'\\
&\qquad-\sum_{j\neq n}i\sqrt{\sigma_2}\,h_2D_j'\zeta_{j-n}\{\sigma_2h_2^2-2(h_1\sin\alpha-jp)^2\}\cos\delta_j'],\\
&-ih_1^2\zeta_{-n}(a-A_0)\{h_1(\lambda_1+2\mu_1\cos^2\alpha)+4\mu_1np\sin\alpha\}\cos\alpha\\
&\quad+2i\mu_1h_1^2\zeta_{-n}(b+B_0)\{-np(\sigma_1-2\sin^2\alpha)+\sigma_1h_1\sin\alpha\cos^2\beta\}\\
&\quad+ih_1\sum_{k=n+1}^{\infty}\zeta_{-k}A_{k-n}[(\lambda_1+2\mu_1\cos^2\alpha_{k-n})+4\mu_1kp\{h_1\sin\alpha+(k-n)p\}]\cos\alpha_{k-n}\\
&\quad-h_1[h_1A_n'(\lambda_1+2\mu_1\cos^2\alpha_n')-\sum_{j\neq n}ih_1^2\zeta_{j-n}A_j'(\lambda_1+2\mu_1\cos^2\alpha_j')\cos\alpha_j'\\
&\qquad-\sum_{j\neq n}4i\mu_1p\zeta_{j-n}A_j'(n-j)(h_1\sin\alpha-jp)\cos\alpha_j']\\
&\quad+2\mu_1\sum_{k=n+1}^{\infty}i\zeta_{-k}B_{k-n}(\sigma_1h_1^2\{h_1\sin\alpha+(k-n)p\}\cos^2\beta_{k-n}\\
&\qquad-kp[\sigma_1h_1^2-2\{h_1\sin\alpha+(k-n)p\}^2])\\
&\quad+2\mu_1[-\sqrt{\sigma_1}\,h_1B_n'(h_1\sin\alpha-np)\cos\beta_n'\\
&\qquad+\sum_{j\neq n}i\sigma_1h_1^2\zeta_{j-n}B_j'(h_1\sin\alpha-jp)\cos^2\beta_j'\\
&\qquad-\sum_{j\neq n}ip\zeta_{j-n}B_j'(n-j)\{\sigma_1h_1^2-2(h_1\sin\alpha-jp)^2\}]\\
&=-ih_2C_0\zeta_{-n}\{h_2^2(\lambda_2+2\mu_2\cos^2\gamma)+4np\mu_2h_1\sin\alpha\}\cos\gamma\\
&\quad+2i\mu_2\zeta_{-n}D_0\{\sigma_2h_1h_2^2\sin\alpha\cos^2\delta-np(\sigma_2h_2^2-2h_1^2\sin^2\alpha)\}\\
&\quad-\sum_{k=n+1}^{\infty}ih_2\zeta_{-k}C_{k-n}[h_2^2(\lambda_2+2\mu_2\cos^2\gamma_{k-n})+4\mu_2kp\{h_1\sin\alpha+(k-n)p\}]\cos\gamma_{k-n}\\
&\quad-[h_2^2C_n'(\lambda_2+2\mu_2\cos^2\gamma_n')+\sum_{j\neq n}ih_2^2\zeta_{j-n}C_j'(\lambda_2+2\mu_2\cos^2\gamma_j')\cos\gamma_j'
\end{aligned}
$$

$$+\sum_{j\neq n} 4ip\mu_2 h_2\zeta_{j-n}C'_j(n-j)(h_1\sin\alpha-jp)\cos\gamma'_j]$$

$$+2i\mu_2\sum_{k=n+1}^{\infty}\zeta_{-k}D_{k-n}(\sigma_2h_2^2\{h_1\sin\alpha+(k-n)p\}\cos^2\delta_{k-n}$$

$$-kp[\sigma_2h_2^2-2\{h_1\sin\alpha+(k-n)p\}^2])$$

$$+2\mu_2[\sqrt{\sigma_2}h_2D'_n(h_1\sin\alpha-np)\cos\delta'_n+\sum_{j\neq n} i\sigma_2h_2^2\zeta_{j-n}D'_j(h_1\sin\alpha-jp)\cos^2\delta'_j$$

$$-\sum_{j\neq n} ip\zeta_{j-n}D'_j(n-j)\{\sigma_2h_2^2-2(h_1\sin\alpha-jp)^2\}],$$

$$ih_1^2\zeta_{-n}(a-A_0)\sin\alpha\cos\alpha-\sum_{k=n+1}^{\infty} ih_1\zeta_{-k}A_{k-n}\{h_1\sin\alpha+(k-n)p\}\cos\alpha_j$$

$$+A'_n(h_1\sin\alpha-np)-\sum_{j\neq n} ih_1(h_1\sin\alpha-jp)\zeta_{j-n}A'_j\cos\alpha'_j$$

$$+i\sigma_1h_1\zeta_{-n}(b+B_0)\cos^2\beta+i\sigma_1h_1^2\sum_{k=n+1}^{\infty}\zeta_{-k}B_{k-n}\cos^2\beta_{k-n}$$

$$-\sqrt{\sigma_1}h_1[B'_n\cos\beta'_n-i\sqrt{\sigma_1}h_1\sum_{j\neq n}\zeta_{j-n}B'_j\cos^2\beta'_j]$$

$$=ih_1h_2C_0\zeta_{-n}\sin\alpha\cos\gamma+\sum_{k=n+1}^{\infty} ih_2C_{k-n}\zeta_{-k}\{h_1\sin\alpha+(k-n)p\}\cos\gamma_{k-n}$$

$$+(h_1\sin\alpha-np)C'_n+\sum_{j\neq n} ih_2\zeta_{j-n}C'_j(h_1\sin\alpha-jp)\cos\gamma'_j+i\sigma_2h_2^2D_0\zeta_{-n}\cos^2\delta$$

$$+i\sigma_2h_2^2\sum_{k=n+1}^{\infty}D_{k-n}\zeta_{-k}\cos^2\delta_{k-n}$$

$$+\sqrt{\sigma_2}h_2[D'_n\cos\delta'_n+i\sqrt{\sigma_2}h_2\sum_{j\neq n}D'_j\zeta_{j-n}\cos^2\delta'_j],$$

$$(a+A_0)ih_1^2\zeta_{-n}\cos^2\alpha+ih_1^2\sum_{k=n+1}^{\infty}A_{k-n}\zeta_{-k}\cos^2\alpha_{k-n}$$

$$-h_1\{A'_n\cos\alpha'_n-ih_1\sum_{j\neq n}A'_j\zeta_{j-n}\cos^2\alpha'_j\}-i\sqrt{\sigma_1}h_1^2\zeta_{-n}(b-B_0)\sin\alpha\cos\beta$$

$$+i\sqrt{\sigma_1}h_1\sum_{k=n+1}^{\infty}\zeta_{-k}B_{k-n}\{h_1\sin\alpha+(k-n)p\}\cos\beta_{k-n}$$

$$-(h_1\sin\alpha-np)B'_n+i\sqrt{\sigma_1}h_1\sum_{j\neq n}\zeta_{j-n}B'_j(h_1\sin\alpha-jp)\cos\beta'_j$$

$$=ih_2^2\zeta_{-n}C_0\cos^2\gamma+ih_2^2\sum_{k=n+1}^{\infty}C_{k-n}\zeta_{-k}\cos^2\gamma_{k-n}$$

$$+h_2\{C'_n\cos\gamma'_n+ih_2\sum_{j\neq n}C'_j\zeta_{j-n}\cos^2\gamma'_j\}-ih_1\sqrt{\sigma_2}h_2D_0\zeta_{-n}\sin\alpha\cos\delta$$

$$-i\sqrt{\sigma_2}h_2\sum_{k=n+1}^{\infty}D_{k-n}\zeta_{-k}\{h_1\sin\alpha+(k-n)p\}\cos\delta_{k-n}$$

$$-(h_1\sin\alpha-np)D'_n-i\sqrt{\sigma_2}h_2\sum_{j\neq n}D'_j\zeta_{j-n}(h_1\sin\alpha-jp)\cos\delta'_j.$$

In these formulae for A_n, B_n, A'_n, B'_n, etc. the values of the first ap-

proximation are used for A_0, B_0, A_j, B_j, etc. As they are of the order of ζ, A_n, B_n, A'_n, B'_n, etc. are of the order of ζ^2.

§ 5. The Case of Normal Incidence on the Mean Surface of the Boundary $\zeta=c\cos px$

As in the incident SH wave, the case of normal incidence on the harmonic boundary surface given by the equation $\zeta=c\cos px$ was calculated. In this case, $\zeta_n=\zeta_{-n}=0$ $(n\neq 1)$, $\zeta_1=\zeta_{-1}=c/2$, $\alpha=\beta=\gamma=\delta=0$, $\sin\alpha_n=np/h_1$, $\sin\alpha'_n=-np/h_1$, $\sin\beta_n=np/\sqrt{\sigma_1}h_1$, $\sin\beta'_n=-np/\sqrt{\sigma_1}h_1$, $\cos\alpha_n=\cos\alpha'_n$, $\cos\beta_n=\cos\beta'_n$, etc.

§ 5.1. The Case of Incidence of the P Wave

In this case, we get the following linear equations from which the solutions of the first approximation for A_0, B_0, C_0 and D_0 are obtained.

$$-\mu_1\sigma_1h_1^2B_0+\mu_2\sigma_2h_2^2D_0=0\ ,$$

$$-h_1^2A_0(\lambda_1+2\mu_1)+h_2^2C_0(\lambda_2+2\mu_2)=h_1^2(\lambda_1+2\mu_1)\ ,$$

$$\sqrt{\sigma_1}h_1B_0+\sqrt{\sigma_2}h_2D_0=0\ ,\qquad h_1A_0+h_2C_0=h_1\ .$$

Therefore, $B_0=D_0=0$,

$$A_0=\{h_2(\lambda_2+2\mu_2)-h_1(\lambda_1+2\mu_1)\}/\{h_2(\lambda_2+2\mu_2)+h_1(\lambda_1+2\mu_1)\}\ ,$$

$$C_0=2h_1^2(2\mu_1+\lambda_1)/[h_2\{h_1(\lambda_1+2\mu_1)+h_2(\lambda_2+2\mu_2)\}]\ ,$$

as far as the solutions of the first approximation are concerned.

With regard to the solutions of the first approximation for A_1, B_1, C_1 and D_1, the following linear equations are obtained.

$$\begin{aligned}&2\mu_1h_1pA_1\cos\alpha_1-\mu_1B_1(\sigma_1h_1^2-2p^2)+2\mu_2ph_2C_1\cos\gamma_1+\mu_2D_1(\sigma_2h_2^2-2p^2)\\&\quad=2i\mu_1h_1^2p\zeta(1+A_0)-2i\mu_2h_2^2p\zeta_1C_0\ ,\\&-h_1^2A_1(\lambda_1+2\mu_1\cos^2\alpha_1)-2\mu_1\sqrt{\sigma_1}h_1pB_1\cos\beta_1\\&\quad+h_2^2C_1(\lambda_2+2\mu_2\cos^2\gamma_1)-2\mu_2\sqrt{\sigma_2}h_2pD_1\cos\delta_1\\&\quad=ih_1^3\zeta_1(\lambda_1+2\mu_1)(1-A_0)-iC_0h_2^3\zeta_1(\lambda_2+2\mu_2)\ ,\\&pA_1-\sqrt{\sigma_1}h_1B_1\cos\beta_1-pC_1-\sqrt{\sigma_2}h_2D_1\cos\delta_1=0\ ,\\&-h_1A_1\cos\alpha_1-pB_1-h_2C_1\cos\gamma_1+pD_1=-ih_1^2\zeta_1(1+A_0)+ih_2^2\zeta_1C_0\ .\end{aligned}$$

We see that the right hand side of the first equation becomes zero by using A_0 and C_0 of the first approximation obtained above.

If this set of linear equations is written in the following form,

$$\begin{aligned}
a_{11}A_1-a_{12}B_1+a_{13}C_1+a_{14}D_1&=0\ ,\\
-a_{21}A_1-a_{22}B_1+a_{23}C_1-a_{24}D_1&=l_2\ ,\\
a_{31}A_1-a_{32}B_1-a_{33}C_1-a_{34}D_1&=0\ ,\\
-a_{41}A_1-a_{42}B_1-a_{43}C_1+a_{44}D_1&=l_4\ ,
\end{aligned}$$

the simultaneous linear equations giving the solutions of the first approximation for A_1', B_1', etc. have the following forms:

$$\begin{aligned}
-a_{11}A_1'-a_{12}B_1'-a_{13}C_1'+a_{14}D_1'&=0\ ,\\
-a_{21}A_1'+a_{22}B_1'+a_{23}C_1'+a_{24}D_1'&=l_2\ ,\\
-a_{31}A_1'-a_{32}B_1'+a_{33}C_1'-a_{34}D_1'&=0\ ,\\
-a_{41}A_1'+a_{42}B_1'-a_{43}C_1'-a_{44}D_1'&=l_4\ .
\end{aligned}$$

By a simple transformation of a set of determinants of the coefficients in the latter equations, the following relations between A_1, B_1, etc. and A_1', B_1', etc. can be obtained.

$$A_1=A_1'\ ,\qquad C_1=C_1'\ ,\qquad B_1=-B_1'\ ,\qquad D_1=-D_1'\ .$$

Since the case of normal incidence is under consideration, these relations are very reasonable and simplify the problem.

For A_0, B_0, etc. of the second approximation by using the relations above obtained, $A_1=A_1'$, $B_1=-B_1'$, etc., we have

$$\begin{aligned}
&-3\mu_1h_1^2A_0+3\mu_2h_2^2C_0\\
&\quad=3\mu_1h_1-2i\mu_1h_1\zeta_1A_1(3h_1^2+2p^2)\cos\alpha_1-4i\mu_1\zeta_1B_1p^3\\
&\qquad-2i\mu_2h_2\zeta_1C_1(3h_2^2+2p^2)\cos\gamma_1+4i\mu_2\zeta_1D_1p^3\ ,\\
&-h_1A_0-h_2C_0=-h_1-2i\zeta_1A_1(h_1^2-p^2)-2i\sqrt{\sigma_1}\zeta_1B_1p\cos\beta_1\\
&\qquad+2i\zeta_1C_1(h_2^2-p^2)-2i\sqrt{\sigma_2}h_2\zeta_1D_1p\cos\delta_1\ ,\\
&-\mu_1\sigma_1h_1^2B_0+\mu_2\sigma_2h_2^2D_0=0\ ,\\
&-\sqrt{\sigma_1}h_1B_0-\sqrt{\sigma_2}h_2D_0=0\ .
\end{aligned}$$

From the last two equations, $B_0=D_0=0$.

With respect to A_1, B_1, etc. of the second approximation, the magnitude of the correction term to those of the first approximation is of the order of ζ^3. Thus as far as the present approximations are concerned, A_1, B_1, etc. of the second approximation are the same as those of the first approximation.

In the second approximation, A_2, B_2, etc. must be taken into consideration and A_n, B_n, etc. $(n>2)$ are quantities of an order higher than ζ^3. Linear equations for A_2, B_2, etc. are as follows:

$$\begin{aligned}
&4\mu_1 pA_2h_1\cos\alpha_2-\mu_1B_2(\sigma_1h_1^2-8p^2)+4\mu_2pC_2h_2\cos\gamma_2+\mu_2D_2(\sigma_2h_2^2-8p^2)\\
&\quad=2i\mu_1pA_1\zeta_1(2h_1^2-3p^2)+3i\mu_1\zeta_1B_1\sqrt{\sigma_1}h_1(2p^2-h_1^2)\cos\beta_1\\
&\qquad-2i\mu_2pC_1\zeta_1(2h_2^2-3p^2)+3i\mu_2\zeta_1D_1\sqrt{\sigma_2}h_2(2p^2-h_2^2)\cos\delta_1\ ,\\
&-\mu_1h_1^2A_1(1+2\cos^2\alpha_2)-4\mu_1\sqrt{\sigma_1}h_1B_2p\cos\beta_2\\
&\qquad+\mu_2h_2^2C_2(1+2\cos^2\gamma_2)-4\mu_2\sqrt{\sigma_2}h_2pD_2\cos\delta_2\\
&\quad=-3i\mu_1h_1\zeta_1A_1(h_1^2-2p^2)\cos\alpha_1-6i\mu_1p\zeta_1B_1(2h_1^2-p^2)\\
&\qquad-3i\mu_2h_2\zeta_1C_1(h_2^2-2p^2)\cos\gamma_1-6i\mu_2p\zeta_1D_1(2h_2^2-p^2)\ ,\\
&2pA_2-\sqrt{\sigma_1}h_1B_2\cos\beta_2-2pC_2-\sqrt{\sigma_2}h_2D_2\cos\delta_2\\
&\quad=ih_1\zeta_1A_1p\cos\alpha_1-i\sigma_1h_1^2\zeta_1B_1\cos^2\beta_1+ih_2\zeta_1C_1p\cos\gamma_1+i\sigma_2h_2^2\zeta_1D_1\cos^2\delta_1\ ,\\
&-h_1A_2\cos\alpha_2-2pB_2-h_2C_2\cos\gamma_2+2pD_2\\
&\quad=-ih_1^2A_1\zeta_1\cos^2\alpha_1-i\sqrt{\sigma_1}h_1\zeta_1B_1p\cos\beta_1\\
&\qquad+ih_2^2C_1\zeta_1\cos^2\gamma_1-i\sqrt{\sigma_2}h_2\zeta_1D_1p\cos\delta_1\ .
\end{aligned}$$

Through the same procedure as already adopted, having obtained the relations $A_1=A_1'$, $B_1=-B_1'$, etc., it is proved readily that the relations $A_2=A_2'$, $B_2=-B_2'$, $C_2=C_2'$ and $D_2=-D_2'$ hold as in A_1, B_1, A_1', B_1', etc.

The numerical constants necessary for the calculations are assumed as follows:

$$V_{p1}/V_{p2}=V_{s1}/V_{s2}=6/8\ ,\qquad \mu_2/\mu_1=2\ ,$$

on Poisson's hypothesis $\lambda_i=\mu_i$.

The formulae are expressed in terms of L/L_{p1}, that is, the ratio of the wave length of corrugation to that of the incident wave, and differ slightly from each other according to the intervals of L/L_{p1}. As an example these formulae for A_1, B_1, etc. are given in the following.

(i) $L/L_{p1}\geq 4/3$

In this range, A_1, B_1, etc. are purely imaginary numbers.

$$2A_1\sqrt{(L/L_{p1})^2-1}-B_1\{3(L/L_{p1})^2-2\}+2C_1(\mu_2/\mu_1)\sqrt{(h_2/h_1)^2(L/L_{p1})^2-1}$$
$$-D_1(\mu_2/\mu_1)\{2-3(h_2/h_1)^2(L/L_{p1})^2\}=0\ ,$$

$$-\{3(L/L_{p1})^2-2\}A_1-2B_1\sqrt{3(L/L_{p1})^2-1}+C_1(\mu_2/\mu_1)\{3(h_2/h_1)^2(L/L_{p1})^2-2\}$$
$$-2D_1(\mu_2/\mu_1)\sqrt{3(h_2/h_1)^2(L/L_{p1})^2-1}$$
$$=3\pi i(c/L_{p1})(L/L_{p1})^2\{1-A_0-C_0(\mu_2/\mu_1)(h_2/h_1)^3\}\ ,$$

$$A_1-B_1\sqrt{3(L/L_{p1})^2-1}-C_1-D_1\sqrt{3(h_2/h_1)^2(L/L_{p1})^2-1}=0\ ,$$

$$-A_1\sqrt{(L/L_{p1})^2-1}-B_1-C_1\sqrt{(h_2/h_1)^2(L/L_{p1})^2-1}+D_1$$
$$=-i\pi(c/L_{p1})(L/L_{p1})\{1+A_0-(h_2/h_1)^2C_0\}\ .$$

For L/L_{p1} smaller than 4/3, A_1, B_1, etc. are complex numbers and A_1 is written as $A_1=RA_1+iIA_1$ and so forth.

(ii) $4/3>L/L_{p1}\geq 1$

$$2RA_1\sqrt{(L/L_{p1})^2-1}-RB_1\{3(L/L_{p1})^2-2\}+2IC_1(\mu_2/\mu_1)\sqrt{1-(h_2/h_1)^2(L/L_{p1})^2}$$
$$-RD_1(\mu_2/\mu_1)\{2-3(h_2/h_1)^2(L/L_{p1})^2\}=0\ ,$$

$$2IA_1\sqrt{(L/L_{p1})^2-1}-IB_1\{3(L/L_{p1})^2-2\}-2RC_1(\mu_2/\mu_1)\sqrt{1-(h_2/h_1)^2(L/L_{p1})^2}$$
$$-ID_1(\mu_2/\mu_1)\{2-3(h_2/h_1)^2(L/L_{p1})^2\}=0\ ,$$

$$-\{3(L/L_{p1})^2-2\}RA_1-2RB_1\sqrt{3(L/L_{p1})^2-1}$$
$$+RC_1(\mu_2/\mu_1)\{3(h_2/h_1)^2(L/L_{p1})^2-2\}$$
$$-2RD_1(\mu_2/\mu_1)\sqrt{3(h_2/h_1)^2(L/L_{p1})^2-1}=0\ ,$$

$$-\{3(L/L_{p1})^2-2\}IA_1-2IB_1\sqrt{3(L/L_{p1})^2-1}$$
$$+IC_1(\mu_2/\mu_1)\{3(h_2/h_1)^2(L/L_{p1})^2-2\}$$
$$-2ID_1(\mu_2/\mu_1)\sqrt{3(h_2/h_1)^2(L/L_{p1})^2-1}$$
$$=3\pi(c/L_{p1})(L/L_{p1})^2\{1-A_0-C_0(\mu_2/\mu_1)(h_2/h_1)^3\}\ ,$$

$$RA_1-RB_1\sqrt{3(L/L_{p1})^2-1}-RC_1-RD_1\sqrt{3(h_2/h_1)^2(L/L_{p1})^2-1}=0\ ,$$

$$IA_1-IB_1\sqrt{3(L/L_{p1})^2-1}-IC_1-ID_1\sqrt{3(h_2/h_1)^2(L/L_{p1})^2-1}=0\ ,$$

$$-RA_1\sqrt{(L/L_{p1})^2-1}-RB_1-IC_1\sqrt{1-(h_2/h_1)^2(L/L_{p1})^2}+RD_1=0\ ,$$

$$-IA_1\sqrt{(L/L_{p1})^2-1}-IB_1+RC_1\sqrt{1-(h_2/h_1)^2(L/L_{p1})^2}+ID_1$$
$$=-\pi(c/L_{p1})(L/L_{p1})\{1+A_0-(h_2/h_1)^2C_0\}$$

(iii) $1>L/L_{p1}\geq 0.770$

In this interval, only the first, second, seventh and eighth equations are slightly different from those in the interval (ii). In the following, only dissimilar equations are given.

$$2IA_1\sqrt{1-(L/L_{p1})^2}-RB_1\{3(L/L_{p1})^2-2\}+2IC_1(\mu_2/\mu_1)\sqrt{1-(h_2/h_1)^2(L/L_{p1})^2}$$
$$-RD_1(\mu_2/\mu_1)\{2-3(h_2/h_1)^2(L/L_{p1})^2\}=0\ ,$$

$$-2RA_1\sqrt{1-(L/L_{p1})^2}-IB_1\{3(L/L_{p1})^2-2\}$$
$$-2RC_1(\mu_2/\mu_1)\sqrt{1-(h_2/h_1)^2(L/L_{p1})^2}$$
$$-ID_1(\mu_2/\mu_1)\{2-3(h_2/h_1)^2(L/L_{p1})^2\}=0\ ,$$

$$-IA_1\sqrt{1-(L/L_{p1})^2}-RB_1-IC_1\sqrt{1-(h_2/h_1)^2(L/L_{p1})^2}+RD_1=0\ ,$$

$$RA_1\sqrt{1-(L/L_{p1})^2}-IB_1+RC_1\sqrt{1-(h_2/h_1)^2(L/L_{p1})^2}+ID_1$$
$$=-\pi(c/L_{p1})(L/L_{p1})\{1+A_0-(h_2/h_1)^2C_0\}\ .$$

(iv) $0.770>L/L_{p1}\geq 0.578$

In this interval, only the third, fourth, fifth and sixth equations given below are slightly different from those in the interval (iii).

$$-\{3(L/L_{p1})^2-2\}RA_1-2RB_1\sqrt{3(L/L_{p1})^2-1}$$
$$+RC_1(\mu_2/\mu_1)\{3(h_2/h_1)^2(L/L_{p1})^2-2\}$$
$$-2ID_1(\mu_2/\mu_1)\sqrt{1-3(h_2/h_1)^2(L/L_{p1})^2}=0\ ,$$

$$-\{3(L/L_{p1})^2-2\}IA_1-2IB_1\sqrt{3(L/L_{p1})^2-1}$$
$$+IC_1(\mu_2/\mu_1)\{3(h_2/h_1)^2(L/L_{p1})^2-2\}+2RD_1(\mu_2/\mu_1)\sqrt{1-3(h_2/h_1)^2(L/L_{p1})^2}$$
$$=3\pi(c/L_{p1})(L/L_{p1})^2\{1-A_0-C_0(\mu_2/\mu_1)(h_2/h_1)^3\}\ ,$$

$$RA_1-RB_1\sqrt{3(L/L_{p1})^2-1}-RC_1-ID_1\sqrt{1-3(h_2/h_1)^2(L/L_{p1})^2}=0\ ,$$

$$IA_1-IB_1\sqrt{3(L/L_{p1})^2-1}-IC_1+RD_1\sqrt{1-3(h_2/h_1)^2(L/L_{p1})^2}=0\ .$$

(v) $0.578>L/L_{p1}$

In this interval, only the third, fourth, fifth and sixth equations given below are slightly different from those in the interval (iv).

$$-\{3(L/L_{p1})^2-2\}RA_1-2IB_1\sqrt{1-3(L/L_{p1})^2}$$
$$+RC_1(\mu_2/\mu_1)\{3(h_2/h_1)^2(L/L_{p1})^2-2\}$$
$$-2ID_1(\mu_2/\mu_1)\sqrt{1-3(h_2/h_1)^2(L/L_{p1})^2}=0\ ,$$

$$-\{3(L/L_{p1})^2-2\}IA_1+2RB_1\sqrt{1-3(L/L_{p1})^2}$$
$$+IC_1(\mu_2/\mu_1)\{3(h_2/h_1)^2(L/L_{p1})^2-2\}$$
$$+2RD_1(\mu_2/\mu_1)\sqrt{1-3(h_2/h_1)^2(L/L_{p1})^2}$$
$$=3\pi(c/L_{p1})(L/L_{p1})^2\{1-A_0-C_0(\mu_2/\mu_1)(h_2/h_1)^3\}\ ,$$

$$RA_1-IB_1\sqrt{1-3(L/L_{p1})^2}-RC_1-ID_1\sqrt{1-3(h_2/h_1)^2(L/L_{p1})^2}=0\ ,$$

$$IA_1+RB_1\sqrt{1-3(L/L_{p1})^2}-IC_1+RD_1\sqrt{1-3(h_2/h_1)^2(L/L_{p1})^2}=0\ .$$

In calculating these formulae, the parametron computor 'PC-1' of

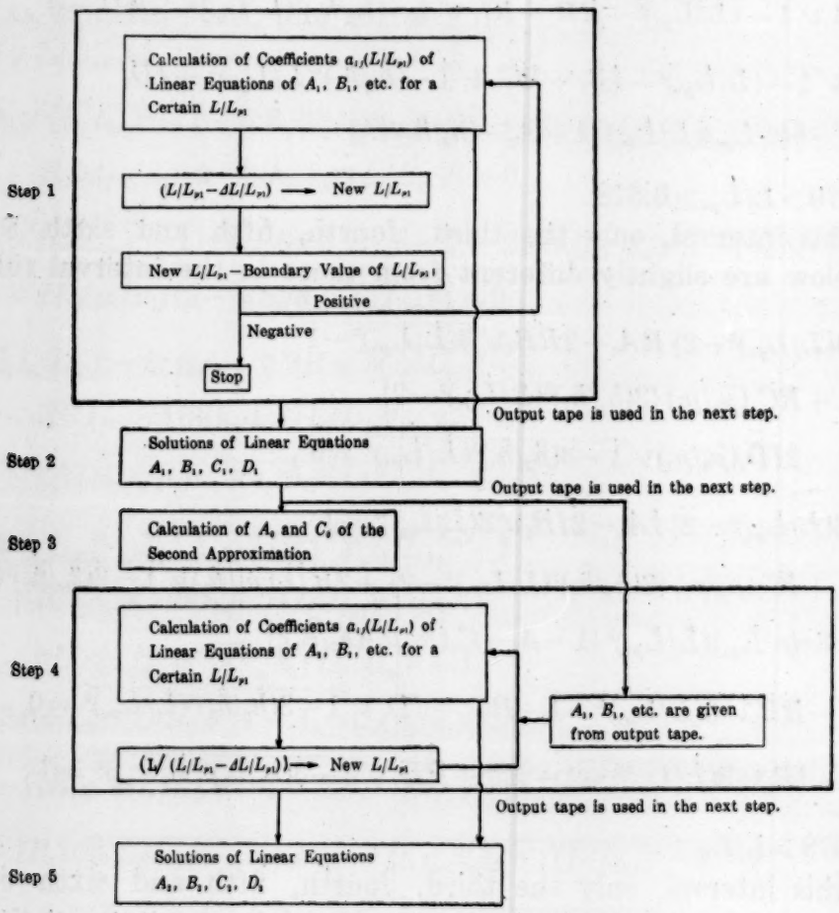

Fig. 2. Flow diagram.

Takahashi Laboratory, Institute of Physics, Faculty of Science, University of Tokyo was used. The memory capacity of this computor is only 256 in long word and is too small for these calculations. The reason why this computor was used depended mostly on the cost, although partly it is because the writer is familiar with the program of this computor. The flow diagram used in these calculations is shown in Fig. 2.

Step 1 is the step to calculate at appropriate intervals $\Delta(L/L_{p1})$ all coefficients of simultaneous linear equations from which A_1, B_1, etc. are determined. The tape on which the coefficients are punched in the output is used directly as an input tape in the next step, Step 2. In Step 2, a revised program of the complete program No. 3 in the PC-1 Library is used, which is a program for obtaining the solution of simultaneous linear equations by using the sweeping out method. The tape punched in the output of Step 2 is edited and used as input tape

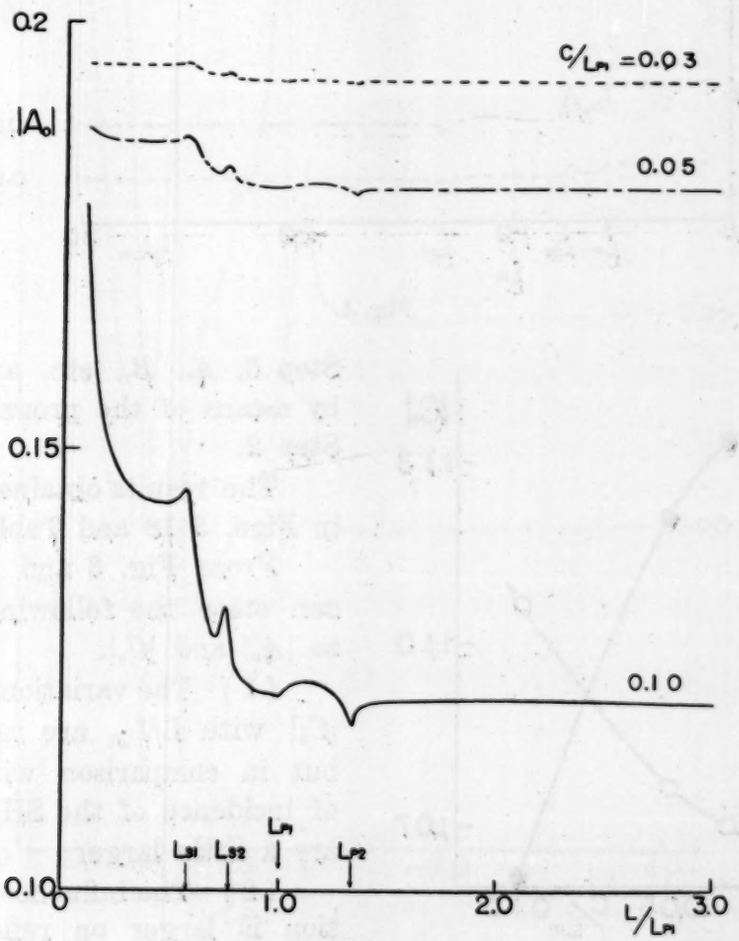

Fig. 3.

in Step 3 and Step 4. In Step 3, A_0 and C_0 of the second approximation are calculated. Step 4 is similar to Step 1, and is the step to obtain all the coefficients of simultaneous linear equations determining A_2, B_2, etc. In

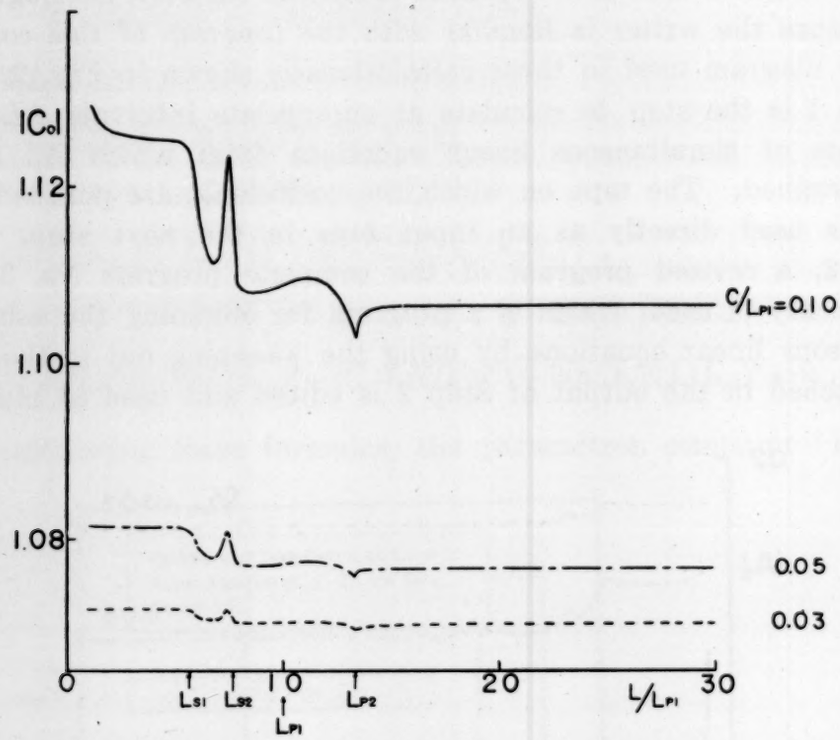

Fig. 4.

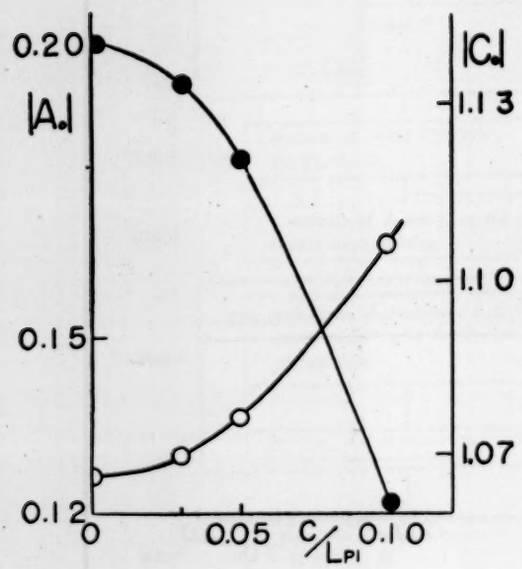

Fig. 5.

Step 5, A_2, B_2, etc. are obtained by means of the program used in Step 2.

The results obtained are given in Figs. 3–18 and Tables 1–5.

From Fig. 3 and Fig. 4, we can state the following points as to $|A_0|$ and $|C_0|$.

(1) The variations of $|A_0|$ and $|C_0|$ with L/L_{p1} are rather small, but in comparison with the case of incidence of the SH wave they are a little larger.

(2) The influence of corrugation is larger on reflection than on refraction. This is also shown

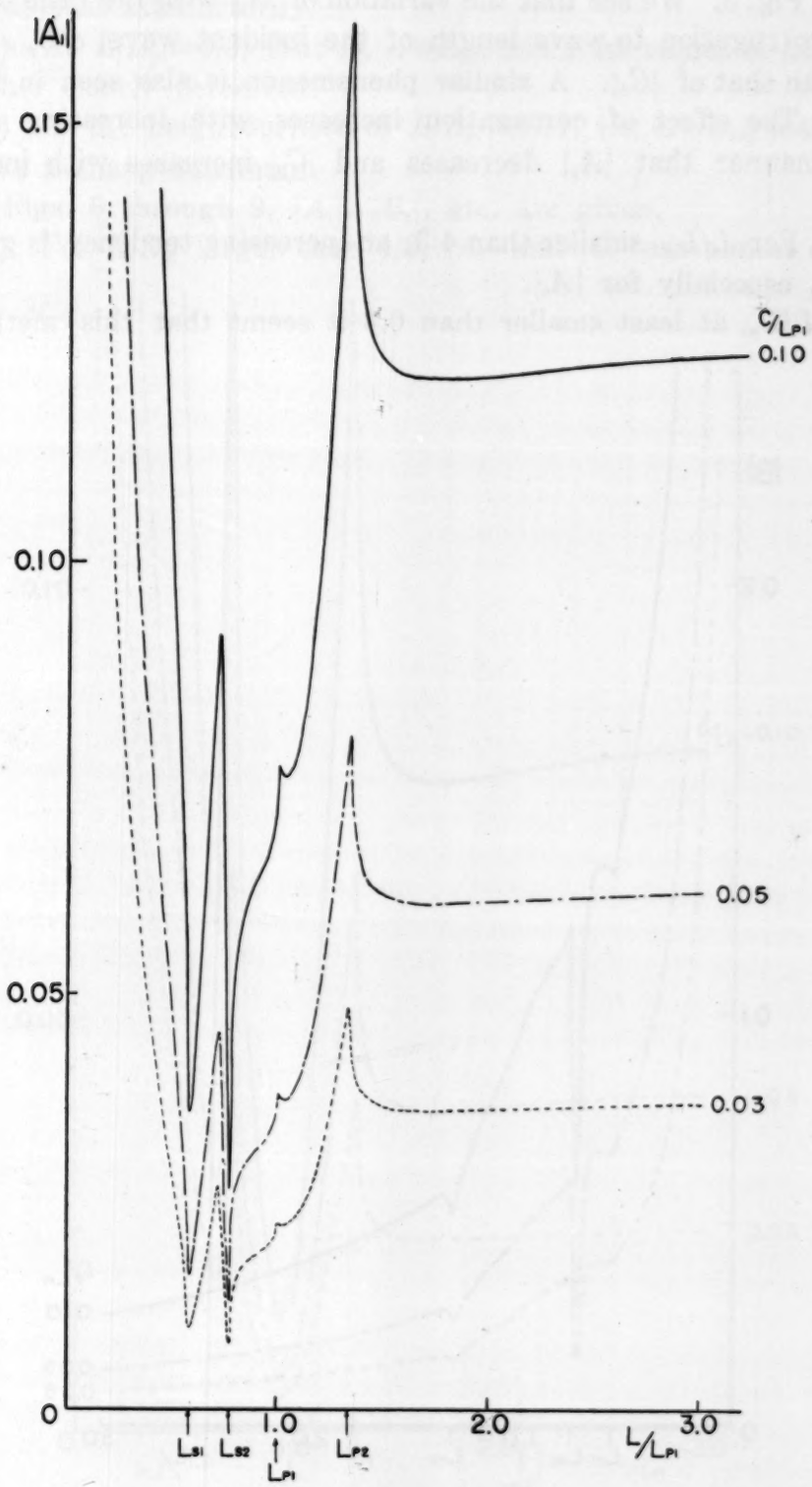

Fig. 6.

clearly in Fig. 5. We see that the variation of $|A_0|$ with the ratio of amplitude of corrugation to wave length of the incident wave, c/L_{p1}, is much larger than that of $|C_0|$. A similar phenomenon is also seen in Fig. 13.

(3) The effect of corrugation increases with increasing c/L_{p1} in such a manner that $|A_0|$ decreases and $|C_0|$ increases with increasing c/L_{p1}.

(4) For L/L_{p1} smaller than 4/3, an increasing tendency is generally observed, especially for $|A_0|$.

For L/L_{p1} at least smaller than 0.3 it seems that this method can

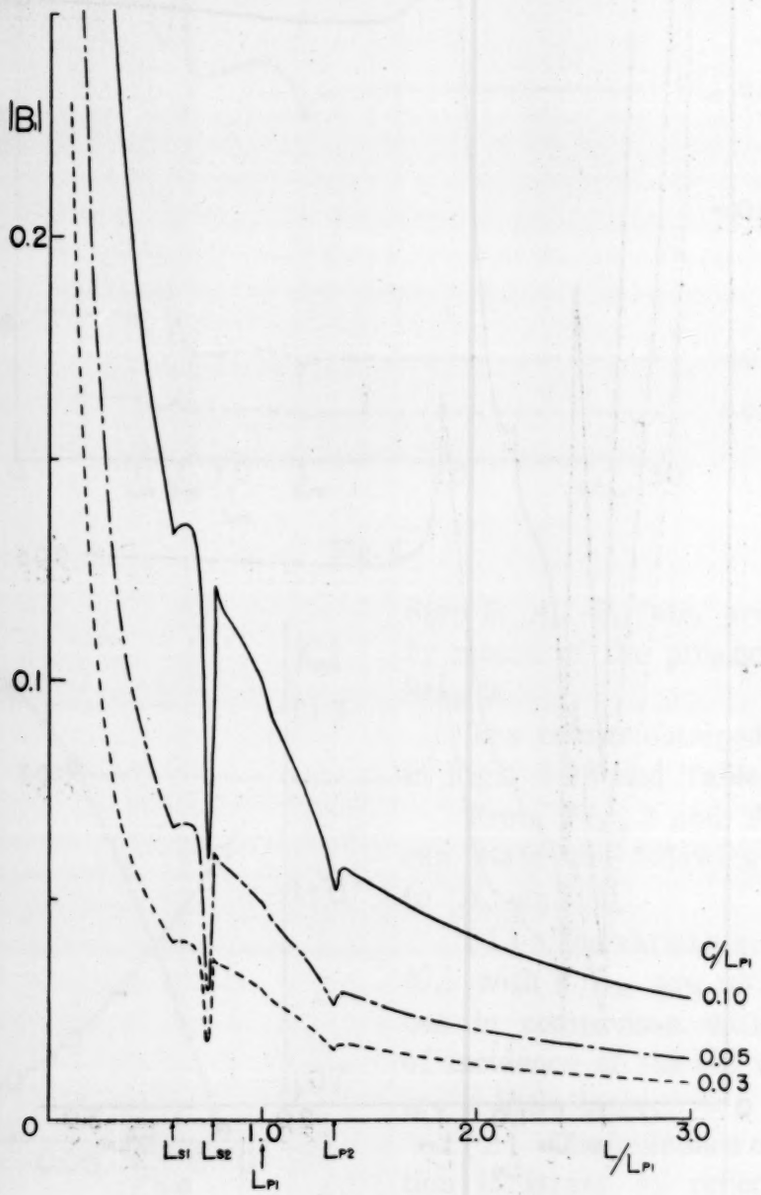

Fig. 7.

not be applied satisfactorily.

(5) At $L/L_{p1}=4/3$, that is, $L=L_{p2}$, minimum values of $|A_0|$ and $|C_0|$ are rather clearly perceived.

(6) In the neighbourhood of $L/L_{p1}=0.77$, i.e. $L=L_{s2}$, both $|A_0|$ and $|C_0|$ have a sharp maximum.

In Figs. 6 through 9, $|A_1|$, $|B_1|$, etc. are given.

(7) For L/L_{p1} larger than 4/3, $|A_1|$ and $|C_1|$ are almost constant.

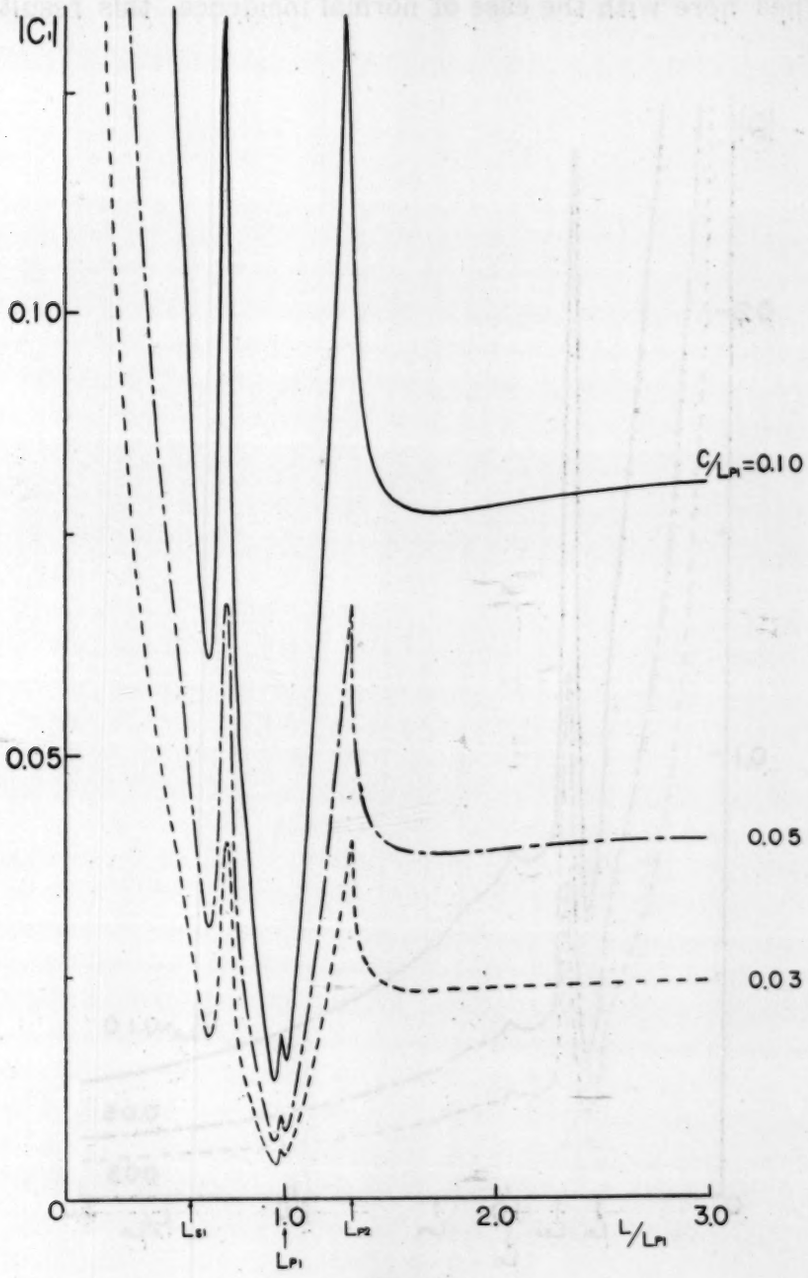

Fig. 8.

(8) At $L/L_{p1}=4/3$, i.e. $L=L_{p2}$, both $|A_1|$ and $|C_1|$ have a sharp maximum and for L/L_{p1} smaller than 4/3 they decrease very rapidly until $|A_1|$ has a sharp minimum at $L/L_{p1}=0.77$, i.e. $L=L_{s2}$ and $|C_1|$ has two minima near $L/L_{p1}=1$.

(9) $|B_1|$ and $|D_1|$, the S wave components of reflected and refracted waves, have an increasing tendency with decreasing L/L_{p1}. Therefore, the vertical component of displacement becomes very large. Since we are concerned here with the case of normal incidence, this result is very reasonable.

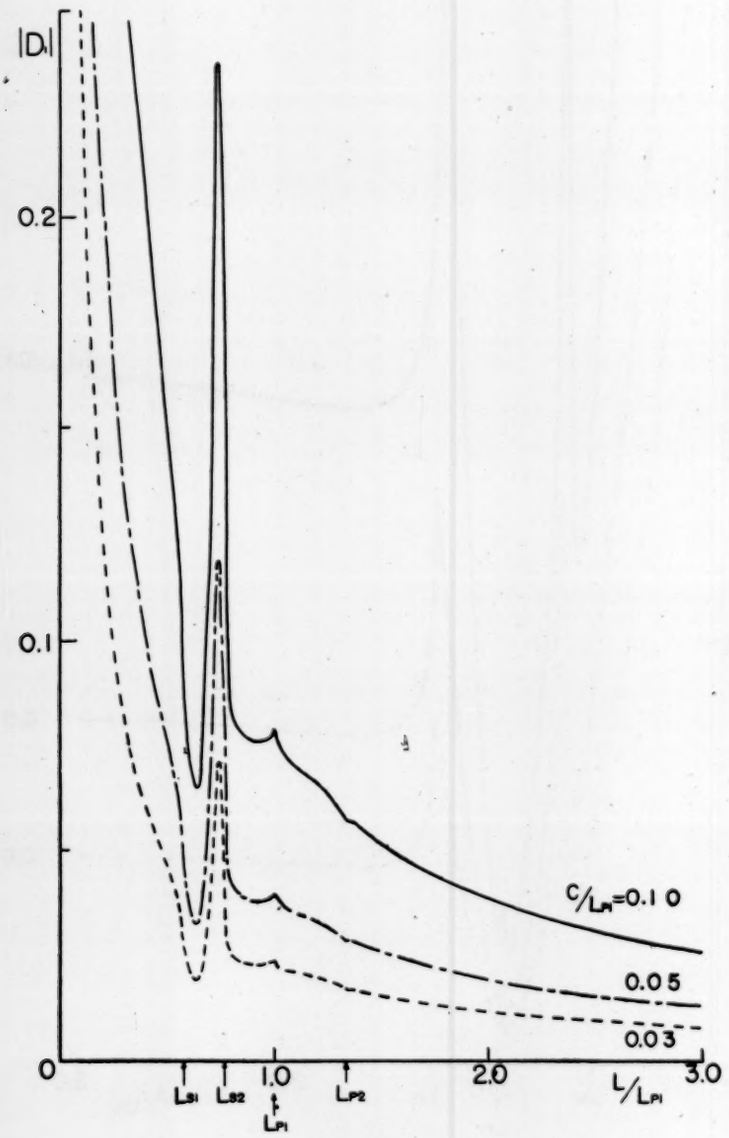

Fig. 9.

(10) It is remarkable that $|B_1|$ decreases very abruptly near $L/L_{p1}=0.77$, i.e. $L=L_{s2}$ and reaches a minimum at $L/L_{p1}=0.74$. Corresponding to this, $|A_1|$, $|C_1|$ and $|D_1|$, especially $|D_1|$ become very large and reach sharp peaks around $L/L_{p1}=0.74$.

(11) The abnormal feature at $L=L_{p1}$ and $L=L_{s1}$ is not as clear as those at $L=L_{p2}$ and $L=L_{s2}$.

(12) For L/L_{p1} smaller than about 0.3, all irregular waves become very large and this tendency impairs the accuracy of this method.

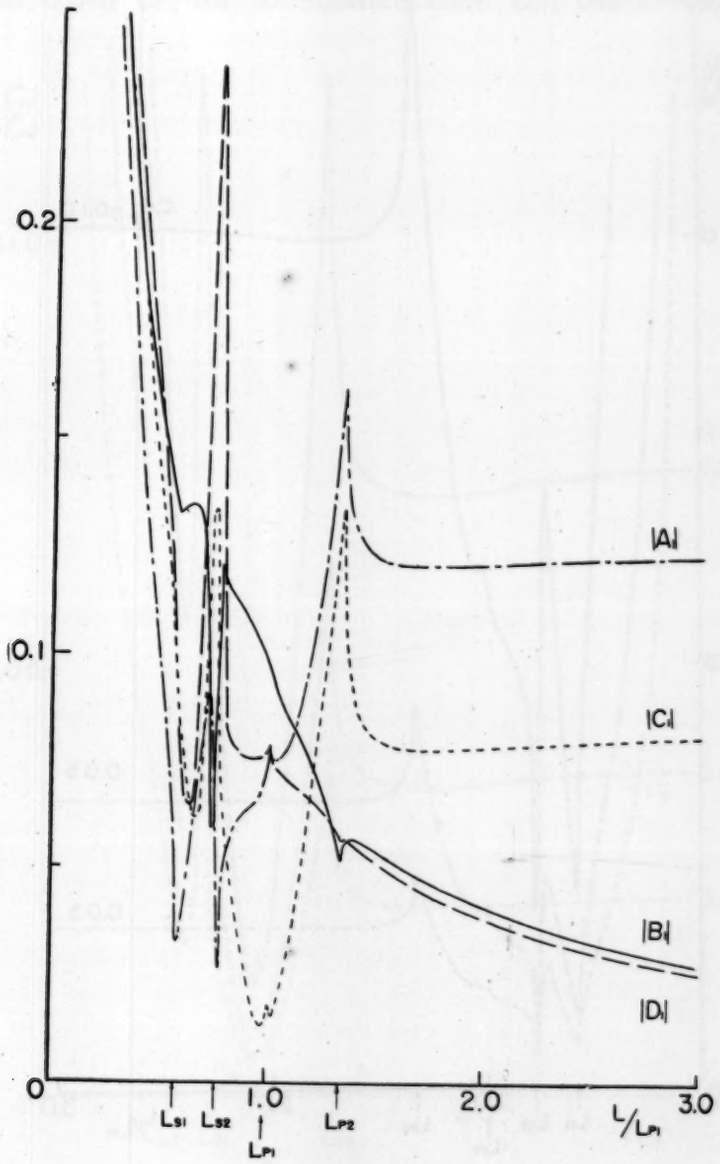

Fig. 10.

In Fig. 10, $|A_1|$, $|B_1|$, $|C_1|$ and $|D_1|$ of $c/L_{p1}=0.1$ are given together for comparison. From this figure, we can see clearly that the S wave component in both reflected and refracted waves increases with decreasing L/L_{p1} and near $L=L_{p1}$ it becomes comparable order to the P wave component. Furthermore, the abnormal character is very conspicuous in the neighbourhood of $L=L_{s2}$.

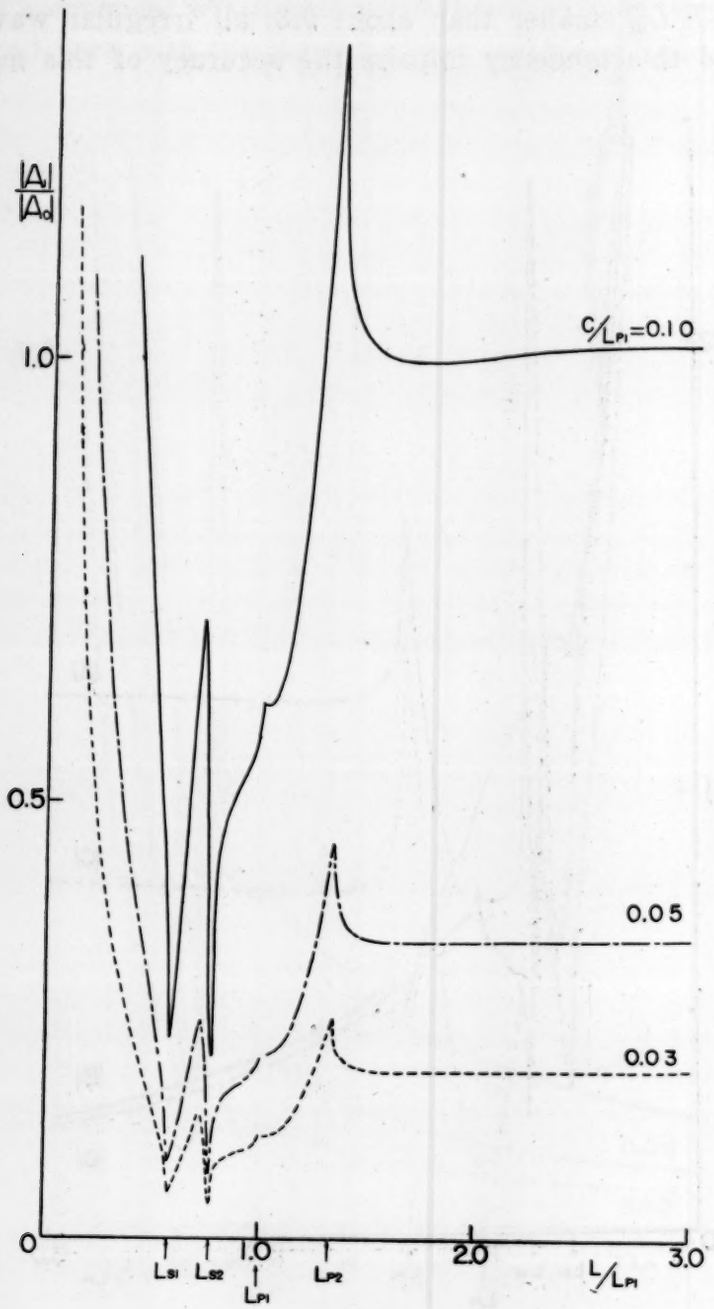

Fig. 11.

(13) According to the value of L/L_{p1}, some irregular waves become boundary waves. That is to say, their amplitude decreases exponentially with increasing $|z|$. The P wave component of an irregularly reflected wave which is represented by $|A_1|$ becomes like the boundary wave for L/L_{p1} smaller than 1, or for L smaller than L_{p1}.

Similar circumstances prevail for the following waves in the ranges of wave lengths specified below:

The S wave component of an irregularly reflected wave B_1, for L/L_{p1} smaller than 0.578 or for L smaller than L_{s1}, the P wave component

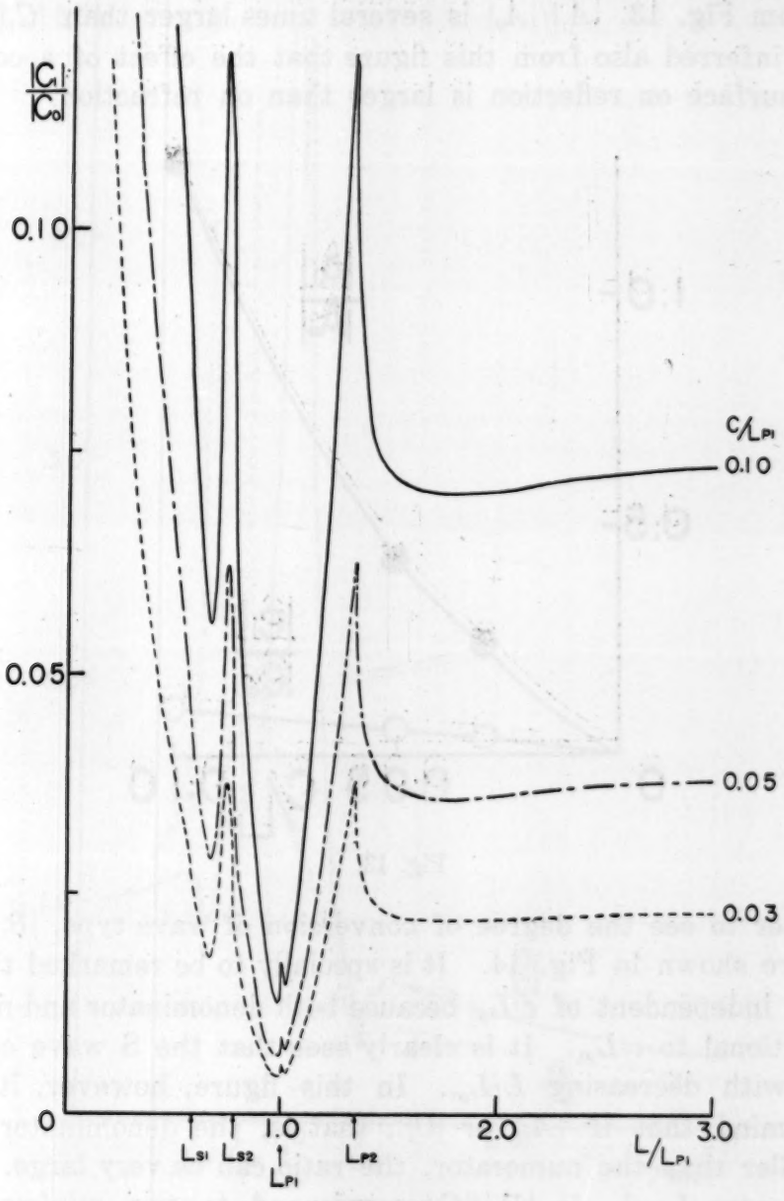

Fig. 12.

of an irregularly refracted wave C_1, for L/L_{p1} smaller than 4/3 or for L smaller than L_{p2}, and the S wave component of an irregularly refracted wave D_1, for L/L_{p1} smaller than 0.77 or for L smaller than L_{s2}.

As in the case of the SH wave, the curves of $|A_1|/|A_0|$ and $|C_1|/|C_0|$ have almost the same tendencies as those of $|A_1|$ and $|C_1|$ themselves, because of small variations of $|A_0|$ and $|C_0|$ with L/L_{p1}. But since it is very interesting to know the values of these ratio, they are given in Figs. 11 through 12. From these figures, it is clear that the effect at $L=L_{p2}$ is most conspicuous in both $|A_1|/|A_0|$ and $|C_1|/|C_0|$. Furthermore, as seen from Fig. 13, $|A_1|/|A_0|$ is several times larger than $|C_1|/|C_0|$ and it may be inferred also from this figure that the effect of a corrugated boundary surface on reflection is larger than on refraction.

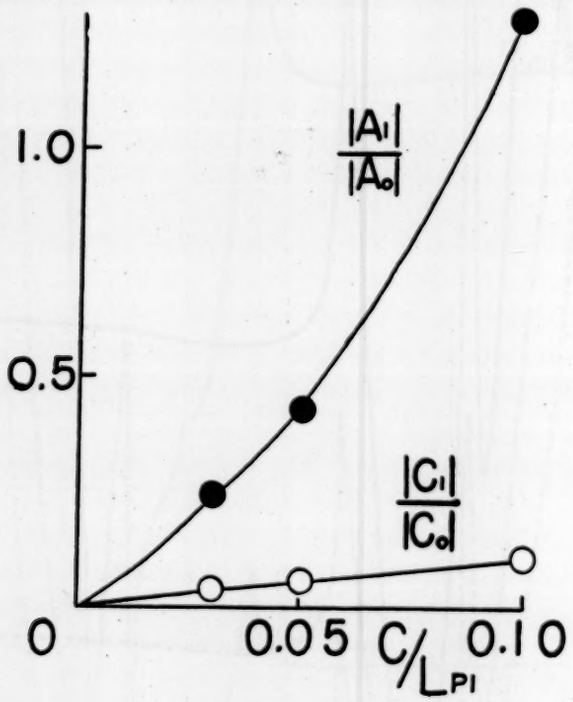

Fig. 13.

In order to see the degree of conversion of wave type, $|B_1|/|A_1|$ and $|D_1|/|C_1|$ are shown in Fig. 14. It is specially to be remarked that these values are independent of c/L_{p1} because both denominator and numerator are proportional to c/L_{p1}. It is clearly seen that the S wave component increases with decreasing L/L_{p1}. In this figure, however, it must be borne in mind that if $|A_1|$ or $|C_1|$, that is, the denominator becomes much smaller than the numerator, the ratio can be very large. In fact, two peaks near $L=L_{p1}$ in $|D_1|/|C_1|$ correspond to two minima of $|C_1|$.

Also two peaks of $|B_1|/|A_1|$ near $L=L_{s1}$ and $L=L_{s2}$ correspond to two minima of $|A_1|$. But it may be permissible to say that for L/L_{p1} below about 1, both $|D_1|/|C_1|$ and $|B_1|/|A_1|$ become comparable to or rather larger than 1.

As for A_2, B_2, etc. computations were carried out only for the case of $c/L_{p1}=0.1$. The results are shown in Figs. 15–18 together with those

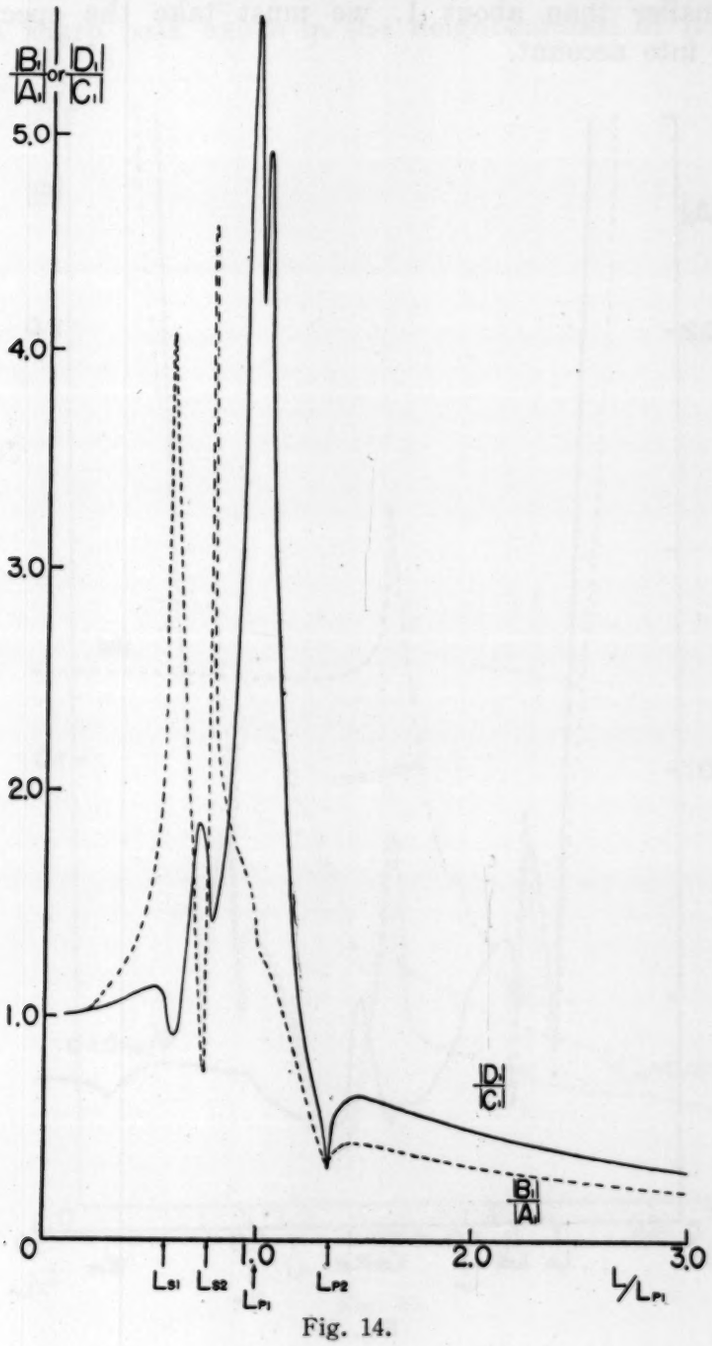

Fig. 14.

of the spectra of the first order, i.e. $|A_1|$, $|B_1|$, etc. for comparison.

(14) In general, for L/L_{p1} smaller than about 1, the values of $|A_2|$, $|B_2|$, etc. are comparable or larger than those of $|A_1|$, $|B_1|$, etc. and much smaller than those of $|A_0|$ and $|C_0|$ for almost all values of L/L_{p1}. Therefore, when we say something about $|A_0|$ or $|C_0|$, it is unnecessary to refer to $|A_2|$ or $|C_2|$. But when attention is paid to irregular waves for L/L_{p1} smaller than about 1, we must take the spectrum of the second order into account.

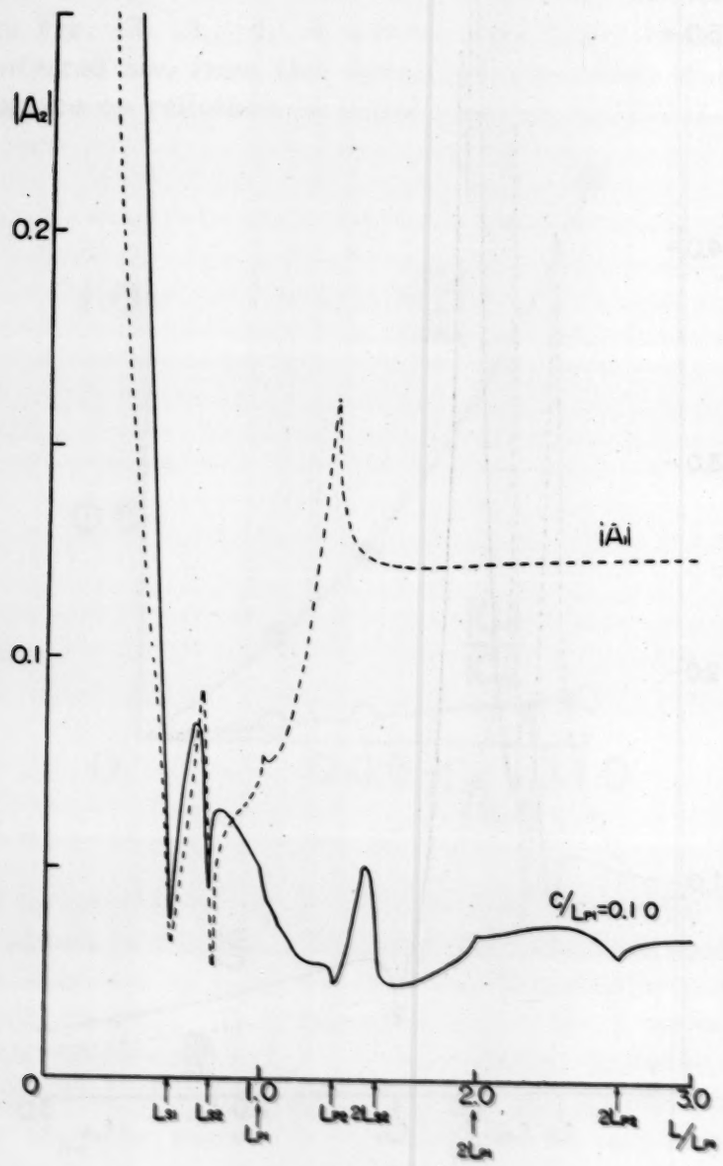

Fig. 15.

(15) As to the P wave component represented by A_n or C_n, $|A_1|$ is much larger than $|A_2|$ for L/L_{p1} larger than about 1; while $|C_1|$ is larger than $|C_2|$ for L/L_{p1} larger than about 1.2. However, the contrary is the case with respect to the S wave component, because both $|B_1|$ and $|D_1|$ are not so large in comparison with $|B_2|$ and $|D_2|$ as in the P wave component, but rather of the same order of magnitude with $|B_2|$ and $|D_2|$.

(16) A sharp peak exists in the neighbourhood of $L=2L_{s2}$ in each

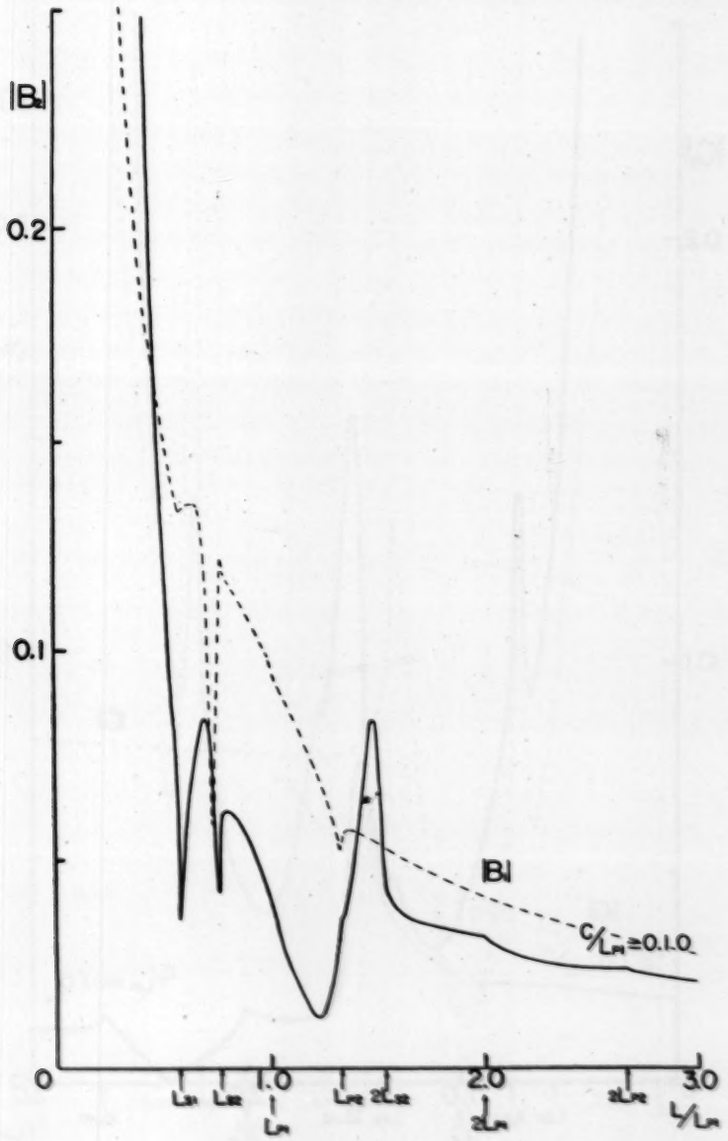

Fig. 16.

irregular wave of the second order. Especially in the S wave components the phenomena are notable.

(17) As a whole, the positions of the maximum or minimum of $|A_2|$, $|B_2|$, etc. especially for L/L_{p1} smaller than about 1 are almost the same as those of $|A_1|$, $|B_1|$, etc.

(18) For L smaller than $2L_{p2}$, some irregular waves become like boundary waves. Such circumstances occur in the ranges specified below: in waves represented by C_2 for L/L_{p1} smaller than 2.667 or for L smaller than $2L_{p2}$, in waves represented by A_2 for L/L_{p1} smaller than

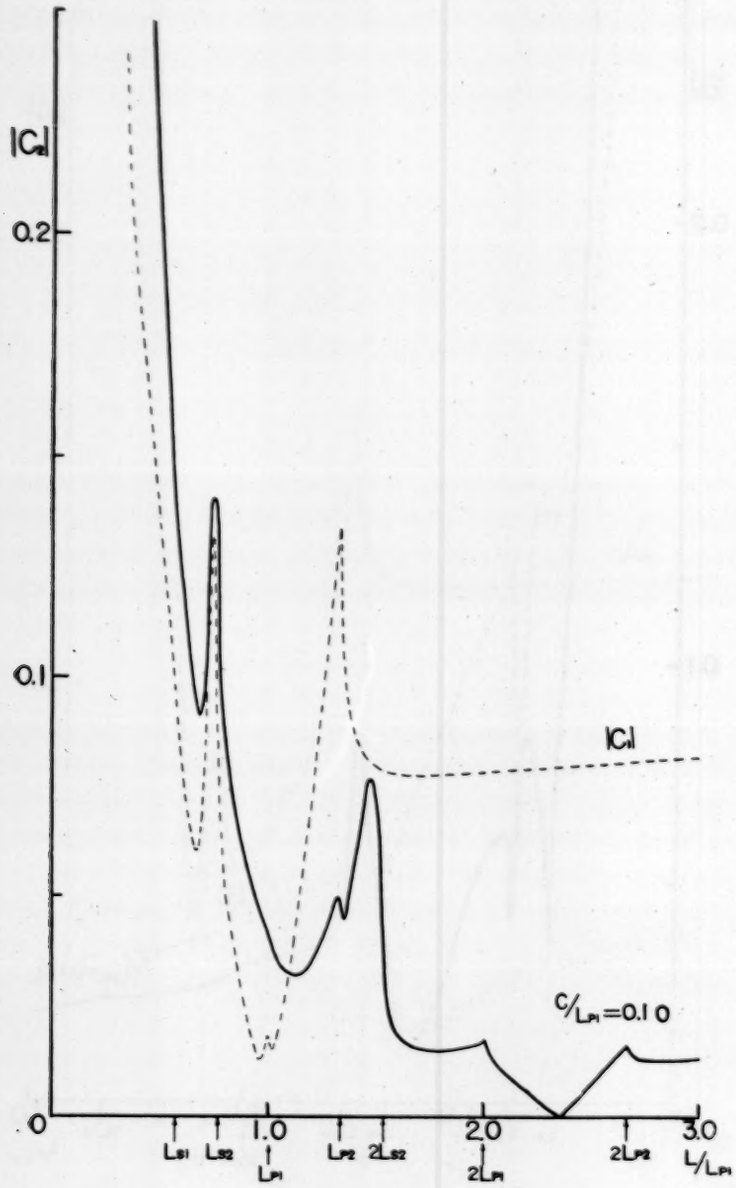

Fig. 17.

2 or for L smaller than $2L_{p1}$, in waves represented by D_2 for L/L_{p1} smaller than 1.539 or for L smaller than $2L_{s2}$, and in waves represented by B_2 for L/L_{p1} smaller than 1.156 or for L smaller than $2L_{s1}$. Therefore, from the practical point of view, it may be permitted to say that only the S wave component of irregularly reflected waves with spectra of the second order has significant contribution to displacement potentials in comparison with those of irregularly reflected and refracted waves with spectra of the first order.

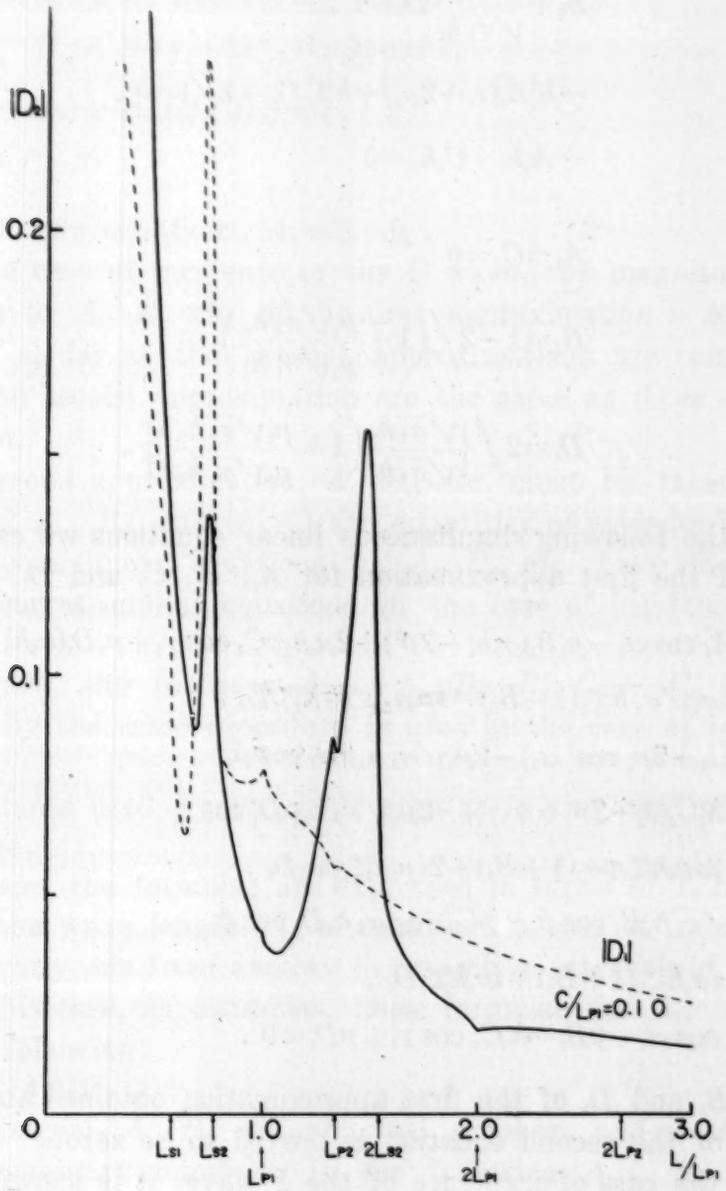

Fig. 18.

§ 5.2. The Case of Incidence of the SV Wave

Putting $a=0$ and $b=1$ in (14), the following simultaneous linear equations, determining solutions of the first approximation for A_0, B_0, C_0 and D_0 are obtained.

$$-B_0+\frac{\mu_2}{\mu_1}\cdot\frac{\sigma_2 h_2^2}{\sigma_1 h_1^2}D_0=1\ ,$$

$$B_0+\frac{\sqrt{\sigma_2}h_2}{\sqrt{\sigma_1}h_1}D_0=1\ ,$$

$$-h_1^2A_0(\lambda_1+2\mu_1)+h_2^2C_0(\lambda_2+2\mu_2)=0\ ,$$

$$-A_0h_1-C_0h_2=0$$

Then

$$A_0=C_0=0\ ,$$

$$B_0=1-2\Big/\left(1+\frac{\mu_2\sqrt{\sigma_2}h_2}{\mu_1\sqrt{\sigma_1}h_1}\right)\ ,$$

$$D_0=2\Big/\left\{\frac{\sqrt{\sigma_2}h_2}{\sqrt{\sigma_1}h_1}\left(1+\frac{\mu_2\sqrt{\sigma_2}h_2}{\mu_1\sqrt{\sigma_1}h_1}\right)\right\}\ .$$

From the following simultaneous linear equations we can obtain the solutions of the first approximation for A_1, B_1, C_1 and D_1,

$$\begin{aligned}
&2\mu_1h_1pA_1\cos\alpha_1-\mu_1B_1(\sigma_1h_1^2-2p^2)+2\mu_2h_2pC_1\cos\gamma_1+\mu_2D_1(\sigma_2h_2^2-2p^2)\\
&\quad=i\mu_1\sigma_1\sqrt{\sigma_1}h_1^3\zeta_1(1-B_0)-i\mu_2\sigma_2\sqrt{\sigma_2}h_2^3\zeta_1D_0\ ,\\
&-h_1^2A_1(\lambda_1+2\mu_1\cos^2\alpha_1)-2\mu_1\sqrt{\sigma_1}h_1pB_1\cos\beta_1\\
&\qquad+h_2^2C_1(\lambda_2+2\mu_2\cos^2\gamma_1)-2\mu_2\sqrt{\sigma_2}h_2pD_1\cos\delta_1\\
&\quad=-2i\mu_1h_1^2\zeta_1p\sigma_1(1+B_0)+2i\mu_2h_2^2\zeta_1p\sigma_2D_0\ ,\\
&pA_1-\sqrt{\sigma_1}h_1B_1\cos\beta_1-pC_1-\sqrt{\sigma_2}h_2D_1\cos\delta_1\\
&\quad=-i\sigma_1h_1^2\zeta_1(1+B_0)+i\sigma_2h_2^2\zeta_1D_0\ ,\\
&-h_1A_1\cos\alpha_1-pB_1-h_2C_1\cos\gamma_1+pD_1=0\ .
\end{aligned}$$

By using B_0 and D_0 of the first approximation obtained above, the right hand side of the second equation is proved to be zero.

As in the case of incidence of the P wave, it is shown readily that there exist the relations $A_1=-A_1'$, $B_1=B_1'$, $C_1=-C_1'$ and $D_1=D_1'$.

As to A_0, B_0, etc. of the second approximation, by using the relations obtained above $A_1=-A_1'$, $B_1=B_1'$, etc., we have

$$
\begin{aligned}
&-\sigma_1\mu_1h_1^2B_0+\sigma_2\mu_2h_2^2D_0\\
&\quad=\sigma_1\mu_1h_1^2+4i\mu_1\zeta_{-1}A_1p^3-2i\mu_1\zeta_{-1}B_1\sqrt{\sigma_1}h_1(\sigma_1h_1^2+2p^2)\cos\beta_1\\
&\qquad-4i\mu_2\zeta_{-1}C_1p^3-2i\mu_2\zeta_{-1}D_1\sqrt{\sigma_2}h_2(\sigma^2h_2^2+2p^2)\cos\delta_1\ ,\\
&-\sqrt{\sigma_1}h_1B_0-\sqrt{\sigma_2}h_2D_0\\
&\quad=-\sqrt{\sigma_1}h_1+2ih_1\zeta_{-1}A_1p\cos\alpha_1-2i\zeta_{-1}B_1\sigma_1h_1^2\cos^2\beta_1\\
&\qquad+2i\zeta_{-1}C_1ph_2\cos\gamma_1+2i\zeta_{-1}D_1\sigma_2h_2^2\cos^2\delta_1\ ,\\
&-h_1^2A_0(\lambda_1+2\mu_1)+h_2^2C_0(\lambda_2+2\mu_2)=0\ ,\\
&-h_1A_0-h_2C_0=0\ .
\end{aligned}
$$

From the last two equations, $A_0=C_0=0_0$.

As in the case of incidence of the P wave, the magnitude of correction terms to A_1, B_1, etc. of the first approximation is of the order of ζ^3. Thus, as far as the present approximations are concerned, A_1, B_1, etc. of the second approximation are the same as those of the first approximation.

In the second approximation, A_2, B_2, etc. must be taken into consideration and A_n, B_n, etc. ($n>2$) are quantities of an order higher than ζ^3. Simultaneous linear equations for A_2, B_2, etc. have the same expressions as corresponding equations in the case of incidence of the P wave.

In this case, the relations $A_2=-A_2'$, $B_2=B_2'$, $C_2=-C_2'$ and $D_2=D_2'$ are obtained by the same procedure as used in the case of incidence of the P wave.

The constants used are the same ones as in the case of incidence of the P wave.

In this case, the formulae are expressed in terms of L/L_{s1}, that is, the ratio of the wave length of corrugation to that of incident wave, and differ slightly one from another in respective intervals of L/L_{s1} concerned. In this case, as examples, these formulae for A_2, B_2, etc. are given in the following:

(i)-(1) $L/L_{s1}\geq 4.619$

In this interval, A_2, B_2, etc. are real numbers and as A_1, B_1, etc. are purely imaginary numbers, in the following A_1/i, B_1/i, etc. are written as A_1, B_1 and so on.

$$4\sqrt{3}\,A_2\sqrt{(L/L_{s1})^2-12}-3B_2\{(L/L_{s1})^2-8\}$$
$$+4\sqrt{3}\,C_2(\mu_2/\mu_1)\sqrt{(h_2/h_1)^2(L/L_{s1})^2-12}+3D_2(\mu_2/\mu_1)\{(h_2/h_1)^2(L/L_{s1})^2-8\}$$
$$=-\frac{\pi(c/L_{s1})}{(L/L_{s1})}[2A_1\{2(L/L_{s1})^2-9\}+3B_1\{6-(L/L_{s1})^2\}\sqrt{(L/L_{s1})^2-1}$$
$$-2C_1(\mu_2/\mu_1)\{2(h_2/h_1)^2(L/L_{s1})^2-9\}$$
$$+3D_1(\mu_2/\mu_1)\{6-(h_2/h_1)^2(L/L_{s1})^2\}\sqrt{(h_2/h_1)^2(L/L_{s1})^2-1}\,],$$

$$3A_2\{(L/L_{s1})^2-8\}+12B_2\sqrt{(L/L_{s1})^2-4}-3C_2(\mu_2/\mu_1)\{(h_2/h_1)^2(L/L_{s1})^2-8\}$$
$$+12(\mu_2/\mu_1)D_2\sqrt{(h_2/h_1)^2(L/L_{s1})^2-4}$$
$$=-\frac{\pi(c/L_{s1})}{\sqrt{3}\,(L/L_{s1})}[3A_1\{(L/L_{s1})^2-6\}\sqrt{(L/L_{s1})^2-3}+6\sqrt{3}\,B_1\{2(L/L_{s1})^2-3\}$$
$$+3C_1(\mu_2/\mu_1)\{(h_2/h_1)^2(L/L_{s1})^2-6\}\sqrt{(h_2/h_1)^2(L/L_{s1})^2-3}$$
$$-6\sqrt{3}\,D_1(\mu_2/\mu_1)\{2(h_2/h_1)^2(L/L_{s1})^2-3\}\,],$$

$$2A_2-B_2\sqrt{(L/L_{s1})^2-4}-2C_2-D_2\sqrt{(h_2/h_1)^2(L/L_{s1})^2-4}$$
$$=-\frac{\pi(c/L_{s1})}{\sqrt{3}\,(L/L_{s1})}[A_1\sqrt{(L/L_{s1})^2-3}-\sqrt{3}\,B_1\{(L/L_{s1})^2-1\}$$
$$+C_1\sqrt{(h_2/h_1)^2(L/L_{s1})^2-3}+\sqrt{3}\,D_1\{(h_2/h_1)^2(L/L_{s1})^2-1\}\,],$$

$$A_2\sqrt{(L/L_{s1})^2-12}+2\sqrt{3}\,B_2+C_2\sqrt{(h_2/h_1)^2(L/L_{s1})^2-12}-2\sqrt{3}\,D_2$$
$$=-\frac{\pi(c/L_{s1})}{\sqrt{3}\,(L/L_{s1})}[A_1\{(L/L_{s1})^2-3\}+3B_1\sqrt{(L/L_{s1})^2-1}$$
$$-C_1\{(h_2/h_1)^2(L/L_{s1})^2-3\}+3D_1\sqrt{(h_2/h_1)^2(L/L_{s1})^2-1}\,].$$

For the value of L/L_{s1} below 4.619, A_2, B_2, etc. become complex numbers and are written as $A_2=RA_2+iIA_2$, etc.

(i)–(2) $4.619>L/L_{s1}\geq 3.464$

$$4\sqrt{3}\,RA_2\sqrt{(L/L_{s1})^2-12}-3RB_2\{(L/L_{s1})^2-8\}$$
$$+4\sqrt{3}\,IC_2(\mu_2/\mu_1)\sqrt{12-(h_2/h_1)^2(L/L_{s1})^2}+3RD_2(\mu_2/\mu_1)\{(h_2/h_1)^2(L/L_{s1})^2-8\}$$
$$=-\frac{\pi(c/L_{s1})}{(L/L_{s1})}[2A_1\{2(L/L_{s1})^2-9\}+3B_1\{6-(L/L_{s1})^2\}\sqrt{(L/L_{s1})^2-1}$$
$$-2C_1(\mu_2/\mu_1)\{2(h_2/h_1)^2(L/L_{s1})^2-9\}$$
$$+3D_1(\mu_2/\mu_1)\{6-(h_2/h_1)^2(L/L_{s1})^2\}\sqrt{(h_2/h_1)^2(L/L_{s1})^2-1}\,],$$

$$4\sqrt{3}\,IA_2\sqrt{(L/L_{s1})^2-12}-3IB_2\{(L/L_{s1})^2-8\}$$
$$-4\sqrt{3}\,RC_2(\mu_2/\mu_1)\sqrt{12-(h_2/h_1)^2(L/L_{s1})^2}$$
$$+3ID_2(\mu_2/\mu_1)\{(h_2/h_1)^2(L/L_{s1})^2-8\}=0\,,$$

$$3RA_2\{(L/L_{s1})^2-8\}+12RB_2\sqrt{(L/L_{s1})^2-4}-3RC_2(\mu_2/\mu_1)\{(h_2/h_1)^2(L/L_{s1})^2-8\}$$
$$+12RD_2(\mu_2/\mu_1)\sqrt{(h_2/h_1)^2(L/L_{s1})^2-4}$$
$$=-\frac{\pi(c/L_{s1})}{\sqrt{3}\,(L/L_{s1})}[3A_1\{(L/L_{s1})^2-6\}\sqrt{(L/L_{s1})^2-3}+6\sqrt{3}\,B_1\{2(L/L_{s1})^2-3\}$$
$$+3C_1(\mu_2/\mu_1)\{(h_2/h_1)^2(L/L_{s1})^2-6\}\sqrt{(h_2/h_1)^2(L/L_{s1})^2-3}$$
$$-6\sqrt{3}\,D_1(\mu_2/\mu_1)\{2(h_2/h_1)^2(L/L_{s1})^2-3\}]\,,$$

$$3IA_2\{(L/L_{s1})^2-8\}+12IB_2\sqrt{(L/L_{s1})^2-4}-3IC_2(\mu_2/\mu_1)\{(h_2/h_1)^2(L/L_{s1})^2-8\}$$
$$+12(\mu_2/\mu_1)ID_2\sqrt{(h_2/h_1)^2(L/L_{s1})^2-4}=0\,,$$

$$2RA_2-RB_2\sqrt{(L/L_{s1})^2-4}-2RC_2-RD_2\sqrt{(h_2/h_1)^2(L/L_{s1})^2-4}$$
$$=-\frac{\pi(c/L_{s1})}{\sqrt{3}\,(L/L_{s1})}[A_1\sqrt{(L/L_{s1})^2-3}-\sqrt{3}\,B_1\{(L/L_{s1})^2-1\}$$
$$+C_1\sqrt{(h_2/h_1)^2(L/L_{s1})^2-3}+\sqrt{3}\,D_1\{(h_2/h_1)^2(L/L_{s1})^2-1\}]\,,$$

$$2IA_2-IB_2\sqrt{(L/L_{s1})^2-4}-2IC_2-ID_2\sqrt{(h_2/h_1)^2(L/L_{s1})^2-4}=0\,,$$

$$RA_2\sqrt{(L/L_{s1})^2-12}+2\sqrt{3}\,RB_2+IC_2\sqrt{12-(h_2/h_1)^2(L/L_{s1})^2}-2\sqrt{3}\,RD_2$$
$$=-\frac{\pi(c/L_{s1})}{\sqrt{3}\,(L/L_{s1})}[A_1\{(L/L_{s1})^2-3\}+3B_1\sqrt{(L/L_{s1})^2-1}$$
$$-C_1\{(h_2/h_1)^2(L/L_{s1})^2-3\}+3D_1\sqrt{(h_2/h_1)^2(L/L_{s1})^2-1}]\,,$$

$$IA_2\sqrt{(L/L_{s1})^2-12}+2\sqrt{3}\,IB_2-RC_2\sqrt{12-(h_2/h_1)^2(L/L_{s1})^2}-2\sqrt{3}\,ID_2=0\,.$$

(i)–(3) $3.464>L/L_{s1}\geq 2.667$

In this interval, the first, second, seventh and eighth equations in (i)–(2) change slightly as follows:

$$4\sqrt{3}\,IA_2\sqrt{12-(L/L_{s1})^2}-3RB_2\{(L/L_{s1})^2-8\}$$
$$+4\sqrt{3}\,IC_2(\mu_2/\mu_1)\sqrt{12-(h_2/h_1)^2(L/L_{s1})^2}$$
$$+3RD_2(\mu_2/\mu_1)\{(h_2/h_1)^2(L/L_{s1})^2-8\}$$

$$=-\frac{\pi(c/L_{s1})}{(L/L_{s1})}[2A_1\{2(L/L_{s1})^2-9\}+3B_1\{6-(L/L_{s1})^2\}\sqrt{(L/L_{s1})^2-1}$$
$$-2C_1(\mu_2/\mu_1)\{2(h_2/h_1)^2(L/L_{s1})^2-9\}$$
$$+3D_1(\mu_2/\mu_1)\{6-(h_2/h_1)^2(L/L_{s1})^2\}\sqrt{(h_2/h_1)^2(L/L_{s1})^2-1}\,,$$
$$-4\sqrt{3}\,RA_2\sqrt{12-(L/L_{s1})^2}-3IB_2\{(L/L_{s1})^2-8\}$$
$$-4\sqrt{3}\,RC_2(\mu_2/\mu_1)\sqrt{12-(h_2/h_1)(L/L_{s1})^2}$$
$$+3ID_2(\mu_2/\mu_1)\{(h_2/h_1)^2(L/L_{s1})^2-8\}=0\,,$$

$$IA_2\sqrt{12-(L/L_{s1})^2}+2\sqrt{3}\,RB_2+IC_2\sqrt{12-(h_2/h_1)^2(L/L_{s1})^2}-2\sqrt{3}\,RD_2$$
$$=-\frac{\pi(c/L_{s1})}{\sqrt{3}\,(L/L_{s1})}[A_1\{(L/L_{s1})^2-3\}+3B_1\sqrt{(L/L_{s1})^2-1}$$
$$-C_1\{(h_2/h_1)^2(L/L_{s1})^2-3\}+3D_1\sqrt{(h_2/h_1)^2(L/L_{s1})^2-1}\,]\,,$$

$$-RA_2\sqrt{12-(L/L_{s1})^2}+2\sqrt{3}\,IB_2-RC_2\sqrt{12-(h_2/h_1)^2(L/L_{s1})^2}-2\sqrt{3}\,ID_2=0.$$

(i)–(4) $2.667>L/L_{s1}\geq 2.309$

In this interval, the third, fourth, fifth and sixth equations in (i)–(3) change slightly as follows:

$$3RA_2\{(L/L_{s1})^2-8\}+12RB_2\sqrt{(L/L_{s1})^2-4}-3RC_2(\mu_2/\mu_1)\{(h_2/h_1)^2(L/L_{s1})^2-8\}$$
$$+12ID_2(\mu_2/\mu_1)\sqrt{4-(h_2/h_1)^2(L/L_{s1})^2}$$
$$=-\frac{\pi(c/L_{s1})}{\sqrt{3}\,(L/L_{s1})}[3A_1\{(L/L_{s1})^2-6\}\sqrt{(L/L_{s1})^2-3}+6\sqrt{3}\,B_1\{2(L/L_{s1})^2-3\}$$
$$+3C_1(\mu_2/\mu_1)\{(h_2/h_1)^2(L/L_{s1})^2-6\}\sqrt{(h_2/h_1)^2(L/L_{s1})^2-3}$$
$$-6\sqrt{3}\,D_1(\mu_2/\mu_1)\{2(h_2/h_1)^2(L/L_{s1})^2-3\}\,]\,,$$

$$3IA_2\{(L/L_{s1})^2-8\}+12IB_2\sqrt{(L/L_{s1})^2-4}-3IC_2(\mu_2/\mu_1)\{(h_2/h_1)^2(L/L_{s1})^2-8\}$$
$$-12RD_2(\mu_2/\mu_1)\sqrt{4-(h_2/h_1)^2(L/L_{s1})^2}=0\,,$$

$$2RA_2-RB_2\sqrt{(L/L_{s1})^2-4}-2RC_2-ID_2\sqrt{4-(h_2/h_1)^2(L/L_{s1})^2}$$
$$=-\frac{\pi(c/L_{s1})}{\sqrt{3}\,(L/L_{s1})}[A_1\sqrt{(L/L_{s1})^2-3}-\sqrt{3}\,B_1\{(L/L_{s1})^2-1\}$$
$$+C_1\sqrt{(h_2/h_1)^2(L/L_{s1})^2-3}+\sqrt{3}\,D_1\{(h_2/h_1)^2(L/L_{s1})^2-1\}\,]\,,$$

$$2IA_2-IB_2\sqrt{(L/L_{s1})^2-4}-2IC_2+RD_2\sqrt{4-(h_2/h_1)^2(L/L_{s1})^2}=0\,.$$

For L/L_{s1} smaller than 2.309 A_1, B_1, etc. become complex numbers and are written as $A_1=RA_1+iIA_1$, etc.

(ii)-(1) $2.309>L/L_{s1}\geq 2$

$$
\begin{aligned}
&4\sqrt{3}\,IA_2\sqrt{12-(L/L_{s1})^2}-3RB_2\{(L/L_{s1})^2-8\}\\
&\quad+4\sqrt{3}\,IC_2(\mu_2/\mu_1)\sqrt{12-(h_2/h_1)^2(L/L_{s1})^2}\\
&\quad+3RD_2(\mu_2/\mu_1)\{(h_2/h_1)^2(L/L_{s1})^2-8\}\\
&=-\frac{\pi(c/L_{s1})}{(L/L_{s1})}[2IA_1\{2(L/L_{s1})^2-9\}+3IB_1\{6-(L/L_{s1})^2\}\sqrt{(L/L_{s1})^2-1}\\
&\qquad-2IC_1(\mu_2/\mu_1)\{2(h_2/h_1)^2(L/L_{s1})^2-9\}\\
&\qquad+3ID_1(\mu_2/\mu_1)\{6-(h_2/h_1)^2(L/L_{s1})^2\}\sqrt{(h_2/h_1)^2(L/L_{s1})^2-1}\,],
\end{aligned}
$$

$$
\begin{aligned}
&-4\sqrt{3}\,RA_2\sqrt{12-(L/L_{s1})^2}-3IB_2\{(L/L_{s1})^2-8\}\\
&\quad-4\sqrt{3}\,RC_2(\mu_2/\mu_1)\sqrt{12-(h_2/h_1)^2(L/L_{s1})^2}\\
&\quad+3ID_2(\mu_2/\mu_1)\{(h_2/h_1)^2(L/L_{s1})^2-8\}\\
&=\frac{\pi(c/L_{s1})}{(L/L_{s1})}[2RA_1\{2(L/L_{s1})^2-9\}+3RB_1\{6-(L/L_{s1})^2\}\sqrt{(L/L_{s1})^2-1}\\
&\qquad-2RC_1(\mu_2/\mu_1)\{2(h_2/h_1)^2(L/L_{s1})^2-9\}\\
&\qquad+3RD_1(\mu_2/\mu_1)\{6-(h_2/h_1)^2(L/L_{s1})^2\}\sqrt{(h_2/h_1)^2(L/L_{s1})^2-1}\,],
\end{aligned}
$$

$$
\begin{aligned}
&-3RA_2\{(L/L_{s1})^2-8\}-12RB_2\sqrt{(L/L_{s1})^2-4}+3RC_2(\mu_2/\mu_1)\{(h_2/h_1)^2(L/L_{s1})^2-8\}\\
&\quad-12(\mu_2/\mu_1)ID_2\sqrt{4-(h_2/h_1)^2(L/L_{s1})^2}\\
&=\frac{\pi(c/L_{s1})}{\sqrt{3}\,(L/L_{s1})}[3IA_1\{(L/L_{s1})^2-6\}\sqrt{(L/L_{s1})^2-3}+6\sqrt{3}\,IB_1\{2(L/L_{s1})^2-3\}\\
&\qquad-3RC_1(\mu_2/\mu_1)\{(h_2/h_1)^2(L/L_{s1})^2-6\}\sqrt{3-(h_2/h_1)^2(L/L_{s1})^2}\\
&\qquad-6\sqrt{3}\,ID_1(\mu_2/\mu_1)\{2(h_2/h_1)^2(L/L_{s1})^2-3\}\,],
\end{aligned}
$$

$$
\begin{aligned}
&-3IA_2\{(L/L_{s1})^2-8\}-12IB_2\sqrt{(L/L_{s1})^2-4}+3IC_2(\mu_2/\mu_1)\{(h_2/h_1)^2(L/L_{s1})^2-8\}\\
&\quad+12RD_2(\mu_2/\mu_1)\sqrt{4-(h_2/h_1)^2(L/L_{s1})^2}\\
&=\frac{\pi(c/L_{s1})}{\sqrt{3}\,(L/L_{s1})}[-3RA_1\{(L/L_{s1})^2-6\}\sqrt{(L/L_{s1})^2-3}\\
&\qquad-6\sqrt{3}\,RB_1\{2(L/L_{s1})^2-3\}
\end{aligned}
$$

$$-3IC_1(\mu_2/\mu_1)\{(h_2/h_1)^2(L/L_{s1})^2-6\}\sqrt{3-(h_2/h_1)^2(L/L_{s1})^2}$$
$$+6\sqrt{3}\,RD_1(\mu_2/\mu_1)\{2(h_2/h_1)^2(L/L_{s1})^2-3\}],$$

$$2RA_2-RB_2\sqrt{(L/L_{s1})^2-4}\,-2RC_2-ID_2\sqrt{4-(h_2/h_1)^2(L/L_{s1})^2}$$
$$=\frac{\pi(c/L_{s1})}{\sqrt{3}\,(L/L_{s1})}[-IA_1\sqrt{(L/L_{s1})^2-3}+\sqrt{3}\,IB_1\{(L/L_{s1})^2-1\}$$
$$+RC_1\sqrt{3-(h_2/h_1)^2(L/L_{s1})^2}-\sqrt{3}\,ID_1\{(h_2/h_1)^2(L/L_{s1})^2-1\}],$$

$$2IA_2-IB_2\sqrt{(L/L_{s1})^2-4}\,-2IC_2+RD_2\sqrt{4-(h_2/h_1)^2(L/L_{s1})^2}$$
$$=\frac{\pi(c/L_{s1})}{\sqrt{3}\,(L/L_{s1})}[RA_1\sqrt{(L/L_{s1})^2-3}\,-\sqrt{3}\,RB_1\{(L/L_{s1})^2-1\}$$
$$+IC_1\sqrt{3-(h_2/h_1)^2(L/L_{s1})^2}+\sqrt{3}\,RD_1\{(h_2/h_1)^2(L/L_{s1})^2-1\}],$$

$$IA_2\sqrt{12-(L/L_{s1})^2}+2\sqrt{3}\,RB_2+IC_2\sqrt{12-(h_2/h_1)^2(L/L_{s1})^2}-2\sqrt{3}\,RD_2$$
$$=-\frac{\pi(c/L_{s1})}{\sqrt{3}\,(L/L_{s1})}[IA_1\{(L/L_{s1})^2-3\}+3IB_1\sqrt{(L/L_{s1})^2-1}$$
$$-IC_1\{(h_2/h_1)^2(L/L_{s1})^2-3\}+3ID_1\sqrt{(h_2/h_1)^2(L/L_{s1})^2-1}],$$

$$-RA_2\sqrt{12-(L/L_{s1})^2}+2\sqrt{3}\,IB_2-RC_2\sqrt{12-(h_2/h_1)^2(L/L_{s1})^2}-2\sqrt{3}\,ID_2$$
$$=\frac{\pi(c/L_{s1})}{\sqrt{3}\,(L/L_{s1})}[RA_1\{(L/L_{s1})^2-3\}+3RB_1\sqrt{(L/L_{s1})^2-1}$$
$$-RC_1\{(h_2/h_1)^2(L/L_{s1})^2-3\}+3RD_1\sqrt{(h_2/h_1)^2(L/L_{s1})^2-1}].$$

(ii)–(2) $2>L/L_{s1}\geq 1.732$

In this interval, the third, fourth, fifth and sixth equations in (ii)–(1) change slightly as follows:

$$-3RA_2\{(L/L_{s1})^2-8\}-12IB_2\sqrt{4-(L/L_{s1})^2}+3RC_2(\mu_2/\mu_1)\{(h_2/h_1)^2(L/L_{s1})^2-8\}$$
$$-12ID_2(\mu_2/\mu_1)\sqrt{4-(h_2/h_1)^2(L/L_{s1})^2}$$
$$=\frac{\pi(c/L_{s1})}{\sqrt{3}\,(L/L_{s1})}[3IA_1\{(L/L_{s1})^2-6\}\sqrt{(L/L_{s1})^2-3}+6\sqrt{3}\,IB_1\{2(L/L_{s1})^2-3\}$$
$$-3RC_1(\mu_2/\mu_1)\{(h_2/h_1)^2(L/L_{s1})^2-6\}\sqrt{3-(h_2/h_1)^2(L/L_{s1})^2}$$
$$-6\sqrt{3}\,ID_1(\mu_2/\mu_1)\{2(h_2/h_1)^2(L/L_{s1})^2-3\}],$$

$$-3IA_2\{(L/L_{s1})^2-8\}+12RB_2\sqrt{4-(L/L_{s1})^2}+3IC_2(\mu_2/\mu_1)\{(h_2/h_1)^2(L/L_{s1})^2-8\}$$
$$+12RD_2(\mu_2/\mu_1)\sqrt{4-(h_2/h_1)^2(L/L_{s1})^2}$$

$$=\frac{\pi(c/L_{s1})}{\sqrt{3}\,(L/L_{s1})}[-3RA_1\{(L/L_{s1})^2-6\}\sqrt{(L/L_{s1})^2-3}$$
$$-6\sqrt{3}\,RB_1\{2(L/L_{s1})^2-3\}$$
$$-3IC_1(\mu_2/\mu_1)\{(h_2/h_1)^2(L/L_{s1})^2-6\}\sqrt{3-(h_2/h_1)^2(L/L_{s1})^2}$$
$$+6\sqrt{3}\,RD_1(\mu_2/\mu_1)\{2(h_2/h_1)^2(L/L_{s1})^2-3\}],$$

$$2RA_2-IB_2\sqrt{4-(L/L_{s1})^2}-2RC_2-ID_2\sqrt{4-(h_2/h_1)^2(L/L_{s1})^2}$$
$$=\frac{\pi(c/L_{s1})}{\sqrt{3}\,(L/L_{s1})}[-IA_1\sqrt{(L/L_{s1})^2-3}+\sqrt{3}\,IB_1\{(L/L_{s1})^2-1\}$$
$$+RC_1\sqrt{3-(h_2/h_1)^2(L/L_{s1})^2}-\sqrt{3}\,ID_1\{(h_2/h_1)^2(L/L_{s1})^2-1\}],$$

$$2IA_2+RB_2\sqrt{4-(L/L_{s1})^2}-2IC_2+RD_2\sqrt{4-(h_2/h_1)^2(L/L_{s1})^2}$$
$$=\frac{\pi(c/L_{s1})}{\sqrt{3}\,(L/L_{s1})}[RA_1\sqrt{(L/L_{s1})^2-3}-\sqrt{3}\,RB_1\{(L/L_{s1})^2-1\}$$
$$+IC_1\sqrt{3-(h_2/h_1)^2(L/L_{s1})^2}+\sqrt{3}\,RD_1\{(h_2/h_1)^2(L/L_{s1})^2-1\}].$$

(iii) $1.732>L/L_{s1}\geq 4/3$

The third, fourth, fifth and sixth equations in (ii)–(2) change slightly as in the preceding interval.

$$-3RA_2\{(L/L_{s1})^2-8\}-12IB_2\sqrt{4-(L/L_{s1})^2}+3RC_2(\mu_2/\mu_1)\{(h_2/h_1)^2(L/L_{s1})^2-8\}$$
$$-12ID_2(\mu_2/\mu_1)\sqrt{4-(h_2/h_1)^2(L/L_{s1})^2}$$
$$=-\frac{\pi(c/L_{s1})}{\sqrt{3}\,(L/L_{s1})}[3RA_1\{(L/L_{s1})^2-6\}\sqrt{3-(L/L_{s1})^2}$$
$$-6\sqrt{3}\,IB_1\{2(L/L_{s1})^2-3\}$$
$$+3RC_1(\mu_2/\mu_1)\{(h_2/h_1)^2(L/L_{s1})^2-6\}\sqrt{3-(h_2/h_1)^2(L/L_{s1})^2}$$
$$+6\sqrt{3}\,ID_1(\mu_2/\mu_1)\{2(h_2/h_1)^2(L/L_{s1})^2-3\}],$$

$$-3IA_2\{(L/L_{s1})^2-8\}+12RB_2\sqrt{4-(L/L_{s1})^2}+3IC_2(\mu_2/\mu_1)\{(h_2/h_1)^2(L/L_{s1})^2-8\}$$
$$+12RD_2(\mu_2/\mu_1)\sqrt{4-(h_2/h_1)^2(L/L_{s1})^2}$$
$$=-\frac{\pi(c/L_{s1})}{\sqrt{3}\,(L/L_{s1})}[3IA_1\{(L/L_{s1})^2-6\}\sqrt{3-(L/L_{s1})^2}$$
$$+6\sqrt{3}\,RB_1\{2(L/L_{s1})^2-3\}$$
$$+3IC_1(\mu_2/\mu_1)\{(h_2/h_1)^2(L/L_{s1})^2-6\}\sqrt{3-(h_2/h_1)^2(L/L_{s1})^2}$$

$$-6\sqrt{3}\,RD_1(\mu_2/\mu_1)\{2(h_2/h_1)^2(L/L_{s1})^2-3\}]\,,$$

$$2RA_2-IB_2\sqrt{4-(L/L_{s1})^2}-2RC_2-ID_2\sqrt{4-(h_2/h_1)^2(L/L_{s1})^2}$$
$$=\frac{\pi(c/L_{s1})}{\sqrt{3}\,(L/L_{s1})}[RA_1\sqrt{3-(L/L_{s1})^2}+\sqrt{3}\,IB_1\{(L/L_{s1})^2-1\}$$
$$+RC_1\sqrt{3-(h_2/h_1)^2(L/L_{s1})^2}-\sqrt{3}\,ID_1\{(h_2/h_1)^2(L/L_{s1})^2-1\}]\,,$$

$$2IA_2+RB_2\sqrt{4-(L/L_{s1})^2}-2IC_2+RD_2\sqrt{4-(h_2/h_1)^2(L/L_{s1})^2}$$
$$=\frac{\pi(c/L_{s1})}{\sqrt{3}\,(L/L_{s1})}[IA_1\sqrt{3-(L/L_{s1})^2}-\sqrt{3}\,RB_1\{(L/L_{s1})^2-1\}$$
$$+IC_1\sqrt{3-(h_2/h_1)^2(L/L_{s1})^2}+\sqrt{3}\,RD_1\{(h_2/h_1)^2(L/L_{s1})^2-1\}]\,,$$

(iv) $4/3>L/L_{s1}\geq 1$

In this interval, the first, second, seventh and eighth equations in (iii) change slightly as follows:

$$4\sqrt{3}\,IA_2\sqrt{12-(L/L_{s1})^2}-3RB_2\{(L/L_{s1})^2-8\}$$
$$+4\sqrt{3}\,IC_2(\mu_2/\mu_1)\sqrt{12-(h_2/h_1)^2(L/L_{s1})^2}$$
$$+3RD_2(\mu_2/\mu_1)\{(h_2/h_1)^2(L/L_{s1})^2-8\}$$
$$=-\frac{\pi(c/L_{s1})}{(L/L_{s1})}[2IA_1\{2(L/L_{s1})^2-9\}+3IB_1\{6-(L/L_{s1})^2\}\sqrt{(L/L_{s1})^2-1}$$
$$-2IC_1(\mu_2/\mu_1)\{2(h_2/h_1)^2(L/L_{s1})^2-9\}$$
$$-3RD_1(\mu_2/\mu_1)\{6-(h_2/h_1)^2(L/L_{s1})^2\}\sqrt{1-(h_2/h_1)^2(L/L_{s1})^2}]\,,$$

$$-4\sqrt{3}\,RA_2\sqrt{12-(L/L_{s1})^2}-3IB_2\{(L/L_{s1})^2-8\}$$
$$-4\sqrt{3}\,RC_2(\mu_2/\mu_1)\sqrt{12-(h_2/h_1)^2(L/L_{s1})^2}$$
$$+3ID_2(\mu_2/\mu_1)\{(h_2/h_1)^2(L/L_{s1})^2-8\}$$
$$=\frac{\pi(c/L_{s1})}{(L/L_{s1})}[2RA_1\{2(L/L_{s1})^2-9\}+3RB_1\{6-(L/L_{s1})^2\}\sqrt{(L/L_{s1})^2-1}$$
$$-2RC_1(\mu_2/\mu_1)\{2(h_2/h_1)^2(L/L_{s1})^2-9\}$$
$$+3ID_1(\mu_2/\mu_1)\{6-(h_2/h_1)^2(L/L_{s1})^2\}\sqrt{1-(h_2/h_1)^2(L/L_{s1})^2}]\,,$$

$$IA_2\sqrt{12-(L/L_{s1})^2}+2\sqrt{3}\,RB_2+IC_2\sqrt{12-(h_2/h_1)^2(L/L_{s1})^2}-2\sqrt{3}\,RD_2$$
$$=-\frac{\pi(c/L_{s1})}{\sqrt{3}\,(L/L_{s1})}[IA_1\{(L/L_{s1})^2-3\}+3IB_1\sqrt{(L/L_{s1})^2-1}$$

$$-IC_1\{(h_2/h_1)^2(L/L_{s1})^2-3\}-3RD_1\sqrt{1-(h_2/h_1)^2(L/L_{s1})^2}\,],$$

$$-RA_2\sqrt{12-(L/L_{s1})^2}+2\sqrt{3}\,IB_2-RC_2\sqrt{12-(h_2/h_1)^2(L/L_{s1})^2}-2\sqrt{3}\,ID_2$$

$$=\frac{\pi(c/L_{s1})}{\sqrt{3}\,(L/L_{s1})}[RA_1\{(L/L_{s1})^2-3\}+3RB_1\sqrt{(L/L_{s1})^2-1}$$

$$-RC_1\{(h_2/h_1)^2(L/L_{s1})^2-3\}+3ID_1\sqrt{1-(h_2/h_1)^2(L/L_{s1})^2}\,].$$

(v) $1>L/L_{s1}$

In this interval, the first, second, seventh and eighth equations in (iv) change slightly as follows:

$$4\sqrt{3}\,IA_2\sqrt{12-(L/L_{s1})^2}-3RB_2\{(L/L_{s1})^2-8\}$$

$$+4\sqrt{3}\,IC_2(\mu_2/\mu_1)\sqrt{12-(h_2/h_1)^2(L/L_{s1})^2}$$

$$+3RD_2(\mu_2/\mu_1)\{(h_2/h_1)^2(L/L_{s1})^2-8\}$$

$$=-\frac{\pi(c/L_{s1})}{(L/L_{s1})}[2IA_1\{2(L/L_{s1})^2-9\}-3RB_1\{6-(L/L_{s1})^2\}\sqrt{1-(L/L_{s1})^2}$$

$$-2IC_1(\mu_2/\mu_1)\{2(h_2/h_1)^2(L/L_{s1})^2-9\}$$

$$-3RD_1(\mu_2/\mu_1)\{6-(h_2/h_1)^2(L/L_{s1})^2\}\sqrt{1-(h_2/h_1)^2(L/L_{s1})^2}\,],$$

$$-4\sqrt{3}\,RA_2\sqrt{12-(L/L_{s1})^2}-3IB_2\{(L/L_{s1})^2-8\}$$

$$-4\sqrt{3}\,RC_2(\mu_2/\mu_1)\sqrt{12-(h_2/h_1)^2(L/L_{s1})^2}$$

$$+3ID_2(\mu_2/\mu_1)\{(h_2/h_1)^2(L/L_{s1})^2-8\}$$

$$=\frac{\pi(c/L_{s1})}{(L/L_{s1})}[2RA_1\{2(L/L_{s1})^2-9\}+3IB_1\{6-(L/L_{s1})^2\}\sqrt{1-(L/L_{s1})^2}$$

$$-2RC_1(\mu_2/\mu_1)\{2(h_2/h_1)^2(L/L_{s1})^2-9\}$$

$$+3ID_1(\mu_2/\mu_1)\{6-(h_2/h_1)^2(L/L_{s1})^2\}\sqrt{1-(h_2/h_1)^2(L/L_{s1})^2}\,],$$

$$IA_2\sqrt{12-(L/L_{s1})^2}+2\sqrt{3}\,RB_2+IC_2\sqrt{12-(h_2/h_1)^2(L/L_{s1})^2}-2\sqrt{3}\,RD_2$$

$$=-\frac{\pi(c/L_{s1})}{\sqrt{3}\,(L/L_{s1})}[IA_1\{(L/L_{s1})^2-3\}-3RB_1\sqrt{1-(L/L_{s1})^2}$$

$$-IC_1\{(h_2/h_1)^2(L/L_{s1})^2-3\}-3RD_1\sqrt{1-(h_2/h_1)^2(L/L_{s1})^2}\,],$$

$$-RA_2\sqrt{12-(L/L_{s1})^2}+2\sqrt{3}\,IB_2-RC_2\sqrt{12-(h_2/h_1)^2(L/L_{s1})^2}-2\sqrt{3}\,ID_2$$

$$=\frac{\pi(c/L_{s1})}{\sqrt{3}\,(L/L_{s1})}[RA_1\{(L/L_{s1})^2-3\}+3IB_1\sqrt{1-(L/L_{s1})^2}$$

$$-RC_1\{(h_2/h_1)^2(L/L_{s1})^2-3\}+3ID_1\sqrt{1-(h_2/h_1)^2(L/L_{s1})^2}\,].$$

Results obtained are given in Figs. 19 through 34 and Tables 6 through 10.

In Fig. 19 and Fig. 20, the following tendencies concerning $|B_0|$ and $|D_0|$ are clearly seen.

(1) The variations of $|B_0|$ and $|D_0|$ with L/L_{s1} (that is, the ratio of the wave length of a corrugated boundary surface to that of an incident wave) are small but larger than in the case of incidence of the SH or P wave.

(2) It is also ascertained in this case, as in the cases of the incidence of SH and P waves, that the influence of corrugation is larger on reflected waves than on refracted waves. This is also shown clearly in Fig. 21. From Fig. 21, we can see that the variation of $|B_0|$ with c/L_{s1}, the ratio of amplitude of corrugation to the wave length of the incident wave, is much larger than that of $|D_0|$. This result is also confirmed by Fig. 29.

(3) The effect of corrugation increases with increasing c/L_{s1} in such a manner that $|B_0|$ decreases and $|D_0|$ increases with increasing c/L_{s1}.

(4) Both $|B_0|$ and $|D_0|$ have a general tendency to increase with decreasing L/L_{s1}. Moreover, the larger the amplitude of the corrugated boundary surface the more remarkable is this increasing tendency. This feature is also observed in the case of incidence of the SH wave.

(5) At $L/L_{s1}=2.309$ or at $L=L_{p2}$, both $|B_0|$ and $|D_0|$ have a steep peak.

(6) In the neighbourhood of $L/L_{s1}=2$, both $|B_0|$ and $|D_0|$ reach minimum.

(7) In the interval between $L/L_{s1}=2$, i.e. $L=2L_{s1}$ and $L/L_{s1}=1.732$, i.e. $L=L_{p1}$, both $|B_0|$ and $|D_0|$ increase rapidly especially for $c/L_{s1}=0.10$.

(8) At $L/L_{s1}=4/3$, i.e. $L=L_{s2}$ both $|B_0|$ and $|D_0|$, especially $|B_0|$ have a steep peak.

(9) It is conspicuous that a very sharp minimum appears in both $|B_0|$ and $|D_0|$ at the value of L just below L_{s2}. This is also common to the cases of the incidence of SH and SV waves and is more remarkable in this case than in the case of incidence of the SH wave. Corresponding to this minimum, all irregular waves have a sharp maximum.

(10) For L/L_{s1} below about 1, the increasing tendency appears in both $|B_0|$ and $|D_0|$.

From Figs. 22 through 25, we can see the following tendencies in $|A_1|$, $|B_1|$, $|C_1|$ and $|D_1|$.

(11) The sharp maxima common to all irregular waves with a

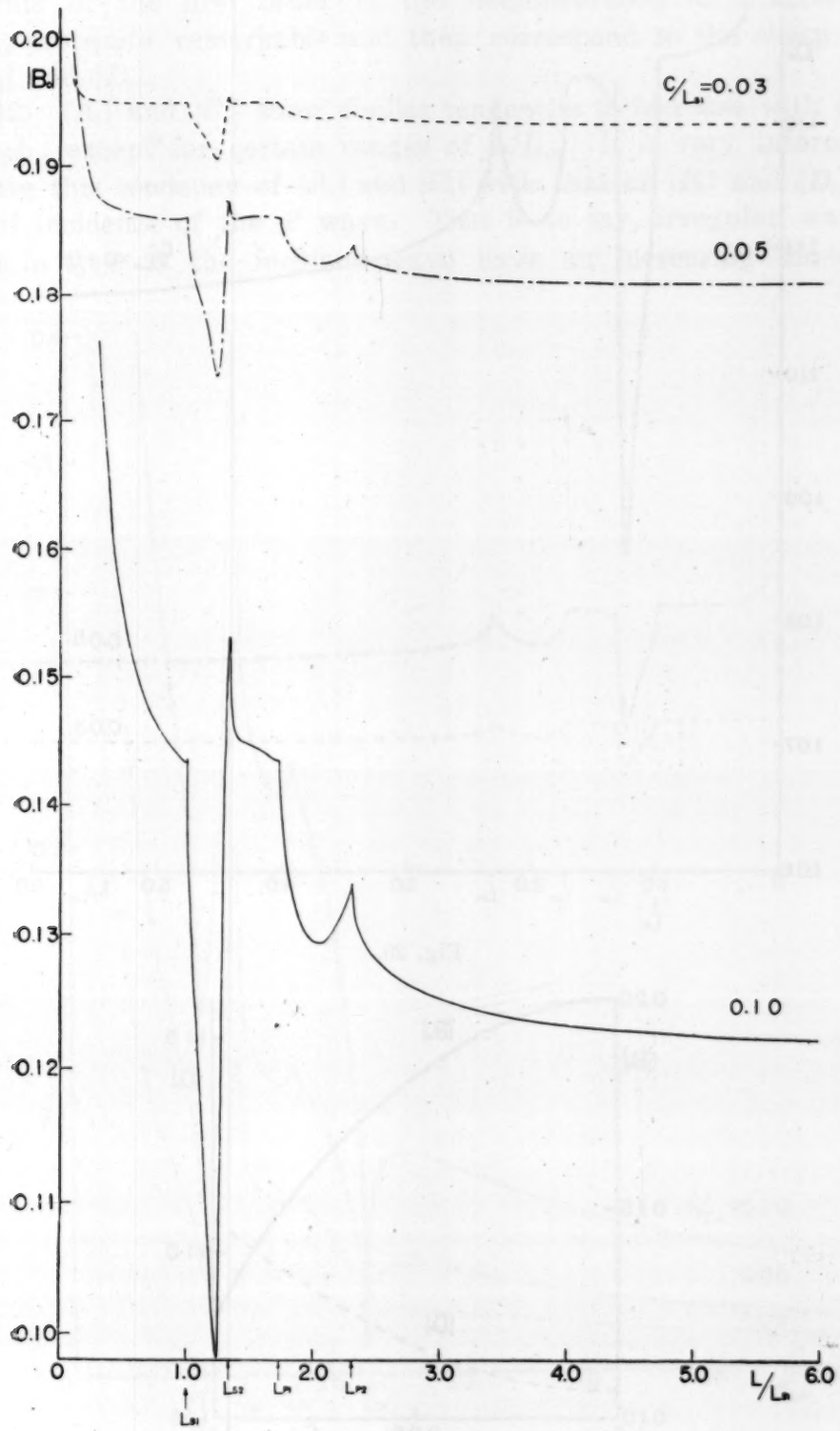
0.20
|B|
0.19
0.18
0.17
0.16
0.15
0.14
0.13
0.12
0.11
0.10
C/L₀₁=0.03
0.05
0.10
0
1.0
2.0
3.0
4.0
5.0
6.0
L/L₀

Fig. 19.

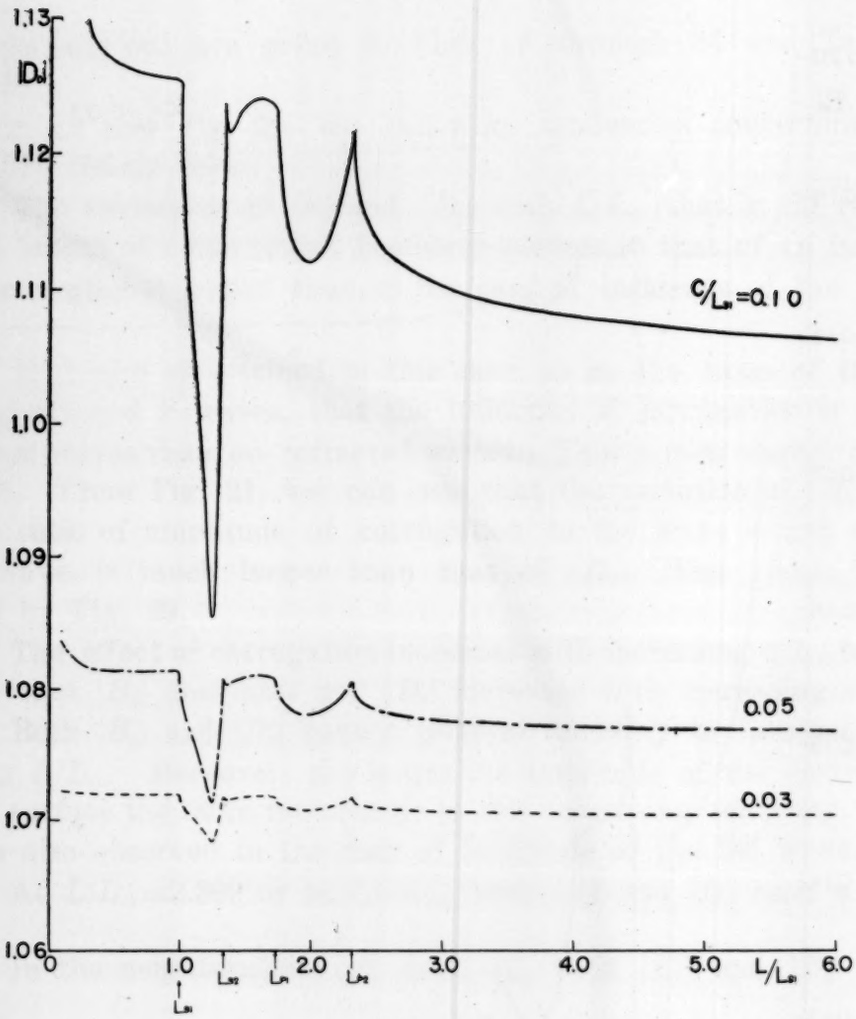
1.13
|D₀|
1.12
1.11
1.10
1.09
1.08
1.07
1.06
C/L₀=0.10
0.05
0.03
0
1.0
2.0
3.0
4.0
5.0
6.0
L/L₀

Fig. 20.

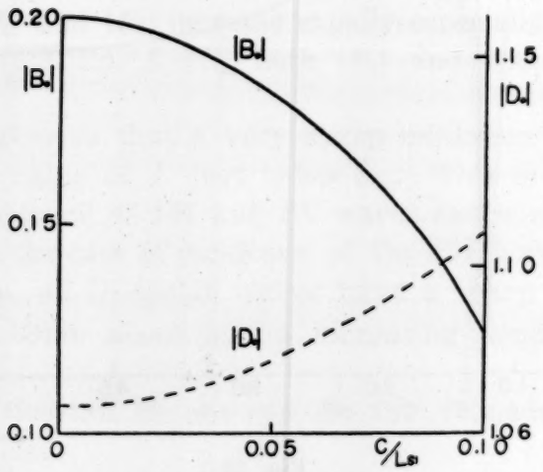
0.20
|B₀|
0.15
0.10
|B₀|
|D₀|
1.15
1.10
1.06
0
0.05
0.10
C/L₀

Fig. 21.

spectrum of the first order in the neighbourhood of $L/L_{s1}=4/3$, i.e. $L=L_{s2}$ are quite remarkable and they correspond to the sharp minima of $|B_0|$ and $|D_0|$.

(12) $|A_1|$ and $|C_1|$ show similar tendencies to increase with decreasing L/L_{s1} except for certain ranges of L/L_{s1}. It is very interesting to compare this tendency of $|A_1|$ and $|C_1|$ with that of $|B_1|$ and $|D_1|$ in the case of incidence of the P wave. That is to say, irregular waves different in type to the incident wave have an increasing tendency in

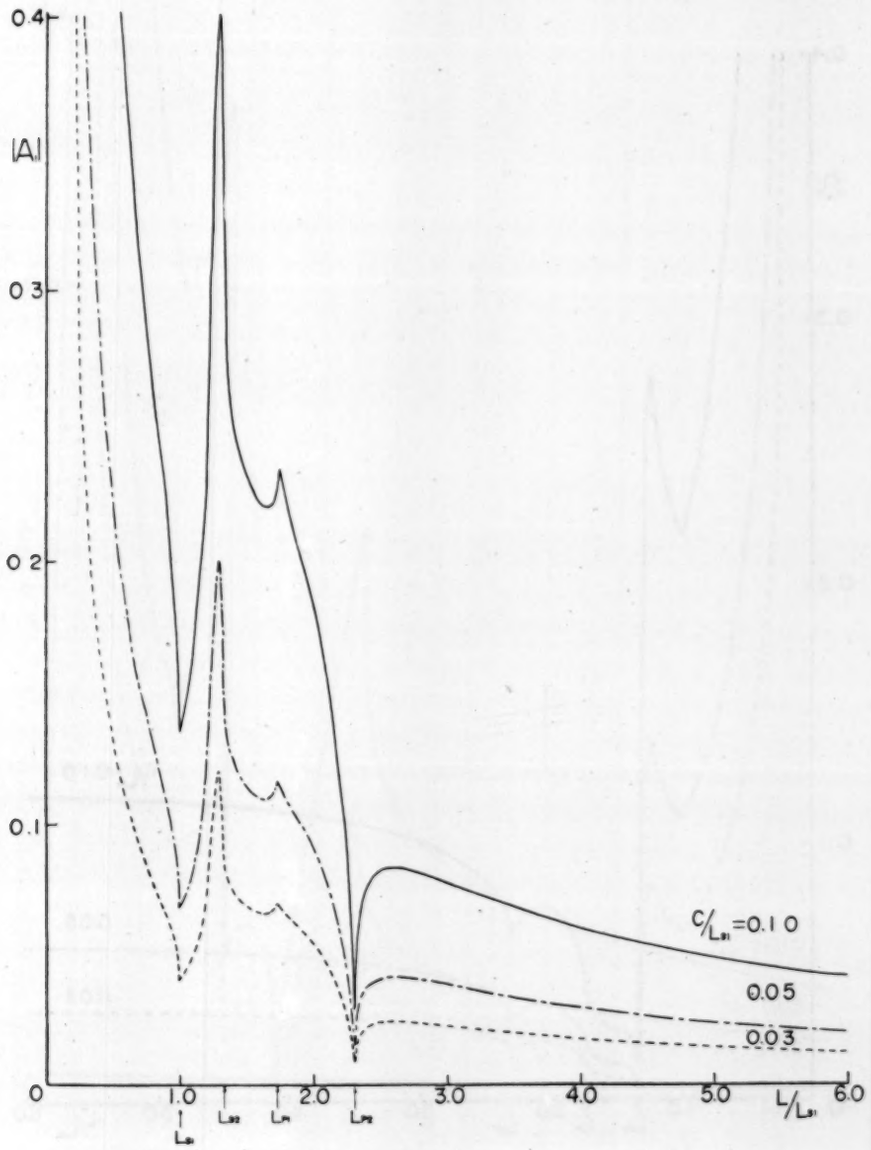

Fig. 22.

general with decreasing L/L_{s1}.

(13) On the contrary, $|B_1|$ and $|D_1|$ decrease as a whole with decreasing L/L_{s1} down to $L/L_{s1}=4/3$ or to $L=L_{s2}$ and to about $L/L_{s1}=1.732$ or to about $L=L_{p1}$ respectively.

(14) For L/L_{s1} smaller than about 1, all irregular waves increase monotonously. This tendency will eventually impair the accuracy of this calculation.

(15) $|A_1|$ has two sharp minima at $L=L_{p2}$ and $L=L_{s1}$ and another small peak at $L=L_{p1}$.

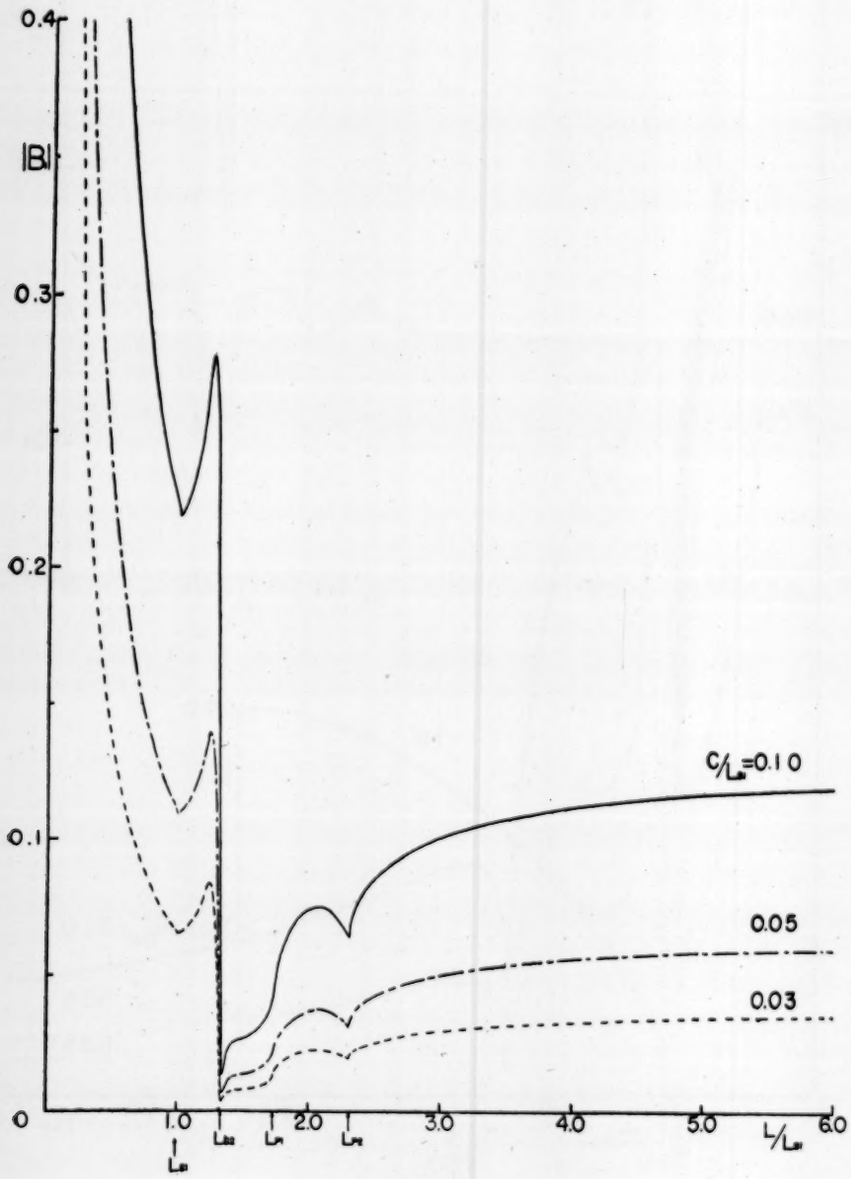

Fig. 23.

(16) $|B_1|$ has a sharp minima at $L=L_{p2}$, $L=L_{s2}$ and $L=L_{s1}$. The minimum at $L=L_{s2}$ is most remarkable and its value is very small.

(17) $|C_1|$ has a sharp maximum at $L=L_{p2}$ and becomes zero at $L=L_{p1}$. In addition to these two abnormal points $|C_1|$ has a sharp minima at $L=L_{s2}$ and near $L=L_{s1}$.

(18) $|D_1|$ is rather simple in comparison with $|A_1|$, $|B_1|$ and $|C_1|$, and has minima in the neighbourhood of $L=L_{p1}$ and $L=L_{s1}$.

(19) For L below L_{p2} some irregular waves become boundary

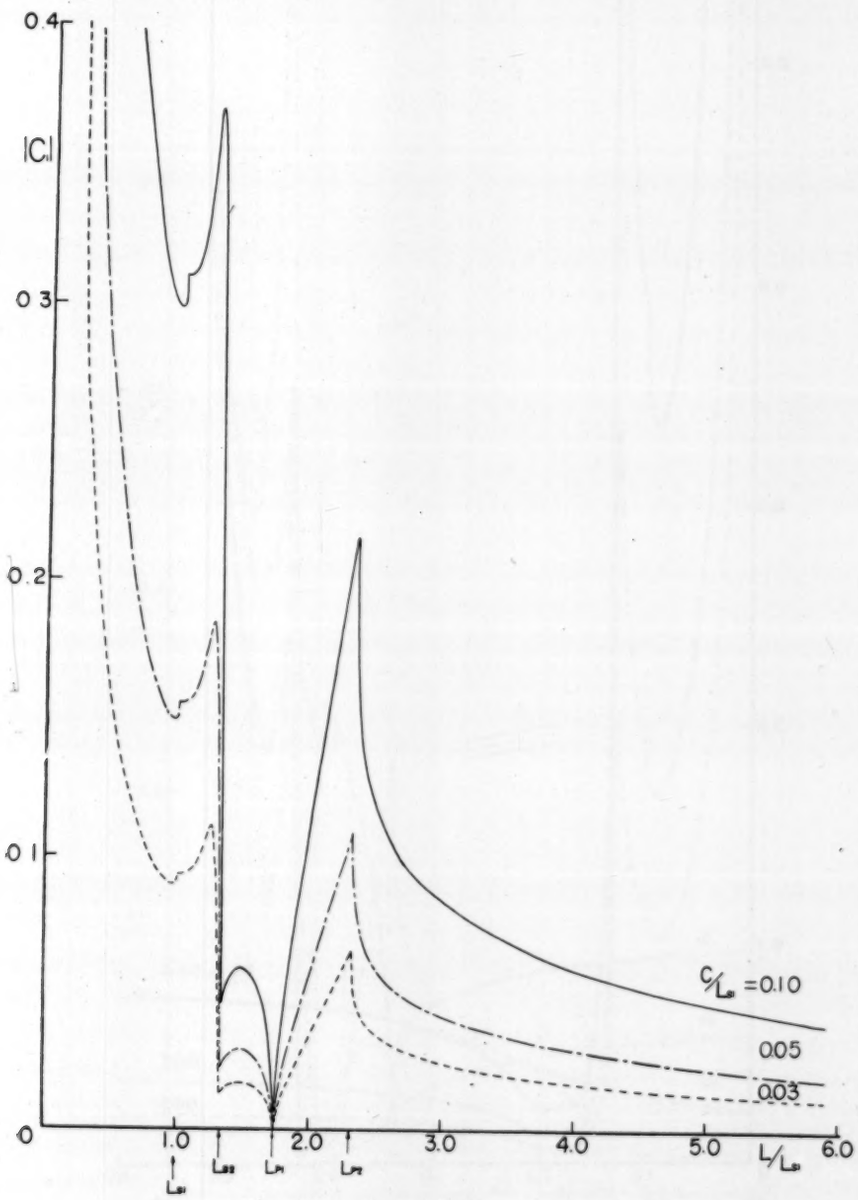

Fig. 24.

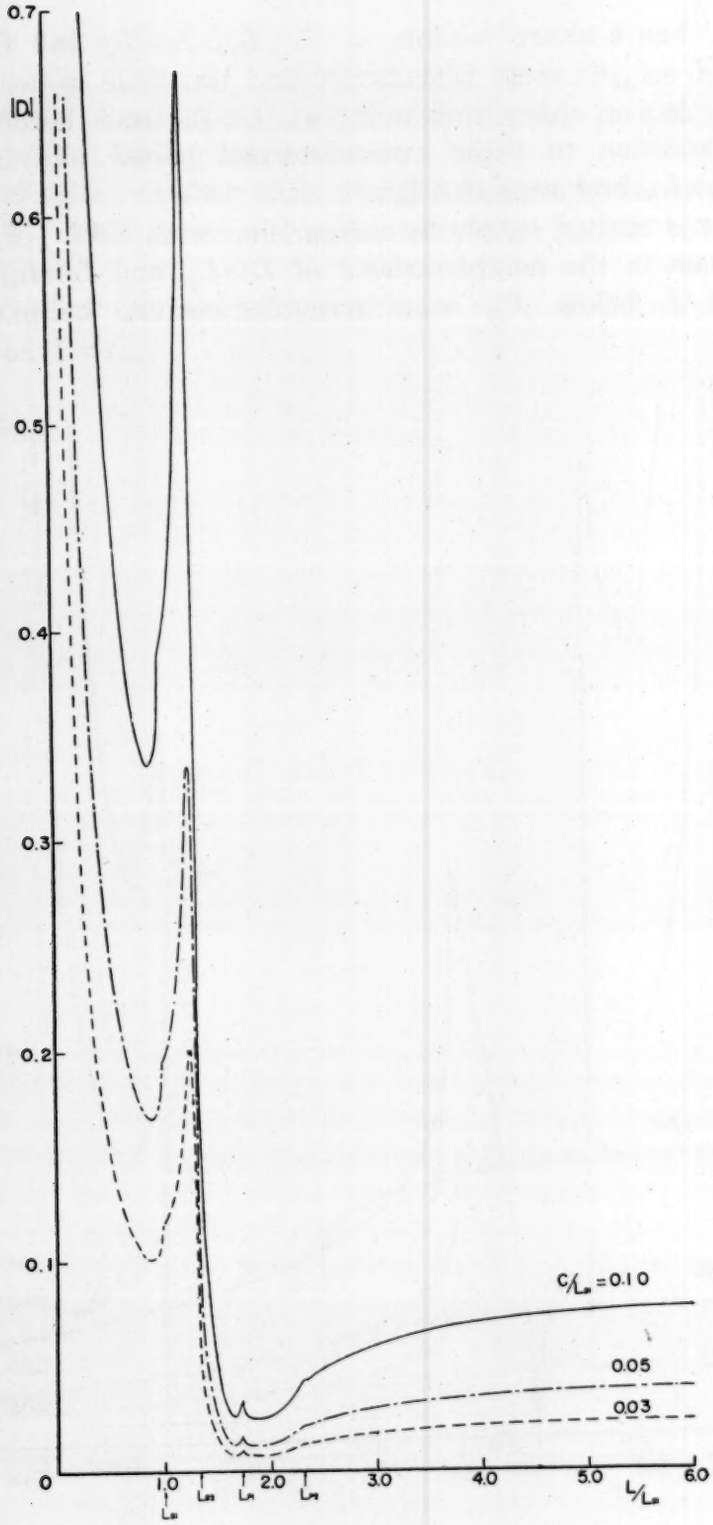

Fig. 25

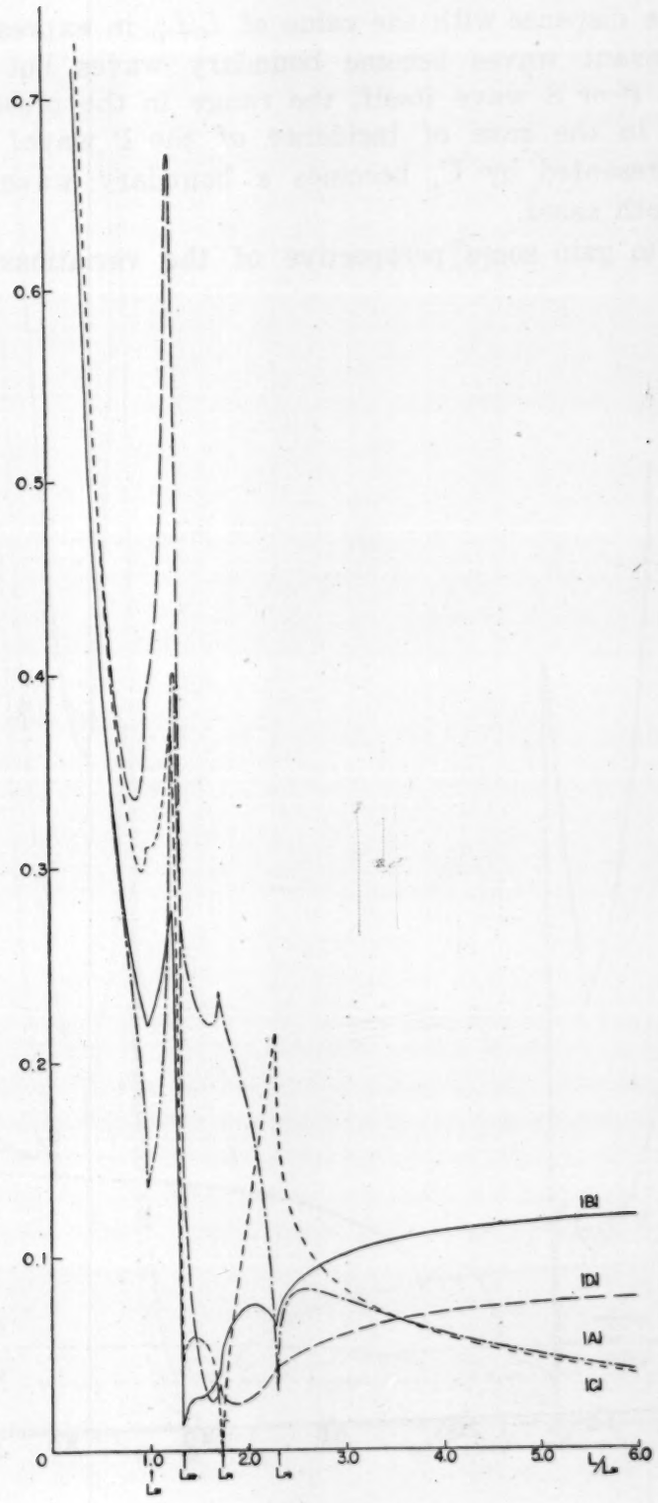

Fig. 26.

waves. If we dispense with the value of L/L_{s1} in expressing the range in which relevant waves become boundary waves but by the wave length of the P or S wave itself, the range in the present case is the same as that in the case of incidence of the P wave. For example, the wave represented by C_1 becomes a boundary wave for L smaller than L_{p2} in both cases.

In order to gain some perspective of the variations of $|A_1|$, $|B_1|$,

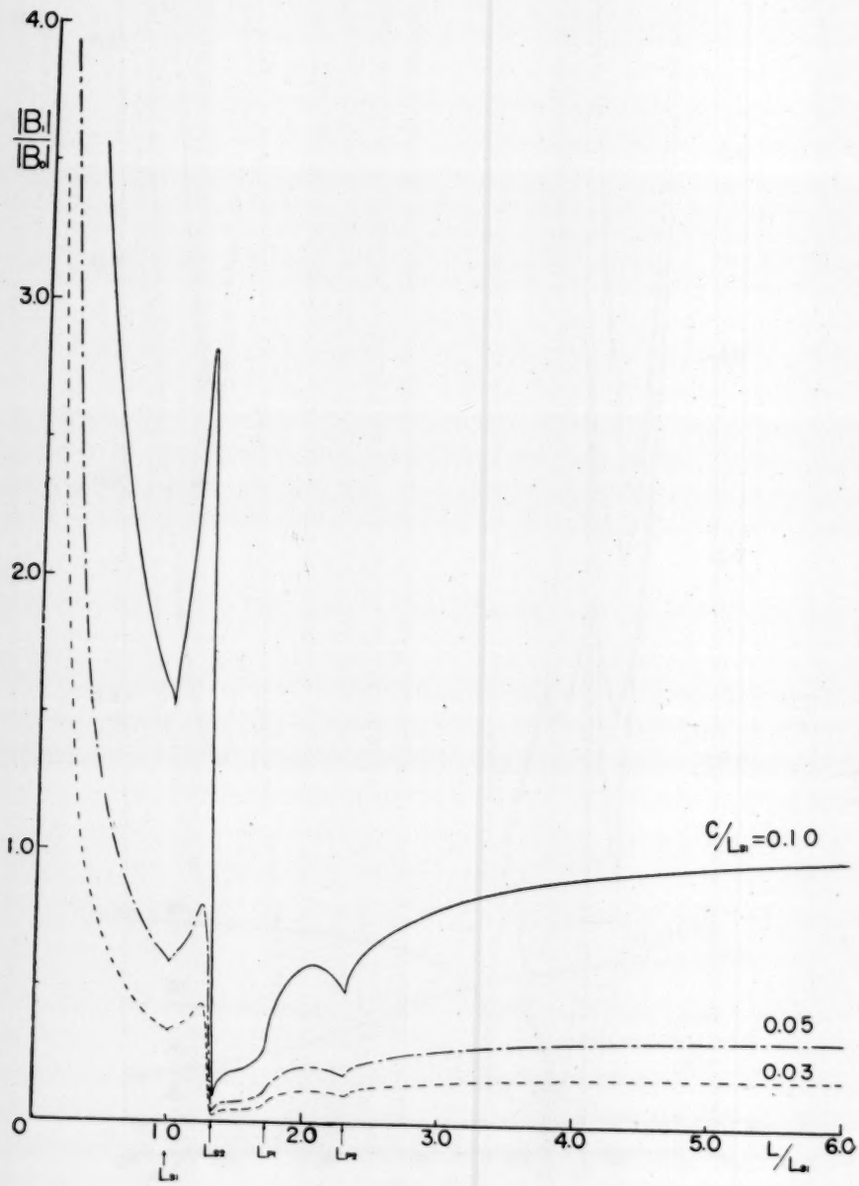

Fig. 27.

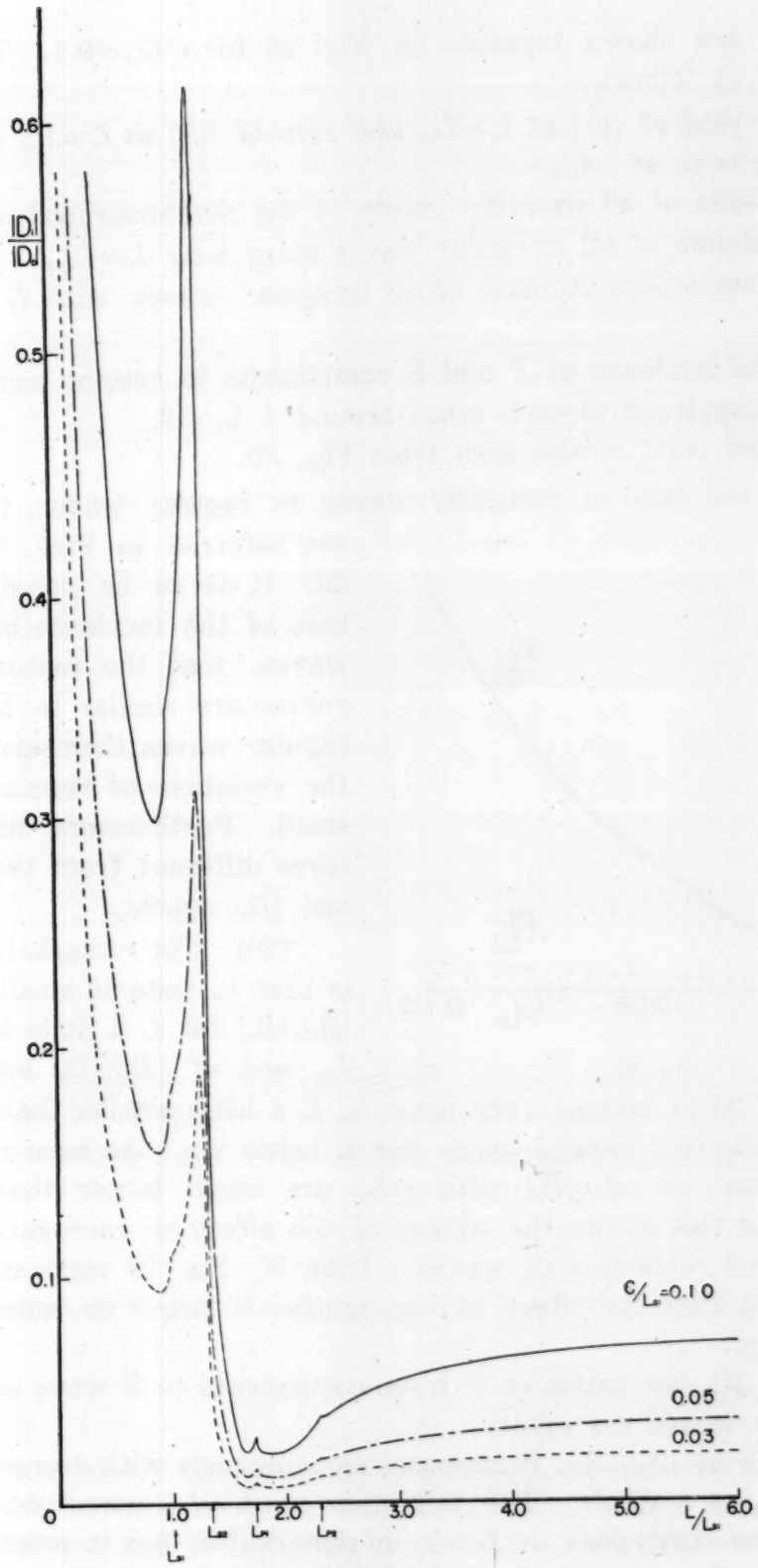

Fig. 28.

etc., they are shown together in Fig. 26 for $c/L_{s1}=0.1$. The notable points are as follows:

(a) a peak of $|C_1|$ at $L=L_{p2}$ and zero of $|C_1|$ at $L=L_{p1}$ corresponding to the peak of $|A_1|$,

(b) peaks of all irregular waves in the neighbourhood of $L=L_{s2}$,

(c) minima of all irregular waves at or near $L=L_{s1}$,

(d) monotonous increase of all irregular waves with L decreasing below L_{s1}.

(e) the tendency of P and S components to become comparable in order of magnitude to each other around $L/L_{s1}=3$.

The last point is also seen from Fig. 30.

As to the ratio of irregular waves to regular waves, the readers are referred to Figs. 27 through 29. It is to be noted as in the case of the incidence of P or SH waves, that the features of the curves are similar to those of irregular waves themselves because the variations of regular ones are small. Furthermore, no new features different from those of $|B_1|$ and $|D_1|$ appear.

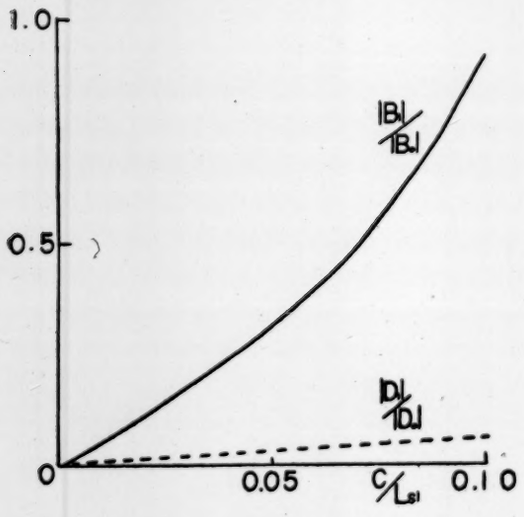

Fig. 29.

(20) The remarkable feature is that in spite of small values of $|B_1|/|B_0|$ for L a little larger than L_{s2} and of $|D_1|/|D_0|$ near $L=L_{p1}$, both these ratios become very large at L a little smaller than L_{s2}. The values of $|B_1|/|B_0|$ become large for L below L_{s2}. As seen in Fig. 29, the variations of $|B_1|/|B_0|$ with c/L_{s1} are much larger than those of $|D_1|/|D_0|$ and this shows the extent of the effect of corrugation on the reflection and refraction of waves. That is, Fig. 29 confirms together with Fig. 21 that the effect of corrugation is larger on reflection than on refraction.

In Fig. 30, the ratios of P wave components to S wave components of irregular waves are given.

(21) As to $|A_1|/|B_1|$, it increases monotonously with decreasing L/L_{s1} down to L_{s2} as a whole. The minimum at $L=L_{p2}$ corresponds to that of $|A_1|$. The sharp peak at $L=L_{s2}$ is remarkable, but it must be borne in mind that this corresponds to the values of L/L_{s1} where the maximum

of $|A_1|$ and the minimum of $|B_1|$ appear. For L below L_{s1}, $|A_1|/|B_1|$ tends to 1.

(22) $|C_1|/|D_1|$ increases monotonously with decreasing L/L_{s1} in the interval of L larger than L_{p2} and decreases as a whole with decreasing L/L_{s1} in the interval of L between L_{p2} and L_{s2}. At $L=L_{p1}$, $|C_1|/|D_1|$ becomes 0 corresponding to the zero of $|C_1|$. For L smaller than L_{s2}, $|C_1|/|D_1|$ increases with decreasing L/L_{s1} and tends to 1.

(23) In comparison with the case of incidence of the P wave, the P wave component becomes comparable in order of magnitude to the S

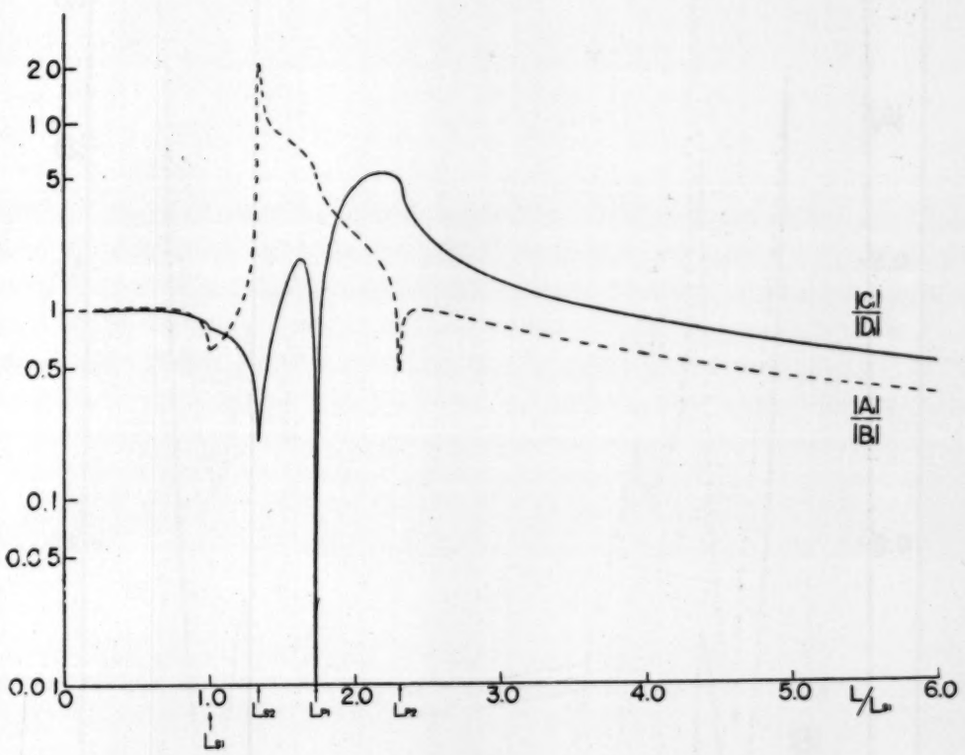

Fig. 30.

wave component from larger values of L, especially in irregularly refracted waves.

From Figs. 31–34, the following features can be seen concerning $|A_2|$, $|B_2|$, etc.

(24) In general, $|A_2|$, $|B_2|$, etc. are much smaller than $|A_1|$, $|B_1|$, etc. respectively. This result is similar to the case of incidence of the SH wave and differs from the case of incidence of the P wave. However, attention must be paid to the ranges of L/L_{s1} where any of $|A_1|$, $|B_1|$, etc. become small.

(25) It is common to all irregular waves that at L, just below L_{s2} there exists a sharp peak, while at $L \approx L_{s1}$ a sharp minimum appears. Furthermore, these features are the same as those with spectra of the first order.

(26) The variations of $|A_2|$, $|B_2|$, etc. with L/L_{s1} are much more complex than those with spectra of the first order.

(27) In this case also, as in the cases of incidence of P and SH waves, some irregular waves become boundary waves. Concerning $|A_2|$,

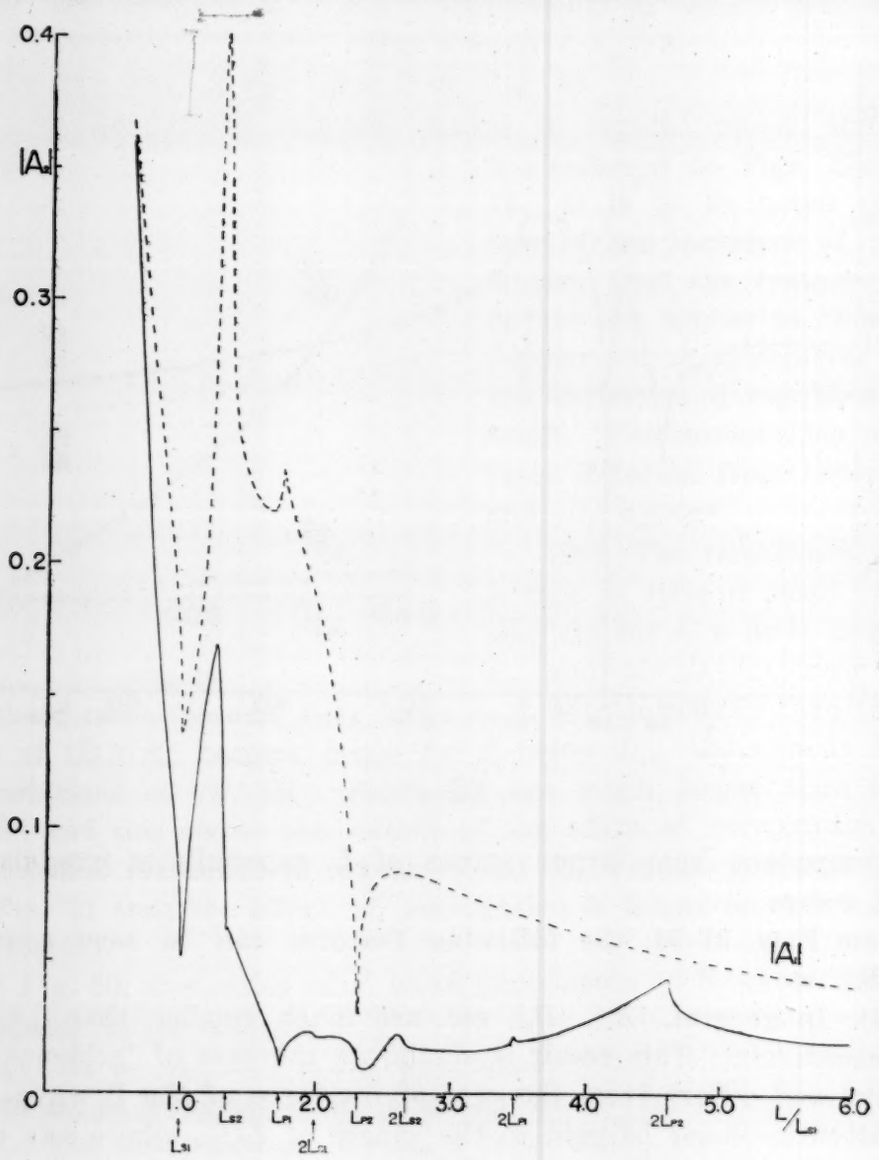

Fig. 31.

$|B_2|$, etc., the range where a certain kind of wave becomes a boundary wave is the same as in the case of incidence of the P wave, if it is expressed in terms of the wave length of P or S waves.

Chapter 4. Discussions and Conclusions

§ 1. Discussions

Now let us first consider the displacement itself. This is very im-

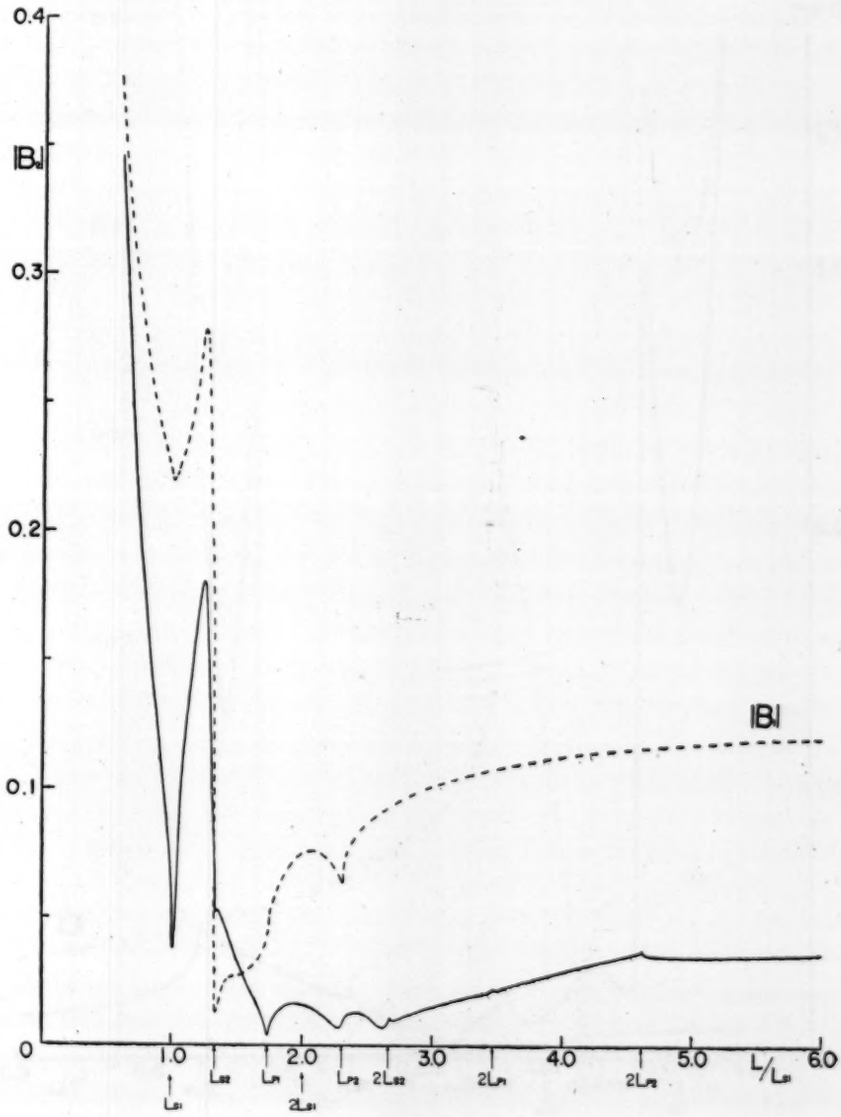

Fig. 32.

portant from the practical point of view since displacement potentials ϕ and ψ can not be observed as they are. But in our above mentioned calculations in cases of the incidence of P and SV waves, only the values of the displacement potentials are given. Therefore some remarks on the relations between displacement and potentials, as given hitherto in the figures, will be set down in the following.

As is well known, the displacement is defined by the relations $u=\partial\phi/\partial x+\partial\psi/\partial z$ and $w=\partial\phi/\partial z-\partial\psi/\partial x$. Because of the difference in the

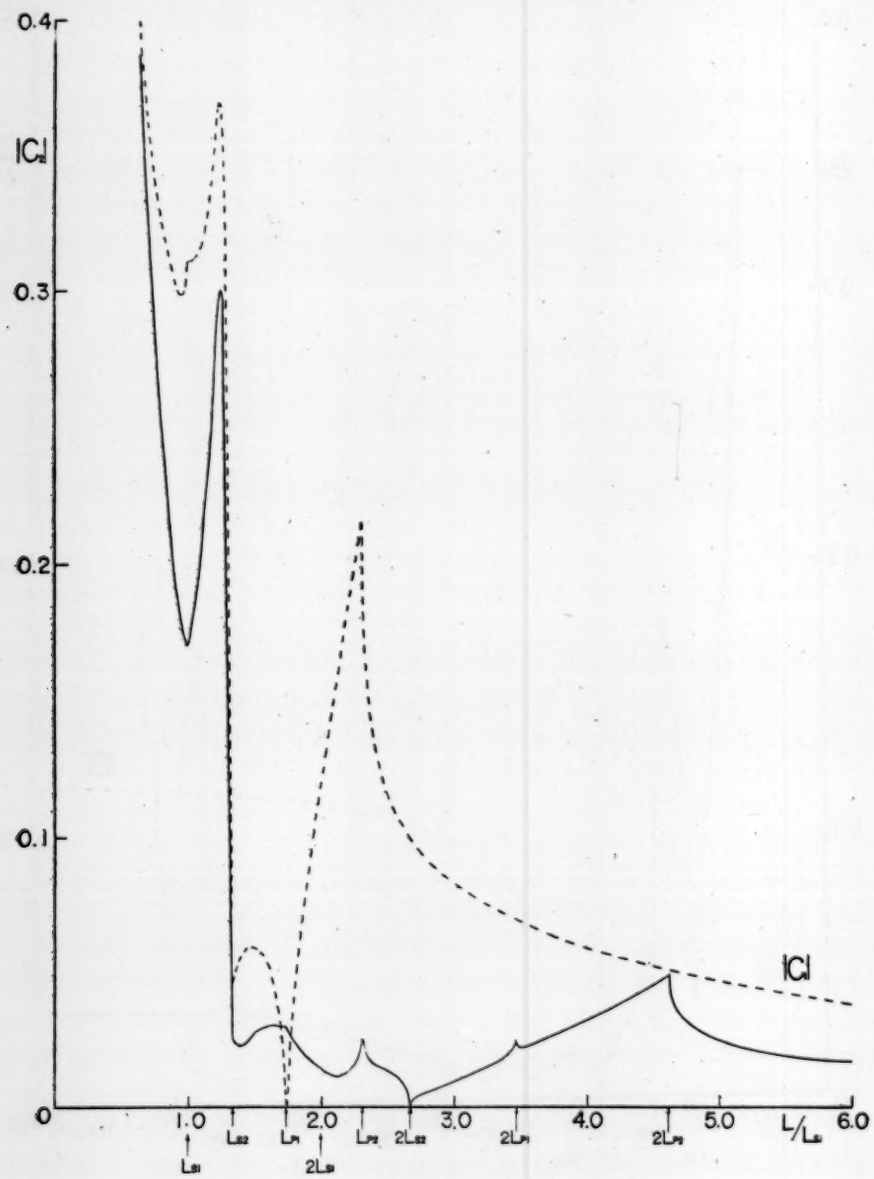

Fig. 33.

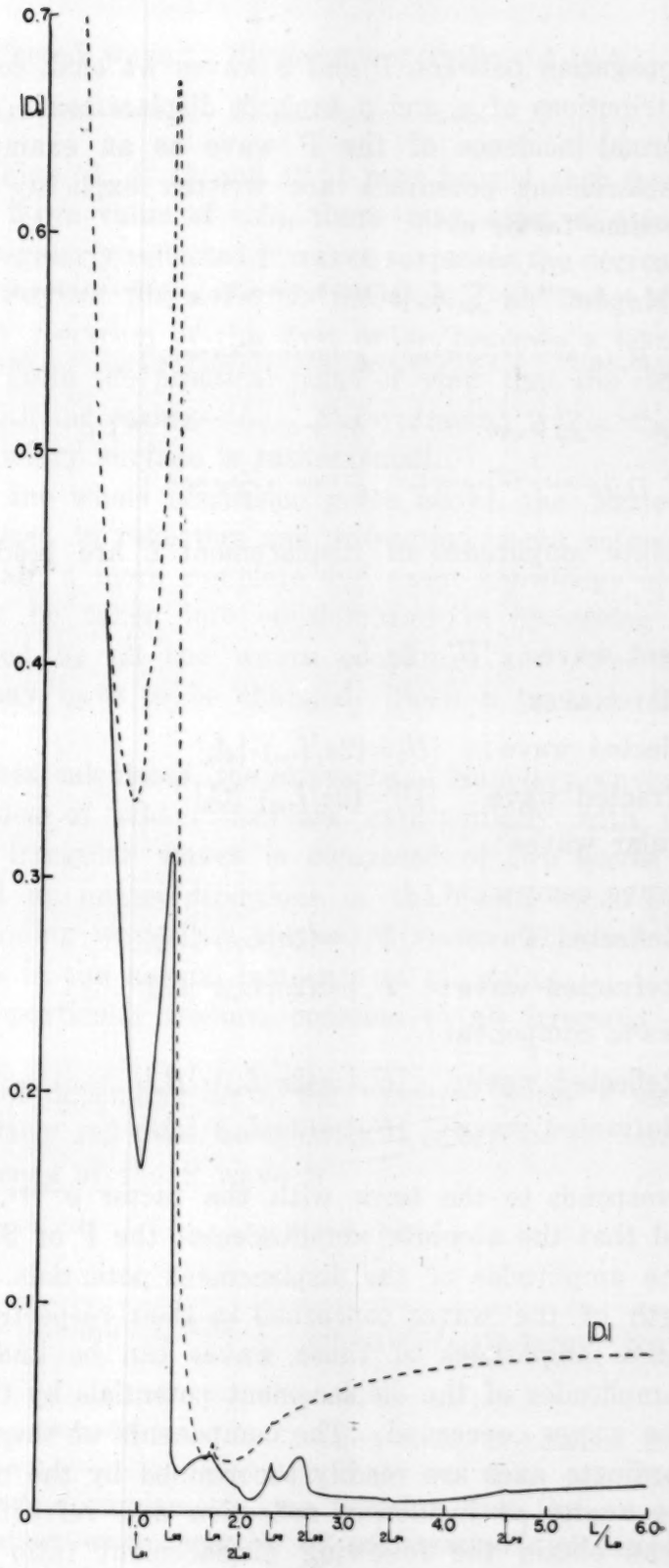

Fig. 34.

velocity of propagation between P and S waves we shall consider separately the contributions of ϕ and ψ towards displacement. Let us take the case of normal incidence of the P wave as an example. In this case, final displacement potentials are written explicitly as follows, neglecting the time factor $e^{i\omega t}$.

$$\phi_1 = e^{ih_1 z} + A_0 e^{-ih_1 z} + \sum A_n \{e^{i(npx - h_1 z\cos\alpha_n)} + e^{-i(npx + h_1 z\cos\alpha_n)}\} ,$$

$$\psi_1 = \sum B_n \{e^{i(npx - \sqrt{\sigma_1} h_1 z\cos\beta_n)} - e^{-i(npx + \sqrt{\sigma_1} h_1 z\cos\beta_n)}\} ,$$

$$\phi_2 = C_0 e^{ih_2 z} + \sum C_n \{e^{i(npx + h_2 z\cos\gamma_n)} + e^{-i(npx - h_2 z\cos\gamma_n)}\} ,$$

$$\psi_2 = \sum D_n \{e^{i(npx + \sqrt{\sigma_2} h_2 z\cos\delta_n)} - e^{-i(npx - \sqrt{\sigma_2} h_2 z\cos\delta_n)}\} .$$

Then the absolute amplitudes of displacement U are readily obtained as follows:

(1) Incident wave: $|U| = 2\pi/L_{p1}$

(2) Regular waves:

Reflected wave: $|U| = (2\pi/L_{p1}) \cdot |A_0|$

Refracted wave: $|U| = (2\pi/L_{p2}) \cdot |C_0|$

(3) Irregular waves:

P wave component:

Reflected wave: $|U_+| = (2\pi/L_{p1}) \cdot |A_n|$

Refracted wave: $|U_+| = (2\pi/L_{p2}) \cdot |C_n|$

S wave component:

Reflected wave: $|U_+| = (2\pi/L_{s1}) \cdot |B_n|$

Refracted wave: $|U_+| = (2\pi/L_{s2}) \cdot |D_n|$

where U_+ corresponds to the term with the factor e^{-inpx}. It is thus to be observed that the absolute amplitudes of the P or SV waves are $2\pi/L'$ times the amplitudes of the displacement potentials, where L' is the wave length of the waves concerned in their respective media, so that the relative amplitudes of these waves can be known only by dividing the amplitudes of the displacement potentials by the respective velocities of the waves concerned. The components of these amplitudes along the coordinate axes are readily ascertained by the nature of the wave and the angles of incidence, reflection and refraction of these waves. We can obtain the following displacement ratio of irregular waves to regular ones from the above formulae.

Reflected wave: displacement ratio $=|A_n|/|A_0|$

Refracted wave: displacement ratio $=|C_n|/|C_0|$

Thus from Figs. 3, 4, 11 and 12 it may be said that for L larger than L_{p1} and for large value of c/L_{p1} there may exist a case where the increase in irregularly reflected P waves surpasses the decrease in regularly reflected P waves. Since for L below L_{p1}, an irregularly reflected P wave with a spectrum of the first order becomes a boundary wave, it can be said from the practical point of view that the reflected P wave decreases with increasing c/L_{p1}. For refracted waves the effect of corrugated boundary surface is rather small.

Now in the whole discussion given above, the phase change which may be induced in reflection and refraction is not referred to. But in order to obtain a more complete and exact knowledge of the phenomena, it must be taken into consideration in discussing the resultant motion caused by all the waves concerned and some of those interpretations may have to be changed. Such a point is left for future study.

In all cases calculated, the existence of boundary waves was indicated the amplitudes of which decrease exponentially with increasing $|z|$. Each of the irregular waves is composed of two waves propagated in plus as well as minus directions of the x-axis which constitute, as a result, a standing wave in a stationary state. This is a common particular feature in the normal incidence of all waves.

Another particular feature, common to all irregular waves is the following:

The factor depending on z, for example in the P wave component of an irregularly reflected wave with a spectrum of n-th order in the case of incidence of the P wave is

$$\phi_n \propto 2A_n e^{-ik_1 z \cos \alpha_n} .$$

Therefore

$$\phi_n \propto 2A_n e^{-i(2\pi/L)z\sqrt{(L/L_{p1})^2-n^2}} \qquad \text{when } L/L_{p1} \text{ is larger than } n ,$$

or

$$\phi_n \propto 2A_n e^{-(2\pi/L)z\sqrt{n^2-(L/L_{p1})^2}} \qquad \text{when } L/L_{p1} \text{ is smaller than } n .$$

From the above formulae, we can perceive that the exponential factor of ϕ_n depends on wave lengths of corrugation and incident wave and the order n of spectrum, in such a way that

(a) the smaller the wave length L of a corrugated boundary surface,
(b) the higher the order n of spectrum, and
(c) the larger the wave length of incident wave L_{p1},

the larger is the rate of decrease in ϕ_n with increase in the distance z from the mean boundary.

As an example, the rate of decrease of the exponential factor of ϕ_1 is estimated, with the result that at a fixed level $z=L/2$, (that is, the level at half a wave length of corrugated boundary surface below the mean boundary surface,) for a wave with $L/L_{p1}=0.7$, the exponential factor becomes only 0.1 approximately, independent of the roughness c/L_{p1}. Therefore, from the practical point of view, it is unnecessary to take these boundary waves into consideration.

It is seen clearly from almost all figures given above that the increasing tendency of amplitudes for the smaller L/L_{p1} or L/L_{s1} is the more prominent. As mentioned previously, this tendency may, in extremity, impair the accuracy of this method of calculation, deteriorating the convergence of series. The amplitude of irregular waves with spectra of the second order gives the measure of the convergence. In cases of the incidence of both SH and SV waves, not only $|B_0|$ and $|D_0|$, but also $|A_1|$ etc. are in general much larger than $|A_2|$, $|B_2|$, etc. Even in these cases where the accuracy is better than in the case of incidence of the P wave $|A_2|$, $|B_2|$, etc. become comparable order to or larger than $|A_1|$, $|B_1|$, etc. for L/L_{s1} below about 0.5. In the case of incidence of the P wave, we must take into consideration the contributions of irregular waves with spectra of the second order from larger values of L/L_{p1} than in the two cases of S waves. However, since fortunately, characteristic features of waves with spectra of the first and second order, that is, the positions of peaks and minima are almost the same, with each other, it is unnecessary to change the results obtained about $|A_1|$, $|B_1|$, etc. by taking $|A_2|$, $|B_2|$, etc. into consideration. Needlessto say, the higher the approximation is advanced, the more information concerning the corrugation of boundary surface can be obtained.

We have had no time to study examples other than the case in which the velocity ratio $V_{p1}/V_{p2}=6/8$ and rigidity ratio $\mu_2/\mu_1=2$. It would therefore be better to abstain from drawing too wide a conclusion, but we cannot refrain from giving a few notices. From figures given above, we have seen that almost all the abnormal points are related to the wavelength of P and S waves. Therefore, since the

wave length is closely connected with velocity itself, many theoretically interesting changes of features will be expected to accompany variations in velocity ratio. Considerations on various cases of velocity contrast will be carried out in the near future. Moreover, the results may depend more or less upon the adopted value of the rigidity ratio and the determining which of the two numerical constants ρ_1/ρ_2 and μ_2/μ_1 has the more effect on these phenomena is a very interesting investigation.

The computations were carried out only for cases of normal incidence on the mean surface of a harmonic boundary $\zeta = c \cos px$. One of the important problems to be considered is the case of the oblique incidence of waves and another is the problem concerning reflection and refraction of waves at an arbitrary form of boundary surface, especially at an isolated trough of large amplitude. If the results obtained above for various L are superposed, we can obtain in principle the solutions to an arbitrary form of boundary surface although the assumptions of small amplitude and periodicity concerning the corrugated boundary surface cannot be dispensed with. To do this will require a very tedious procedure and other appropriate methods may be applied much more easily. It is very interesting to solve the same problems by using other methods and to compare the results with one another and it is hoped that some tests will be carried out on these problems.

§ 2. Conclusions

In the present paper the effect of corrugation of boundary surface on reflection and refraction of elastic waves was considered by the method introduced by Lord Rayleigh in his problem of sound and light. The solutions were obtained for the cases of incidence of P and SV waves with an arbitrary angle of incidence on a corrugated periodic boundary surface which can be expanded in Fourier's series.

In Chapter 2 of the present paper, the fundamental equations such as equations of boundary surface, equations of motion and formulae of boundary conditions were presented. In Chapter 3, the solutions of the case of incidence of P and SV waves were obtained to the order of magnitude of ζ^2. That is to say, the solutions of the first and second approximation were obtained. Numerical calculations were carried out for the case of normal incidence of all waves on the mean surface of a harmonic boundary $\zeta = c \cos px$ by using the electronic computor PC–1. The results thus obtained were given in Figs. 3–18 and Tables 1–5 for

Table 1. $|A_0|$, $|C_0|$, etc. for $c/L_{p1}=0.03$ in the case of incidence of P wave.

L/L_{p1}	$\lvert A_0\rvert$	$\lvert C_0\rvert$	$\lvert A_1\rvert$	$\lvert B_1\rvert$	$\lvert C_1\rvert$	$\lvert D_1\rvert$	$\lvert A_1\rvert/\lvert A_0\rvert$	$\lvert C_1\rvert/\lvert C_0\rvert$
3.00	0.19291	1.07025	0.037083	0.008157	0.024288	0.007646	0.19223	0.022694
2.95	0.192910	1.070234	0.037064	0.008296	0.024261	0.007776		
2.90	0.192911	1.070235	0.037043	0.008439	0.024233	0.007910		
2.85	0.192911	1.070235	0.037022	0.008587	0.024204	0.008048		
2.80	0.192912	1.070236	0.037000	0.008740	0.024173	0.008192		
2.75	0.192912	1.070236	0.036976	0.008899	0.024140	0.008341		
2.70	0.192913	1.070237	0.036952	0.009064	0.024106	0.008496		
2.65	0.192914	1.070238	0.036926	0.009235	0.024071	0.008656		
2.60			0.036899	0.009412	0.024034	0.008823		
2.55	0.192915	1.070239	0.036871	0.009597	0.023995	0.008996		
2.50	0.19293	1.07025	0.036842	0.009788	0.023954	0.009176		
2.45	0.192916	1.070240	0.036811	0.009988	0.023911	0.009363		
2.40	0.192916	1.070240	0.036779	0.010196	0.023867	0.009558		
2.35	0.192918	1.070242	0.036746	0.010412	0.023820	0.009761		
2.30	0.192919	1.070242	0.036711	0.010638	0.023772	0.009974		
2.25	0.192920	1.070243	0.036675	0.010873	0.023721	0.010196		
2.20	0.19292	1.07024	0.036638	0.011120	0.023669	0.010428	0.18991	0.022116
2.15	0.192922	1.070245	0.036599	0.011377	0.023615	0.010671		
2.10	0.192927	1.070254	0.036560	0.011646	0.023560	0.010925		
2.05	0.192929	1.070255	0.036520	0.011929	0.023504	0.011192		
2.00	0.192931	1.070255	0.036480	0.012224	0.023447	0.011473		
1.95	0.192933	1.070255	0.036441	0.012534	0.023392	0.011767		
1.90	0.192936	1.070255	0.036404	0.012860	0.023338	0.012078		
1.85	0.192939	1.070254	0.036370	0.013202	0.023289	0.012405		
1.80	0.192943	1.070252	0.036341	0.013561	0.023249	0.012751		
1.75			0.036323	0.013938	0.023221	0.013117		
1.70	0.192953	1.070245	0.036320	0.014334	0.023215	0.013505		
1.65			0.036342	0.014748	0.023243	0.013917		
1.60	0.192969	1.070227	0.036404	0.015180	0.023327	0.014355		
1.55	0.192981	1.070209	0.036535	0.015626	0.023506	0.014823		
1.50	0.192999	1.070181	0.036786	0.016078	0.023855	0.015322	0.19060	0.022290
1.45	0.193028	1.070132	0.037275	0.016515	0.024538	0.015856		
1.40	0.193082	1.070035	0.038323	0.016869	0.026007	0.016424	0.19848	0.024305
1.35	0.193246	1.069762	0.041575	0.016797	0.030552	0.016993	0.21514	0.028560
1.333334	0.192680	1.069902	0.048559	0.015559	0.040177	0.016974	0.25202	0.037552
1.32	0.192748	1.069996	0.046455	0.016379	0.038159	0.017366	0.24101	0.035663
1.30	0.192838	1.070122	0.043330	0.017529	0.035057	0.017896	0.22470	0.032760
1.28	0.192913	1.070226	0.040379	0.018575	0.032037	0.018358		
1.26	0.192974	1.070311	0.037626	0.019532	0.029115	0.018762		
1.24	0.193022	1.070379	0.035089	0.020414	0.026304	0.019117	0.18179	0.024574
1.20	0.193085	1.070469	0.030712	0.021995	0.021046	0.019713	0.15906	0.019661

1.18	0.193103	1.070496	0.028887	0.022714	0.018610	0.019969		
1.16	0.193114	1.070512	0.027308	0.023397	0.016307	0.020208		
1.14	0.193118	1.070521	0.025971	0.024052	0.014139	0.020438	0.13448	0.013208
1.12	0.193117	1.070523	0.024869	0.024689	0.012108	0.020668		
1.10	0.193112	1.070519	0.023989	0.025315	0.010220	0.020907	0.12422	0.009547
1.08	0.193102	1.070512	0.023317	0.025941	0.008482	0.021168	0.12075	0.007923
1.06	0.193088	1.070501	0.022839	0.026580	0.006916	0.021468	0.11828	0.006461
1.04	0.193068	1.070488	0.022545	0.027254	0.005565	0.021833	0.11677	0.005199
1.02	0.193040	1.070472	0.022446	0.028014	0.004567	0.022329	0.11628	0.004266
1.00			0.022935	0.029393	0.005591	0.023530		
0.98	0.192985	1.070436	0.020834	0.030124	0.004091	0.022817	0.107957	0.003822
0.96	0.192995	1.070422	0.020107	0.030692	0.003952	0.022664	0.104184	
0.94	0.193002	1.070407	0.019640	0.031253	0.004747	0.022609	0.101761	0.004435
0.92	0.193010	1.070394	0.019294	0.031810	0.006012	0.022610	0.099964	0.005617
0.90	0.193021	1.070384	0.018994	0.032364	0.007477	0.022661	0.098404	0.006985
0.88			0.018689	0.032909	0.009043	0.022773		0.008436
0.86	0.193058	1.070377	0.018329	0.033440	0.010690	0.022974	0.094940	0.009987
0.84	0.193087	1.070383	0.017855	0.033947	0.012444	0.023329	0.092471	0.011626
0.82	0.193125	1.070398	0.017174	0.034425	0.014388	0.023980	0.088927	0.013442
0.80	0.193175	1.070425	0.016088	0.034882	0.016738	0.025286	0.083282	0.015637
0.78	0.193240	1.070465	0.013871	0.035542	0.020338	0.028668	0.071781	0.018999
0.769			0.008002	0.036430	0.028618	0.042816		
0.76	0.193706	1.071294	0.009992	0.027078	0.036107	0.059843	0.051583	0.033704
0.749			0.018038	0.018063	0.040085	0.070224		
0.74	0.193908	1.071796	0.023585	0.017514	0.039469	0.071235	0.121630	0.036825
0.729			0.026985	0.024551	0.034912	0.064440		
0.72	0.193664	1.071176	0.027418	0.030131	0.030181	0.055961	0.141575	0.028176
0.709			0.026412	0.034686	0.025113	0.045773		
0.70	0.193577	1.070752	0.025103	0.036963	0.022083	0.038697	0.129680	0.020624
0.689			0.023329	0.038632	0.019697	0.031806		
0.66	0.193771	1.070684	0.018966	0.040277	0.018425	0.021439	0.097878	0.017209
0.64			0.016335	0.040467	0.019760	0.019308		
0.62	0.194147	1.070969	0.013936	0.040381	0.021813	0.019924	0.071781	0.020368
0.60	0.194419	1.071207	0.011704	0.040172	0.024239	0.022266	0.060200	0.022628
0.58	0.194910	1.071651	0.009800	0.039909	0.027158	0.026473	0.050280	0.025342
0.55	0.195059	1.071873	0.020228	0.042017	0.033703	0.037693	0.103703	0.031443
0.50	0.194919	1.071942	0.028835	0.045806	0.040460	0.045437	0.147934	0.037745
0.45			0.036655	0.050687	0.047624	0.052661		
0.40	0.194873	1.071954	0.045072	0.056831	0.055651	0.060343	0.231290	0.051915
0.35	0.194866	1.071957	0.054971	0.064838	0.065675	0.069911	0.282096	0.061266
0.30	0.194864	1.071960	0.067362	0.075559	0.078612	0.082314	0.345688	0.073335
0.25	0.194870	1.071962	0.083930	0.090600	0.096286	0.099408	0.430700	0.089822
0.20	0.194888	1.071966	0.107948	0.113188	0.122302	0.124820	0.553899	0.114091
0.15	0.194929	1.071974	0.146983	0.150861	0.165049	0.166947	0.754030	0.153967
0.10	0.195057	1.071995	0.223674	0.226237	0.249668	0.250937	1.146710	0.232900

Table 2. $|A_0|$, $|C_0|$, etc. for $c/L_{p1}=0.05$ in the case of incidence of P wave.

L/L_{p1}	$\lvert A_0\rvert$	$\lvert C_0\rvert$	$\lvert A_1\rvert$	$\lvert B_1\rvert$	$\lvert C_1\rvert$	$\lvert D_1\rvert$	$\lvert A_1\rvert/\lvert A_0\rvert$	$\lvert C_1\rvert/\lvert C_0\rvert$
3.00	0.18030	1.07658	0.061806	0.013596	0.040481	0.012743	0.34281	0.037601
2.95	0.180306	1.076577	0.061773	0.013826	0.040436	0.012959		
2.90	0.180307	1.076579	0.061739	0.014064	0.040389	0.013183		
2.85	0.180309	1.076580	0.061703	0.014311	0.040339	0.013414		
2.80	0.180310	1.076581	0.061666	0.014567	0.040288	0.013654		
2.75	0.180312	1.076583	0.061627	0.014832	0.040234	0.013902		
2.70	0.180314	1.076584	0.061586	0.015106	0.040177	0.014159		
2.65	0.180316	1.076586	0.061543	0.015391	0.040118	0.014427		
2.60	0.180317	1.076588	0.061499	0.015687	0.040056	0.014704		
2.55	0.180319	1.076589	0.061452	0.015994	0.039991	0.014993		
2.50	0.18033	1.07659	0.061403	0.016314	0.039923	0.015293		
2.45	0.180323	1.076593	0.061352	0.016646	0.039852	0.015605		
2.40	0.180324	1.076593	0.061299	0.016993	0.039778	0.015930		
2.35	0.180328	1.076597	0.061243	0.017353	0.039700	0.016270		
2.30	0.180330	1.076599	0.061185	0.017730	0.039619	0.016624		
2.25	0.180333	1.076601	0.061125	0.018122	0.039536	0.016993		
2.20	0.18038	1.07663	0.061063	0.018533	0.039449	0.017380	0.33862	0.036643
2.15	0.180338	1.076605	0.060999	0.018962	0.039359	0.017785		
2.10	0.180341	1.076607	0.060933	0.019411	0.039267	0.018209		
2.05	0.180343	1.076610	0.060867	0.019881	0.039173	0.018654		
2.00			0.060800	0.020374	0.039079	0.019121		
1.95	0.180349	1.076614	0.060735	0.020891	0.038986	0.019612		
1.90			0.060673	0.021433	0.038897	0.020130		
1.85	0.180354	1.076617	0.060616	0.022003	0.038816	0.020676		
1.80	0.180356	1.076618	0.060569	0.022601	0.038748	0.021252		
1.75	0.180357	1.076618	0.060538	0.023230	0.038702	0.021862		
1.70			0.060534	0.023890	0.038691	0.022509		
1.65	0.180357	1.076613	0.060570	0.024580	0.038738	0.023195		
1.60	0.180354	1.076607	0.060674	0.025300	0.038878	0.023925		
1.55	0.180347	1.076596	0.060891	0.026044	0.039177	0.024704		
1.50	0.180333	1.076575	0.061310	0.026797	0.039759	0.025536	0.33998	0.036931
1.45	0.180307	1.076538	0.062124	0.027524	0.040896	0.026426		
1.40	0.180250	1.076459	0.063871	0.028115	0.043345	0.027374	0.35435	0.040266
1.35	0.180071	1.076212	0.069292	0.027995	0.050921	0.028321	0.38436	0.047135
1.333334	0.179667	1.075654	0.080932	0.025931	0.066961	0.028290	0.450456	0.062251
1.32	0.179856	1.075915	0.077425	0.027299	0.063598	0.028944	0.43048	0.059110
1.30	0.180106	1.076264	0.072216	0.029216	0.058428	0.029826	0.40096	0.054288
1.28	0.180315	1.076554	0.067299	0.030959	0.053395	0.030579		
1.26	0.180483	1.076791	0.062710	0.032554	0.048526	0.031271		
1.24	0.180617	1.076978	0.058481	0.034023	0.043840	0.031862	0.32378	0.040706
1.20	0.180792	1.077229	0.051186	0.036658	0.035078	0.032854	0.28312	0.032563

1.18	0.180843	1.077303	0.048145	0.037856	0.031017	0.033281		
1.16	0.180872	1.077349	0.045514	0.038994	0.027179	0.033680		
1.14	0.180884	1.077373	0.043285	0.040087	0.023565	0.034064	0.23930	0.021873
1.12	0.180882	1.077378	0.041448	0.041148	0.020181	0.034447		
1.10	0.180866	1.077369	0.039982	0.042192	0.017033	0.034846	0.22106	0.015810
1.08	0.180839	1.077347	0.038862	0.043235	0.014137	0.035280	0.21490	0.013122
1.06	0.180800	1.077317	0.038066	0.044300	0.011526	0.035779	0.21054	0.010699
1.04	0.180746	1.077280	0.037574	0.045423	0.009275	0.036389	0.20788	0.008610
1.02	0.180666	1.077237	0.037410	0.046689	0.007612	0.037214	0.20707	0.007066
1.00			0.038224	0.048988	0.009318	0.039216		
0.98	0.180513	1.077138	0.034724	0.050207	0.006819	0.038028	0.19236	0.006331
0.96	0.180541	1.077098	0.033511	0.051154	0.006586	0.037773		
0.94	0.180561	1.077057	0.032734	0.052088	0.007911	0.037681	0.18129	0.007345
0.92	0.180584	1.077021	0.032156	0.053017	0.010021	0.037683		
0.90	0.180615	1.076994	0.031657	0.053940	0.012462	0.037769	0.17527	0.011571
0.88	0.180658	1.076977	0.031149	0.054849	0.015072	0.037954	0.17242	0.013995
0.86	0.180718	1.076975	0.030548	0.055733	0.017816	0.038290		
0.84	0.180799	1.076992	0.029758	0.056579	0.020740	0.038882	0.16459	0.019257
0.82	0.180906	1.077033	0.028623	0.057375	0.023979	0.039966		
0.80	0.181046	1.077108	0.026814	0.058137	0.027897	0.042142	0.14811	0.025900
0.78	0.181229	1.077218	0.023118	0.059236	0.033896	0.047780	0.12756	0.031466
0.769			0.013335	0.060722	0.047697	0.071366		
0.76	0.182527	1.079522	0.016654	0.045130	0.060178	0.099738	0.091241	0.055745
0.749			0.030076	0.030110	0.066811	0.117040		
0.74	0.183079	1.080916	0.039308	0.029191	0.065780	0.118722	0.214705	0.060856
0.729			0.044984	0.040922	0.058189	0.107401		
0.72	0.182400	1.079193	0.045697	0.050219	0.050301	0.093267	0.250532	0.046610
0.709			0.044033	0.057812	0.041868	0.076290		
0.70	0.182161	1.078016	0.041838	0.061606	0.036805	0.064495	0.229676	0.034141
0.689			0.038895	0.064388	0.032837	0.053009		
0.66	0.182700	1.077825	0.031611	0.067129	0.030708	0.035730	0.173021	0.028491
0.64	0.183170	1.078145	0.027225	0.067445	0.032934	0.032180	0.148632	0.030547
0.62	0.183747	1.078618	0.023227	0.067301	0.036356	0.033206	0.126408	0.033707
0.60	0.184503	1.079279	0.019506	0.066953	0.040399	0.037110	0.105722	0.037431
0.58	0.185865	1.080512	0.016333	0.066515	0.045263	0.044122	0.087876	0.041890
0.55	0.186325	1.081128	0.033713	0.070029	0.056172	0.062821	0.180939	0.051956
0.50	0.185895	1.081320	0.048059	0.076343	0.067434	0.075729	0.258525	0.062363
0.45			0.061091	0.084479	0.079373	0.087769		
0.40	0.185794	1.081357	0.075120	0.094718	0.092751	0.100572	0.404321	0.085773
0.35	0.185797	1.081369	0.091618	0.108064	0.109458	0.116519	0.493110	0.101222
0.30	0.185830	1.081381	0.112271	0.125931	0.131020	0.137189	0.604157	0.121160
0.25	0.185907	1.081397	0.146750	0.159106	0.193091	0.165680	0.789377	0.178557
0.20	0.186067	1.081423	0.179913	0.188647	0.203837	0.208033	0.966928	0.188489
0.15	0.186428	1.081477	0.244971	0.251436	0.275082	0.278246	1.314026	0.254358
0.10	0.187480	1.081622	0.372790	0.377061	0.416113	0.418229	1.988424	0.384712

Table 3. $|A_0|$, $|C_0|$, etc. for $c/L_{p1}=0.10$ in the case of incidence of P wave.

L/L_{p1}	$\lvert A_0\rvert$	$\lvert C_0\rvert$	$\lvert A_1\rvert$	$\lvert B_1\rvert$	$\lvert C_1\rvert$	$\lvert D_1\rvert$	$\lvert A_1\rvert/\lvert A_0\rvert$	$\lvert C_1\rvert/\lvert C_0\rvert$
3.00	0.12128	1.10633	0.123611	0.027191	0.080962	0.025487	0.34281	0.037601
2.95	0.121223	1.106310	0.123546	0.027652	0.080871	0.025919		
2.90	0.121229	1.106315	0.123478	0.028129	0.080777	0.026365		
2.85	0.121235	1.106320	0.123407	0.028622	0.080678	0.026828		
2.80	0.121242	1.106326	0.123332	0.029134	0.080575	0.027307		
2.75	0.121248	1.106331	0.123254	0.029663	0.080467	0.027804		
2.70			0.123172	0.030212	0.080354	0.028319		
2.65	0.121262	1.106344	0.123087	0.030782	0.080236	0.028853		
2.60	0.121270	1.106350	0.122997	0.031374	0.080112	0.029409		
2.55	0.121277	1.106357	0.122904	0.031989	0.079982	0.029985		
2.50			0.122806	0.032628	0.079846	0.030585		
2.45	0.121294	1.106372	0.122704	0.033293	0.079704	0.031210		
2.40	0.121294	1.106372	0.122597	0.033985	0.079555	0.031861		
2.35	0.121312	1.106387	0.122486	0.034707	0.079401	0.032539		
2.30	0.121321	1.106395	0.122370	0.035459	0.079239	0.033247		
2.25	0.121331	1.106404	0.122250	0.036245	0.079071	0.033987		
2.20			0.122126	0.037066	0.078897	0.034760	0.33862	0.036643
2.15	0.121352	1.106421	0.121998	0.037924	0.078718	0.035569		
2.10	0.121362	1.106430	0.121867	0.038821	0.078533	0.036417		
2.05	0.121373	1.106439	0.121734	0.039762	0.078346	0.037307		
2.00	0.121384	1.106447	0.121601	0.040747	0.078158	0.038242		
1.95	0.121395	1.106455	0.121470	0.041781	0.077972	0.039225		
1.90	0.121405	1.106462	0.121345	0.042866	0.077794	0.040260		
1.85	0.121415	1.106467	0.121232	0.044006	0.077632	0.041351		
1.80	0.121423	1.106471	0.121138	0.045203	0.077495	0.042504	0.99765	0.070038
1.75	0.121429	1.106471	0.121077	0.046460	0.077403	0.043724		
1.70			0.121067	0.047779	0.077382	0.045017		
1.65	0.121446	1.106448	0.121140	0.049160	0.077475	0.046390		
1.60	0.121415	1.106428	0.121348	0.050600	0.077756	0.047851		
1.55			0.121783	0.052088	0.078354	0.049409		
1.50	0.121334	1.106301	0.122620	0.053595	0.079518	0.051073	0.33998	0.036931
1.45	0.121228	1.106150	0.124248	0.055048	0.081793	0.052852		
1.40	0.121000	1.105834	0.127742	0.056231	0.086689	0.054748	1.05572	0.078392
1.35	0.120283	1.104848	0.138584	0.055990	0.101841	0.056642	1.152150	0.092176
1.333334	0.118667	1.102617	0.161864	0.051862	0.133922	0.056581	1.364014	0.121458
1.32	0.119435	1.103664	0.154850	0.054598	0.127196	0.057887	1.29652	0.11525
1.30	0.120450	1.105061	0.144433	0.058431	0.116856	0.059652	1.19911	0.10575
1.28	0.121286	1.106223	0.134598	0.061918	0.106790	0.061194		
1.26	0.121960	1.107168	0.125421	0.065108	0.097052	0.062542		
1.24	0.122490	1.107917	0.116962	0.068047	0.087681	0.063725	0.95487	0.079140
1.20	0.123184	1.108918	0.102372	0.073316	0.070155	0.065709	0.83105	0.063264

1.18	0.123381	1.109213	0.096291	0.075712	0.062035	0.066563		
1.16	0.123496	1.109399	0.091027	0.077989	0.054357	0.067360		
1.14	0.123543	1.109494	0.086571	0.080174	0.047130	0.068127	0.70074	0.042479
1.12	0.123530	1.109514	0.082896	0.082296	0.040361	0.068894		
1.10	0.123467	1.109475	0.079963	0.084383	0.034066	0.069691	0.64765	0.030705
1.08	0.123357	1.109390	0.077725	0.086470	0.028275	0.070561	0.63008	0.025487
1.06	0.123200	1.109270	0.076131	0.088600	0.023052	0.071559	0.61795	0.020781
1.04	0.122984	1.109122	0.075149	0.090846	0.018549	0.072777	0.61105	0.016724
1.02	0.122666	1.108949	0.074821	0.093378	0.015223	0.074429	0.60996	0.013727
1.00			0.076448	0.097977	0.018635	0.078433		
0.98	0.122058	1.108554	0.069448	0.100415	0.013637	0.076056	0.56898	0.012302
0.96	0.122172	1.108391	0.067023	0.102308	0.013173	0.075547		
0.94	0.122257	1.108229	0.065468	0.104175	0.015823	0.075362	0.53549	0.014278
0.92	0.122353	1.108086	0.064312	0.106035	0.020042	0.075367		
0.90	0.122482	1.107975	0.063314	0.107880	0.024925	0.075538	0.51692	0.022496
0.88	0.122663	1.107908	0.062297	0.109698	0.030143	0.075909	0.50787	0.027207
0.86	0.122914	1.107900	0.061097	0.111466	0.035632	0.076580		
0.84	0.123252	1.107969	0.059515	0.113158	0.041479	0.077765	0.48287	0.037437
0.82	0.123700	1.108137	0.057245	0.114750	0.047958	0.079932		
0.80	0.124290	1.108438	0.053627	0.116274	0.055794	0.084285	0.43147	0.050336
0.78			0.046236	0.118472	0.067793	0.095560	0.26338	0.058757
0.769			0.026697	0.121448	0.095403	0.142735		
0.76	0.130375	1.118140	0.033308	0.090260	0.120356	0.199477	0.255478	0.107639
0.749			0.060161	0.060234	0.133627	0.234083		
0.74	0.132365	1.123665	0.078616	0.058382	0.131561	0.237447		
0.729			0.089973	0.081852	0.116385	0.214806		
0.72	0.129614	1.116783	0.091394	0.100437	0.100603	0.186537	0.705127	0.090083
0.709			0.088069	0.115627	0.083741	0.152584		
0.70	0.128681	1.112069	0.083676	0.123212	0.073610	0.128990	0.650261	0.066192
0.689			0.077796	0.128781	0.065679	0.106022		
0.66	0.130900	1.111300	0.063221	0.134258	0.061417	0.071462	0.482971	0.055266
0.64	0.132797	1.112586	0.054450	0.134889	0.065868	0.064361	0.410024	0.059203
0.62	0.135117	1.114478	0.046454	0.134602	0.072712	0.066413	0.343806	0.065243
0.60	0.138137	1.117128	0.039012	0.133906	0.080797	0.074219	0.282416	0.072326
0.58	0.143557	1.122062	0.032666	0.133030	0.090526	0.088244	0.227548	0.080678
0.55	0.145135	1.124515	0.067427	0.140057	0.112343	0.125642	0.464582	0.099904
0.50	0.143790	1.125292	0.096117	0.152687	0.134868	0.151457	0.668454	0.119852
0.45			0.122182	0.168958	0.158745	0.175538		
0.40	0.144074	1.125502	0.150241	0.189435	0.185502	0.201145	1.042799	0.164817
0.35	0.144685	1.125606	0.183236	0.216127	0.218916	0.233037	1.266452	0.194487
0.30	0.145741	1.125742	0.224541	0.251862	0.262041	0.274379	1.540680	0.232771
0.25	0.147567	1.125951	0.279768	0.301999	0.320953	0.331361	1.895875	0.285050
0.20	0.150944	1.126318	0.359827	0.377295	0.407673	0.416066	2.383836	0.361952
0.15	0.158060	1.127102	0.489942	0.502871	0.550164	0.556491	3.099721	0.488123
0.10	0.176877	1.129317	0.745580	0.754122	0.832226	0.836457	4.215247	0.736928

Table 4. $|B_1|/|A_1|$ and $|D_1|/|C_1|$ in the case of incidence of P wave.

L/L_{p1}	$\lvert B_1\rvert/\lvert A_1\rvert$	$\lvert D_1\rvert/\lvert C_1\rvert$	L/L_{p1}	$\lvert B_1\rvert/\lvert A_1\rvert$	$\lvert D_1\rvert/\lvert C_1\rvert$
3.00	0.21997	0.31479	0.96	1.59129	4.76311
2.50	0.26568	0.38306	0.94	1.52643	
2.20	0.30351	0.44057	0.92	1.70391	3.76040
2.00	0.33509	0.48929	0.90	1.76088	2.51818
1.80	0.37316	0.54847	0.86	1.90126	1.87473
1.75	0.38372		0.82	2.16820	1.51063
1.65	0.40581		0.80	2.56232	1.40961
1.60	0.41699		0.76	2.7099	1.65738
1.55	0.42770		0.74	0.74262	1.80483
1.50	0.43707	0.64227	0.72	1.09896	1.85418
1.45	0.44306	0.64618	0.70	1.47249	1.75234
1.40	0.44017	0.63154	0.66	2.12360	1.16354
1.35	0.40402	0.55618	0.64	2.47732	0.97711
1.32	0.35258	0.37649	0.62	2.89753	0.91336
1.30	0.40455	0.51047	0.60	3.43243	0.91859
1.24	0.58178	0.72678	0.58	4.07243	0.97479
1.20	0.71617	0.93660	0.55	2.07717	1.11838
1.14	0.92611	1.44553	0.50	1.58855	1.12300
1.10	1.05528	2.04579	0.45	1.38284	1.10578
1.08	1.11254	2.49558	0.40	1.26088	1.08433
1.06	1.16380	3.10420	0.35	1.17950	1.06451
1.04	1.20887	3.92334	0.30	1.12168	1.04708
1.02	1.24806	4.88886	0.20	1.04855	1.02059
1.00	1.28158	4.20863	0.15	1.02639	1.01150
0.98	1.44591	5.57677	0.10	1.01146	1.00508

Table 5. $|A_2|$, $|B_2|$, etc. for $c/L_{p1}=0.10$ in the case of incidence of P wave.

L/L_{p1}	$\lvert A_2\rvert$	$\lvert B_2\rvert$	$\lvert C_2\rvert$	$\lvert D_2\rvert$
3.00	0.034329	0.020961	0.013187	0.015756
2.95	0.034128	0.021302	0.012989	0.015991
2.90	0.033901	0.021657	0.012802	0.016231
2.85	0.033634	0.022029	0.012643	0.016476
2.80	0.033299	0.022426	0.012548	0.016725
2.75	0.032827	0.022861	0.012610	0.016975
2.70	0.031987	0.023099	0.013225	0.016977
2.65	0.030214	0.024152	0.015567	0.017440
2.60	0.032687	0.024061	0.012709	0.017829
2.55	0·034455	0.024061	0.009962	0.018152
2.50	0.035671	0.024154	0.007340	0.018419
2.45	0.036445	0.024343	0.004848	0.018641
2.40	0.036860	0.024624	0.002485	0.018827
2.35	0.036983	0.024997	0.000244	0.018988
2.30	0.036871	0.025459	0.001886	0.019129
2.25	0.036568	0.026011	0.003926	0.019258
2.20	0.036118	0.026655	0.005902	0.019378
2.15	0.035559	0.027404	0.007861	0.019489
2.10	0.034938	0.028284	0.009891	0.019582
2.05	0.034337	0.029378	0.012218	0.019615
2.00	0.034462	0.031623	0.017514	0.019060
1.99	0.032700	0.031794	0.016733	0.020179
1.97	0.031246	0.032014	0.016200	0.021181
1.95	0.030198	0.032214	0.015854	0.021980
1.90	0.028208	0.032699	0.015272	0.023759
1.85	0.026633	0.033191	0.014902	0.025521
1.80	0.025281	0.033718	0.014711	0.027431

(to be continued)

Table 5. (continued)

L/L_{p1}	$\lvert A_2\rvert$	$\lvert B_2\rvert$	$\lvert C_2\rvert$	$\lvert D_2\rvert$
1.75	0.024096	0.034313	0.014750	0.029642
1.65	0.022401	0.036036	0.016126	0.036113
1.60	0.022415	0.037653	0.018344	0.042052
1.58	0.022879	0.038686	0.019972	0.045852
1.56	0.024021	0.040241	0.022625	0.051723
1.54	0.028442	0.043798	0.030074	0.067743
1.53	0.038501	0.059316	0.046294	0.100602
1.51	0.047055	0.074757	0.063112	0.133084
1.50	0.049597	0.079779	0.069462	0.144790
1.49	0.050802	0.082603	0.073986	0.152627
1.47	0.049189	0.081325	0.076727	0.155397
1.45	0.044051	0.073552	0.072803	0.145077
1.40	0.030657	0.050705	0.055976	0.107705
1.35	0.023199	0.036563	0.044614	0.082836
1.333334	0.022607	0.035882	0.046651	0.083223
1.33	0.025194	0.034077	0.049271	0.085968
1.32	0.026654	0.030193	0.049459	0.084414
1.30	0.027307	0.023678	0.047166	0.078058
1.28	0.027437	0.018415	0.044319	0.071289
1.26	0.027531	0.014499	0.041540	0.064891
1.24	0.027697	0.012203	0.039000	0.059038
1.20	0.028368	0.012658	0.034862	0.049067
1.18	0.028948	0.014448	0.033299	0.044921
1.16	0.029985	0.016573	0.032061	0.041344
1.14	0.032648	0.019216	0.031990	0.040219
1.12	0.034154	0.021839	0.032001	0.038579
1.10	0.035695	0.024455	0.032369	0.037358
1.08	0.036505	0.026436	0.032606	0.036207
1.06	0.039137	0.029725	0.034373	0.036595
1.04	0.041169	0.032490	0.036071	0.037165
1.02	0.043672	0.035579	0.038334	0.038486
1.00	0.049192	0.041257	0.042047	0.041438
0.98	0.051371	0.044990	0.044010	0.042227
0.96	0.053131	0.047636	0.046706	0.044316
0.94	0.054894	0.050122	0.049825	0.047012
0.92	0.056646	0.052494	0.053339	0.050233
0.90	0.058354	0.054744	0.057253	0.053953
0.88	0.059967	0.056837	0.061594	0.058176
0.86	0.061420	0.058714	0.066426	0.062951
0.84	0.062609	0.060281	0.071874	0.068390
0.82	0.063364	0.061371	0.078208	0.074753
0.80	0.063331	0.061636	0.086105	0.082712
0.78	0.061367	0.059961	0.098148	0.094864
0.77	0.056954	0.055912	0.113927	0.110809
0.76	0.044418	0.042371	0.138446	0.134647
0.74	0.064207	0.062096	0.140502	0.136401
0.72	0.082516	0.081298	0.112367	0.108664
0.70	0.084281	0.083557	0.094923	0.091578
0.66	0.075114	0.074675	0.095668	0.092781
0.64	0.068544	0.068071	0.102692	0.099974
0.62	0.060521	0.059901	0.111396	0.108826
0.60	0.050240	0.049272	0.121322	0.118886
0.58	0.037502	0.035477	0.132566	0.130257
0.575	0.051392	0.049196	0.138078	0.135816
0.55	0.085516	0.083900	0.158268	0.156155
0.50	0.130900	0.129934	0.199855	0.197988
0.45	0.182550	0.182042	0.257916	0.256257
0.40	0.249145	0.249011	0.332279	0.330768
0.35	0.345645	0.345768	0.448616	0.447209
0.30	0.494434	0.494702	0.635275	0.633909
0.25	0.744708	0.744971	0.963989	0.962578

Table 6. $|B_0|$, $|D_0|$, etc. for $c/L_{s1}=0.03$ in the case of incidence of SV wave.

L/L_{s1}	$\lvert B_0\rvert$	$\lvert D_0\rvert$	$\lvert A_1\rvert$	$\lvert B_1\rvert$	$\lvert C_1\rvert$	$\lvert D_1\rvert$	$\lvert B_1\rvert/\lvert B_0\rvert$	$\lvert D_1\rvert/\lvert D_0\rvert$
5.900	0.192978	1.070298	0.012372	0.035926	0.011780	0.023334	0.186169	0.021801
5.800	0.192981	1.070301	0.012582	0.035863	0.011988	0.023271		
5.700	0.192984	1.070304	0.012799	0.035796	0.012204	0.023204		
5.600	0.192987	1.070307	0.013025	0.035726	0.012428	0.023133		
5.500	0.192991	1.070311	0.013258	0.035651	0.012660	0.023059	0.184731	0.021544
5.400	0.192995	1.070314	0.013499	0.035572	0.012902	0.022980		
5.300	0.192999	1.070318	0.013749	0.035488	0.013153	0.022897		
5.200	0.193003	1.070322	0.014008	0.035400	0.013415	0.022809		
5.100	0.193008	1.070327	0.014277	0.035305	0.013688	0.022715		
5.000	0.193013	1.070331	0.014557	0.035205	0.013972	0.022616	0.182400	0.021130
4.900	0.193018	1.070336	0.014847	0.035098	0.014269	0.022510		
4.800	0.193023	1.070342	0.015148	0.034984	0.014580	0.022398		
4.700	0.193029	1.070347	0.015462	0.034863	0.014905	0.022278		
4.600	0.193036	1.070353	0.015788	0.034732	0.015245	0.022150		
4.500	0.193043	1.070360	0.016128	0.034593	0.015603	0.022013	0.179199	0.020566
4.400	0.193050	1.070367	0.016482	0.034443	0.015979	0.021867		
4.300	0.193058	1.070375	0.016851	0.034281	0.016374	0.021709		
4.200	0.193067	1.070383	0.017235	0.034107	0.016792	0.021540		
4.100	0.193076	1.070392	0.017637	0.033919	0.017233	0.021358		
4.000	0.193086	1.070402	0.018055	0.033716	0.017700	0.021162	0.174616	0.019770
3.900	0.193097	1.070413	0.018492	0.033495	0.018196	0.020950		
3.800	0.193109	1.070425	0.018948	0.033254	0.018725	0.020720		
3.700	0.193123	1.070438	0.019424	0.032991	0.019290	0.020470		
3.600	0.193138	1.070452	0.019920	0.032703	0.019896	0.020199		
3.500	0.193154	1.070468	0.020436	0.032386	0.020549	0.019902	0.167673	0.018592
3.400	0.193172	1.070486	0.020973	0.032037	0.021257	0.019578		
3.300	0.193192	1.070506	0.021527	0.031649	0.022028	0.019222		
3.200	0.193215	1.070529	0.022098	0.031217	0.022877	0.018831		
3.100	0.193241	1.070555	0.022679	0.030733	0.023820	0.018399		
3.000	0.193270	1.070585	0.023262	0.030187	0.024882	0.017920	0.156191	0.016738
2.900	0.193304	1.070621	0.023830	0.029564	0.026099	0.017387		
2.800	0.193345	1.070663	0.024351	0.028846	0.027532	0.016791		
2.700	0.193393	1.070716	0.024768	0.028006	0.029281	0.016123		
2.600	0.193453	1.070783	0.024957	0.026996	0.031544	0.015371		
2.500	0.193532	1.070876	0.024617	0.025727	0.034772	0.014521	0.132937	0.013560
2.400	0.193652	1.071029	0.022739	0.023948	0.040418	0.013569	0.123667	0.012669
2.300	0.193669	1.071051	0.022346	0.023715	0.041286	0.013470		
2.200	0.193687	1.071076	0.021881	0.023463	0.042257	0.013371		

2,370	0,193707	1,071104	0.021324	0.023190	0.043360	0.013273		
2,360	0,193730	1,071135	0.020646	0.022889	0.044634	0.013176		
2,350	0,193756	1,071172	0.019803	0.022551	0.046141	0.013081		0.012212
2,340	0,193788	1,071217	0.018717	0.022158	0.047988	0.012993		
2,330	0,193827	1,071273	0.017237	0.021681	0.050384	0.012915		
2,320	0,193882	1,071355	0.014969	0.021036	0.053868	0.012863		
2,310	0,194007	1,071544	0.009218	0.019670	0.062127	0.012949	0.101388	0.012085
2,300			0.012677	0.019484	0.064287	0.012786		
2,290	0,193965	1,071473	0.019859	0.020039	0.062340	0.012269	0.103314	0.011451
2,280	0,193911	1,071383	0.024936	0.020535	0.060372	0.011776	0.105900	0.010991
2,270	0,193862	1,071299	0.029028	0.020974	0.058387	0.011306	0.108193	0.010554
2,260	0,193817	1,071221	0.032505	0.021358	0.056390	0.010863	0.110199	0.010140
2,250	0,193776	1,071148	0.035546	0.021689	0.054384	0.010446	0.111929	
2,240	0,193740	1,071020	0.040695	0.022197	0.050360	0.009696	0.114589	0.009053
2,230	0,193684	1,070965	0.042918	0.022377	0.048347	0.009363		
2,220	0,193663	1,070916	0.044956	0.022509	0.046336	0.009059	0.116230	0.008459
2,210			0.046254		0.044559	0.008832		
2,200	0,193636	1,070836	0.048580	0.022635	0.042322	0.008534	0.116897	0.007970
2,190	0,193630	1,070805	0.050204	0.022630	0.040321	0.008313		
2,180	0,193629	1,070780	0.051726	0.022580	0.038322	0.008117	0.116619	
2,170	0,193633	1,070761	0.053156	0.022486	0.036325	0.007945		0.007421
2,160	0,193643	1,070748	0.054508	0.022348	0.034327	0.007797	0.115409	0.007283
2,150	0,193658	1,070742	0.055791	0.022164	0.032327	0.007671		
2,140	0,193678	1,070741	0.057014	0.021934	0.030319	0.007565	0.113252	0.007066
2,130	0,193705	1,070747	0.058187	0.021657	0.028299	0.007479		
2,120	0,193738	1,070760	0.059319	0.021331	0.021331	0.007411		
2,110	0,193778	1,070781	0.060417	0.020952	0.024195	0.007362	0.108126	0.006875
2,100	0,193825	1,070809	0.061491	0.020517	0.022090	0.007331		0.006847
2,090	0,193881	1,070846	0.062551	0.020021	0.019931	0.007323	0.103265	0.006839
2,080	0,193947	1,070893	0.063608	0.019454	0.017694	0.007342		0.006856
2,070	0,194025	1,070952	0.064675	0.018806	0.015345	0.007399		0.006909
2,060	0,194119	1,071026	0.065773	0.018057	0.012827	0.007512	0.093021	0.007015
2,050	0,194236	1,071122	0.066934	0.017172	0.010035	0.007723	0.088408	0.007211
2,040	0,194389	1,071252	0.068224	0.016074	0.006728	0.008125	0.082692	0.007585
2,030	0,194632	1,071465	0.069884	0.014483	0.009069	0.009069	0.074414	0.008465
2,028	0,194679	1,071499	0.070111	0.014249	0.001255	0.009253		
2,027	0,194692	1,071519	0.070235	0.014118	0.000851	0.009361		
2,026	0,194715	1,071540	0.070370	0.013976	0.000404	0.009485		
2,025	0,194743	1,071565	0.070520	0.013815	0.000103	0.009630		

(to be continued)

Table 6. (continued)

L/L_{r1}	$\lvert B_0\rvert$	$\lvert D_0\rvert$	$\lvert A_1\rvert$	$\lvert B_1\rvert$	$\lvert C_1\rvert$	$\lvert D_1\rvert$	$\lvert B_1\rvert/\lvert B_0\rvert$	$\lvert D_1\rvert/\lvert D_0\rvert$
1.734	0.194775	1.071594	0.070692	0.013627	0.000708	0.009809		
1.733	0.194817	1.071633	0.070911	0.013384	0.001502	0.010055	0.068703	0.009383
1.730	0.195022	1.071621	0.069878	0.012406	0.004193	0.010078	0.063616	0.009405
1.728	0.195081	1.071651	0.069325	0.012223	0.004879	0.009839	0.062660	0.009182
1.726	0.195190	1.071712	0.068922	0.012080	0.005465	0.009655	0.061891	0.009009
1.720	0.194904	1.071769	0.068090	0.011749	0.006869	0.009239	0.060281	0.008621
1.700	0.194905	1.071794	0.066704	0.010991	0.009890	0.008386	0.056392	0.007825
1.680	0.194909	1.071810	0.066096	0.010424	0.011847	0.007908	0.053484	0.007378
1.660	0.194913	1.071821	0.065848	0.009952	0.013291	0.007704	0.051060	0.007188
1.640	0.194917	1.071828	0.065827	0.009548	0.014413	0.007771	0.048987	0.007251
1.620	0.194920	1.071832	0.065969	0.009203	0.015306	0.008115		0.007572
1.600	0.194922	1.071833	0.066240	0.008912	0.016023	0.008737		
1.580	0.194922	1.071830	0.066620	0.008675	0.016595	0.009628	0.044505	0.008984
1.560	0.194921	1.071824	0.067096	0.008487	0.017044	0.010778		
1.540	0.194917	1.071815	0.067661	0.008347	0.017381	0.012180	0.042824	0.011364
1.520	0.194912	1.071802	0.068315	0.008246	0.017616	0.013837		
1.500	0.194903	1.071785	0.069059	0.008174	0.017752	0.015766	0.041942	0.014710
1.480	0.194893	1.071764	0.069902	0.008115	0.017791	0.017997		
1.460	0.194880	1.071739	0.070856	0.008045	0.017727	0.020583	0.041286	0.019205
1.440	0.194864	1.071710	0.071944	0.007929	0.017555	0.023607		
1.420	0.194848	1.071676	0.073201	0.007713	0.017259	0.027205		
1.400	0.194833	1.071638	0.074690	0.007308	0.016816	0.031601	0.037511	0.029489
1.380	0.194825	1.071600	0.076521	0.006560	0.016184	0.037223		
1.360	0.194843	1.071570	0.078923	0.005183	0.015281	0.045042	0.026604	0.042034
1.340	0.194981	1.071603	0.082581	0.003993	0.013968	0.058752	0.020482	0.054826
1.338	0.195022	1.071621	0.083105	0.004460	0.013818	0.061115	0.022872	
1.336	0.195081	1.071651	0.083696	0.005383	0.013683	0.064078	0.027597	
1.334	0.195190	1.071712	0.084422	0.007401	0.013618	0.068612	0.037919	0.064021
1.333	0.195303	1.071767	0.086788	0.011689	0.016672	0.078076	0.059854	0.072848
1.328	0.195150	1.071617	0.094590	0.019818	0.028435	0.098393	0.101554	0.091818
1.323	0.194958	1.071452	0.099984	0.026154	0.037056	0.112738	0.134152	0.105220
1.320	0.194817	1.071336	0.102907	0.029835	0.041987	0.120740	0.153143	
1.300	0.193388	1.070252	0.117567	0.053786	0.073461	0.167806	0.278129	0.156791
1.290			0.120528	0.064354	0.087112	0.185164		
1.280	0.191625	1.069023	0.119865	0.072754	0.097830	0.196230	0.379671	0.183560
1.270			0.116019	0.078521	0.105061	0.200797		
1.260	0.190605	1.068386	0.110058	0.081820	0.109074	0.200057	0.429266	0.187252
1.255	0.190506	1.068338	0.106654	0.082713	0.110105	0.198255		

1.250	0.190457	1.068324	0.103134	0.083210	0.110633	0.195797	0.436899	0.183275
1.245	0.190450	1.068338	0.099595	0.083390	0.110760	0.192875		
1.240	0.190474	1.068373	0.096109	0.083320	0.110578	0.189651	0.437436	0.177514
1.220	0.190762	1.068629	0.083492	0.081598	0.108120	0.175873	0.427752	
1.200	0.191156	1.068940	0.073535	0.079048	0.104798	0.163262	0.413529	0.152733
1.180	0.191541	1.069235	0.065951	0.076555	0.101722	0.152844		
1.160	0.191891	1.069499	0.060168	0.074368	0.099182	0.144500	0.387553	0.135110
1.140	0.192207	1.069738	0.055699	0.072519	0.097192	0.137864		
1.120	0.192498	1.069958	0.052184	0.070973	0.095692	0.132582		
1.100	0.192774	1.070170	0.049367	0.069682	0.094608	0.128366	0.361474	0.119950
1.080	0.193045	1.070382	0.047068	0.068601	0.093873	0.124994		
1.060	0.193327	1.070606	0.045158	0.067690	0.093429	0.122293		
1.040	0.193637	1.070859	0.043539	0.066920	0.093228	0.120123		
1.020	0.194021	1.071179	0.042128	0.066265	0.093218	0.118352		
1.000	0.194902	1.071944	0.040683	0.065704	0.093151	0.116445	0.337118	0.108630
0.990	0.194873	1.071951	0.048148	0.066788	0.090619	0.109152	0.342726	0.101826
0.980			0.051303	0.067334	0.089958	0.106491		
0.970			0.053751	0.067861	0.089662	0.104704		
0.960			0.055839	0.068406	0.089579	0.103407		
0.950			0.057703	0.068978	0.089645	0.102443		
0.940			0.059414	0.069580	0.089826	0.101730		
0.930			0.061016	0.070212	0.090100	0.101215		
0.920			0.062536	0.070876	0.090455	0.100865		
0.910			0.063993	0.071570	0.090881	0.100655		
0.900	0.194854	1.071958	0.065403	0.072295	0.091369	0.100565	0.371021	0.093815
0.850	0.194854	1.071959	0.072061	0.076365	0.094604	0.101546		0.094730
0.800	0.194857	1.071960	0.078565	0.081183	0.098965	0.104343	0.416630	0.097339
0.750	0.194860	1.071962	0.085327	0.086797	0.104375	0.108606		
0.700	0.194865	1.071963	0.092638	0.093310	0.110887	0.114248	0.478847	0.106578
0.650	0.194871	1.071964	0.100767	0.100883	0.118644	0.121331		
0.600	0.194879	1.071966	0.110014	0.109748	0.127884	0.130041	0.563160	0.121311
0.550	0.194890	1.071967	0.120750	0.120230	0.138958	0.140691		
0.500	0.194904	1.071970	0.133473	0.132797	0.152374	0.153767	0.681345	0.143444
0.450	0.194923	1.071973	0.148886	0.148126	0.168881	0.169998		
0.400	0.194951	1.071977	0.168026	0.167241	0.189611	0.190503	0.857863	0.177712
0.350	0.194991	1.071983	0.192521	0.191755	0.216352	0.217059		
0.300	0.195054	1.071992	0.225068	0.224357	0.252090	0.252645		
0.250	0.195157	1.072007	0.270521	0.269891	0.302206	0.302634	1.382941	0.282306
0.150	0.195761	1.072091	0.451863	0.451455	0.503011	0.503239		
0.100	0.196934	1.072261	0.678233	0.677955	0.754226	0.754372	3.442552	0.703534

Table 7. $|B_0|$, $|D_0|$, etc. for $c/L_{s1}=0.05$ in the case of incidence of SV wave.

L/L_{s1}	$\lvert B_0\rvert$	$\lvert D_0\rvert$	$\lvert A_1\rvert$	$\lvert B_1\rvert$	$\lvert C_1\rvert$	$\lvert D_1\rvert$	$\lvert B_1\rvert/\lvert B_0\rvert$	$\lvert D_1\rvert/\lvert D_0\rvert$
5.900	0.180494	1.076755	0.020620	0.059877	0.019633	0.038890	0.331742	0.036118
5.800	0.180503	1.076763	0.020970	0.059772	0.019980	0.038785		
5.700	0.180512	1.076772	0.021333	0.059661	0.020340	0.038674		
5.600	0.180521	1.076781	0.021708	0.059543	0.020713	0.038556		
5.500			0.022096	0.059419	0.021101	0.038432		
5.400	0.180542	1.076800	0.022499	0.059287	0.021504	0.038301		0.035569
5.300	0.180553	1.076811	0.022915	0.059148	0.021923	0.038162		
5.200	0.180565	1.076822	0.023348	0.059000	0.022359	0.038015		
5.100	0.180578	1.076834	0.023796	0.058843	0.022813	0.037859		
5.000	0.180591	1.076847	0.024261	0.058676	0.023288	0.037694	0.324910	0.035004
4.900	0.180606	1.076861	0.024745	0.058498	0.023783	0.037518		
4.800	0.180621	1.076876	0.025247	0.058308	0.024300	0.037330		
4.700	0.180638	1.076891	0.025770	0.058105	0.024842	0.037131		
4.600	0.180656	1.076908	0.026314	0.057888	0.025409	0.036917		
4.500	0.180675	1.076927	0.026880	0.057655	0.026005	0.036689	0.319110	0.034068
4.400			0.027470	0.057405	0.026631	0.036445		
4.300	0.180718	1.076968	0.028085	0.057136	0.027291	0.036182		
4.200	0.180742	1.076991	0.028726	0.056846	0.027986	0.035901		
4.100	0.180768	1.077016	0.029395	0.056533	0.028722	0.035597		
4.000	0.180796	1.077043	0.030093	0.056193	0.029500	0.035270	0.310811	0.032747
3.900	0.180827	1.077073	0.030821	0.055825	0.030328	0.034916		
3.800	0.180860	1.077106	0.031581	0.055423	0.031209	0.034533		
3.700	0.180898	1.077142	0.032374	0.054985	0.032150	0.034117		
3.600	0.180893	1.077182	0.033200	0.054505	0.033160	0.033665		
3.500	0.180984	1.077227	0.034061	0.053977	0.034249	0.033171	0.298246	0.030793
3.400	0.181034	1.077276	0.034955	0.053395	0.035428	0.032631		
3.300	0.181090	1.077332	0.035879	0.052749	0.036714	0.032038		
3.200	0.181153	1.077396	0.036830	0.052029	0.038129	0.031385		
3.100	0.181225	1.077468	0.037799	0.051223	0.039700	0.030665		
3.000	0.181307	1.077552	0.038771	0.050312	0.041470	0.029866	0.277496	0.027717
2.900	0.181402	1.077651	0.039716	0.049274	0.043499	0.028978		
2.800	0.181513	1.077769	0.040585	0.048078	0.045887	0.027986		
2.700	0.181648	1.077915	0.041280	0.046677	0.048803	0.026872		
2.600	0.181814	1.078102	0.041595	0.044994	0.052574	0.025618		
2.500	0.182034	1.078361	0.041028	0.042879	0.057954	0.024202	0.235556	0.022443
2.400	0.182368	1.078785	0.037898	0.039914	0.067363	0.022616	0.218866	0.020964
2.390	0.182414	1.078847	0.037243	0.039525	0.068810	0.022451	0.216677	0.020810
2.380	0.182465	1.078915	0.034684	0.039106	0.070429	0.022286		

2.370	0.182521	1.078992	0.035540	0.038651	0.072267	0.022121	0.211764	0.020502
2.360	0.182585	1.079080	0.034411	0.038149	0.074390	0.021960		
2.350	0.182658	1.079182	0.033006	0.037585	0.076902	0.021803	0.205770	0.020203
2.340	0.182744	1.079306	0.031196	0.036931	0.079980	0.021655		
2.330	0.182853	1.079464	0.028729	0.036135	0.083973	0.021525	0.197619	0.019940
2.320	0.183006	1.079690	0.024948	0.035060	0.089781	0.021439		
2.310	0.183353	1.080214	0.015364	0.032783	0.103546	0.021583	0.178799	0.019980
2.300	0.183400	1.080279	0.021129	0.032473	0.107145	0.021310	0.177064	0.019726
2.280	0.183239	1.080018	0.033099	0.033398	0.103901	0.020449	0.182268	
2.260	0.183090	1.079770	0.041561	0.034225	0.100612	0.019626	0.186933	
2.240	0.182953	1.079537	0.048381	0.034957	0.097312	0.018844	0.191073	
2.220	0.182828	1.079319	0.054176	0.035597	0.093983	0.018105	0.194704	
2.200	0.182716	1.079117	0.059244	0.036148	0.090641	0.017410	0.197840	0.016134
2.160	0.182532	1.078762	0.067826	0.036995	0.083934	0.016160	0.202677	
2.140	0.182460	1.078609	0.071530	0.037295	0.080579	0.015605	0.204401	0.014468
2.120	0.182401	1.078473	0.074927	0.037515	0.077226	0.015099		
2.080	0.182326	1.078250	0.080966	0.037725	0.070537	0.014224	0.206913	0.013192
2.060	0.182309	1.078164	0.083674	0.037717	0.067201	0.013854	0.206882	
2.040	0.182306	1.078094	0.086210	0.037634	0.063870	0.013528		0.012548
2.020	0.182317	1.078042	0.088594	0.037478	0.060542	0.013243		
2.000	0.182343	1.078006	0.090847	0.037246	0.057213	0.012996	0.204266	0.012056
1.980	0.182385	1.077987	0.092985	0.036940	0.053878	0.012786		
1.960	0.182442	1.077986	0.095024	0.036557	0.050532	0.012609	0.200379	0.011697
1.940	0.182515	1.078003	0.096979	0.036095	0.047165	0.012465		
1.920	0.182606	1.078039	0.098865	0.035551	0.043768	0.012352		
1.900	0.182717	1.078096	0.100695	0.034920	0.040325	0.012270	0.191118	0.011381
1.880	0.182848	1.078174	0.102486	0.034196	0.036817	0.012219		0.011333
1.860	0.183003	1.078276	0.104252	0.033368	0.033218	0.012205		0.011319
1.840	0.183187	1.078407	0.106013	0.032424	0.029490	0.012237	0.177002	0.011347
1.820	0.183404	1.078571	0.107792	0.031344	0.025575	0.012331	0.170901	0.011433
1.800	0.183666	1.078777	0.109622	0.030095	0.021378	0.012521	0.163858	0.011606
1.780	0.183990	1.079042	0.111556	0.028620	0.016725	0.012872	0.155551	
1.760	0.184415	1.079403	0.113708	0.026790	0.011214	0.013541	0.145273	
1.740	0.185089	1.079996	0.116474	0.024139	0.003290	0.015116	0.130417	0.013996
1.738	0.185195	1.080091	0.116852	0.023748	0.002092	0.015422		
1.737	0.185255	1.080145	0.117059	0.023531	0.001418	0.015603		
1.736	0.185321	1.080205	0.117284	0.023293	0.000673	0.015808		
1.735	0.185397	1.080273	0.117533	0.023025	0.000173	0.016050		
1.734	0.185487	1.080355	0.117821	0.022711	0.001180	0.016349		

(to be continued)

Table 7. (continued)

L/L_{s1}	$\lvert B_0\rvert$	$\lvert D_0\rvert$	$\lvert A_1\rvert$	$\lvert B_1\rvert$	$\lvert C_1\rvert$	$\lvert D_1\rvert$	$\lvert B_1\rvert/\lvert B_0\rvert$	$\lvert D_1\rvert/\lvert D_0\rvert$
1.733	0.185605	1.080463	0.118185	0.022307	0.002503	0.016759		0.015510
1.730	0.185859	1.080767	0.116464	0.020677	0.006989	0.016797	0.111253	0.015542
1.728	0.185853	1.080788	0.115541	0.020372	0.008132	0.016399	0.109617	0.015173
1.726	0.185850	1.080804	0.114870	0.020134	0.009108	0.016091	0.108335	
1.720	0.185847	1.080840	0.113483	0.019581	0.011448	0.015399	0.105364	0.014247
1.700	0.185852	1.080912	0.111173	0.018318	0.016484	0.013977	0.098564	0.012931
1.680	0.185865	1.080957	0.110160	0.017374	0.019745	0.013180	0.093477	0.012192
1.660	0.185880	1.080987	0.109748	0.016587	0.022152	0.012840	0.089237	0.011878
1.640	0.185894	1.081007	0.109712	0.015914	0.024022	0.012952	0.085608	0.011981
1.620	0.185906	1.081018	0.109949	0.015338	0.025511	0.013526	0.082508	0.012512
1.600	0.185914	1.081020	0.110401	0.014854	0.026706	0.014563	0.079901	0.013471
1.580	0.185919	1.081013	0.111034	0.014458	0.027659	0.016048	0.077768	
1.560	0.185919	1.080997	0.111826	0.014146	0.028406	0.017964	0.076089	0.016618
1.540	0.185914	1.080971	0.112769	0.013912	0.028969	0.020300		
1.520	0.185903	1.080936	0.113859	0.013743	0.029361	0.023062	0.073930	
1.500	0.185886	1.080890	0.115099	0.013624	0.029588	0.026276	0.073293	0.024310
1.480	0.185863	1.080833	0.116504	0.013526	0.029651	0.029995		
1.460	0.185834	1.080764	0.118093	0.013409	0.029546	0.034305	0.072159	
1.440	0.185800	1.080684	0.119906	0.013216	0.029258	0.039346		
1.420	0.185765	1.080591	0.122002	0.012855	0.028765	0.045341	0.069201	
1.400	0.185735	1.080480	0.124484	0.012180	0.028027	0.052669		0.048745
1.380	0.185729	1.080385	0.127535	0.010933	0.026973	0.062039	0.058867	
1.360	0.185799	1.080304	0.131540	0.008639	0.025469	0.075071		
1.340	0.186213	1.080397	0.137635	0.006656	0.023280	0.097920	0.035745	0.090633
1.338	0.186330	1.080449	0.138508	0.007343	0.023031	0.101858	0.039898	
1.336	0.186499	1.080533	0.139494	0.008972	0.022805	0.106797	0.048111	
1.334	0.186810	1.080702	0.140703	0.012335	0.022697	0.114354	0.066033	0.105814
1.333	0.187138	1.080857	0.144646	0.019483	0.027787	0.130126	0.104110	
1.328	0.186763	1.080445	0.157650	0.033030	0.047393	0.163988	0.176857	0.151779
1.323	0.186269	1.079989	0.166640	0.043590	0.061760	0.187897	0.234015	
1.320	0.185903	1.079671	0.171512	0.049725	0.069979	0.201235	0.267479	0.186385
1.300	0.182054	1.076667	0.195946	0.089644	0.122436	0.279677	0.492406	0.259762
1.290			0.200881	0.107257	0.145187	0.308607		
1.280		1.073246	0.199775	0.121257	0.163051	0.327050		0.304730
1.270			0.193365	0.130868	0.175103	0.334663		
1.260	0.174120	1.071461	0.183431	0.136367	0.181790	0.333428	0.783179	0.311190
1.255	0.173809	1.071325	0.177757	0.137856	0.183509	0.330425		
1.250	0.173642	1.071284	0.171890	0.138684	0.184389	0.326329	0.798682	0.304615

1.245	0.173593	1.071320	0.165992	0.138983	0.184600	0.321459		
1.240	0.173639	1.071415	0.160183	0.138867	0.184297	0.316085	0.799750	0.295017
1.220	0.174383	1.072122	0.139154	0.135998	0.180200	0.293122	0.779882	0.273404
1.200	0.175452	1.072984	0.122559	0.131747	0.174664	0.272104	0.750900	
1.180	0.176514	1.073802	0.109918	0.127591	0.169537	0.254740		
1.160	0.177482	1.074536	0.100281	0.123947	0.165303	0.240833	0.698362	0.224128
1.140	0.178358	1.075198	0.092832	0.120865	0.161987	0.229774		
1.120	0.179163	1.075810	0.086973	0.118289	0.159487	0.220970	0.660231	
1.100	0.179928	1.076398	0.082279	0.116137	0.157681	0.213944		0.198760
1.080	0.180683	1.076987	0.078447	0.114335	0.156455	0.208324	0.632795	
1.060	0.181464	1.077609	0.075264	0.112818	0.155715	0.203822		
1.040	0.182327	1.078312	0.072565	0.111534	0.155380	0.200206	0.611725	0.185666
1.020	0.183392	1.079201	0.070213	0.110442	0.155363	0.197253		
1.000	0.185840	1.081327	0.067805	0.109508	0.155252	0.194076	0.589260	0.179480
0.990	0.185765	1.081347	0.080246	0.111313	0.151033	0.181920	0.599216	0.168235
0.980			0.085506	0.112223	0.149930	0.177486		
0.970			0.089586	0.113103	0.149438	0.174508		
0.960			0.093065	0.114011	0.149299	0.172345		
0.950			0.096172	0.114964	0.149408	0.170739		
0.940			0.099024	0.115966	0.149710	0.169550		
0.930			0.101694	0.117021	0.150168	0.168693		
0.920			0.104226	0.118127	0.150759	0.168109		
0.910			0.106655	0.119284	0.151468	0.167758		
0.900	0.185748	1.081372	0.109005	0.120491	0.152282	0.167609	0.648683	0.154997
0.850			0.120102	0.127275	0.157673	0.169244		
0.800			0.130942	0.135305	0.164943	0.173905		
0.750			0.142212	0.144662	0.173959	0.181010		
0.700			0.154397	0.155517	0.184811	0.190413		
0.650			0.167945	0.168139	0.197740	0.202219		
0.600	0.186007	1.081418	0.183356	0.182913	0.213141	0.216735	0.983369	0.200417
0.550			0.201250	0.200384	0.231597	0.234486		
0.500			0.222456	0.221328	0.253957	0.256278		
0.450			0.248143	0.246877	0.281469	0.283330		
0.400			0.280044	0.278735	0.316019	0.317505		
0.350			0.320868	0.319592	0.360587	0.361765		
0.300	0.187431	1.081615	0.375114	0.373928	0.420151	0.420175	1.995015	0.389302
0.250			0.450868	0.449819	0.503677	0.504390		
0.150			0.753105	0.752425	0.838352	0.838731		
0.100	0.201984	1.083737	1.130388	1.129924	1.257043	1.257286		

Table 8. $|B_0|$, $|D_0|$, etc. for $c/L_{s1}=0.10$ in the case of incidence of SV wave.

L/L_{s1}	$\lvert B_0\rvert$	$\lvert D_0\rvert$	$\lvert A_1\rvert$	$\lvert B_1\rvert$	$\lvert C_1\rvert$	$\lvert D_1\rvert$	$\lvert B_1\rvert/\lvert B_0\rvert$	$\lvert D_1\rvert/\lvert D_0\rvert$
5.900	0.121979	1.107022	0.041240	0.119755	0.039267	0.077781	0.981772	0.070262
5.800	0.122013	1.107054	0.041941	0.119544	0.039961	0.077570		
5.700	0.122049	1.107088	0.042666	0.119322	0.040681	0.077348		
5.600	0.122086	1.107124	0.043416	0.119087	0.041427	0.077113		
5.500	0.122127	1.107162	0.044193	0.118838	0.042203	0.076865	0.973073	0.069425
5.400	0.122169	1.107202	0.044998	0.118575	0.043008	0.076603		
5.300	0.122214	1.107245	0.045831	0.118296	0.043846	0.076325		
5.200	0.122262	1.107290	0.046696	0.118000	0.044719	0.076031		
5.100	0.122313	1.107339	0.047592	0.117686	0.045627	0.075719		
5.000	0.122367	1.107390	0.048523	0.117352	0.046576	0.075388	0.959020	0.068077
4.900	0.122425	1.107445	0.049490	0.116996	0.047566	0.075036		
4.800	0.122487	1.107504	0.050495	0.116616	0.048601	0.074661		
4.700	0.122553	1.107568	0.051541	0.116210	0.049684	0.074262		
4.600	0.122624	1.107636	0.052628	0.115776	0.050819	0.073835		
4.500	0.122701	1.107709	0.053761	0.115310	0.052011	0.073378	0.939770	0.066243
4.400	0.122783	1.107787	0.054940	0.114810	0.053263	0.072890		
4.300	0.122872	1.107873	0.056170	0.114272	0.054582	0.072365		
4.200	0.122968	1.107965	0.057452	0.113692	0.055973	0.071802		
4.100	0.123072	1.108065	0.058790	0.113066	0.057444	0.071195		
4.000	0.123185	1.108175	0.060186	0.112387	0.059001	0.070541	0.912344	0.063655
3.900	0.123309	1.108294	0.061642	0.111650	0.060656	0.069833		
3.800	0.123444	1.108426	0.063162	0.110847	0.062418	0.069067		
3.700	0.123592	1.108570	0.064748	0.109971	0.064301	0.068235		
3.600	0.123755	1.108730	0.066401	0.109011	0.066321	0.067330		
3.500	0.123936	1.108908	0.068122	0.107955	0.068498	0.066342	0.871062	0.059827
3.400	0.124137	1.109107	0.069910	0.106790	0.070857	0.065262		
3.300	0.124361	1.109331	0.071759	0.105499	0.073429	0.064076		
3.200	0.124614	1.109584	0.073661	0.104059	0.076253	0.062771		
3.100	0.124901	1.109875	0.075599	0.102446	0.079400	0.061330		
3.000	0.125229	1.110211	0.077542	0.100624	0.082940	0.059733	0.803521	0.053803
2.900	0.125609	1.110606	0.079433	0.098542	0.086999	0.057856		
2.800	0.126056	1.111080	0.081171	0.096156	0.091775	0.055972		
2.700	0.126592	1.111662	0.082561	0.093354	0.097606	0.053745		
2.600	0.127259	1.112411	0.083191	0.089989	0.105148	0.051237		
2.500	0.128139	1.113447	0.082056	0.085759	0.115909	0.048404	0.669265	0.043473
2.400	0.129473	1.115141	0.075797	0.079828	0.134727	0.045232	0.616565	0.040562
2.390	0.129659	1.115389	0.074487	0.079050	0.137620	0.044902	0.609679	0.040257
2.380	0.129863	1.115663	0.072936	0.078213	0.140859	0.044572		

2.370	0.130088	1.115971	0.071080	0.077303	0.144535	0.044243	0.594237	0.039645
2.360	0.130341	1.116322	0.068822	0.076299	0.148781	0.043920		
2.350	0.130632	1.116731	0.066012	0.075170	0.153805	0.043606	0.575440	0.039048
2.340	0.130978	1.117226	0.062393	0.073863	0.159960	0.043310		
2.330	0.131414	1.117857	0.057458	0.072270	0.167946	0.043050	0.549945	0.038512
2.320	0.132025	1.118761	0.049897	0.070121	0.179563	0.042878		
2.310	0.133414	1.120860	0.030729	0.065567	0.207092	0.043166	0.491456	0.038511
2.300	0.133614	1.121122	0.042259	0.064947	0.214291	0.042621	0.486081	0.038016
2.280	0.132994	1.120081	0.066198	0.066797	0.207803	0.040899	0.502261	
2.260	0.132415	1.119094	0.083122	0.068451	0.201242	0.039253	0.516945	
2.240	0.131879	1.118165	0.096763	0.069915	0.194625	0.037689	0.530142	
2.220	0.131390	1.117296	0.108352	0.071195	0.187967	0.036210	0.541859	
2.200	0.130948	1.116491	0.118488	0.072297	0.181281	0.034821	0.552105	0.031188
2.160	0.130214	1.115071	0.135653	0.073990	0.167868	0.032320	0.568219	
2.140	0.129924	1.114460	0.143061	0.074590	0.161158	0.031211	0.574106	0.028005
2.100	0.130266	1.114243	0.154182		0.148531	0.029441		
2.080	0.129373	1.113023	0.161933	0.075451	0.141075	0.028448	0.583205	0.025559
2.060	0.129299	1.112677	0.167349	0.075435	0.134403	0.027709	0.583412	0.024903
2.040	0.129281	1.112397	0.172420	0.075269	0.127741	0.027057		
2.020	0.129320	1.112184	0.177189	0.074955	0.121084	0.026486		
2.000	0.129418	1.112040	0.181694	0.074493	0.114426	0.025992	0.575602	0.023374
1.980	0.129577	1.111963	0.185969	0.073881	0.107757	0.025572		
1.960	0.129798	1.111958	0.190048	0.073115	0.101064	0.025219	0.563296	0.022680
1.940	0.130087	1.112024	0.193958	0.072191	0.094331	0.024931		
1.920	0.130446	1.112167	0.197730	0.071103	0.087536	0.024705		
1.900	0.130883	1.112391	0.201391	0.069841	0.080650	0.024540	0.533616	0.022060
1.880	0.131405	1.112702	0.204972	0.068392	0.073634	0.024439		0.021964
1.860	0.132023	1.113111	0.208505	0.066736	0.066436	0.024411		0.021931
1.840	0.132754	1.113631	0.212027	0.064849	0.058980	0.024474	0.488490	0.021977
1.820	0.133622	1.114286	0.215585	0.062688	0.051150	0.024663	0.469145	0.022133
1.800	0.134667	1.115111	0.219244	0.060190	0.042757	0.025042	0.446957	0.022457
1.780	0.135961	1.116171	0.223113	0.057240	0.033451	0.025745	0.420811	0.023065
1.760	0.137663	1.117614	0.227415	0.053581	0.022429	0.027083	0.389222	0.024233
1.740	0.140358	1.119984	0.232948	0.048278	0.006581	0.030232	0.343961	0.026993
1.738	0.140782	1.120365	0.233704	0.047497	0.004185	0.030845		
1.737	0.141022	1.120581	0.234118	0.047063	0.002837	0.031206		
1.736	0.141287	1.120821	0.234568	0.046586	0.001347	0.031617	0.329731	0.028209
1.735	0.141589	1.121095	0.235066	0.046051	0.000346	0.032101		
1.734	0.141948	1.121422	0.235642	0.045423	0.002360	0.032699		

(to be continued)

Table 8. (continued)

L/L_{s1}	$\lvert B_0\rvert$	$\lvert D_0\rvert$	$\lvert A_1\rvert$	$\lvert B_1\rvert$	$\lvert C_1\rvert$	$\lvert D_1\rvert$	$\lvert B_1\rvert/\lvert B_0\rvert$	$\lvert D_1\rvert/\lvert D_0\rvert$
1.733	0.142420	1.121855	0.236370	0.044615	0.005007	0.033518	0.313263	0.029877
1.730	0.143441	1.123071	0.232928	0.041355	0.013978	0.033595	0.288306	0.029914
1.728	0.143428	1.123155	0.231083	0.040745	0.016264	0.032798	0.284083	0.029201
1.726	0.143423	1.123220	0.229740	0.040268	0.018217	0.032183	0.280768	0.028652
1.720	0.143427	1.123363	0.226967	0.039163	0.022897	0.030798	0.273053	0.027416
1.700	0.143512	1.123657	0.222346	0.036637	0.032968	0.027955	0.255288	0.024879
1.680	0.143630	1.123844	0.220321	0.034748	0.039491	0.026359	0.241930	0.023455
1.660	0.143759	1.123974	0.219496	0.033174	0.044304	0.025681	0.230765	0.022848
1.640	0.143889	1.124061	0.219425	0.031828	0.048045	0.025904	0.221199	0.023045
1.620	0.144018	1.124111	0.219899	0.030677	0.051022	0.027052	0.213012	0.024065
1.600	0.144141	1.124127	0.220803	0.029709	0.053412	0.029126	0.206115	0.025909
1.580	0.144257	1.124108	0.222068	0.028917	0.055319	0.032096	0.200457	0.028552
1.560	0.144364	1.124054	0.223653	0.028293	0.056813	0.035928	0.195984	0.031963
1.540	0.144619	1.123963	0.225539	0.027824	0.057939	0.040601		
1.520	0.144549	1.123833	0.227718	0.027487	0.058722	0.046125	0.190161	0.041043
1.500	0.144629	1.123663	0.230199	0.027248	0.059176	0.052553	0.188403	0.046769
1.480	0.144702	1.123449	0.233008	0.027052	0.059303	0.059990		
1.460	0.144774	1.123191	0.236187	0.026819	0.059092	0.068610	0.185250	0.061085
1.440	0.144856	1.122886	0.239813	0.026432	0.058517	0.078692		
1.420	0.144969	1.122538	0.244005	0.025710	0.057531	0.090683	0.177351	0.080784
1.400	0.145153	1.122155	0.248968	0.024361	0.056055	0.105338		
1.380	0.145504	1.121768	0.255070	0.021867	0.053946	0.124078	0.150283	0.110609
1.360	0.146281	1.121486	0.263079	0.017278	0.050939	0.150143		
1.340	0.148676	1.121922	0.275271	0.013312	0.046561	0.195840	0.089539	0.174558
1.338	0.149244	1.122141	0.277017	0.014868	0.046063	0.203717	0.099625	0.181543
1.336	0.150028	1.122484	0.278989	0.017945	0.045610	0.213594	0.119612	0.190287
1.334	0.151394	1.123176	0.281407	0.024671	0.045395	0.228708	0.162962	0.203626
1.333	0.153010	1.123822	0.289293	0.038965	0.055574	0.260253	0.254661	0.231578
1.328	0.152762	1.122256	0.315299	0.066061	0.094786	0.327977	0.432443	0.292248
1.323	0.151840	1.120496	0.333280	0.087180	0.123521	0.375794	0.574157	0.335382
1.320	0.151009	1.119257	0.343024	0.099450	0.139958	0.402470	0.658570	0.359586
1.300	0.139606	1.107400	0.391893	0.179289	0.244873	0.559355	1.284253	0.505106
1.290			0.401762	0.214515	0.290374	0.617215		
1.280	0.120304	1.093593	0.399550	0.242515	0.326102	0.654100	2.015843	0.598120
1.270			0.386730	0.261737	0.350206	0.669326		
1.260	0.104186	1.086184	0.366862	0.272735	0.363581	0.666857	2.617759	0.613944
1.255	0.101758	1.085582	0.355514	0.275712	0.367019	0.660851		
1.250	0.199998	1.085369	0.343781	0.277369	0.368778	0.652658	2.773752	0.601323

1.245	0.098840	1.085470	0.331985	0.277966	0.369201	0.642919	
1.240	0.098200	1.085815	0.320366	0.277735	0.368595	0.632170	2.828261
1.220	0.099094	1.088559	0.278308	0.271996	0.360401	0.586245	2.744808
1.200	0.102500	1.091974	0.245118	0.263495	0.349329	0.544209	2.570688
1.180	0.106378	1.095229	0.219837	0.255183	0.339075	0.509481	
1.160	0.110090	1.098158	0.200562	0.247894	0.330606	0.481667	2.251730
1.140	0.113515	1.100800	0.185665	0.241731	0.323975	0.459548	
1.120	0.116700	1.103247	0.173947	0.236578	0.318975	0.441941	2.027238
1.100	0.119738	1.105596	0.164558	0.232275	0.315362	0.427889	
1.080	0.128442	1.113036	0.153666	0.228603			
1.060		1.110440	0.150528	0.225636	0.311431	0.407644	
1.040	0.129311	1.113248	0.145130	0.223068	0.310761	0.400412	1.725049
1.020	0.133570	1.116804	0.140427	0.220884	0.310727	0.394507	
1.000	0.143361	1.125311	0.135610	0.219016	0.310505	0.388153	1.527718
0.990	0.143187	1.125402	0.160493	0.222627	0.302066	0.363841	1.554801
0.980			0.171013	0.224447	0.299860	0.354972	
0.970			0.179171	0.226206	0.298876	0.349016	
0.960			0.186130	0.228022	0.298598	0.344691	
0.950	0.143513	1.125510	0.192344	0.229928	0.298817	0.341479	1.602133
0.940			0.198049	0.231933	0.299420	0.339101	
0.930			0.203388	0.234042	0.300336	0.337386	
0.920			0.208453	0.236254	0.301519	0.336218	
0.910			0.213311	0.238568	0.302936	0.335516	
0.900	0.144080	1.125594	0.218011	0.240983	0.304564	0.335219	1.672564
0.850			0.240205	0.254551	0.315347	0.338489	
0.800			0.261884	0.270611	0.329886	0.347810	
0.750			0.284425	0.289324	0.347919	0.362020	
0.700			0.308795	0.311035	0.369623	0.380826	
0.650			0.335891	0.336279	0.395481	0.404438	
0.600	0.149823	1.126229	0.366713	0.365827	0.426283	0.433470	2.441732
0.550			0.402501	0.400769	0.463195	0.468972	
0.500			0.444912	0.442656	0.507915	0.512557	
0.450			0.496286	0.493754	0.562938	0.566660	
0.400	0.161316	1.127494	0.560089	0.557471	0.632038	0.635010	3.455760
0.350			0.641737	0.639184	0.721174	0.723531	
0.300	0.176071	1.129238	0.750228	0.747856	0.840303	0.842151	4.247456

	0.582208		
	0.538551		
	0.498371		
	0.438613		
	0.400582		
	0.387021		
	0.367101		
	0.359679		
	0.344929		
	0.323299		
	0.303399		
	0.297815		
	0.384886		
	0.563204		
	0.745768		

Table 9. $|A_1|/|B_1|$ and $|C_1|/|D_1|$ in the case of incidence of SV wave.

L/L_{s1}	$\lvert A_1\rvert/\lvert B_1\rvert$	$\lvert C_1\rvert/\lvert D_1\rvert$	L/L_{s1}	$\lvert A_1\rvert/\lvert B_1\rvert$	$\lvert C_1\rvert/\lvert D_1\rvert$
5.800	0.350843	0.515165	1.720	5.79540	0.743466
5.500	0.371879	0.549052	1.700	6.06891	1.179315
5.000	0.413488	0.617812	1.660		1.725168
4.500	0.466229	0.708805	1.640	6.89401	1.854708
4.000	0.535524	0.836417	1.620		1.886049
3.500	0.631025	1.032497	1.600	7.43202	1.833826
3.000	0.770611	1.388504	1.500	8.44813	1.126023
2.700	0.884386	1.816076	1.460		0.861276
2.600	0.924458	2.052164	1.420	9.49052	0.634423
2.500	0.956831		1.400	10.21977	
2.400	0.949505	2.978540	1.380	11.66464	0.43478
2.390	0.942277		1.360	15.22550	
2.360	0.902000	3.387550	1.340	20.67780	0.237752
2.340	0.844715		1.338	18.63113	
2.330	0.795049	3.901118	1.336	15.54668	
2.320	0.711589		1.334	11.40614	0.198485
2.310	0.468679	4.797511	1.333	7.42428	0.213541
2.300	0.650675		1.328	4.77286	0.289002
2.280	0.991028		1.323	3.82289	0.328694
2.260	1.214331	5.126709	1.320	3.44921	
2.220		5.190949	1.300	2.18581	
2.200	1.638900	5.206064	1.280	1.64753	0.498551
2.160		5.193938	1.260	1.34512	
2.140	1.917959	5.163477	1.200	0.930258	0.641902
2.060	2.218462	4.850389	1.100	0.708461	0.737017
2.000	2.439059	4.402231	1.060	0.667126	
1.980	2.517155	4.213867	1.020	0.635750	
1.940	2.686715		1.000	0.619181	0.789956
1.900	2.88356	3.286443	0.990	0.720907	0.830210
1.860	3.12429	2.721508	0.950	0.836541	0.875068
1.820	3.43900		0.900	0.904672	0.908552
1.800	3.64251	1.707372	0.800	0.967754	0.948466
1.760	4.24430	0.828148	0.700	0.992799	0.970582
1.740	4.82515	0.217690	0.600	1.002421	0.983418
1.738		0.135698	0.550	1.004321	
1.737		0.090940	0.500	1.005096	
1.736		0.042609	0.450	1.005129	
1.735	5.10443	0.010788	0.400	1.004695	
1.734		0.072195	0.300	1.003171	0.997806
1.733	5.29799	0.149409	0.200	1.000904	
1.730	5.63241	0.416077	0.100	1.000410	0.999807

Table 10. $|A_2|$, $|B_2|$, etc. for $c/L_{s1}=0.10$ in the case of incidence of SV wave.

L/L_{s1}	$\|A_2\|$	$\|B_2\|$	$\|C_2\|$	$\|D_2\|$
5.800	0.019907	0.035127	0.017583	0.014945
5.700	0.020410	0.035000	0.018045	0.014765
5.600	0.020955	0.034871	0.018644	0.014573
5.500	0.021552	0.034740	0.019313	0.014370
5.400	0.022213	0.034611	0.020068	0.014152
5.300	0.022955	0.034485	0.020933	0.013921
5.200	0.023801	0.034368	0.021943	0.013673
5.100	0.024792	0.034266	0.023154	0.013408
5.000	0.025988	0.034192	0.024653	0.013124
4.900	0.027508	0.034170	0.026607	0.012820
4.800	0.029605	0.034255	0.029375	0.012497
4.700	0.033067	0.034611	0.034053	0.012170
4.639001	0.037661	0.035342	0.040347	0.012028
4.619001	0.043073	0.036420	0.047783	0.012154
4.618	0.043813	0.036531	0.048786	0.012157
4.600	0.043301	0.036294	0.048302	0.011984
4.500	0.040447	0.034978	0.045570	0.011067
4.400	0.037628	0.033675	0.042801	0.010240
4.300	0.034896	0.032395	0.040047	0.009511
4.000	0.027632	0.028700	0.032216	0.007899
3.900	0.025619	0.027495	0.029833	0.007529
3.800	0.023854	0.026278	0.027599	0.007225
3.700	0.022363	0.025024	0.025546	0.006980
3.600	0.021187	0.023682	0.023752	0.006797
3.500	0.020443	0.022090	0.022541	0.006759
3.84001	0.020405	0.021756	0.022526	0.006802
3.460	0.021676	0.022398	0.024588	0.008216
3.440	0.019303	0.020900	0.021405	0.007637
3.420	0.018790	0.020788	0.020516	0.007803
3.400	0.018439	0.020448	0.019808	0.007850
3.300	0.017203	0.019368	0.016776	0.008117
3.200	0.016589	0.018150	0.014288	0.008278
3.100	0.016349	0.016807	0.012051	0.008438
3.000	0.016378	0.015339	0.009949	0.008646
2.900	0.016610	0.013745	0.007917	0.008962
2.800	0.017020	0.012018	0.005883	0.009549
2.700	0.017737	0.010265	0.003531	0.011275
2.687001	0.017897	0.010123	0.003105	0.011857
2.667001	0.018341	0.010907	0.002259	0.014341
2.660	0.019681	0.009660	0.004131	0.018056
2.640	0.021559	0.007044	0.006749	0.022444
2.600	0.022950	0.000701	0.010379	0.027163
2.500	0.015882	0.011731	0.013901	0.023143
2.400	0.009791	0.013598	0.015780	0.016878
2.390	0.009562	0.013497	0.016170	0.016774
2.370	0.009285	0.013187	0.017123	0.016914
2.350	0.009244	0.012717	0.018390	0.017609
2.330	0.009485	0.012019	0.020236	0.019162
2.310	0.010740	0.010554	0.024907	0.024393
2.300	0.014719	0.008003	0.021760	0.020298
2.260	0.018749	0.007492	0.016770	0.013987
2.220	0.020480	0.009324	0.014227	0.010672
2.140	0.021713	0.013023	0.011851	0.006876
2.100	0.021487	0.014125	0.011932	0.006413
2.060	0.021670	0.015325	0.012326	0.007576
2.020	0.021547	0.015919	0.013592	0.009854
2.000001	0.021899	0.016078	0.014836	0.012297

(to be continued)

Table 10. (continued)

L/L_{s1}	$\lvert A_2\rvert$	$\lvert B_2\rvert$	$\lvert C_2\rvert$	$\lvert D_2\rvert$
1.980	0.023187	0.016475	0.015437	0.012825
1.940	0.023503	0.016702	0.016817	0.014219
1.900	0.023134	0.016496	0.018485	0.015878
1.860	0.022198	0.015780	0.020445	0.017810
1.820	0.020593	0.014375	0.022720	0.020048
1.780	0.018007	0.011854	0.025397	0.022699
1.740	0.013228	0.006310	0.028992	0.026343
1.737	0.012597	0.005420	0.029401	0.026771
1.735	0.012094	0.004652	0.029727	0.027115
1.733	0.011429	0.003520	0.030164	0.027581
1.730	0.012894	0.003493	0.030317	0.027634
1.728	0.013779	0.004263	0.030228	0.027483
1.726	0.014464	0.004885	0.030177	0.027383
1.720	0.016032	0.006350	0.030112	0.027204
1.680	0.022311	0.012408	0.030276	0.026908
1.640	0.027038	0.017040	0.030398	0.026694
1.620	0.029270	0.019239	0.030348	0.026488
1.580	0.033698	0.023625	0.029941	0.025776
1.540	0.038219	0.028131	0.029042	0.024581
1.520	0.040550	0.030464	0.028384	0.023786
1.480	0.045396	0.035334	0.026663	0.021869
1.440	0.050536	0.040518	0.024605	0.019942
1.400	0.055970	0.045988	0.023039	0.019458
1.360	0.061338	0.051293	0.023767	0.022958
1.340	0.062819	0.052672	0.024849	0.026317
1.338	0.062689	0.052553	0.024904	0.026736
1.336	0.062356	0.052261	0.024986	0.027288
1.334	0.061444	0.051503	0.025384	0.028453
1.333	0.061824	0.052335	0.030022	0.033465
1.328	0.070449	0.061230	0.047711	0.049893
1.323	0.077473	0.068240	0.064136	0.065982
1.320	0.081650	0.072391	0.074788	0.076659
1.300	0.111538	0.104066	0.163634	0.168718
1.290	0.127783	0.123534	0.212580	0.220355
1.280	0.143247	0.143252	0.254408	0.264671
1.270	0.155821	0.159934	0.283180	0.295175
1.260	0.164173	0.171440	0.297909	0.310706
1.255	0.166727	0.175137	0.300818	0.313707
1.250	0.168316	0.177599	0.301425	0.314240
1.245	0.169075	0.178991	0.300238	0.312849
1.240	0.169142	0.179488	0.297713	0.310022
1.200	0.157744	0.167722	0.262483	0.271205
1.160	0.142597	0.150384	0.234160	0.239706
1.120	0.128482	0.133977	0.216533	0.219564
1.080	0.109112	0.111727	0.193341	0.193540
1.000	0.050506	0.037413	0.169576	0.163377
0.990	0.071027	0.058021	0.170064	0.163890
0.970	0.086704	0.073772	0.174423	0.168265
0.950	0.098486	0.085596	0.179983	0.173834
0.900	0.124187	0.111351	0.197493	0.191358
0.850	0.149952	0.137138	0.219829	0.213709
0.800	0.178445	0.165641	0.247537	0.241439
0.750	0.211458	0.198662	0.281770	0.275703
0.700	0.250873	0.238088	0.324304	0.318283
0.650	0.299078	0.286311	0.377737	0.371780
0.600	0.359373	0.346638	0.445904	0.440035
0.550	0.436568	0.423882	0.534599	0.528850
0.500	0.537989	0.525378	0.652861	0.647276
0.450	0.675311	0.662814	0.815434	0.810076

the case of incidence of the P wave, and in Figs. 19–34 and Tables 6–10 for the case of incidence of the SV wave. The last section of Chapter 3 was devoted to a study of the detailed features of the figures concerned.

Since these detailed features can be referred to last sections of Part 1 and Chapter 3, the writer will only mention the characteristics common to the three cases in the remaining part of this section.

(1) The larger the amplitude of a corrugated boundary surface, the larger is its effect on reflection and refraction. The effect is such that with respect to regular waves the reflected wave decreases and the refracted one increases with the increase in the ratio of amplitude of corrugation to the wave length of the incident wave.

(2) $|A_1|$, $|B_1|$, etc. which represent irregular waves with a spectrum of the first order are proportional to the amplitude of the corrugated boundary surface in the present approximation and they vary with the wave length of the corrugated boundary surface.

(3) In general, the effect of corrugation on reflection is larger than on refraction.

(4) The S component of both irregularly reflected and refracted waves increases in general with decreasing L/L_{p1} in the case of incidence of the P wave. The P component of both irregularly reflected and refracted waves also increases as a whole with decreasing L/L_{s1} in the case of incidence of the SV wave.

(5) When the wave length of corrugation is equal to or near one of the wave length as of P or S waves in any medium, abnormal features appear in both regular and irregular waves. Furthermore it is very interesting to note that in general the abnormal features are more sensitive to the wave length of P or S waves in the refracted side than to that of P or S waves in the incident side. Whether this feature depends on adopted velocity ratio or not, will be of much interest and will be studied in detail in the near future.

(6) In a certain range of L there exist boundary waves of which the amplitude decreases exponentially with the distance from the boundary surface. Its rate of decrease depends on the wave length of the corrugated boundary surface and incident wave and the order of spectrum. Although they become standing waves in a stationary state as far as cases of normal incidences are considered, it will be inferred that there is a possibility of the existence of pure boundary waves caused by corrugation in the case of oblique incidence.

(7) When the wave length of the corrugated boundary surface is smaller than that of the incident wave, almost all irregular waves become boundary waves. Therefore, from the practical point of view it is enough to take only regular waves into practical consideration. In the present cases, the reflected wave becomes the smaller and the refracted wave the larger as the corrugation becomes larger.

The possibility of obliteration of the reflected wave from the Mohorovičić discontinuity in mountainous regions as suggested by H. E. Tatel and others[11] may be inferred from the results just obtained. That is, if the roughness of the boundary surface is interpreted as a corrugation of the boundary surface of a shorter wave length than that of the incident wave, it is possible for reflected waves to be rendered too small to be observed for the instruments of given sensitivity. In Japan, the Research Group for Explosion Seismology has several times carried out observations of reflected waves from the Mohorovičić discontinuity. The success in catching them may depend on the technical circumstances and the ground conditions near the observation stations. But there are a few examples under almost the same observational circumstances concerning observers and instruments. The first example is given by the fifth experiment carried out in 1953 by the Group in north-eastern Japan[12] and the experiment carried out by the Group in 1954 near Kamaisi Mine in north-eastern Japan[13]. The chief observer and instruments used were the same in both cases although the observation stations were in different places. Another difference was the amount of explosives used. Explosives of 42 tons were used in the former case and in the latter experiment explosives of only 1 or 0.1 ton were used. In the former experiment it succeeded in catching reflected waves, while in the latter it failed, although the experiment was repeated four times under slightly different conditions of shooting. The failure may be partly attributed to the decrease of reflected wave caused by a corrugated boundary surface in addition to the smaller quantity of explosives used in the latter experiment. The next example seems to be better than the first. It is supplied from the observation at Sano in the Kanto District on the occasion of the second Hokoda

11) H. E. TATEL, L. H. ADAMS and M. A. TUVE, *loc. cit.*, 3).

12) THE RESEARCH GROUP FOR EXPLOSION SEISMOLOGY, *Bull. Earthq. Res. Inst.*, **33** (1955), 699.
T. MATUZAWA, *Bull. Earthq. Res. Inst.*, **37** (1959), 123.

13) THE RESEARCH GROUP FOR EXPLOSION SEISMOLOGY, *Bull. Earthq. Res. Inst.*, **37** (1959), 89.

explosion in 1957[14] and the observation at Kamioka in central Japan on the occasion of the third Miboro explosion in 1958[15]. In this example also the chief observer and instruments used were the same at both sites and the same as in the first example. The different conditions were the positions of the observation stations and shot point, quantities of explosives, method of detonation, etc. In the former explosion, explosives of one ton were detonated simultaneously and in the latter, explosives of 100 tons were not detonated simultaneously, but almost at the one time by means of delayed shot. In the former observation it was successful in catching manifested reflected wave from the Mohorovičić discontinuity, whereas in the latter the reflected wave observed was not so clear although the amount of explosives used was much larger. The former station was in the Kanto Plain and the latter station was set up in the mountainous region of Japan. Therefore, this may be interpreted by the results obtained. That is to say, one may interpret the difference in two cases as being partly due to the decrease of reflected wave caused by the roughness of the Mohorovičić discontinuity. From these speculations it may be said that the experiment would be better if carried out on plain, and if not, excessive amounts of explosives must be used in the observation of reflected wave from deep seated discontinuities which are expected to be rough. Concerning these respects there are not yet sufficient relevant data.

We can now say with confidence that if elaborate experiments are carried out and knowledge of the variation in amplitude of reflected or refracted waves is further increased, it is possible to gain knowledge about the character of the boundary surface concerned.

Acknowledgement

In concluding, the writer expresses his hearty thanks to Professor Hirosi Kawasumi for his useful advice and encouragements. Also the writer's sincere thanks are due to Dr. Ryosuke Sato for his valuable advice and discussion. To members of Takahashi Laboratory, Institute of Physics, Faculty of Science, University of Tokyo, and especially to Dr. M. Ariyama, Mr. K. Nakagawa and Mr. Y. Ishida the writer

14) THE RESEARCH GROUP FOR EXPLOSION SEISMOLOGY, *Bull. Earthq. Res. Inst.*, **37** (1959), 495.
T. MATUZAWA, T. MATUMOTO and S. ASANO, *Bull. Earthq. Res. Inst.*, **37** (1959), 509.

15) THE RESEARCH GROUP FOR EXPLOSION SEISMOLOGY, *Bull. Earthq. Res. Inst.*, **39** (1961), 285.
T. MIKUMO *et al.*, *Bull. Earthq. Res. Inst.*, **39** (1961), 321.

is greatly thankful for their kind instructions in the programming of PC-1. To Mr. Masumi Yanagisawa, Miss Junko Takahashi and Miss Sachiko Terashi the writer is also indebted for their assistance in the calculation and preparation of tables and text figures. Also his gratitude is due to his wife, Miyako, for her assistance in preparing original tables and original text figures.

---

13. 波型の境界面における弾性波の反射，屈折　第2報

地震研究所　浅　野　周　三

本報では，第1報で用いた Rayleigh の方法により，Fourier 級数に展開可能な境界面に，任意の入射角で P 及び SV 波が入射する場合の解を主に述べた．境界面の振巾と入射波の波長の比が小さいとして，この2乗の程度まで近似をたかめた．計算に用いた構造は SH 波の場合と同じく，$\lambda_4=\mu_4$，$V_{p1}/V_{p2}=3/4$，$\mu_2/\mu_1=2$ なる値を用い，低速側から高速側へ入射する場合に対して計算した．簡単のために，第1報と同様に，境界面は $\zeta=c\cos px$ なる形にとり，平面 P 波或いは SV 波が垂直に入射することを仮定した．

結果は，P 波入射の場合には Figs. 3-18, Tables 1-5, SV 波入射の場合には Figs. 19-34, Tables 6-10 に与えられている．

細かい点を除き，P, SH, SV 波に共通している結果は大体，次の通りである．

（1） 凹凸振巾が大きくなると，効果は大となる．regular wave について反射波は減少し，屈折波は増加する．

（2） 凹凸の効果は屈折よりも反射に大きい．

（3） irregular wave について凹凸と同じ波長で変化するもの A_1, B_1, … はこの程度の近似では凹凸振巾に比例する．

（4） 反射波，屈折波とも P 波入射の時は irregular wave の S 波の成分が凹凸の波長が小さくなるにつれて，増加する一般的傾向を有し，SV 波入射の時は irregular wave の P 波の成分が増加する一般的傾向を有する．

（5） 凹凸の波長が入射，或いは屈折側の P 波或いは S 波の波長に等しくなるか，或いは近くなると regular wave, irregular wave とも異常を示す．興味深い点はこのモデルに関する限り入射側より屈折側の量に，より敏感である点である．

（6） 凹凸波長の比によるが，境界面から離れるにつれ，指数関数的に急に減少する境界波が存在する．

（7） 凹凸の波長が入射波の波長に比べて小さい場合には，irregular wave は殆んどすべて指数関数的に減衰する境界波となるので，実際的には regular wave のみ考えれば十分である．すなわち，凹凸が増すと反射波は減少し屈折波は増加する．

若し，H. E. Tatel や M. A. Tuve がいう粗な境界面とは，入射波の波長に比べて凹凸の波長が小さい場合と解釈するならば (7) より反射波は減少するから Moho 面よりの反射波が観測されないことはあり得ると推察される．また，これらの結果は地震探鉱法にも参考になるものと思われる．

以上，述べた結果は1つのモデルに対する簡単な場合であるが，弾性波動の立場からはこのような結果が弾性定数の相異や，斜め入射の場合，更には境界面の形が異なった場合等により，どの程度，修正が必要かを調べることは，極めて興味深いので近い将来，報告する予定である．

BULLETIN OF THE EARTHQUAKE
RESEARCH INSTITUTE
Vol. 39 (1961), pp. 467-476

14. *Archaeomagnetic Study on Volcanic Rocks in Oshima Island, Japan.**

By Takesi YUKUTAKE,

Graduate School, University of Tokyo.

(Read Dec. 20, 1960.—Received June 20, 1961.)

Summary

Variation in the geomagnetic field for the past one thousand years has been inferred from the direction of the remanent magnetization of rocks ejected at periods known from historical records. The results show an agreement with those of instrumental observations which have been conducted since the sixteenth century. Periodical changes are found both in declination and in inclination: inclination varies rather slowly within a period of about 600–700 *years*, while declination changes within a 400–500 *year* period.

1. Introduction

Recent studies of palaeomagnetism have yielded much material that may enable us to trace back the variation in the geomagnetic field during the geologic time[1),2),3),4),5)] such as the migration of the pole and the variation in field intensity that is likely to have accompanied the reversal of the magnetic field. Concerning the phenomena of the historical time scale, only a little study has been done on this[6),7)]. It may due to the precision required not only in the orientation of samples or in the measurement of magnetization but also in knowledge about the periods of magnetization of the specimens.

A geological survey of the historical age of Oshima Island has been

*) Communicated by T. RIKITAKE.

1) E. IRVING, *Royal. Astron. Soc. Geophys. Journ.*, **2** (1959), 51.

2) P. M. S. BLACKETT, J. A. CLEGG and P. H. S. STUBBS, *Proc. Roy. Soc.*, **A**, **256** (1960), 291.

3) A. COX and R. R. DOELL, *Bull. Geol. Soc. Amer.*, **71** (1960), 645.

4) TH. SIGURGEIRSSON, *Advances in Physics*, **6** (1957), 240.

5) K. MOMOSE, Thesis (1961).

6) É. THELLIER and O. THELLIER, *Annales Géophysique*, **15** (1959), 285.

7) R. M. COOK and J. C. BELSHE, *Antiquity*, **32** (1958), 167.

8) K. NAKAMURA, *Sci. Papers Coll. Gener. Educ. Univ. Tokyo*, **10** (1960) 125.

thoroughly carried out by K. Nakamura[8], and the age when each lava layer was formed has been ascertained fairly accurately from historical records or human remains. From the study of these lava the writer has tried to infer the time variation in the direction of the geomagnetic field for a few thousand years. The obtained results agree fairly well with those inferred by N. Watanabe[9] from archaeomagnetic study of old hearth stones in Japan.

2. Collection and Measurement of Specimens

It seems that the field direction seldom varied more than 20–30 degrees of arc for a few thousand years. It requires higher accuracy than has been attained by the usual method of palaeomagnetism. In this study, at every step from the sampling to the measurement any sources that may produce errors of more than several degrees have been carefully removed.

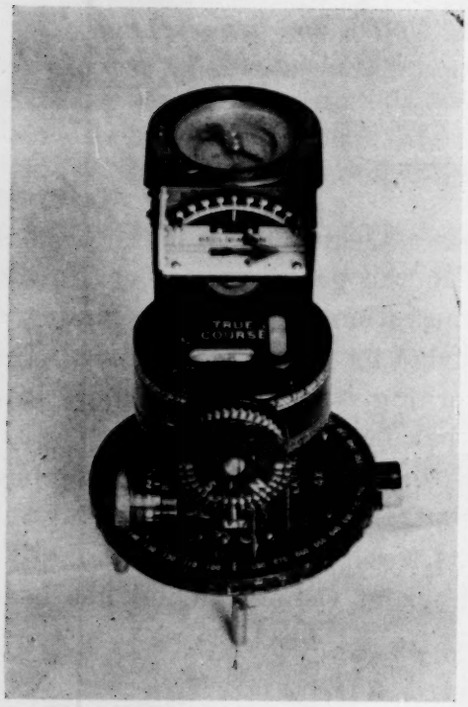

Fig. 1. Rock-compass

Natural remanent magnetization of the lava (all basaltic) in Oshima Island is due to the very fine particles of magnetite[10]. Therefore it is unlikely that the direction of N.R.M. has been altered from the original one by the varying geomagnetic field, so long as the rock has been firmly occupying the same position since its solidification.

It is known that the strong intensity of the N.R.M. of lava in Oshima Island put the needle of a compass, closely attached to the rocks, out of the direction of the normal field there[11]. Deviation from the normal field sometimes exceeds ten degrees. In order to avoid this embarrassment the writer has made use of a rock-compass devised by D.E.T. Bidgood and W.B. Harland[12], which has a theodolite on a rigid tripod (Fig. 1). The sighting arm of

9) N. WATANABE, *Jour. Fac. Sci. Univ. Tokyo, Sec. 5*, **2** (1959), 1.
10) T. NAGATA, *Bull. Earthq. Res. Inst.*, **21** (1943), 1.
11) T. NAGATA, *loc. cit.*, 10).
12) D. E. T. BIDGOOD and W. B. HARLAND, *Bull. Geol. Soc. Amer.*, **70** (1959), 641.

the rock-compass mounted on a specimen was sighted by a telescope settled 5 to 30 *m* apart from the rock. The direction of the sighting arm was read with reference to a compass attached to the telescope. Although there still remains the effect of the local anomaly of the magnetic field which is less than several degrees, the influence of the extremely disturbed field near the rock on the orientation of the specimens is presumed to have been removed. After the reorientation in the laboratory by using the rock-compass again, the specimens were fixed with plaster in cubic moulds of aluminium (15 *cm* or 25 *cm* in size), lest their orientation should get out of order in the course of measuring.

In order to test the accuracy of the astatic magnetometer a magnetic needle was measured in place of a rock sample. The test revealed that the direction of the needle obtained by an analysis of the results of the measurement did not deviate more than 8 minutes of arc from the true direction.

Measurements have been carried out at every 90° around one axis of rotation. Then the sample has been turned upside down and measurements at intervals of ninety degrees have been repeated. With regard to the other two axes, the same procedure has been followed. It has been ascertained that the direction of magnetization obtained after Fourier analyses of the above measurements agree within a range of one degree or so with those of measurements at 30° intervals.

It may safely be expected that the total errors produced from sampling to measuring would not exceed several degrees of arc.

There are other sources of errors which are difficult to assess, that is, the movements of rocks after magnetization. Specimens were collected from rocks of lava layers which, according to Mr. Nakamura, had not moved. It may, however, exert a crucial influence upon the result whether or not a block of lava at the very point of collection has moved with time, even if the lava layer shows no movement as a whole. Avoiding the natural surface of lava produced at the cooling stage, the writer collected specimens from exposures of the inner part of lava layers such as at a roadside cutting.

3. The Locality of Specimens and the Result of Measurements

During the past two thousand years Volcano Mihara has likely repeated great eruptions and produced a great deal of lava over an area a few kilometers in radius. Some of the lava reached the seashore. K. Nakamura has scrutinized the distribution of lava and published a

map as is shown in Fig. 2. The first and the second columns of Table 1 represent the layers of scoria and lava covering Volcano Mihara and the probable ages when they were ejected. The specimens have mainly been collected from lava layers. Their locations are indicated in Fig. 2 by solid circles. From each layer, samples of ten or so have been taken. As a representative of Y_5 formation (Motomati lava) a large driblet near the presumed crater has been adopted. Direction of magnetization of the samples are shown by the equal area projection as in Fig. 5. They were averaged by means of Fisher's method. Table 1 shows these results with a 95% level of confidence. With reference to the present local anomaly of the geomagnetic field[13], which is caused by the magnetization of the volcano as a whole, the results are corrected and reduced to the declination and the inclination in Tokyo. They are shown in Table 2 together with the inferred time of solidification. In Fig. 3 these values are plotted by full circles.

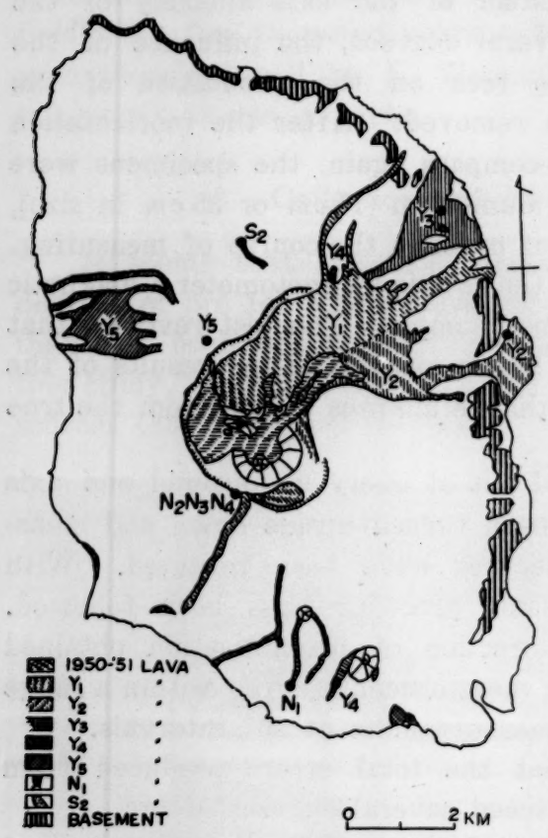

Fig. 2 Distribution of lava and of the sampling sites.

Since the beginning of the sixteenth century, the geomagnetic field has been measured every now and then in Japan[14),15)]. These records show that the declination at the beginning of the seventeenth century was 2.1°E and reached the maximum value 5.4°E at the end of that century. Declination obtained from the Y_2-layer agrees well with these instrumental observations. The hollow circles in Fig. 3 are the inclination and declination obtained either by instrumental observations or from palaeomagnetic studies in Japan. From these, Watanabe inferred the secular variation of the geomagnetic field in Japan as is shown by the

13) I. YOKOYAMA, *Bull. Earthq. Res. Inst.*, **35** (1957), 327.
14) Y. KATO and T. NAGATA, *Proc. Seventh Pacific Sci. Congr.*, **2** (1953), 562.
15) S. IMAMITI, *Mem. Kakioka Mag. Obs.*, **7** (1956), 49.

Table 1.

Formations	Time of Eruption	Declination (E)	Inclination	No. of samples	Fisher's θ for $p=0.05$	N.R.M.+) (*emu/gr*)
Y_2	1684	11°20′E	35°20′	9	4°29′	8.63×10^{-3}
Y_3	1552	9 10	39 50	12	5 34	—
Y_4	1421	1 50	48 40	10	5 06	—
Y_5	1300	10 40	56 10	6	5 22	—
N_1		1 00	46 10	11	1 03	2.97×10^{-3}
N_2*)		8 20		11		(1.6×10^{-3})
N_3*)	838	− 6 50		9		(0.8×10^{-3})
N_4		−13 30	55 30	8	2 20	1.24×10^{-2}
S_2	200	6 10	40 10	9	4 31	(1.2×10^{-2})
Tatunokuti lava.		16 20	53 10	7	5 35	—

*) Specimens of N_2 and N_3 were collected from layers of tuff.
+) Intensity of NRM was tentatively measured.

Table 2.

Formations	Adopted Time of Eruption	Declination	Inclination
Y_2	1684	5.0° E	35.5°
Y_3	1552	3.0	40.0
Y_4	1421	− 4.0	50.0
Y_5	1300	6.0	53.0
N_4	1075	− 5.0	48.0
N_2	925	4.5	—
N_3	838	−11.0	—
N_4	650	−17.5	52.5
S_2	325	1.0	39.0

dotted curves in Fig. 3.

The magnetic measurements of rocks in Oshima Island seem to confirm Watanabe's inference, excepting that the period of the oscillatory variation of inclination seems to be about 600 *years*, while Watanabe assumed an 800-*year* period. The results suggest that the magnitude of the variation in inclination amounted to about 20° during the past one thousand years. Periodical variation is also seen in declination. The period is about 400 *years* which is a little shorter than that of inclination. Easterly deviation from the meridian plane seems to have reached the maxima at about 1250 and 1650 A.D. amounting to 6° and 6.3°E respectively. On the other hand, the maximum of westerly declina-

tion is seen in 1450 A.D.

The magnitude of the field variation for a thousand years or so, obtained in this study, is small compared with the variation in geologic time such as polar wandering, but by far larger than the variation of

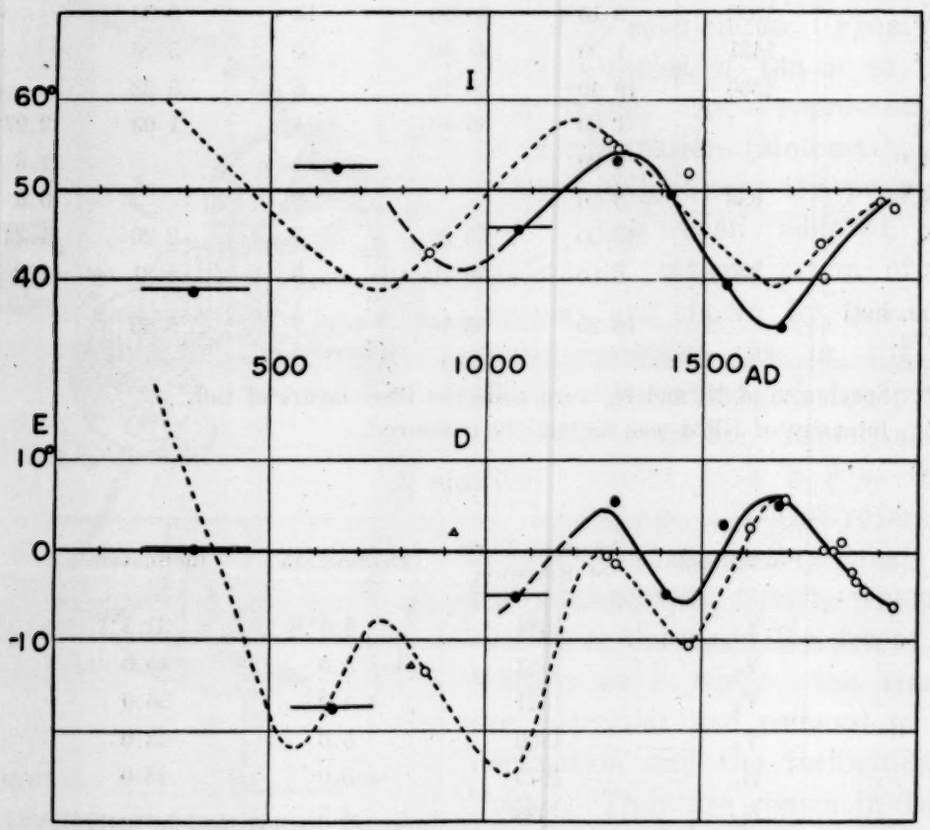

Fig. 3. Time variation in the geomagnetic field. The upper curve represents the variation in inclination and the lower curve in declination. The full circles are the results obtained from the measurement of lava specimens in Oshima Island, the triangles are those from tuff. The hollow circles are the values already known either by instrumental observations or by the other palaeomagnetic studies. The dotted curves are variation curves by N. Watanabe.

the order of a decade. As will be discussed in another paper, such variations as in Fig. 3 may well be understood as the result of the westward drift of non-dipoles part of the geomagnetic field. The archaeomagnetic study of this kind seems to afford important clues to the study of the geomagnetic field and its secular variation.

4. Magnetization of Rokcs in Bore-holes

Oshima Development Co. Ltd. has drilled two bores at the foot of the somma wall in the northeastern part of the caldera. The bores

Table 3.

L	Depth	Inclination	L	Depth	Inclination
1	5.0m	48°00′	18	229.0m	48°15′
2	17.3	31 30	19	233.0	—
3	42.5	50 00	20	235.0	—
4	61.0	(27 00)	21	238.0	48 45
5	77.5	49 00	22	248.0	37 40
6	80.5	51 00	23	251.3	27 10
7	104.0	44 00	24	252.0	—
8	128.0	—	25	254.0	—
9	162.0	56 30	26	255.0	—
10	193.2	47 30	27	258.0	39 15
11	196.0	23 00	28	262.0	43 50
12	202.0	14 00	29	268.9	52 50
13	207.0	31 00	30	275.0	40 55
14	214.6	42 00	31	281.5	32 20
15	219.0	44 00	Tuff	286.8	53 40
16	222.0	—	Tuff	290.0	63 40
17	224.5	38 30			

reached the depth of 300 *m* and 290 *m*, cutting off many layers of lava and scoria. The magnetization of the cores of these bores was measured. As the drilling accompanies the rotation of the cores, we have no means of supposing in what direction the cores were magnetized in the horizontal plane. If we assume, however, that the bores were vertically drilled, we can ascertain the dip component of magnetization. Taking one or two samples from every lava layer, the inclination has been measured. The results from one of the cores are shown in Table 3 and Fig. 4. Being unknown which end of a sample was the top or the bottom, inclination in Table 3 are all assumed to be normal. At the depth of 202 *m* the dip decreases to 14°. The cores of another bore are now being

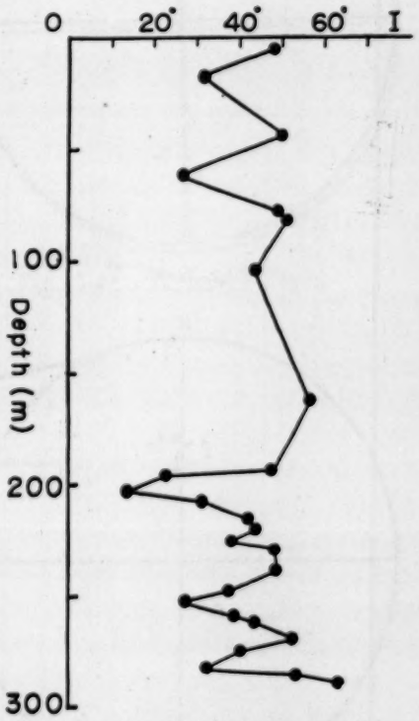

Fig. 4. Variation in inclination obtained from the measurement of the cores of a bore.

measured.

Acknowledgments

The writer expresses his sincere thanks to Dr. T. Rikitake for his suggestions and support, and to Prof. T. Nagata for his interest in this study. Dr. S. Akimoto and Dr. S. Uyeda have given advice and instruction on various problems. The writer owe much to Mr. I. Tanaoka and Mr. E. Kimoto, who collaborated in the collection and preparation of the samples. As for the dating and the location of samples, the writer depended entirely on Mr. Nakamura's help. The writer is also grateful to the members of Oshima Development Co. Ltd. who provided facilities for the collection of samples and measurement of the cores of the bores.

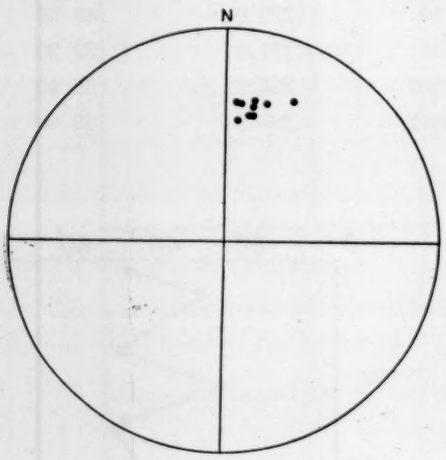

Fig. 5-a. Y_2

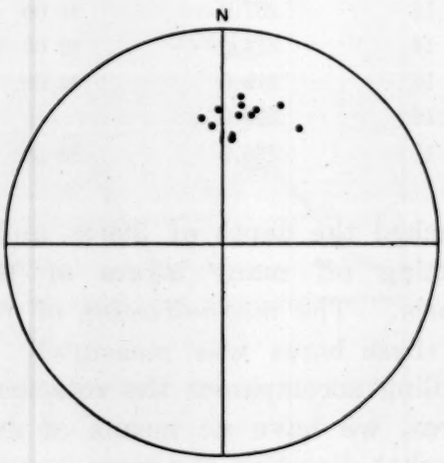

Fig. 5-b. Y_3

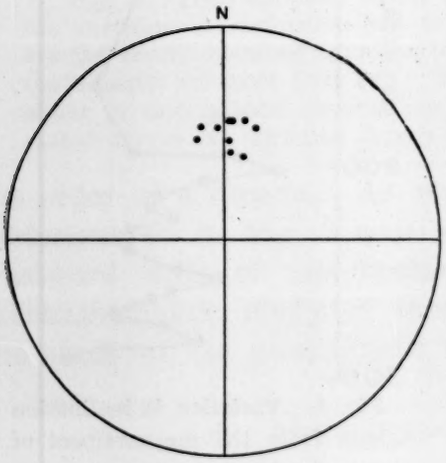

Fig. 5-c. Y_4

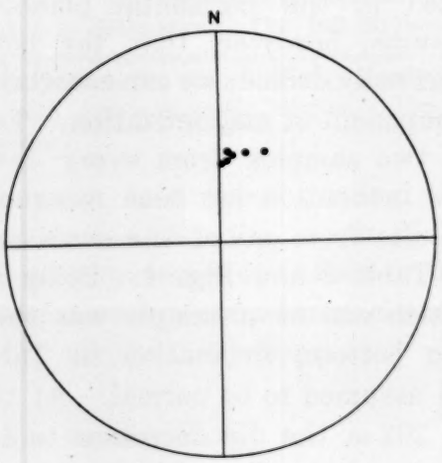

Fig. 5-d. Y_5

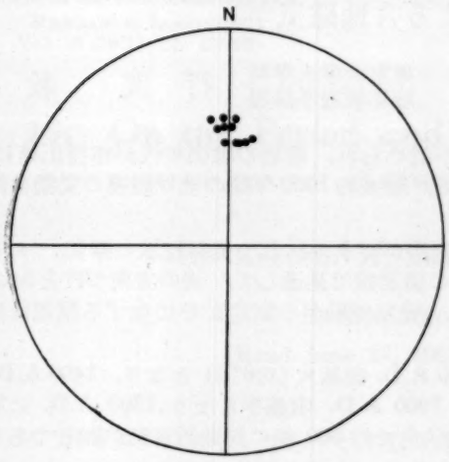

Fig. 5-e. N_1

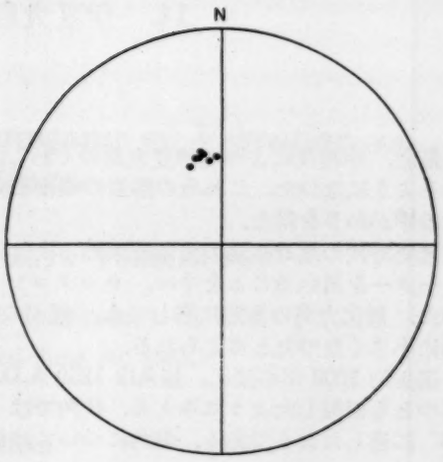

Fig. 5-f. N_4

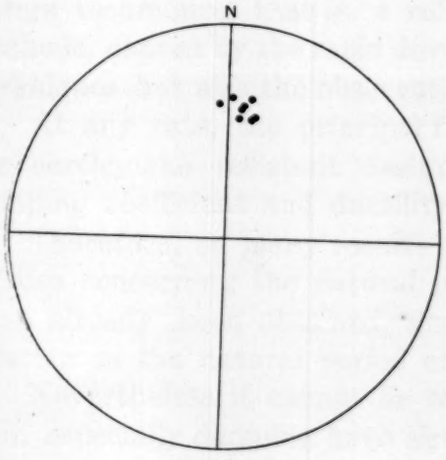

Fig. 5-g. S_2

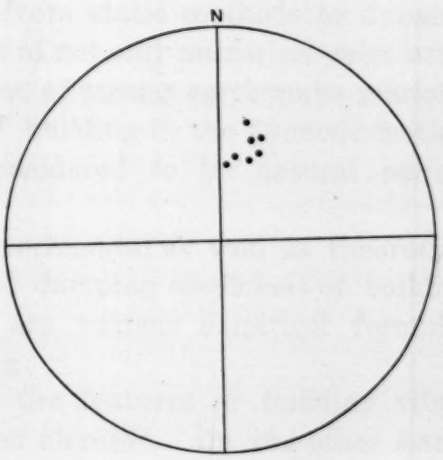

Fig. 5-h. Tatunokuti-lava

14. 伊豆大島熔岩による古地磁気学

東京大学大学院
地球物理学課程 行武 毅

最近，中村氏によつて伊豆大島のくわしい地質調査が進められ，熔岩の噴出年代が相当正確に知れるようになつた．これらの熔岩の残留磁気を測定して，過去約1000年間の地球磁場の変動を推定する手がかりを得た．

歴史時代の地球磁場の変動を求めるには，高精度の測定が要求される．資料採取の際に，クリノメーターを用いることをやめ，ロックコンパスを遠方の望遠鏡で見通して，岩の方向づけをおこなつた．磁化方向の測定に際しても，種々の注意を払い，資料採取から測定までに生ずる誤差は画期的に小さくなつたと考えられる．

過去約1000年の間に，偏角は1250 A.D.および1650 A.D.頃極大（約6°E）となり，1400 A.D.頃もつとも西偏したようにみえる．伏角では1600 A.D. 1000 A.D.頃極小となり，1300 A.D.に極大53°に達したようである．偏角については約400年，伏角で約600年の周期的変動が顕著である．

Bulletin of the Earthquake
Research Institute
Vol. 39 (1961), pp. 477-489

15. *On the Period and the Damping of Vibration in Actual Buildings.*

By Kiyoshi Kanai and Shizuyo Yoshizawa,

Earthquake Research Institute.

(Read June 27, 1961.—Received June 30, 1961.)

1. Introduction

The time is rapidly ripening for a reformation in earthquake resistant design techniques, that is, a reforming from static methods to dynamic methods, caused by the rapid development of not only numerical calculation techniques but also the observation system of strong earthquake motions.

At any rate, the principal factors of building in the dynamic method for earthquake resistant design are considered to be natural period, damping coefficient and ductility factor.

Therefore, so many results from experimental as well as theoretical studies concerning the natural period and damping coefficient of building have already been obtained, and there are various empirical formulae relating to the natural period of building.

Nevertheless it cannot be said that the features of building vibration, especially damping have already been clarified. On the other hand, it may be said that the study of the ductility problem in building is developing rapidly.

In the present investigation, a large number of measurement data of natural periods as well as damping coefficients of actual buildings more than several stories high of various types will be dealt with from some new view points.

2. The Values of the Fundamental Period of Actual Buildings

The relation among height (H), length parallel to vibration direction (D), effective stiffness (G), mass (m), natural period (T) of building and connection factor of building base to ground (ξ) can be written as follows:

$$T=f(H, D, G, m, \xi)\,. \qquad (1)$$

Now, for simplicity, it is assumed that the relationship of (1) may

be rewritten as the following formula:

$$T=f_1(H)\cdot f_2(D)\,. \qquad (2)$$

In that case the ratio of the period (T_1) for vibration parallel of the long side (D_1) to the one (T_2) of the short side (D_2) of a building

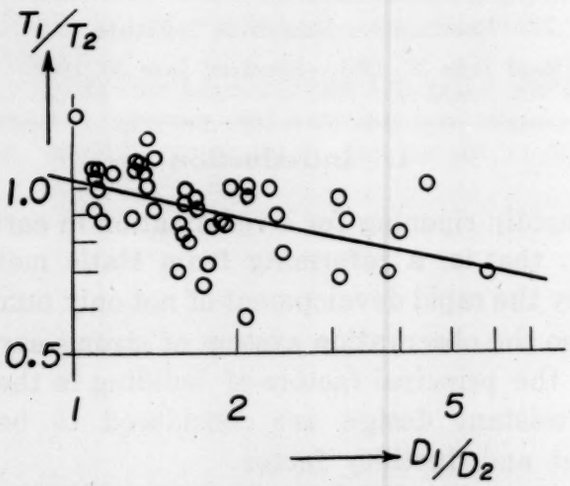

Fig. 1. Relation between the fundamental period and the depth parallel to the vibration direction of actual buildings in Japan. Suffix 1 and 2 represent the long and the short sides, respectively.

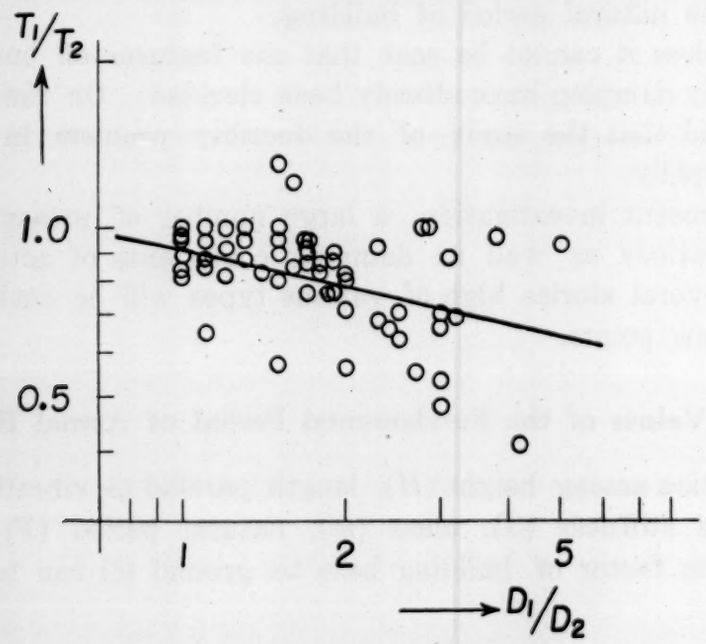

Fig. 2. Relation between the fundamental period and the depth parallel to the vibration direction of actual buildings in the U.S.A. Suffix 1 and 2 represent the long and the short sides, respectively.

becomes, as follows:

$$\frac{T_1}{T_2}=\frac{f_1(D_1)}{f_2(D_2)}\,, \tag{3}$$

Under the consideration of (3), Figs. 1 and 2 were obtained from the results of vibration experiments of actual buildings including reinforced concrete, steel frame and reinforced concrete, steel-concrete composite constructions in Japan[1] and in the U.S.A.[2]

From Figs. 1 and 2, by means of the least square method, we get the empirical formulae as follows:

$$\text{Japan}\,;\quad \frac{T_1}{T_2}=1.03\left(\frac{D_1}{D_2}\right)^{-0.21}, \tag{4}$$

$$\text{U.S.A.}\,;\quad \frac{T_1}{T_2}=0.92\left(\frac{D_1}{D_2}\right)^{-0.24}. \tag{5}$$

It will be said from (4) and (5) that the empirical formulae of the period of building obtained from the data in Japan and in the U.S.A. coincide well within their errors.

Next, for the present, let us assume that the fundamental periods of buildings (T) are proportional to their height (H). Under the above assumption, the relations between T/H and the length parallel to the vibration direction (D) of actual buildings in Japan and in the U.S.A. are shown in Figs. 3 and 4.

The empirical formula of the problem obtained from Fig. 3 is presented by (6) as well as by a straight line in Fig. 3.

$$\left.\begin{aligned}&\frac{T}{H}=0.034\,D^{-0.19}\,,\\ &\text{or}\quad T=\frac{0.034H}{D^{0.19}}\,.\end{aligned}\right\} \tag{6}$$

---

1) K. KANAI and S. YOSHIZAWA, "On the damping of vibration of actual buildings. I", *Bull. Earthq. Res. Inst.*, **30** (1952), 121-126.

T. NAITO and S. NASU, "Vibration tests of actual buildings", *Memoirs Faculty Sci. and Egg., Waseda Univ.*, **16** (1952), 54-61.

H. KAWASUMI and K. KANAI, "Vibrations of buildings in Japan", *Proc. World Conf. Earthq. Engg.*, (1956), Berkeley, 7_1-1-14.

K. NAKAGAWA, "Vibrational characteristics of reinforced concrete buildings existing in Japan", *Proc. II. World Conf. Earthq. Engg.*, (1960), Tokyo, 95-2-1-10.

2) *Earthq. Invest. in Calif., 1934-1935, U.S.C.G.S. Special Public.* **201**, p. 54, Table 3.

It can be said that the present assumption, in which the fundamental period of buildings is proportional to the height of the buildings embodies the conditions of actual buildings, because the degree of the power to D in (4) as well as (5) and (6) coincides approximately with one another.

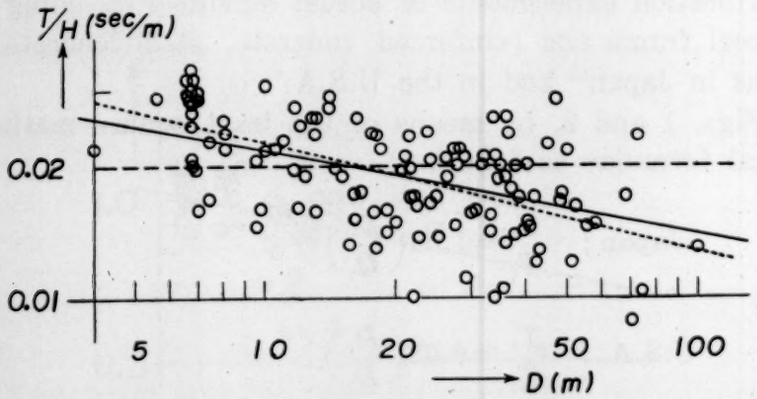

Fig. 3. Relation among the fundamental period, the height and the depth of actual buildings in Japan.

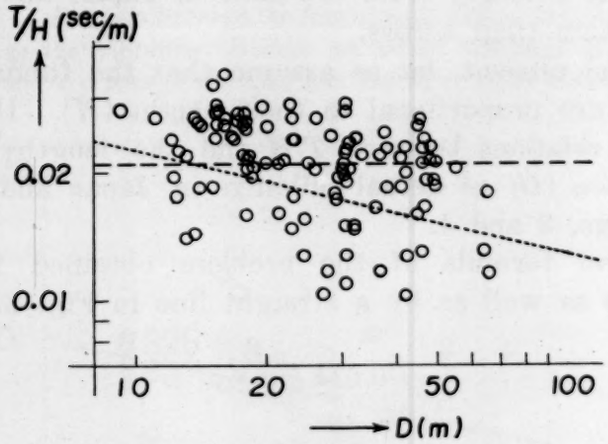

Fig. 4. Relation among the fundamental period, the height and the depth of actual buildings in the U.S.A.

Consequently, an empirical formula to obtain the fundamental period of building for practical use may be written as follows:

$$T=\frac{0.04\,H}{\sqrt[4]{D}}, \tag{7}$$

in which T is in sec and H and D are in m. The results of (7), as a reference, are shown by the dotted lines is Figs. 3 and 4.

Nevertheless, in general, the empirical formula to be taken regardless of D will be more practical because the degree of the power to D in the empirical formulae obtained above are fairly small. Then, when we adopt the mean values of ordinates in Figs. 3 and 4 (two values are about the same), the empirical formula shown by broken lines in the respective figures becomes as follows:

$$\left.\begin{aligned} T&=0.02\,H\,,\\ \text{or}\quad T&=0.08\,N\,, \end{aligned}\right\} \tag{8}$$

in which N represents the number of stories.

3. Mathematical Interpretation

The results of experiments using a vibration generator attached to actual buildings showed us that, in general, there take place (a) a relative displacement at the base to the ground and (b) a rocking-like vibration at the base together with (c) elastic deformation of the upper structure. The ratios among (a), (b) and (c) depend mainly on the kinds of soil as well as the types of construction. For instance, a rigid structure standing on soft ground is has strong influence of (b), on the contrary, a flexible structure standing on hard ground acts mainly upon (c). Fig. 5 shows, as an example, the distribution of horizontal displacement in a reinforced concrete apartment-house with six metre concrete piles[3] which stands on crushed stone.

It seems from Fig. 5 that the boundary conditions at the joints of vertical and horizontal members of building may be adopted as follows.

That is

$$x_n=l_n\,,\quad x_{n+1}=0\,;\qquad y_n=y_{n+1}, \tag{9}$$

$$\frac{\partial y_n}{\partial x_n}=0,\qquad \frac{\partial y_{n+1}}{\partial x_{n+1}}=0\,, \tag{10), (11}$$

$$-E_nI_n\frac{\partial^3 y_n}{\partial x_n^3}+m_n\frac{\partial^2 y_n}{\partial t^2}=-E_{n+1}I_{n+1}\frac{\partial^3 y_{n+1}}{\partial x_{n+1}^3}\,, \tag{12}$$

in which x=the ordinate, y=the displacement, E=Young's modulus, I=the moment of inertia of the crosssection, m=the concentrated mass at the joint, l=floor height, n=the number of floor.

3) K. KANAI, T. TANAKA and T. SUZUKI, "Rocking and Elastic Vibrations of Actual Buildings. I", *Bull. Earthq. Res. Inst.*, **36** (1958), 193, Fig. 19.

Strictly speaking, the boundary conditions at the base of a building are not simple, although, it is considered that they are at least between the following alternative assumptions.

(i) $x_1=0$;

$$y_1=0\,,\quad \frac{\partial y_1}{\partial x_1}=0\,,\quad (13),(14)$$

(ii) $x_1=0$;

$$y_1=0\,,\quad \frac{\partial^2 y_1}{\partial x_1^2}=0\,,\quad (15),(16)$$

when $E_1I_1=E_2I_2=\cdots\cdots$, $m_1=m_2=\cdots\cdots$, $l_1=l_2=\cdots\cdots$, we have[4]

(i) $$T\simeq 2\pi\sqrt{\frac{ml^3}{EI}}\times(0.18N+0.106)\,,\qquad (17)$$

(ii) $$T\simeq 2\pi\sqrt{\frac{ml^3}{EI}}\times(0.295)\,(N+1)\,,\qquad (18)$$

in which N represents the number of stories. It follows from these equations that the periods of free vibrations increase linearly as the number of stories increases. It follows, therefore, that the results of theoretical study are in good agreement with those obtained from experimental studies.

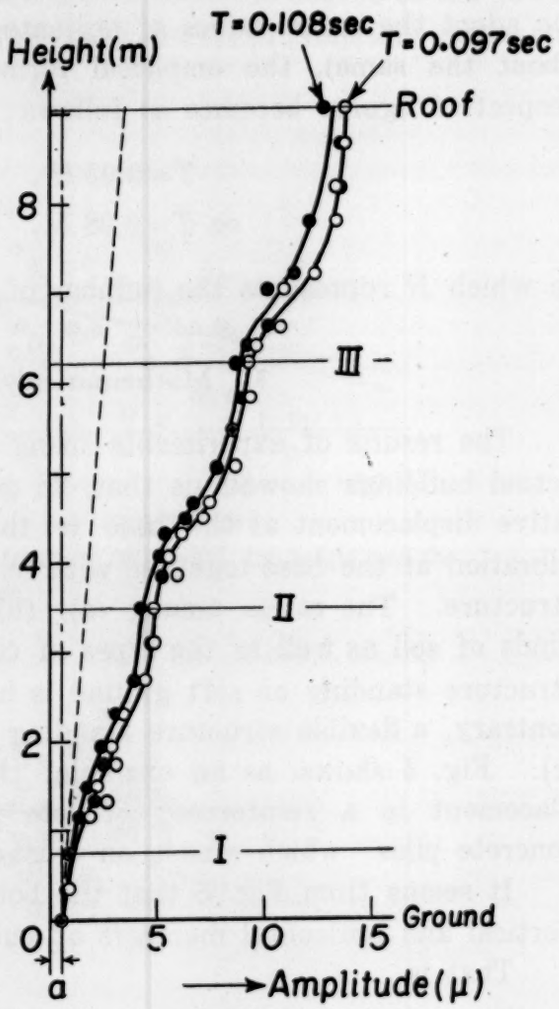

Fig. 5. Amplitude distuributions of the horizontal component of an apartment-house in the case of vibration experiments.

According to the theory concerning shearing vibrations of a building, the period of such vibrations is denoted by[5]

$$T=4H\sqrt{\frac{\rho}{\mu}}\,,\qquad (19)$$

4) K. SEZAWA and K. KANAI, "Some New Problems of Free Vibrations of a Structure", *Bull. Earthq. Res. Inst.*, **12** (1934), 816, equation (48).

5) K. SUYEHIRO, "The Theory of the Vibration of Structures and a Method of Measuring It", *Journ. Inst. Japanese Archit.*, **40** (1926), 531–559, (in Japanese).

where H, μ and ρ represent the height, the shearing modulus and the density of the building, respectively. Comparing (19) with (17) or (18) we find that μ and ρ are respectively equivalent to

$$\text{(i)} \quad \rho=\frac{m}{al}, \qquad \mu\fallingdotseq 12.4\frac{EI}{al^3}, \tag{20}$$

$$\text{(ii)} \quad \rho=\frac{m}{al}, \qquad \mu\fallingdotseq 4.7\frac{EI}{al^3}. \tag{21}$$

4. Damping Coefficient of Actual Buildings

Roughly speaking, the damping factor of building, represented by the fraction of critical damping, h, can be written as follows:

$$h=\frac{T}{2\pi}\xi\cdot f(m,H), \tag{22}$$

in which T and ξ represent the period and damping coefficient of building and $f(m,H)$ means the function of mass and height of building. In that case, the ratio of the damping factor for vibration parallel to the long side of a building (suffix 1) to that of the short side of it (suffix 2) become as follows:

$$\frac{h_1}{h_2}=\frac{T_1\xi_1}{T_2\xi_2}, \tag{23}$$

or

$$\frac{h_1T_2}{h_2T_1}=\frac{\xi_1}{\xi_2}. \tag{23'}$$

On the other hand, the relation between h_1T_2/h_2T_1 and D_1/D_2 of actual buildings was obtained from Table 1 and is shown in Fig. 6[6]. An empirical formula obtained from Fig. 6 becomes as follows:

$$\frac{h_1T_2}{h_2T_1}=1.1\frac{D_1}{D_2}. \tag{24}$$

From (23') and (24), we get

6) Original data are presented in the following:

K. KANAI and S. YOSHIZAWA, "On the Damping of Vibration of Actual Buildings. I", *Bull. Earthq. Res. Inst.*, **30** (1959), 125, Table 2.

K. NAKAGAWA, "Vibrational Characteristics of Buildings", *Proc. II Word Conf. Earthq. Engg.*, (1960), Tokyo, 95-2-6, Table 1.

$$\frac{\xi_1}{\xi_2}=1.1\frac{D_1}{D_2}\ . \tag{25}$$

Table 1.

S	Name	No.	H	D		T	h	h_1T_2/h_2T_1
a	Yotsuya	2	11.0	D_1	56.0	0.36	—	4.5
				D_2	10.0	0.37	—	
b	Honmura-cho	4	11.1	D_1	32.3	0.175	—	3.7
				D_2	6.8	0.225	—	
c	Ōkura	5(1)	21.8	D_1	33.7	0.22	0.0609	—
				D_2	16.4	0.38	0.0376	
d	Mantetsu	6(1)	25.4	D_1	70.0	0.50	—	2.3
				D_2	28.0	0.44	—	
e	Tachikawa	4(1)	13.2	D_1	11.6	0.20	—	2.8
				D_2	4.4	0.31	—	
f	Kanzai	3(1)	14.7	D_1	28.8	0.31	0.0666	—
				D_2	18.4	0.32	0.0275	
g	Manpei	4(2)	17.8	D_1	44	0.40	—	1.6
				D_2	21	0.41	—	
h	Sannō-B	4(1)	12.7	D_1	21	0.21	—	1.7
				D_2	13	0.19	—	
i	Nonomiya	7(1)	24.3	D_1	16.5	0.39	—	1.5
				D_2	10.5	0.48	—	
j	Fujiginkō	6(1)	27.7	D_1	105	0.56	—	1.4
				D_2	75	0.54	—	
l	Sannō-A	4(1)	12.9	D_1	12	0.24	—	1.3
				D_2	10	0.275	—	
m	Itō-chū	8(2)	29.9	D_1	31.9	0.63	0.217	—
				D_2	27.7	0.60	0.159	

S=symbol of building, No.=no. of stories above (under) G. L., H=height in m, D=depth in m, suffix 1 and 2 represent the long and the short sides, respectively, T=period in sec, h=fraction of critical damping.

Now, if the vibration damping of a building is caused by resistance proportional to the velocity of a rocking-like movement at the base of the building, the damping coefficient of the building (ξ') can be obtained as follows:

$$\xi'=2\int_0^{D/2}\xi_0 Lx\,dx=\frac{1}{4}\xi_0 LD^2\,, \tag{26}$$

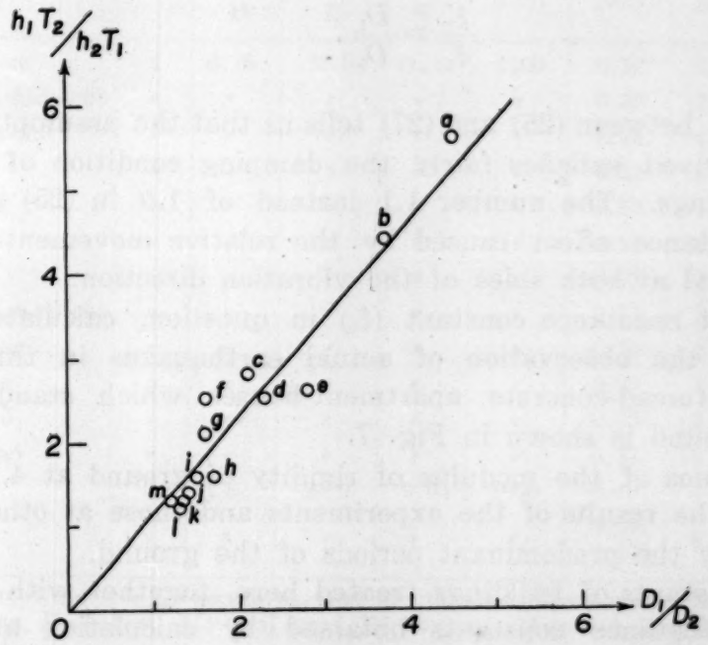

Fig. 6. Relation between the damping factor and the depth parallel to vibration direction of actual buildings. Suffix 1 and 2 repesent the long and the short sides, respectively.

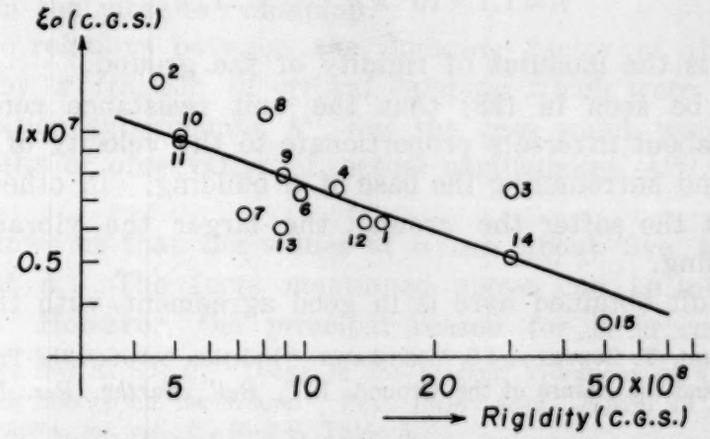

Fig. 7. Relation between the modulus of damping resistance and the rigidity modulus of various kinds of subsoil.

in which ξ_0, x, D and L represent the resistance constant of unit area, distance from the central axis of the rocking-like movement of the base, length parallel to vibration direction and length normal to the above. From (26) we can find easily the ratio of ξ' for the vibration parallel to the long side (suffix 1) to the one of the short side (suffix 2) of a building as follows

$$\frac{\xi_1'}{\xi_2'}=\frac{D_1}{D_2}. \tag{27}$$

The relation between (25) and (27) tells us that the assumption on which (27) was derived satisfies fairly the damping condition of vibration in actual buildings. The number 1.1 instead of 1.0 in (25) is considered as the resistance effect caused by the relative movement of the base to the ground at both sides of the vibration direction.

The unit resistance constant (ξ_0) in question, calculated from the results[7] of the observation of actual earthquakes in three and four storied reinforced-concrete apartment-houses which stand on various kinds of ground is shown in Fig. 7.

The values of the modulus of rigidity of ground at 4, 6 and 14 in Fig. 7 are the results of the experiments and those at other points are estimated by the predominant periods of the ground.

The constants of buildings treated here, together with the values of the unit resistance constants obtained by calculation are shown in Table 2.

From Fig. 7 the empirical formula can be written as follows:

$$\xi_0=1.1\times10^{10}\times\mu^{-0.35}\quad C.G.S., \tag{28}$$

in which μ is the modulus of rigidity of the ground.

It will be seen in (28) that the unit resistance constant (ξ_0) in question is about inversely proportionate to the velocity of the S-waves of the ground surrounding the base of a building. In other words, (28) tells us that the softer the ground, the larger the vibration damping of the building.

The result obtained here is in good agreement with the dissipation

7) K. KANAI, T. SUZUKI and S. YOSHIZAWA, "Relation between the Property of Building Vibration and the Nature of the Ground. III", *Bull. Earthq. Res. Inst.*, **34** (1956), 61-86.

K. KANAI, T. TANAKA and T. SUZUKI, "Rocking and Elastic Vibrations of Actual Buildings. II", *Bull. Earthq. Res. Inst.*, **36** (1958), 212-226.

theory which is based upon the idea that at the time of an earthquake, the vibration energy of a building dissipates to the ground again as the elastic waves that start from the base of it[8].

Table 2.

No.	Location	No.	Dimension (m)			M (ton)	T (sec)	Roof / Base	$\xi_0 \times 10^{-6}$ (C.G.S.)
			D	L	H				
1	Komagome	4	6.76	32.3	11.1	1400	0.32	3.7	6.2
2	Senju-hashido-chō	〃	〃	〃	〃	〃	0.28	2.0	13.1
3	Ishikawa-chō	〃	〃	〃	〃	〃	0.22	4.0	8.3
4	Totsuka	〃	〃	〃	〃	〃	0.33	3.0	7.4
6	Gōtokuji	〃	〃	〃	〃	〃	0.32	3.2	7.2
7	Taishidō	〃	〃	〃	〃	〃	0.32	3.5	6.5
8	Kyōdō	〃	〃	〃	〃	〃	0.32	2.1	10.9
9	Dairokuten-machi	〃	〃	〃	〃	〃	0.31	3.0	7.9
10	Nakarokugō	〃	〃	〃	〃	〃	0.30	2.5	9.8
11	Kugahara	〃	〃	〃	〃	〃	0.35	2.2	9.5
12	Sakae-chō	〃	〃	〃	〃	〃	0.35	3.4	6.2
13	Maeno-chō	〃	〃	〃	〃	〃	0.37	3.3	6.0
14	Hitachi	3	6.8	30.0	9.04	1000	0.18	4.0	5.1
15	Hitachi	〃	〃	〃	〃	〃	0.097 0.108	9.6	4.0 3.6

No.=number of stories, D=length parallel to vibration direction, L=length normal to vibration direction, H=height, M=total mass, T=fundamental period, Roof/Base=amplitude ratio of roof to base.

At any rate, the results mentioned above tell us that the upper parts of a building of any type of construction, seem to have slight influence upon the vibration damping.

Next, the relations between the damping factor of the buildings represented by a fraction of critical damping which were obtained by artificial vibration experiments, h[9], and the ones which were calculated from the results of observation of actual earthquakes, h'[10], are shown in Fig. 8.

Fig. 8 shows us that the values of h' are about five times larger than those of h. The facts mentioned above can be interpreted in various ways. However, the principal reason for it is considered as

8) K. SEZAWA and K. KANAI, "Decay in the Seismic Vibrations of a Structure by Dissipation of their Energy into the Ground", *Proc. Impr. Acad., Japan*, **11** (1935) 174-176.

9) K. NAKAGAWA, *loc. cit.*, 6), 95-2-9, Table 3.
K. KANAI and others, *loc. cit.*, 3).

10) K. KANAI, and others, *loc. cit.*, 7).

that the number of successive actual seismic waves, in which the periods closely approximate the natural period of building, was unsatisfactory.

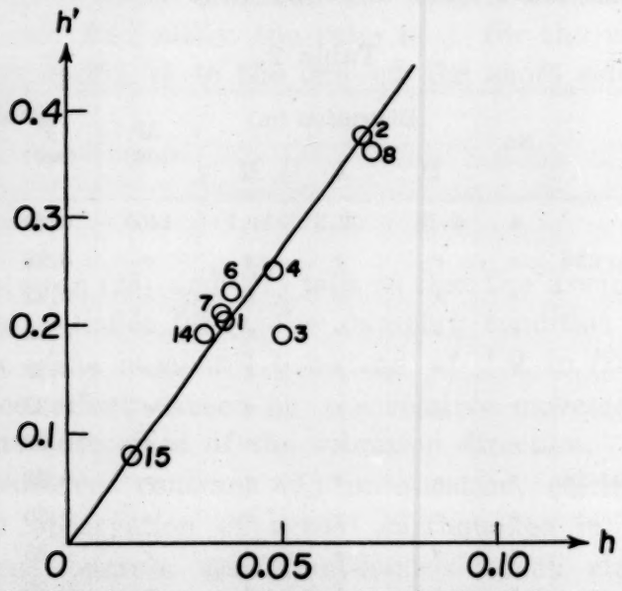

Fig. 8. Relation between the fraction of critical damping of buildings obtained by actual earthquake observations(h') and that obtained by artificial vibration experiments(h).

In other words, it seems that the synchronization of seismic waves to actual buildings was not sufficient.

5. Conclusion

From a statistical investigation of the fundamental periods of actual buildings more than several stories high, including various types which were obtained in Japan as well as in the U.S.A., the empirical formula obtained is as follows:

$$T=\frac{0.04\,H}{\sqrt[4]{D}}. \tag{7}$$

And, in practical use, the empirical formula in question may be taken as follows:

$$\left.\begin{aligned} T&=0.02\,H, \\ \text{or}\quad T&=0.08\,N. \end{aligned}\right\} \tag{8}$$

The present investigation also showed us that the vibration damping of actual buildings depends mostly upon the resistance between their

base and the ground on which they stand. And the empirical formula concerning the unit resistance constant at the base of a building was obtained as follows:

$$\xi_0=1.1\times10^{10}\times\mu^{-0.35}\quad C.G.S. \tag{28}$$

At any rate, from the present investigation, it may be said that the period of a building more than several stories high, depends mostly on the height and is slightly subject to the effect of the foundation, on the contrary, the conditions concerning the damping are just the reverse of those mentioned above.

---

15. 実在建物の周期と減衰

地震研究所 金井 清
吉沢 静代

日本およびアメリカ合衆国の実在建物の振動実験結果を統計的にしらべて，次のような実験式を得た．即ち，固有周期の式としては，

$$T=\frac{0.04H}{\sqrt[4]{D}}, \tag{7}$$

但し，T は秒，H と D は高さと振動方向の巾で，単位は m である．(7) から次の実用式も得られた．

$$\left.\begin{aligned} &T=0.02\,H,\\ \text{又は}\quad &T=0.08\,N,\end{aligned}\right\} \tag{8}$$

ここに，N は層数である．

又，減衰の大部分は基礎部分の傾斜運動による，基礎と土との間の抵抗に原因することがわかり，その抵抗常数として次の値を得た．

$$\xi_0=1.1\times10^{10}\times\mu^{-0.35}\quad C.G.S., \tag{28}$$

但し，μ は土の剛性率である．即ち，この結果は，地震時に建物の振動勢力が地中に逸散するという考から出た理論結果と定性的には，よく合う．

とにかく，この研究で，数階建以上の建物の周期は上部構造できまり，基礎の影響は少く，反対に，減衰は基礎と土との間で主におこり，上部構造では，あまり生じないことがわかつた．

BULLETIN OF THE EARTHQUAKE
RESEARCH INSTITUTE
Vol. 39 (1961), pp. 491-521

16. *Observations at Miyagi-Enoshima Tsunami Observatory during the IGY Period.*

By Ryutaro TAKAHASI, Kintaro HIRANO, Isamu AIDA,
Tokutaro HATORI and Shizuko SHIMIZU,

Earthquake Research Institute.

(Read January 26, 1960.—Received June 30, 1961.)

1. Miyagi-Enoshima Station-site

Miyagi-Enoshima is a small rocky island only 800 m in diameter, situated about 15 km east of Onagawa harbour, a fishery base for the Sanriku fishing grounds. The island, roughly speaking, is conical in shape, surrounded by cliffs 10–30 m high, but it has two small indentations on its northern coast. The western and larger one furnishes the only landing-place on the island. About 1200 inhabitants, mostly fishermen and their families, live on the steep slope around this landing place. This is the sole inhabited remote island on the north-eastern Pacific coast of Honshu, which is the main island of Japan. It directly faces the Sanriku seismic region frequented with tsunamis.

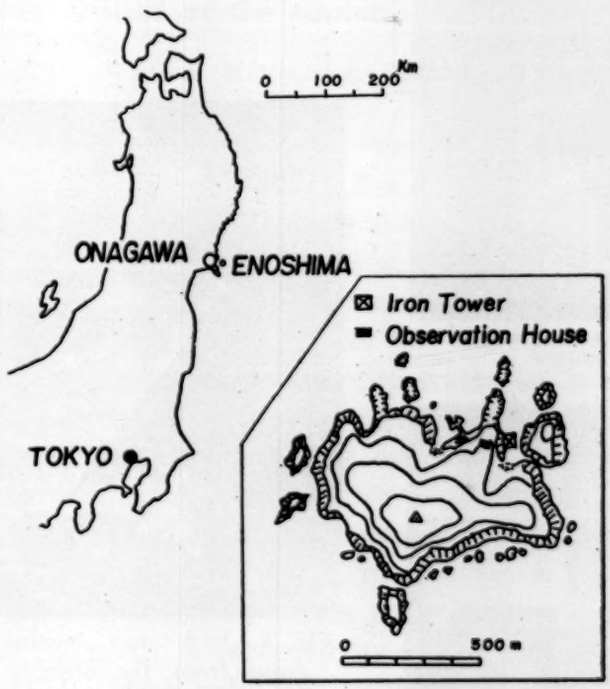

Fig. 1. The map of Enoshima.

The depth of the sea around the island is about 100 m, and the distance to the nearest margin of the island shelf of Honshu from this island is about 25 km.

Miyagi-Enoshima is usually called Enoshima, without using the prefix Miyagi, but since there is another Enoshima in Kanagawa prefecture, we sometimes refer to

the island in question by adding the name of the prefecture to which it belongs.

In 1941, the Earthquake Research Institute installed on the island a tide-gauge specially designed for recording tsunami. The tide-gauge was installed in a wooden shelter on the top of a concrete pedestal 2.5×2.5 m wide and 3.5 m high above MSL, erected in water 3 m in depth in the eastern indentation mentioned above. This indentation is incomplete but it has a rock in front of it, to shelter the tide-gauge from rough seas and swells. Numerous sea-gulls gather on this rock.

Unfortunately however this tide-gauge was washed away by an unusually heavy storm in 1942, and was not restored till 1954, when an iron tower was erected on the concrete pedestal that remained, and a pressure-type tide-gauge was installed in a tide-gauge well at the centre of the pedestal. The recording part of the instrument was installed in a small shed on the cliff nearest to the iron-tower, the pressure changes

Fig. 2. Observation house.

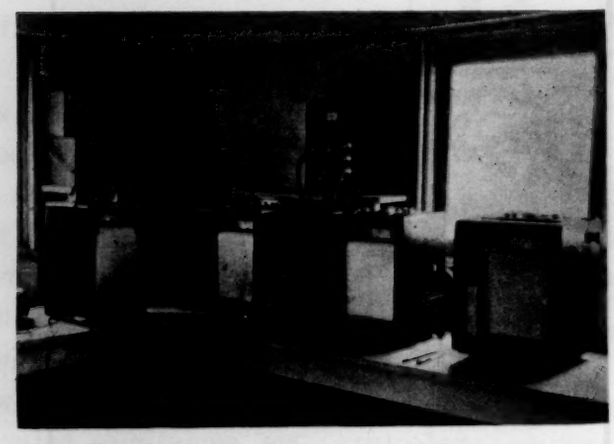

Fig. 3. Interior of observation house.

Fig. 4. Iron tower, looking down from the observation house.

produced at the sensing part in the well being led by a thin copper tube, spanned from the iron tower to the shed.

In 1956, an ERI-III tsunami recorder was installed in the well under the iron tower. This is essentially a differential tide-gauge which records tides and long waves separately. The details of this instrument will be given below.

In April, 1957, a long wave recorder of the Van Dorn type was installed in the same well as the ERI-III tsunami recorder. The recording galvanometers for these two gauges were installed in a newly built observation house as shown in Figs. 2~4. Cables were spanned from the iron tower to a concrete anchor half way down the cliff and then to the station house.

During the IGY period of 1957–58, this station participated in long wave observations. Its CSAGI No. is C-118 and the geographic position 141°36′E, 38°24′N. Observations of sea and swell, microbarometric oscillations and other conventional meteorological elements were also carried out.

In the following we will give some explanations of each instrument which is used at the station and the results of the observations.

2. Instruments

a) *ERI-III tsunami recorder.* Two identical 6″ galvanized iron pipes, C_1 and C_2, each 5.5 m long, are erected in the sea, with a float F in each of them. They differ only in the diameters of the copper capillary tubes R_1 and R_2 at the lower end of each iron pipe, through which the sea water communicates with the interior of the pipes. The water surface in C_1 follows the sea surface variation of periods longer than about 2 min., while the water surface in C_2 follows the sea surface variation of periods longer than 120 min. The rise and fall of each float are transmitted to a pully by means of nylon string. The pulley rotates a low-torque potentiometer (Helicalohm) on its axis. The potentiometers are fed with 6 volts. Thus the motions of the floats are transformed into DC electric signals. The difference of the electric signals from the two potentiometers, which follows thus the long waves of periods from 2 to 120 min., is recorded by two recording galvanometers, connected in parallel. Each recording galvanometer has a transistor amplifier fed with 24 v. The sensitivity of one galvanometer is $0\sim\pm1.5$ volts for full scale, and can record the long waves of heights $0\sim\pm2.5$ m. The other recording galvanometer is of the range $0\sim\pm0.3$ volts full scale which

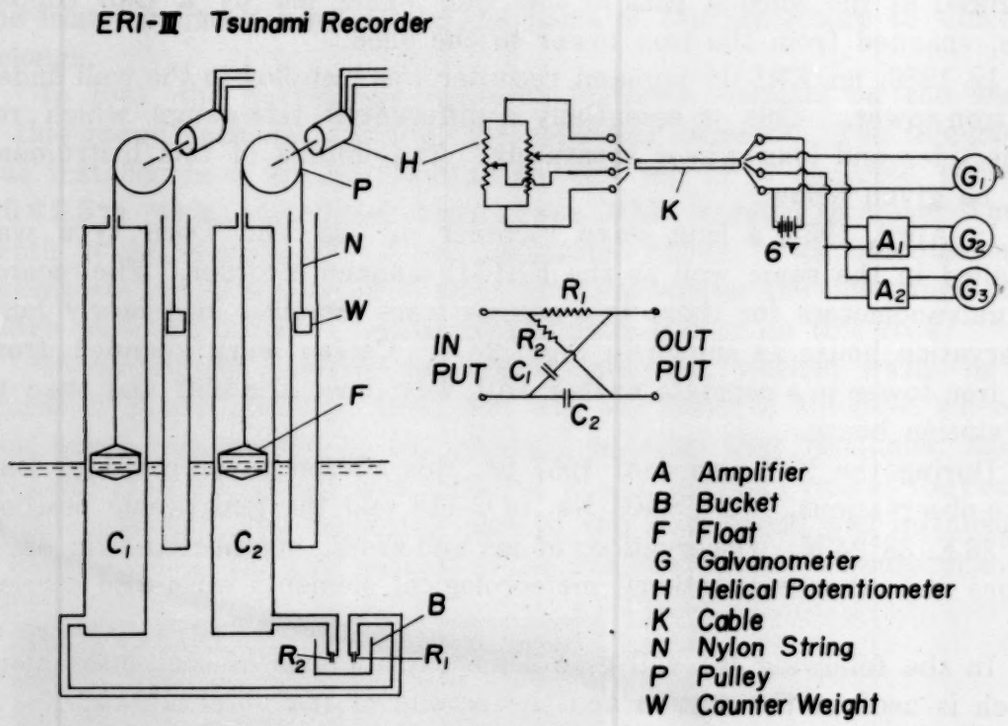

Fig. 5. The ERI-III tsunami recorder and its equivalent circuit.

corresponds to the long waves of the range $0 \sim \pm 0.5$ m. Beside these two galvanometers there is another one with the range $0 \sim 6$ volts full scale, and is fed with an electric signal directly from one of the potentiometers for the purpose of recording tide. Recording charts are driven at the speed of 6 cm/hr for long waves and 2 cm/hr for the tide.

The sensitivity of this long wave recorder is adjusted to show the maximum value of 0.53 div. per cm of wave height at the central period of 12 min. and fall at the rate of 6 db/octave on both sides of this central period.

Results obtained by this ERI-III long wave recorder are not given in the present report because they were almost the same as those obtained from the Van Dorn long wave recorder.

b) *The Van Dorn long wave recorder.* This instrument, invented by Dr. W. G. Van Dorn of the Scripps Institution of Oceanography, was provided by him in March, 1957, and was installed in the same well as ERI-III. The observation of long waves with the use of this instrument has been executed since April 1, 1957 without any serious interruption.

No detailed descriptions of this instrument will be given here but

only a brief explanation just necessary for the present report, since details would be given elsewhere by the inventor. The present recorder is entirely different from that written by him in 1956.[1)]

The recorder is shown schematically in Fig. 6. It consists of a standpipe C_1, a hydraulic filter C_0, and a piece of rubber hose connecting them. The hydraulic filter consists of two capillary tubes of different diameters R_1, and R_2, a U-tube C_2 which contain mercury, and a wire-strain pressure transducer T of high sensitivity. The hydraulic filter is installed just under the L. W. level. A long vinyl hose is connected to the bottom of the filter. Sea water is led into the hydraulic filter through this vinyl hose and a strainer at the other end of the hose. The strainer has been fixed in a bucket placed on the bottom of the well to facilitate the step-function calibration. The hydraulic filter is filled with silicon oil. The hydraulic filter and the stand pipe are fixed to a 3 inch galvanized iron pipe and have been installed in the concrete well mentioned above.

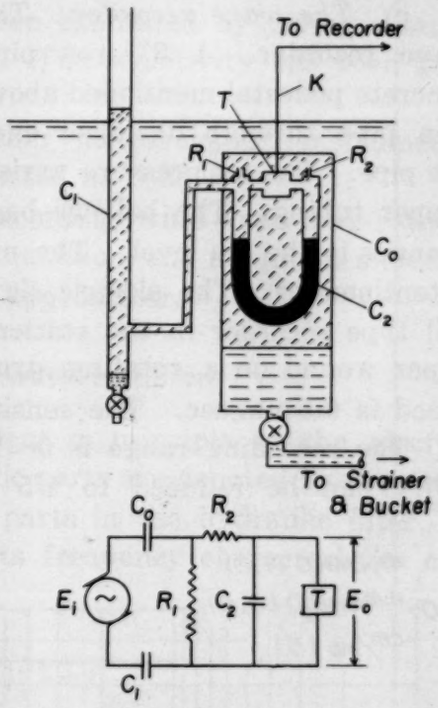

Fig. 6. The Van Dorn L. W. recorder and its equivalent circuit.

The pressure differences produced between two legs of the mercury U-tube are transformed by the pressure transducer into electric signals and are sent to a transistor amplifier and then to the Esterline-Angus recording galvanometer, both installed in the station house on the cliff.

The over-all sensitivity of the Van Dorn L. W. recorder, as calibrated by giving a step-function input, is about 1.35 division on the chart for 1 cm change in the sea level at the central period of 20 min. Since the width of 1 div is 2.4 mm at the centre of the chart, the Van Dorn instrument describes the long waves with the minification of about 1/3 the actual height. The chart speed was kept at 3″/hour.

The sensitivity remained fairly constant during the IGY period, although small fluctuations have been noticed, which seem to have their

1) VAN DORN, W. G. "A portable tsunami recorder," *Trans. Amer. Geophys. Union*, **37** (1956), 27–30.

cause in the change in viscosity of silicon oil, due to the sea water temperature change.

In the actual observation, an additional low pass filter, consisting of a 40000μF shunt condenser, was inserted in front of the amplifier for the purpose of cutting off the 2.5 min. oscillations inherent to the station site.

c) *The wave recorder.* This is essentially a stand-pipe type wind wave recorder. A 3″ iron pipe is fixed to the outer surface of the concrete pedestal mentioned above. The sea water flows in and out the iron pipe through its lower end and compresses and rarefies the air in the pipe. The air pressure variation is fed to a metalic bellows through copper tubing. The bellows has a slow leak capillary to eliminate slow changes in the sea level. The motion of the bellows turns a low torque potentiometer. The electric signal thus produced is sent to the moving coil type recorder in the station house. The record is made on smoked paper wound on a rotating drum run by a spring motor. Recording speed is 0.5 mm/sec. The sensitivity characteristic is shown in Fig. 7.

The recording range is 0~1.2 m. In case of heavy seas the sensitivity can be reduced to 1/5 of the usual value, the recording range

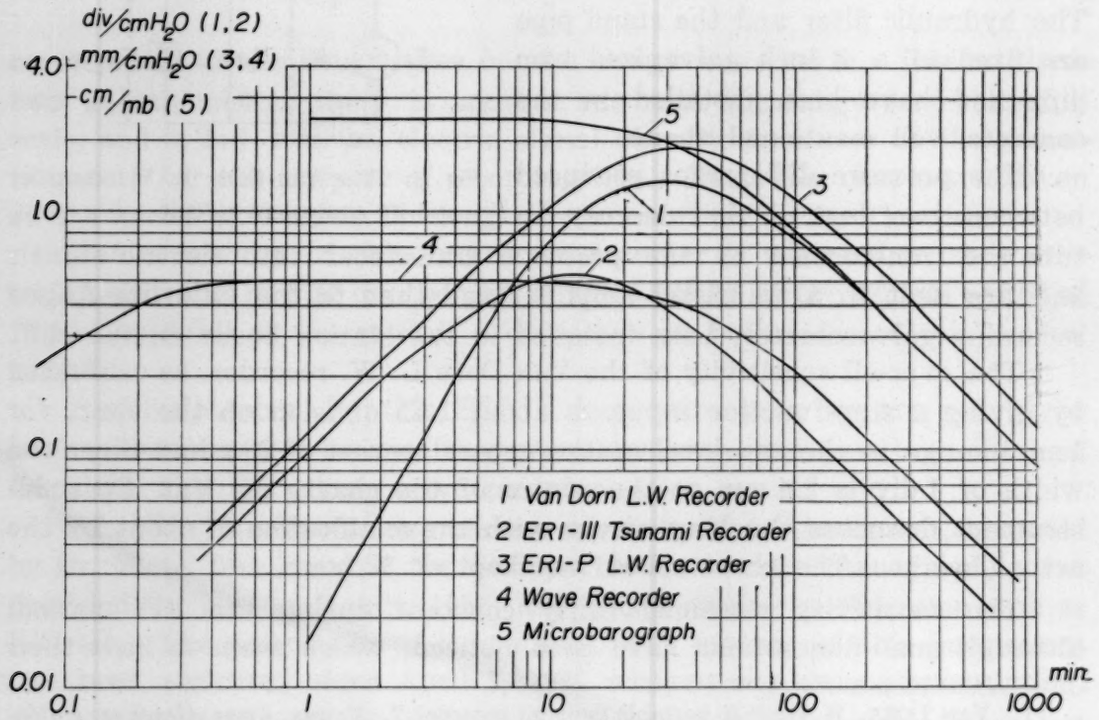

Fig. 7. The sensitivity characteristics of various instruments at Enoshima.

being accordingly increased to 0~6 m.

d) *Microbarograph.* This is a one-cup microbarograph to record the oscillation of the atmospheric pressure of periods shorter than 100 min. An 18-litre glass bottle provided with a slow leak is connected with the interior of the microbarograph cup. The glass bottle is buried in the ground to avoid the effect of air temperature changes. The sensitivity of the microbarograph has been calibrated by giving a step-wise pressure change to the glass bottle. The sensitivity has been 2.42 cm for a change of one millibar.

e) *Other instruments.* Various other meteorological instruments are installed at the station. They are listed as follows:

1 barograph; 1 thermograph; 1 recording wind vane and 1 wind speed recorder; 1 hygrograph; 1 maximum and minimum mercury thermometer; 1 dry and wet bulb hygrometer.

3. Calibration of long wave recorders

The Van Dorn instrument is equivalent in principle to the electric band-pass filter shown in Fig. 6. Electric parts are denoted by the same letters as the corresponding mechanical parts in the hydraulic filter.

Since the filter is heavily tapered, its frequency characteristics can be shown as

$$E_0/E_i = j\frac{\omega}{\omega_1}\Big/\left(1+j\frac{\omega}{\omega_1}\right)\left(1+j\frac{\omega}{\omega_2}\right),$$

where ω is the angular frequency of the pressure variation E_i, and $\omega_1=1/CR_1$, $1/C=1/C_0+1/C_1$, $\omega_2=1/C_2R_2$.

The sensistivity of the filter takes the maximum value of $\omega_2/(\omega_1+\omega_2)$ at the central frequency $\omega_0=\sqrt{\omega_1\omega_2}$. For small values of ω, $E_0/E_i \fallingdotseq j\omega/\omega_1$, and for large values of ω, $E_0/E_i \fallingdotseq \omega_2/j\omega$.

The calibration of the Van Dorn long-wave recorder has been made at intervals of 3~6 months during the IGY period. The calibration was made by lifting the bucket B, Fig. 6, above the sea level to make an artificial sea surface in the bucket. The height of the bucket was then suddenly changed (lifted and/or lowered) by about 10 cm. Corresponding to this step-function imput, the recorder will describe on the chart a response

$$R(t)=D\cdot H\frac{\omega_2}{\omega_2-\omega_1}\left(e^{-\omega_1 t}-e^{-\omega_2 t}\right),$$

where H is the height of the imput step function, D the deflection which would be produced on the chart when a pressure equivalent to 1 cm of water column was applied across the pressure transducer T. D, ω_1 and ω_2 are three quantities to be determined by the calibration. The quickest and easiest way of getting their values is to plot $R(t)$ on a sheet of logarithmic section paper. Since $R(t)/H$ can be approximated by $D\frac{\omega_2}{\omega_2-\omega_1}e^{-\omega_1 t}$ for large values of t, we can easily read off the values $\omega_2 D/(\omega_2-\omega_1)$ and ω_1 from the logarithmic section paper. Then the values of $D\frac{\omega_2}{\omega_2-\omega_1}e^{-\omega_1 t}$ for small values of t are read on the section paper by producing the tail of the response curve. The differences of these values from $R(t)$ represent $D\frac{\omega_2}{\omega_2-\omega_1}e^{-\omega_2 t}$. Plotting these values again on the same logarithmic section paper, we can obtained ω_2. From $\omega_2 D/(\omega_2-\omega_1)$, ω_1 and ω_2 thus obtained, we calculated D, ω_1, ω_2 and $\omega_0=\sqrt{\omega_1\omega_2}$.

The results of calibration have been reported to the IGY World Data Centers in the form of spectral sensitivity curves attached to the monthly report. We will here briefly summarize the results of calibration carried out during the IGY period.

Table 1.

Date	(div/cmH_2O) D	(rad/min) ω_1	(rad/min) ω_2	(min) $T_1=2\pi/\omega_1$	(min) $T_2=2\pi/\omega_2$
1957 III 31	1.55	0.0886	0.627	71.0	10.0
VI 29	1.60	0.121	0.744	52.0	8.45
XII 11	1.60	0.105	0.530	60.0	11.9
1958 III 26	1.59	0.109	0.609	57.7	10.3
X 12	1.75	0.129	0.649	48.8	9.7
1959 IV 28	1.58	0.0948	0.635	66.4	9.9

The calibrations have been done with and without the additional electric low-pass filter of which the cut-off frequency ω_3 is almost the same as ω_2. In the actual observation, the spectral sensitivity of the recorder showed therefore the decrease of 12 db per octave for frequencies larger than ω_2, and the decrease of 6 db per octave for frequencies smaller than ω_1.

The ERI-III tsunami recorder is equivalent in function to the elec-

tric circuit shown in Fig. 5. The spectral response is therefore

$$E_0/E_i=\frac{\omega_2-\omega_1}{\omega_2}\cdot\frac{j\omega/\omega_1}{(1+j\omega/\omega_1)(1+j\omega/\omega_2)},$$

which has the maximum value of $(\omega_2-\omega_1)/(\omega_2+\omega_1)$ at $\omega_0=\sqrt{\omega_1\omega_2}$, and decreases at the rate of 6 db/octave on both side of ω_0. Calibration for the ERI-III recorder has been made separately for the recording galvanometer and for two capillary tubes R_1, R_2. Effective values for R_1 or R_2 have been obtained in the laboratory by the discharge test of water through the capillary tube under consideration.

Fig. 7 shows the average sensitivity curves for various long wave recorders, the wave-meter and the microbarograph which are being used at Enoshima.

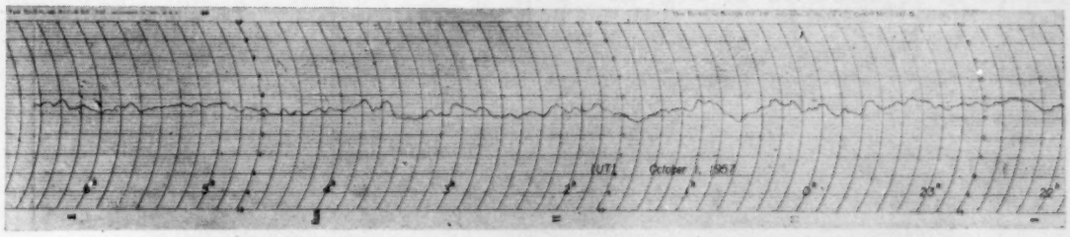

Fig. 8. Feature of long wave record obtained at Enoshima on an ordinary day.

4. Results of Observations

Fig. 8 shows the typical feature of the record obtained by the Van Dorn long wave recorder at Miyagi-Enoshima on an ordinary day. The incessant fluctuations of the sea level of periods ranging from 10 to 70 min. have been observed. The ranges of these fluctuations, measured from a trough to the following crest, were mostly less than 4 divisions on the chart, or about 3 cm in actual scale. In the IGY monthly report sent to the World Data Centres, all remarkable fluctuations which surpassed 4 divisions in height have been given, together with the time of starting and the termination, the mean period, the maximum amplitude and its time of occurrence, etc.

Some of these remarkable disturbances resulted from obvious causes such as a tsunami, a nuclear explosion or typhoons: on Sept. 27, 1958 the typhoon "Kanogawa" passed 15 km east of Enoshima, the atmospheric pressure at the centre having been 980 mb. approximately. On this occasion, the long wave attained as much as 26 divisions in height, the highest value observed during the IGY period. The long waves developed to 4 divisions in height as early as 0517, 26th UT and lasted for about 32 hours. The maximum wind speed during these hours was

17.0 m/s blowing from ESE.

A similar remarkable disturbance was experienced on 26th December, 1958, which had been due to a heavy cyclone. The Van Dorn recorder was out of order for forty hours on account of this storm (From 0650, Dec. 27 to 2300 Dec. 28, 1958, UT). According to the ERI-recorder, the maximum height of the long wave during this storm was 21.5 cm.

On November 6th, 1958, a tsunami caused by an earthquake near Iturup Is. was observed. This was the only seismic tsunami observed in Japan during the IGY period. The origin time of the earthquake was 2258 Nov. 6, 1958 UT, the epicentre being at 44°3N, 148°5E. At Enoshima, the tsunami started at 0005 Nov. 7, UT, the maximum amplitude of 14.5 divisions having been observed at 0129 of the same day. The record is reproduced in Fig. 9.

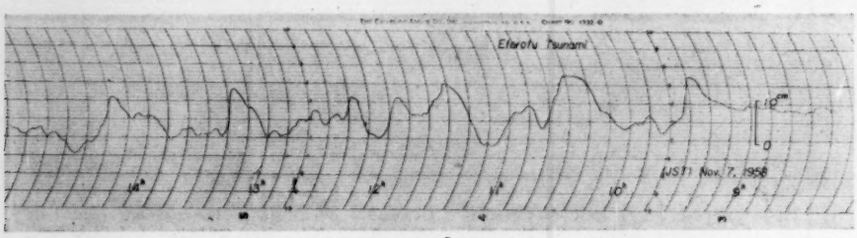

Fig. 9. Record of Iturup Tsunami on Nov. 7, 1958.

A minute disturbance, about 4 divisions in amplitude, was observed on June 29, 1958. This was probably the tsunami caused by the nuclear explosion near Eniwetok atoll on June 28, 1958, UT. The waves started at 0024 UT and lasted for about 9 hours.

The incessant disturbances, of lengthy periods but of small height, which form the back-ground noise to the remarkable long waves, seem to have a close relation with the fact that Enoshima lies on the continental shelf along Honshu. We seldom observed such back-ground noise at Hachijo Island, which stands on a deep ocean floor. These disturbances might be shelf seiches or edge waves generated by meteorological disturbances which are progressing on or outside the coastal waters.

To see the relation between the growth and decay of long waves and various meteorological elements, we have made summary diagrams of various observed quantities at Enoshima for each month during the IGY. They are shown in Figs 10~27, and contain : daily weather, wind wave height, long wave period, long wave height, atmospheric pressure, microbarometric oscillations of long and short periods, wind velocity and direction.

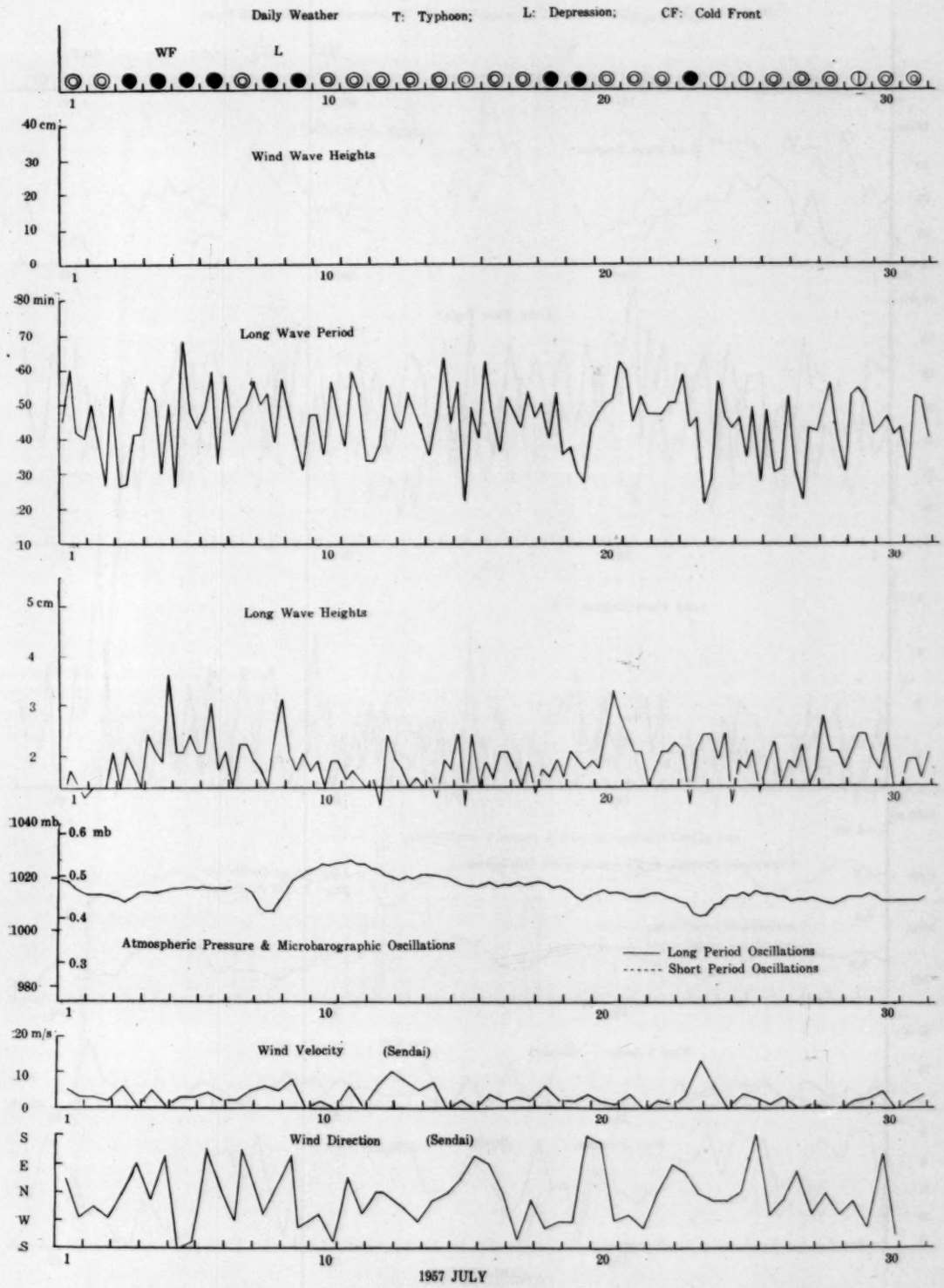

Fig. 10. Summary diagram of Long Period Wave Measurements at Miyagi-Enoshima in July 1957.

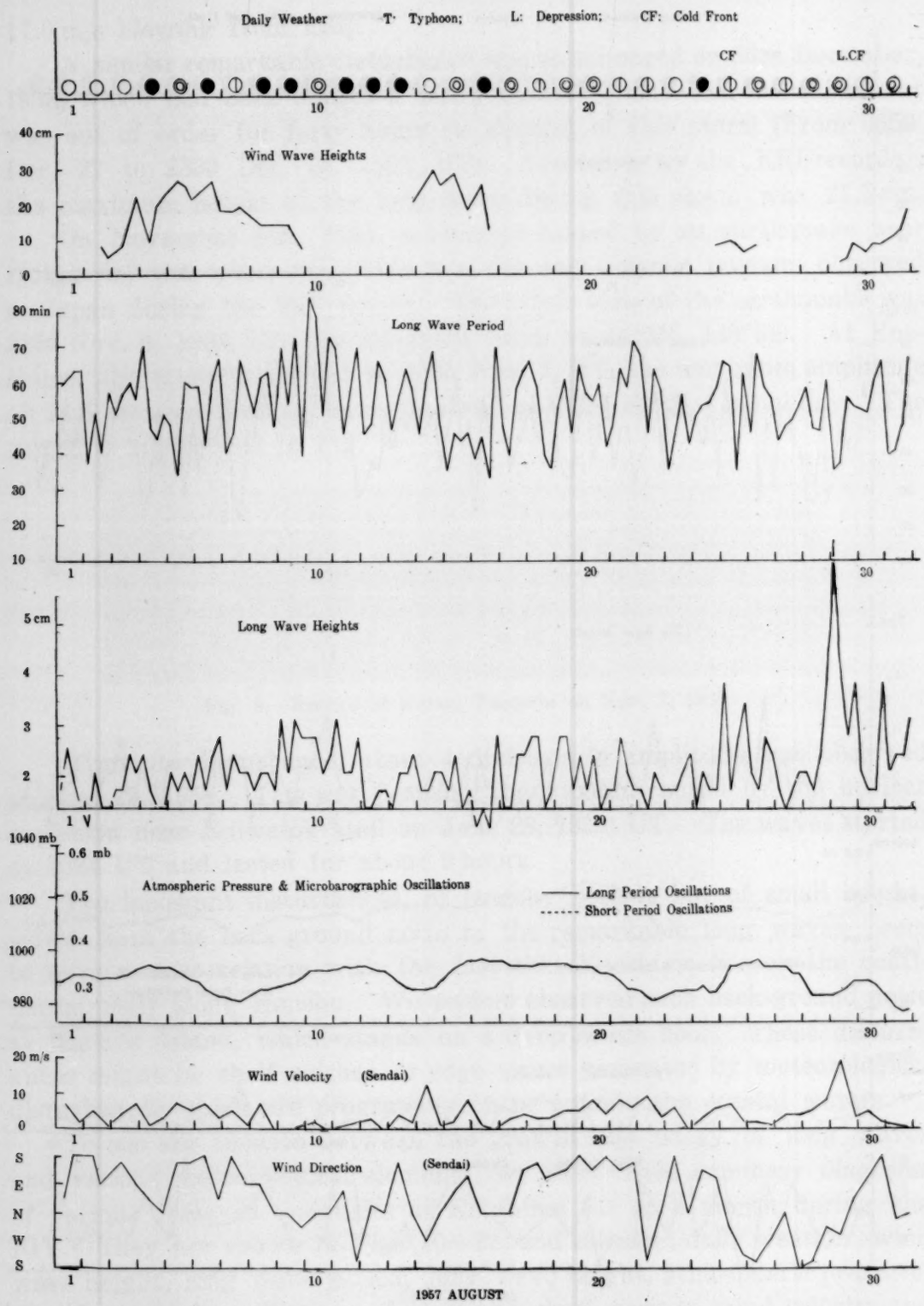

Fig. 11. Summary diagram of Long Period Wave Measurements at Miyagi-Enoshima in August 1957.

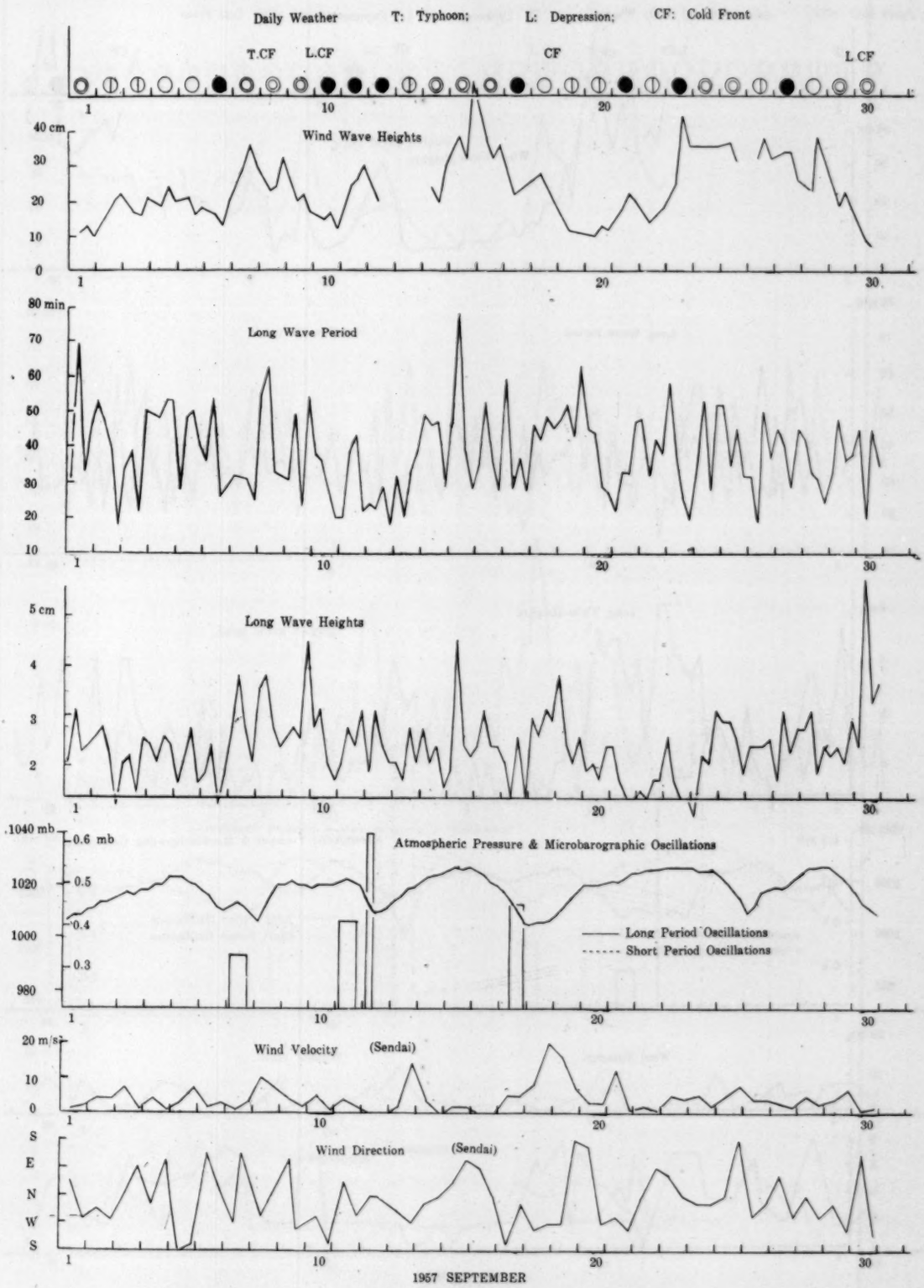

Fig. 12. Summary diagram of Long Period Wave Measurements of Miyagi-Enoshima in September 1957.

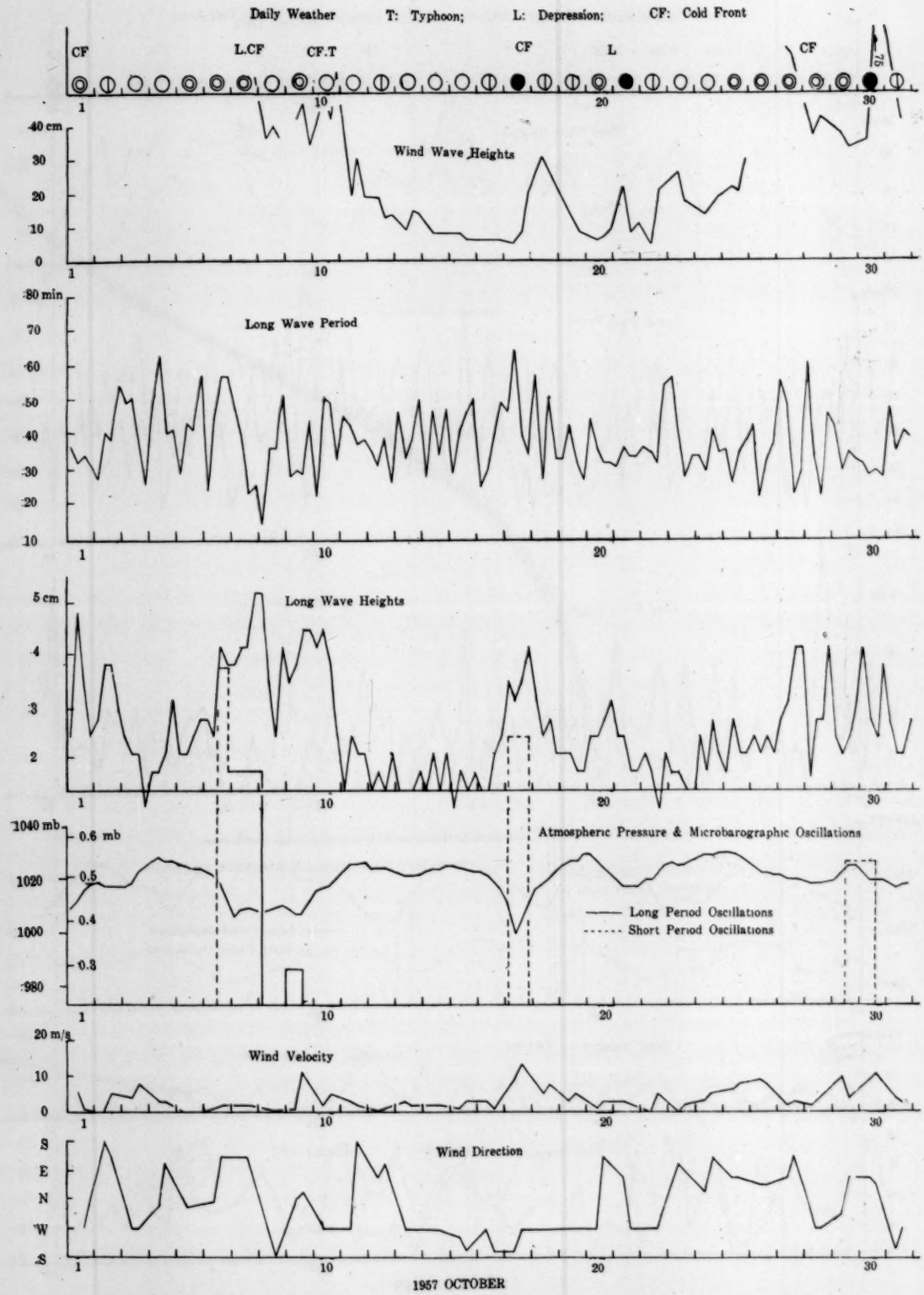

Fig. 13. Summary diagram of Long Period Wave Measurements at Miyagi-Enoshima in October 1957.

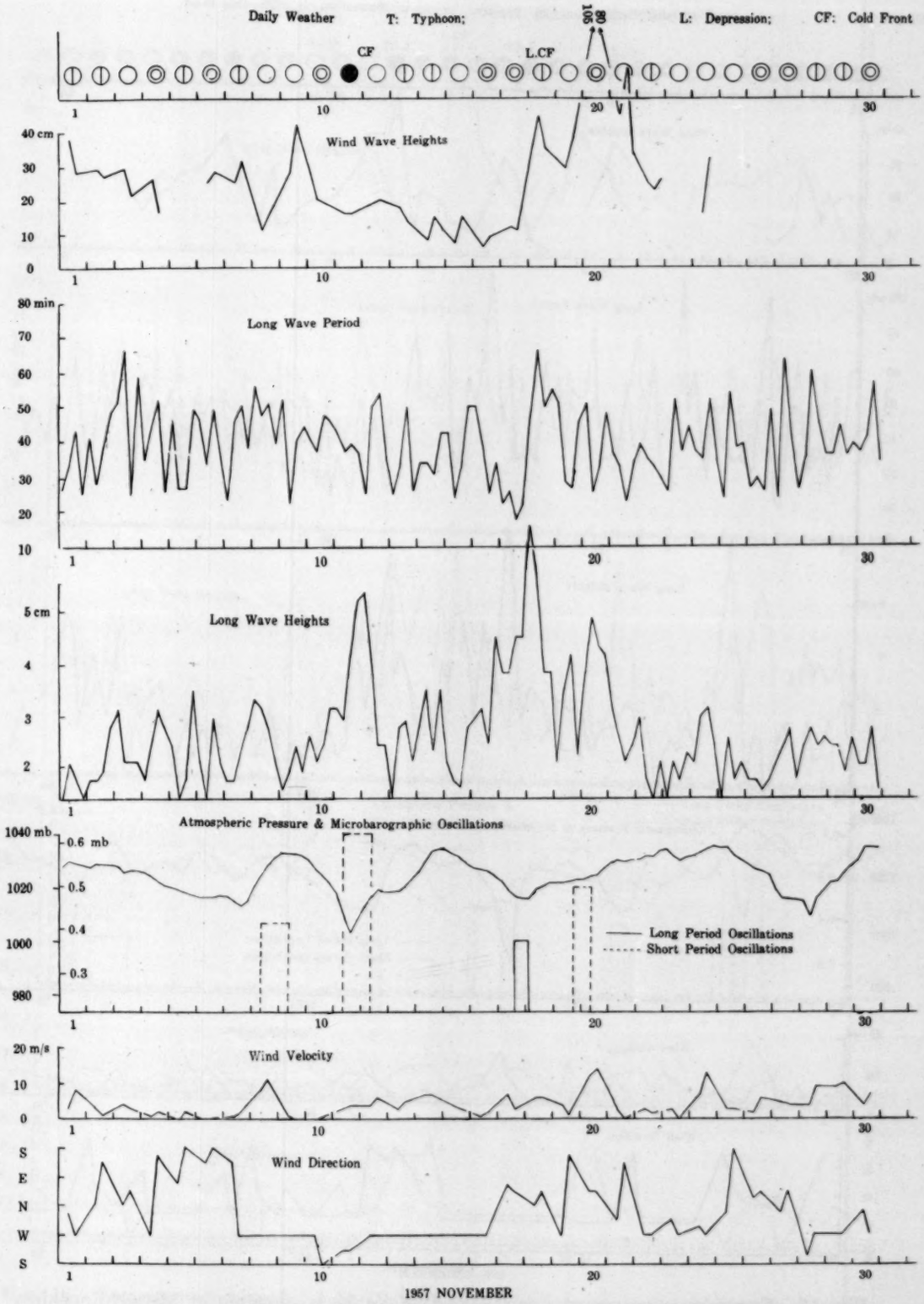

Fig. 14. Summary diagram of Long Period Wave Measurements at Miyagi-Enoshima in November 1957.

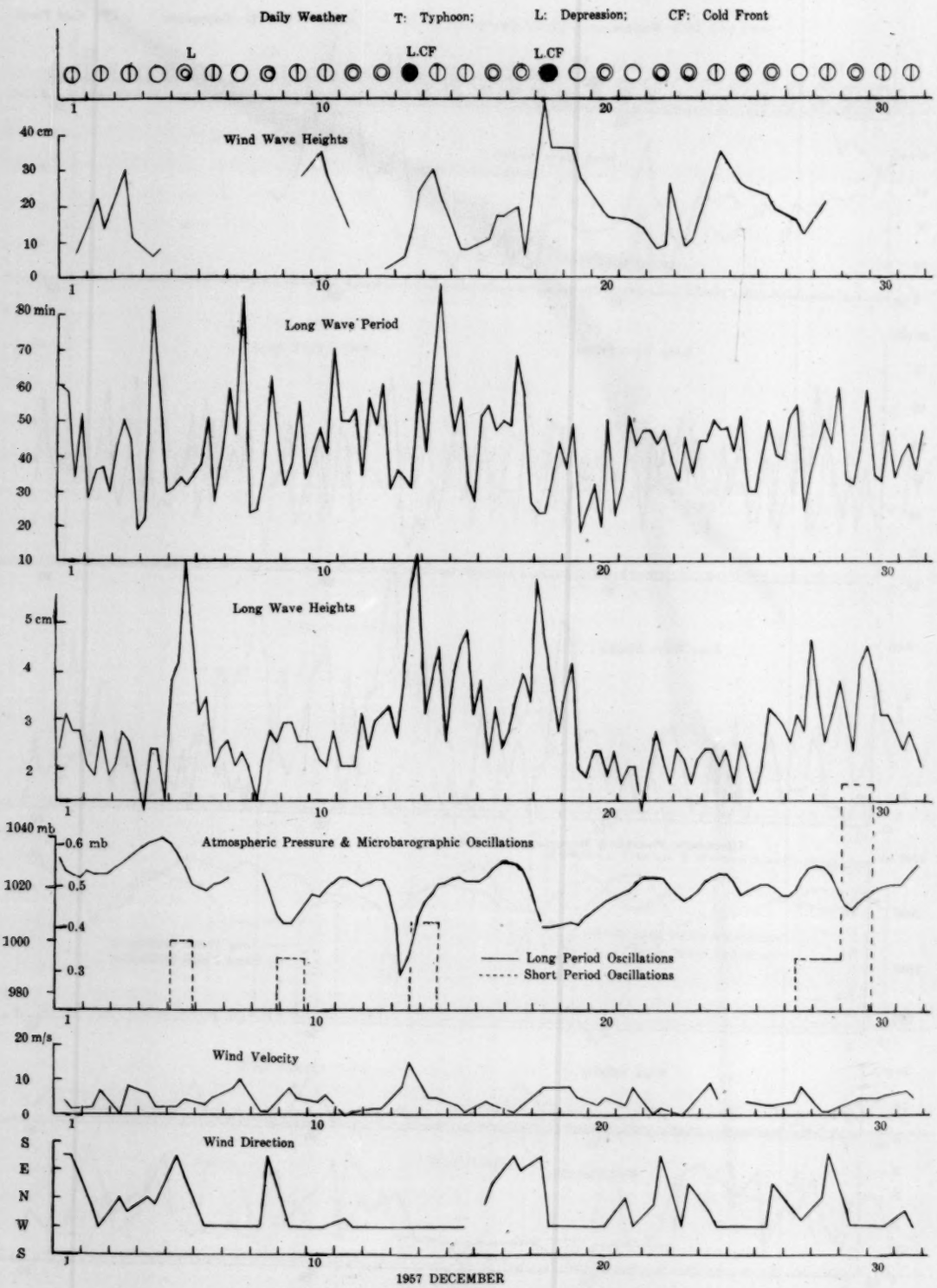

Fig. 15. Summary diagram of Long Period Wave Measurements at Miyagi-Enoshima in December 1957.

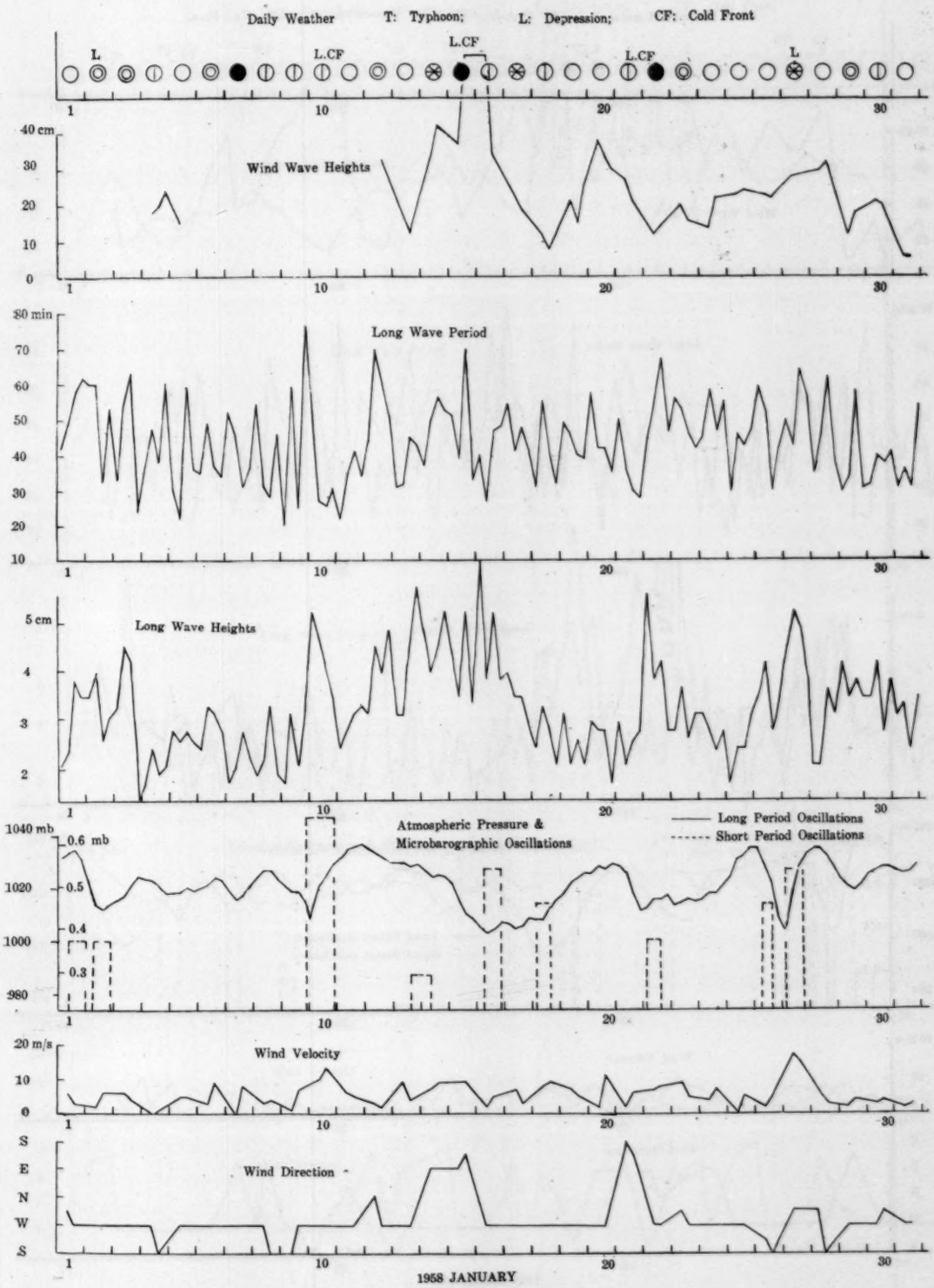

Fig. 16. Summary diagram of Long Period Wave Measurements at Miyagi-Enoshima in January 1958.

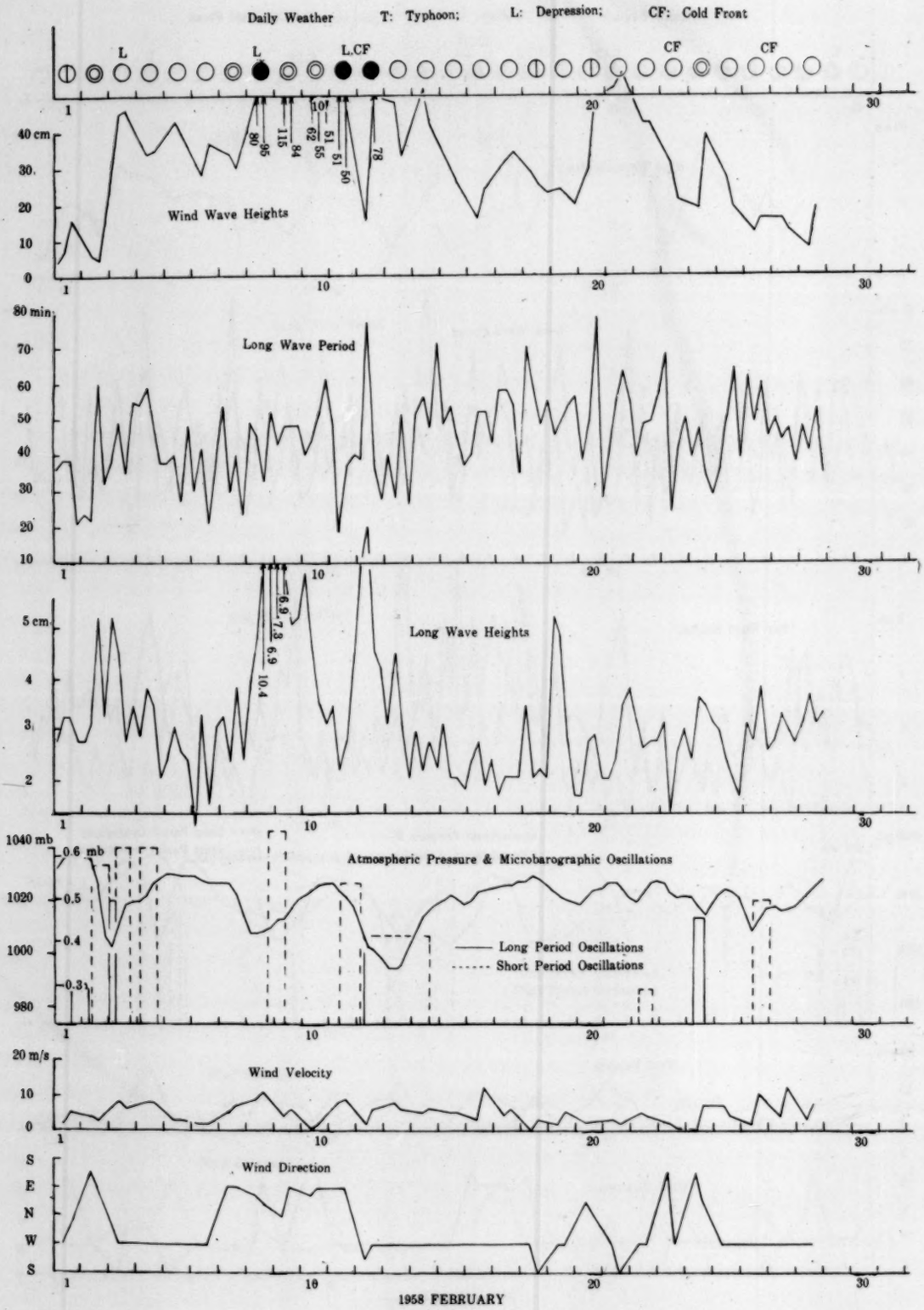

Fig. 17. Summary diagram of Long Period Wave Measurements at Miyagi-Enoshima in February 1958.

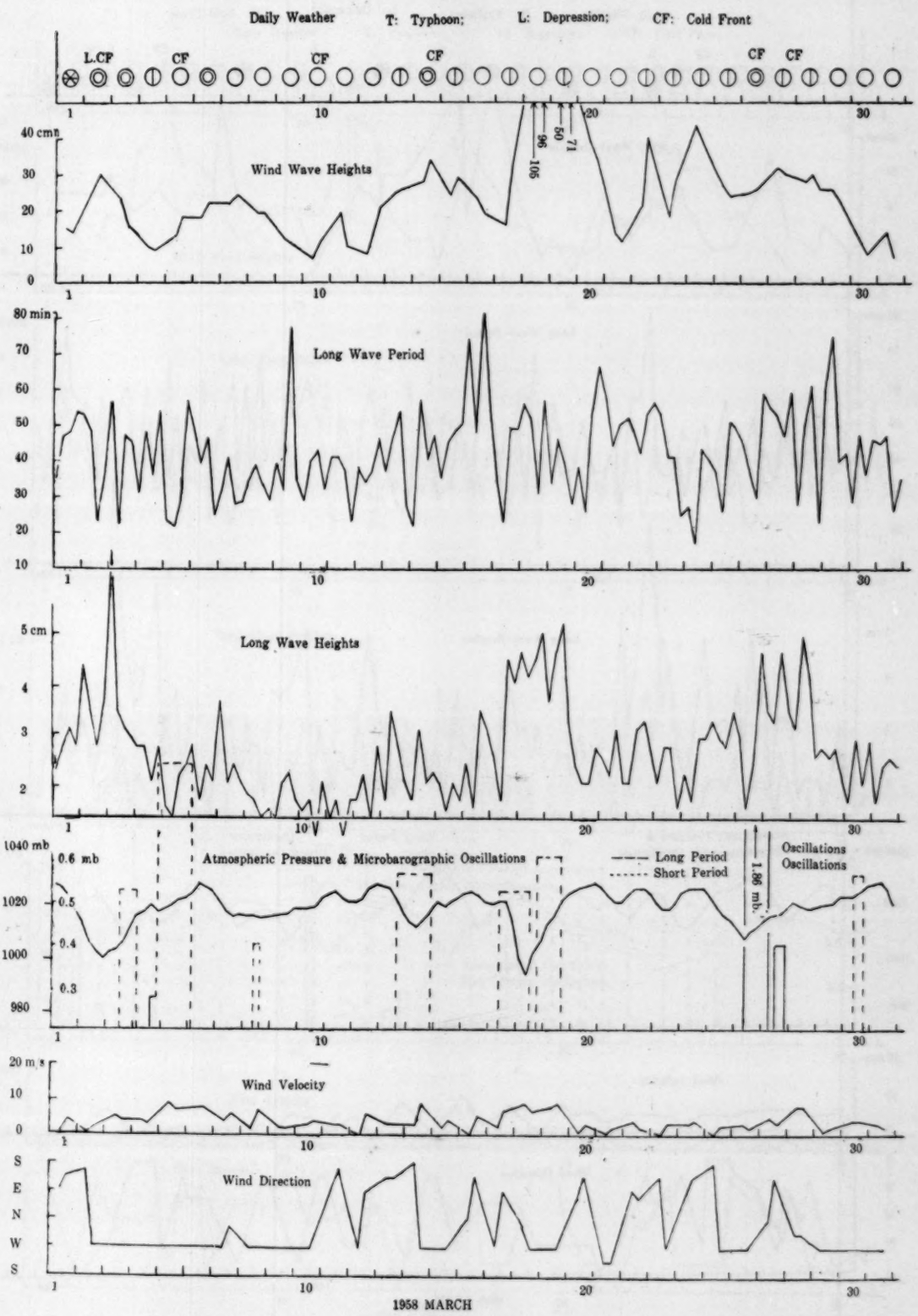

Fig. 18. Summary diagram of Long Period Wave Measurements at Miyagi-Enoshima in March 1958.

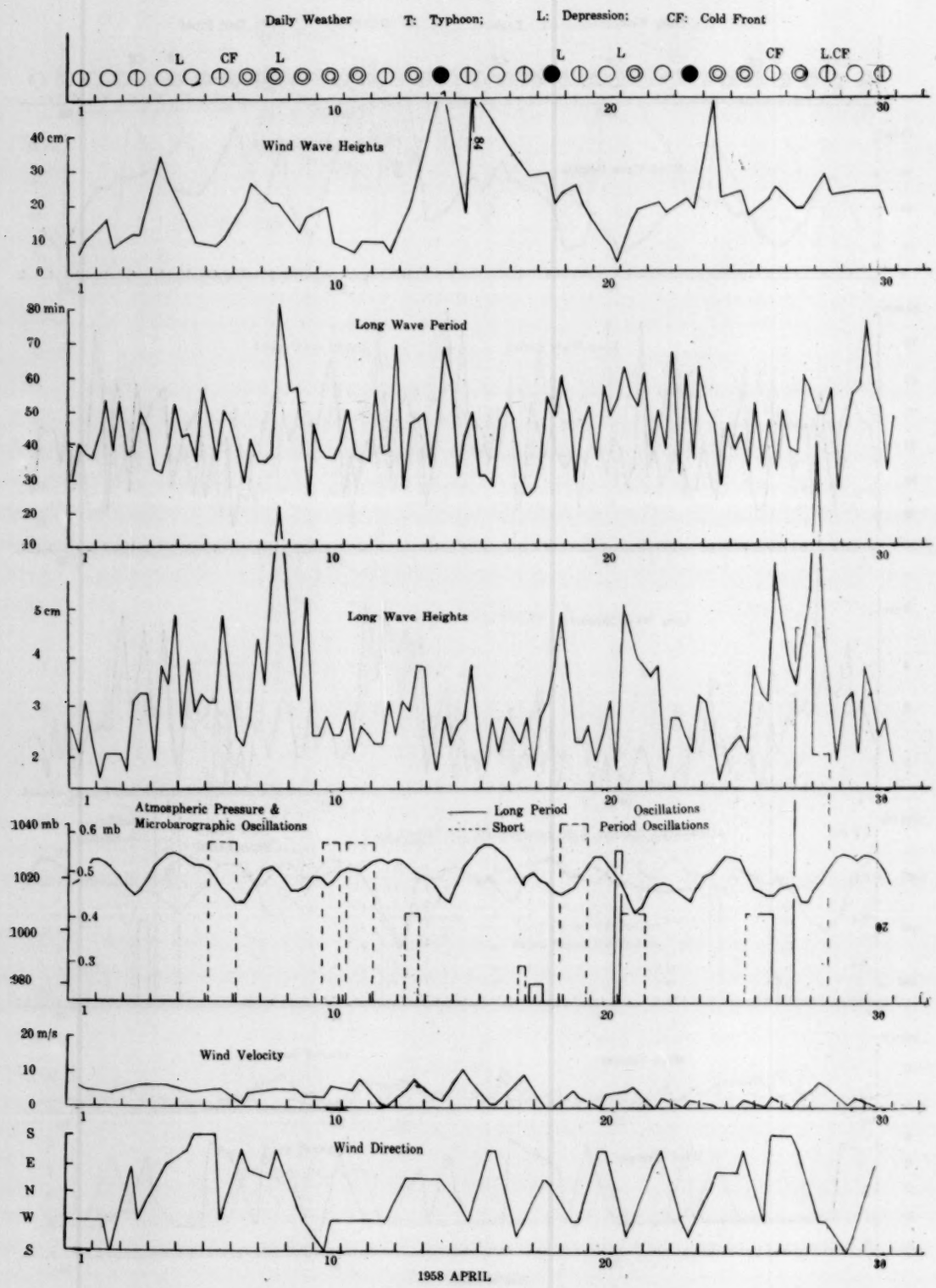

Fig. 19. Summary diagram of Long Period Wave Measurements at Miyagi-Enoshima in April 1958.

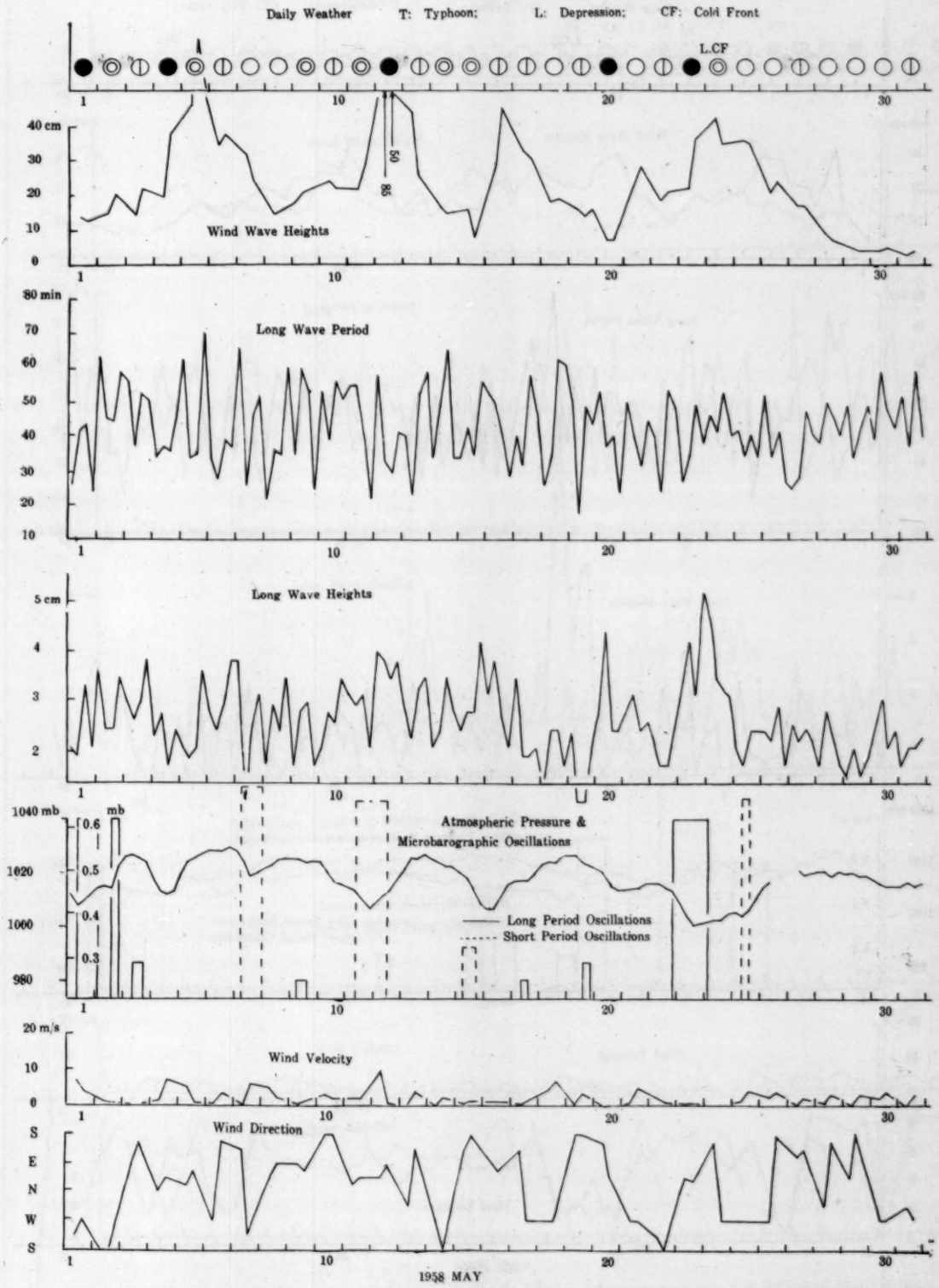

Fig. 20. Summary diagram of Long Period Wave Measurements at Miyagi-Enoshima in May 1958.

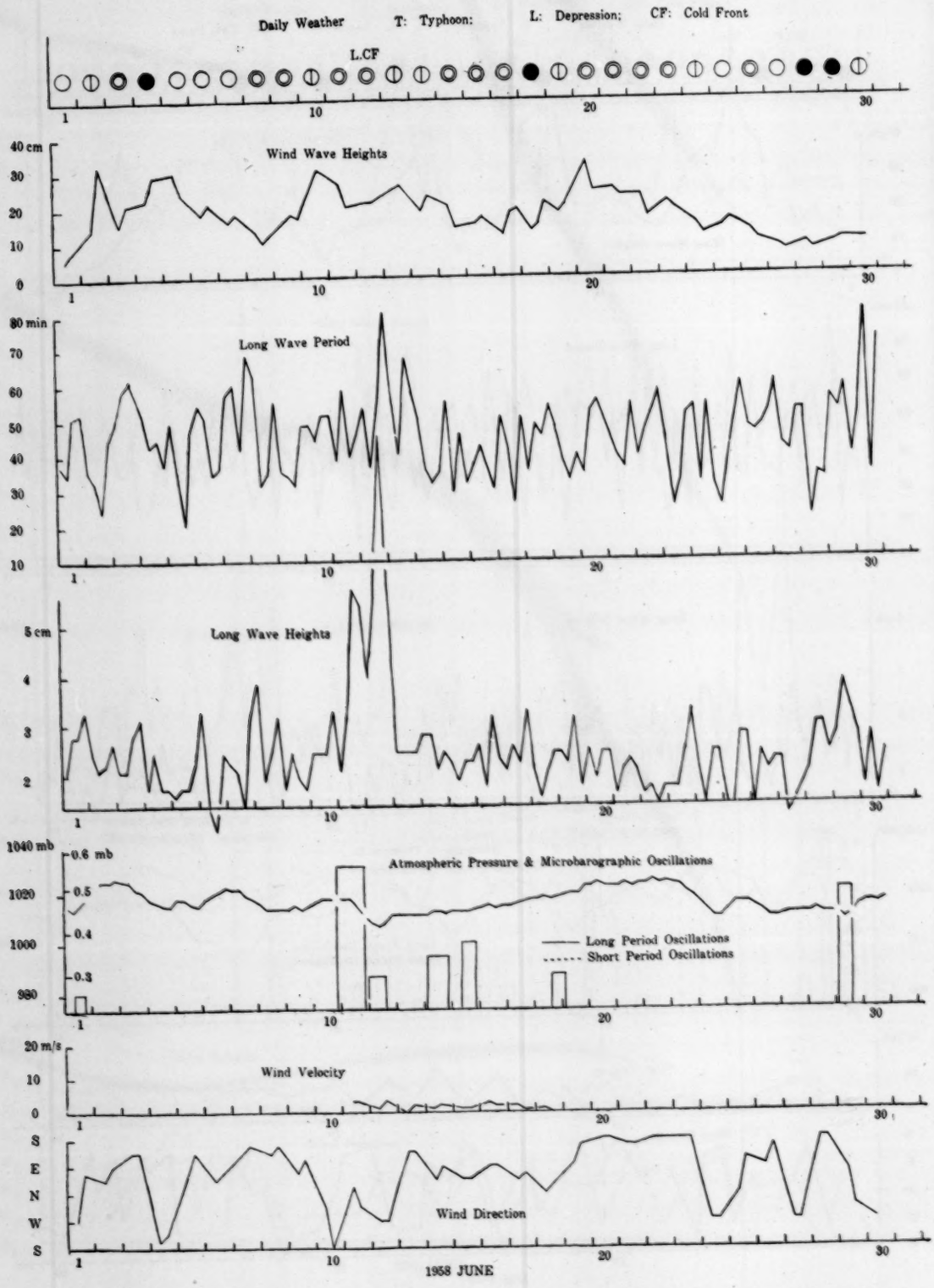

Fig. 21. Summary diagram of Long Period Wave Measurements at Miyagi-Enoshima in June 1958.

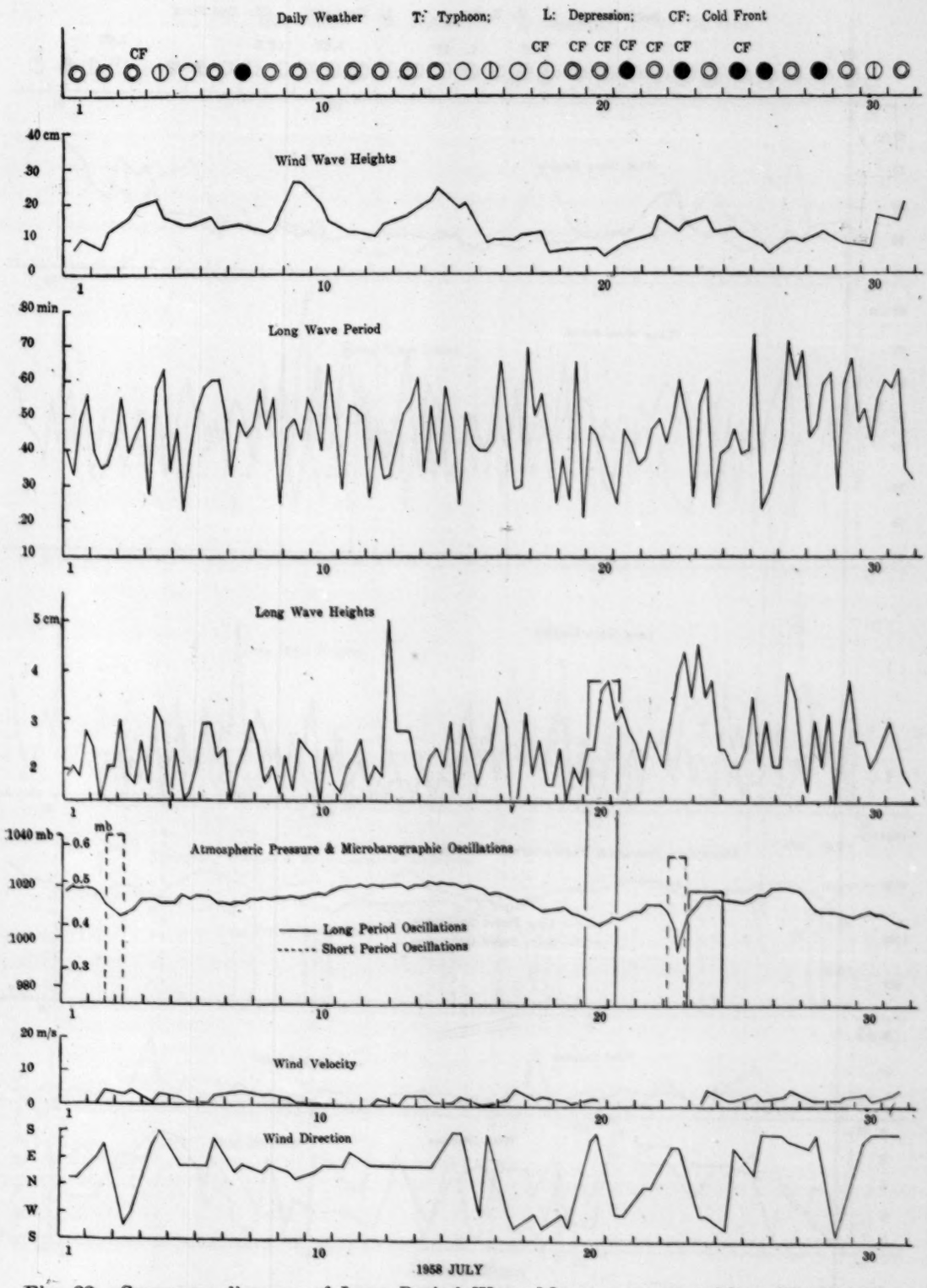

Fig. 22. Summary diagram of Long Period Wave Measurements at Miyagi-Enoshima in July 1958.

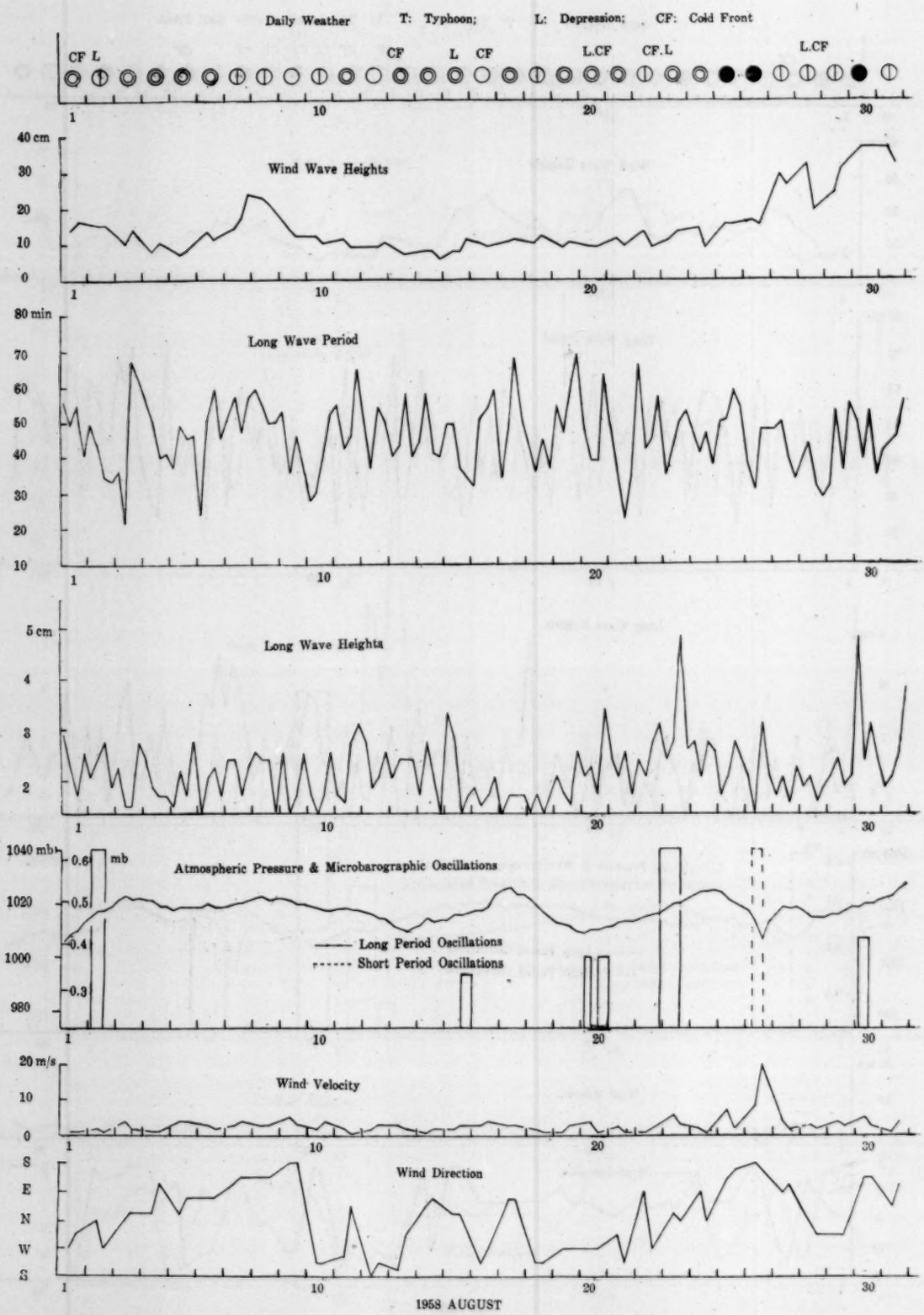

Fig. 23. Summary diagram of Long Period Wave Measurements at Miyagi-Enoshima in August 1958.

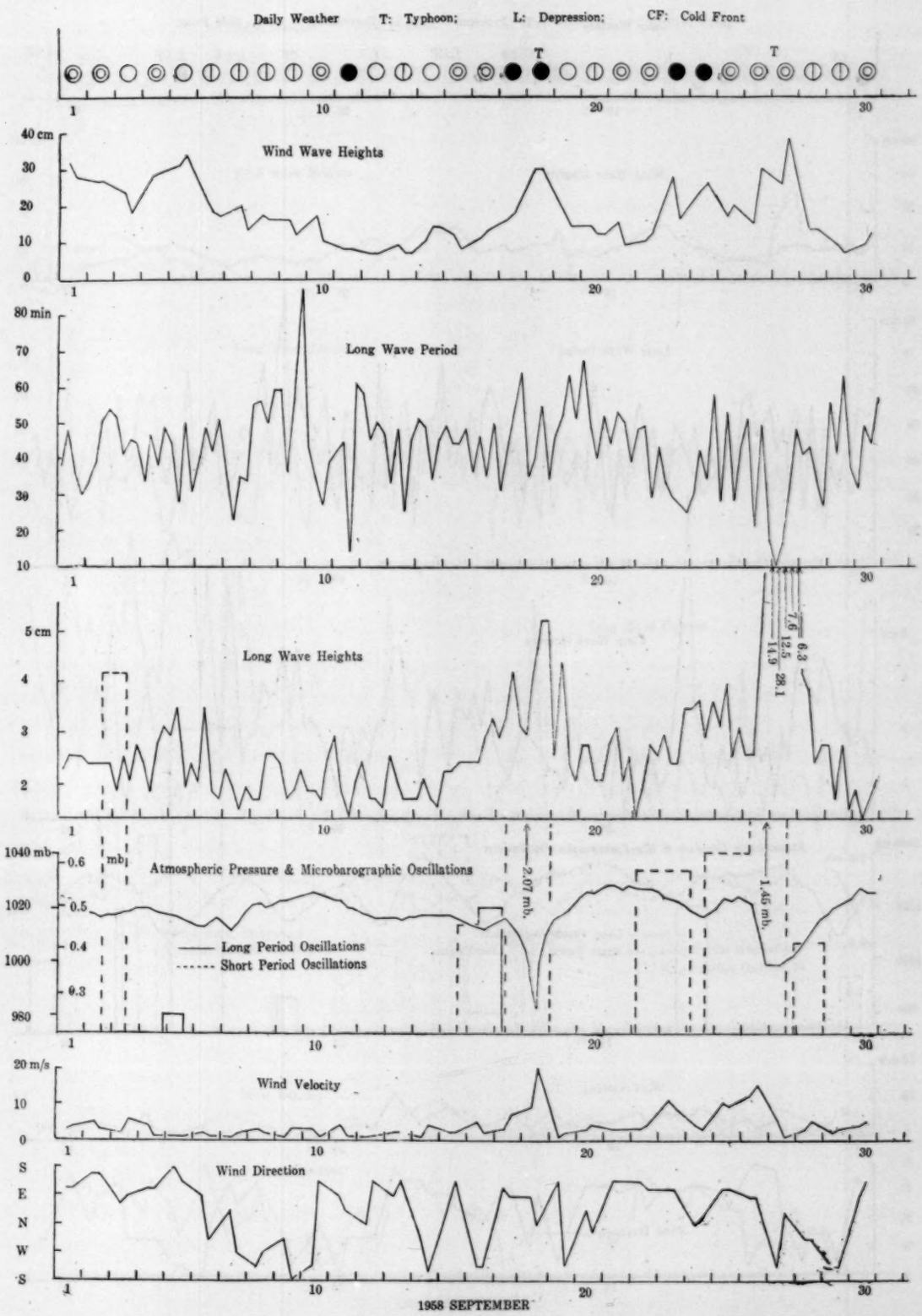

Fig. 24. Summary diagram of Long Period Wave Measurements at Miyagi-Enoshima in September 1958.

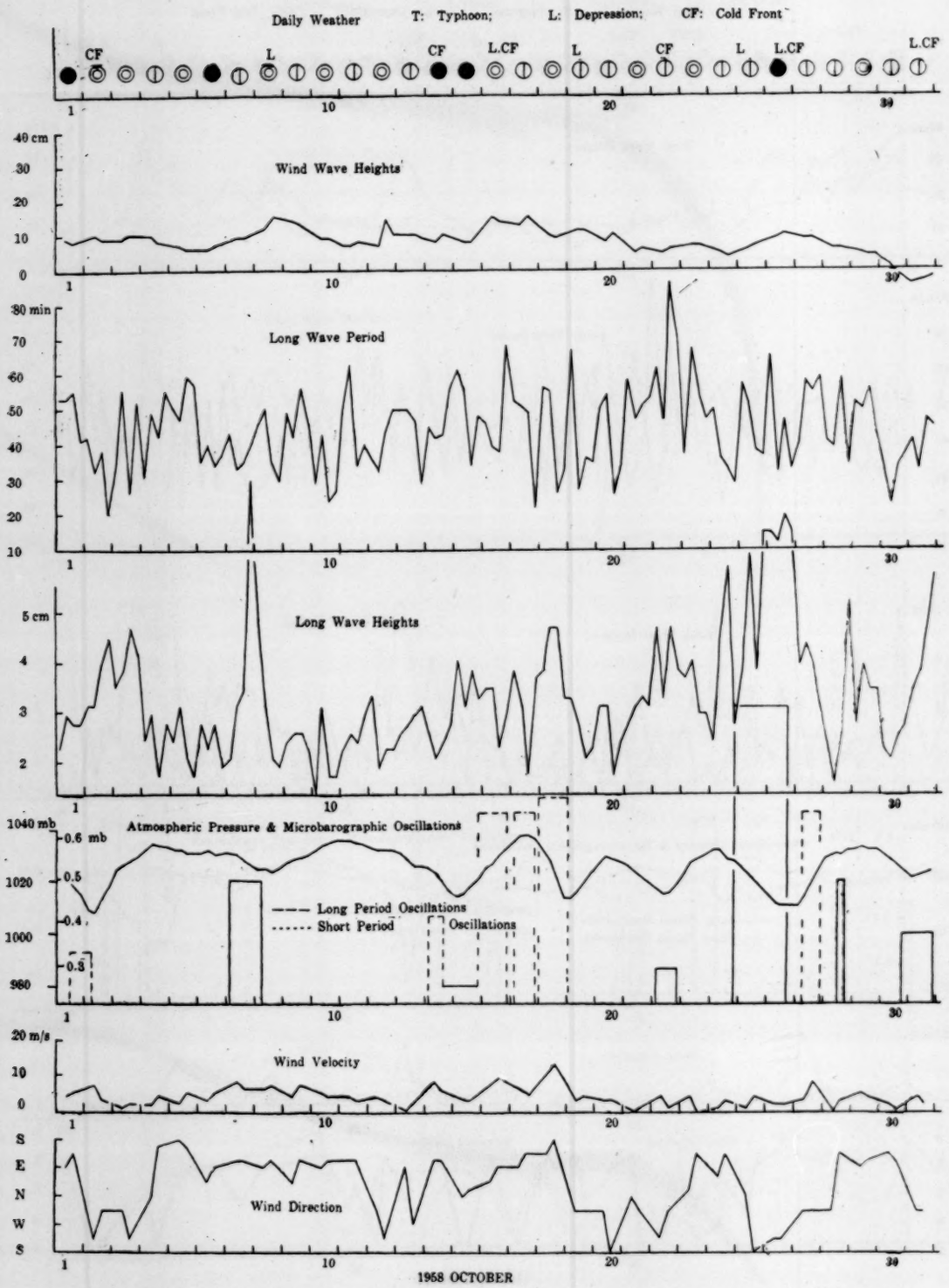

Fig. 25. Summary diagram of Long Period Wave Measurements at Miyagi-Enoshima in October 1958.

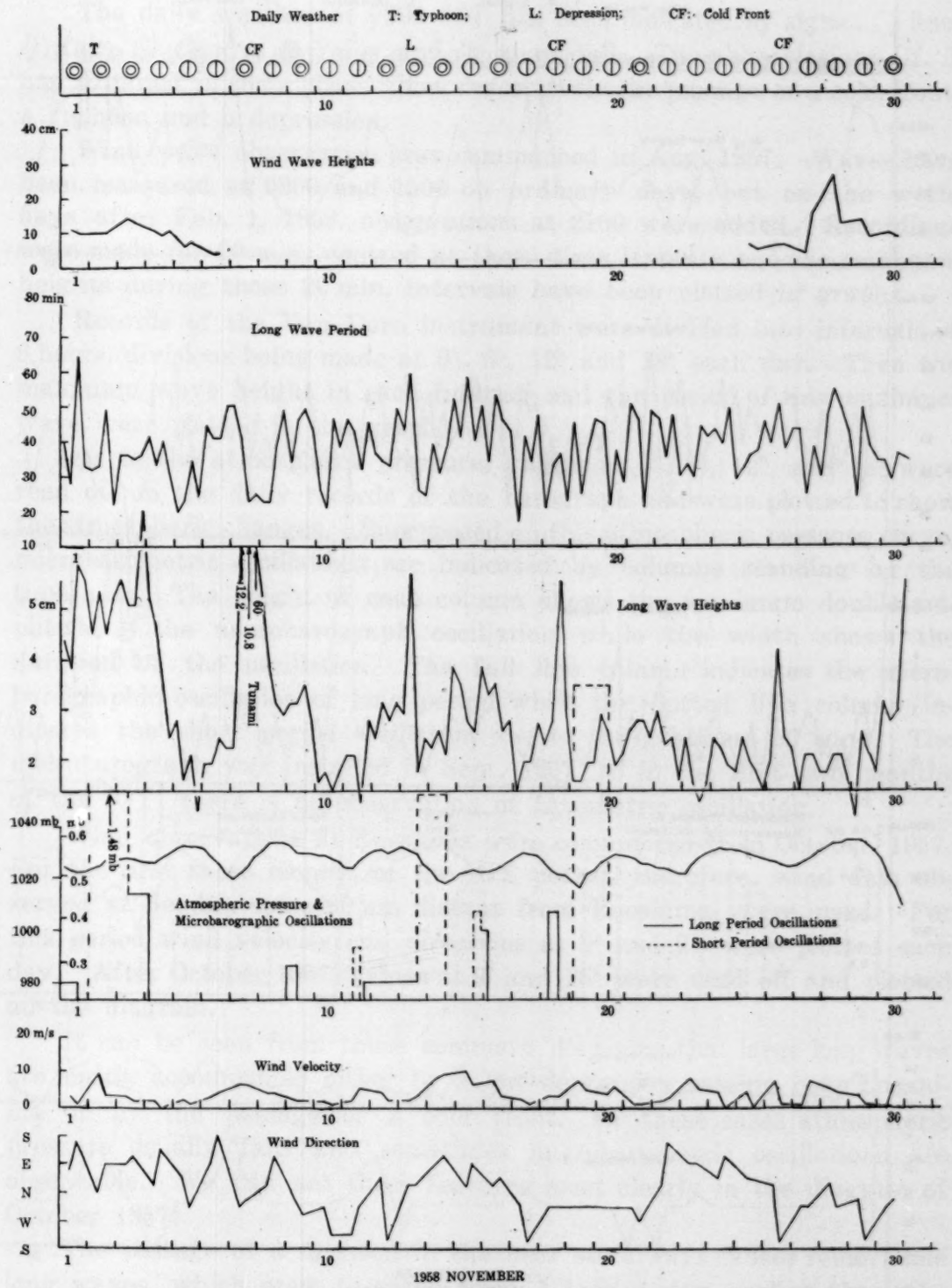

Fig. 26. Summary diagram of Long Period Wave Measurements at Miyagi.Enoshima in November 1958.

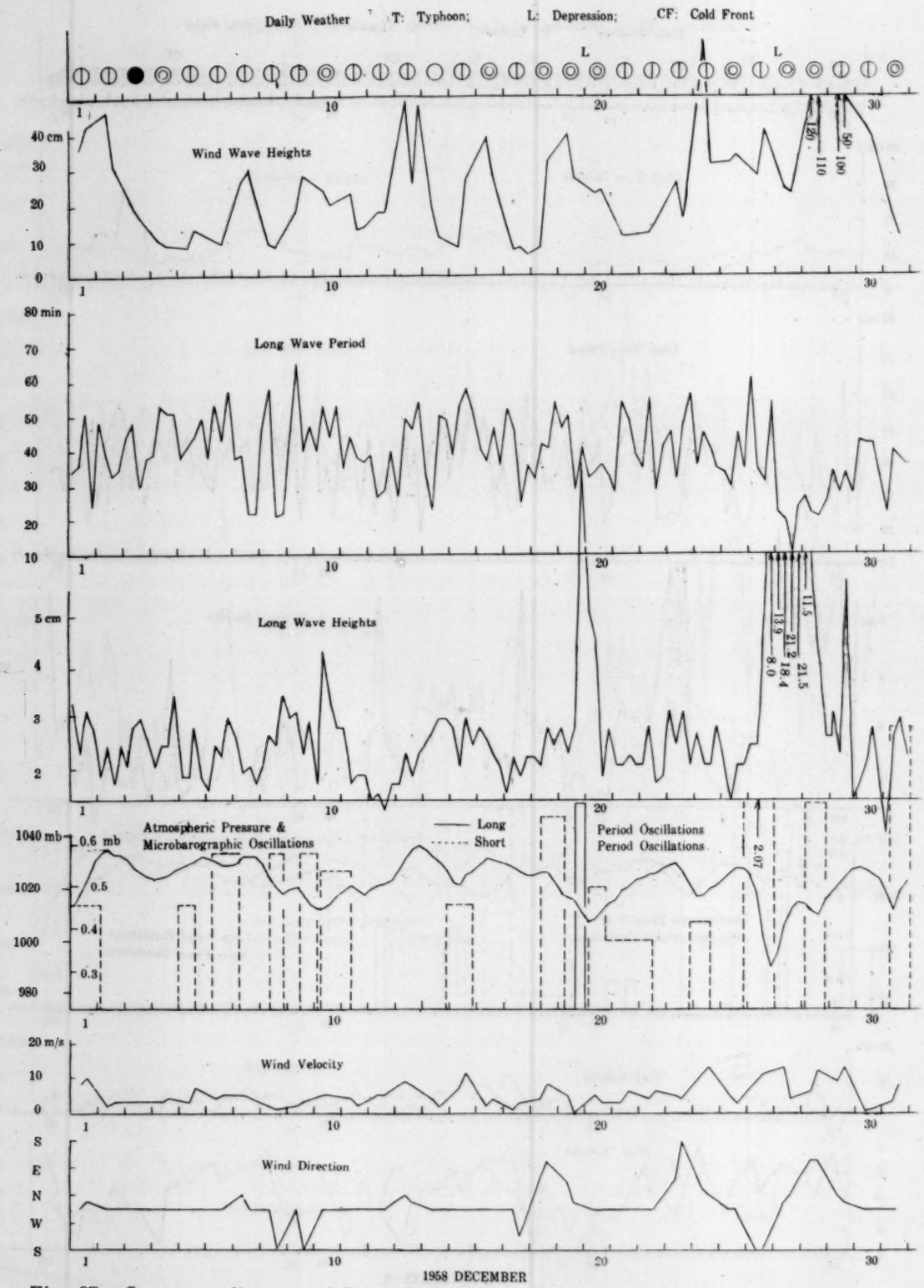

Fig. 27. Summary diagram of Long Period Wave Measurements at Miyagi-Enoshima in December 1958.

The daily weather at 0900 JST has been indicated by signs: ○ fine, ① fair, ◎ cloudy, ● rainy and ⊛ snow fall. The abbreviations Cf. T and L noted in some places show respectively the passage of a cold front, a typhoon and a depression.

Wind wave observation was commenced in Aug. 1957. Waves have been measured at 0900 and 1500 on ordinary days, but on the world days after Feb. 1, 1958, observations at 2100 were added. Recordings were made for 20 min. centred at these time instants and the maximum heights during those 20 min. intervals have been plotted in graphs.

Records of the Van Dorn instrument were divided into intervals of 6 hours, divisions being made at 0^h, 6^h, 12^h and 18^h each day. Then the maximum wave height in each interval and the period of this maximum wave were plotted in the graph.

As to the atmospheric pressure, values at 0^h, 6^h, 12^h, and 18^h were read off on the daily records of the barograph and were plotted to show the atmospheric changes. Superposed on this atmospheric pressure curve, microbarometric oscillations are indicated by columns standing on the time axis. The height of each column shows the maximum double amplitude of the microbarograph oscillation while the width shows the duration of the oscillation. The full line column indicates the microbarographic oscillation of long period while the dotted line column indicates the short period oscillation due to the gustiness of wind. The microbarograph was installed in Sept. 1957, so in the first two months of the IGY, there is no observation of barometric oscillation.

Wind observations at Enoshima were commenced from October, 1957. For the first three months of the IGY period, therefore, wind data observed at Sendai, some 60 km distant from Enoshima, were used. For this period wind velocity and directions at 9^h and 21^h were plotted each day. After October 1957, values at 9^h and 15^h were read off and plotted on the diagram.

It can be seen from these summary diagrams that large long waves are mostly accompanied either by a low depression passing near Enoshima or by the passage of a cold front. In these cases atmospheric pressure usually falls and sometimes microbarometric oscillations are observable. We can see these features most clearly in the diagram of October 1957.

The passage of a typhoon in the near sea always causes remarkable long waves, which seem to occur from 1/2 to 1 day earlier than the full development of ordinary wind waves. Roughly speaking, there is

a general tendency that the development and decay of sea and swell go parallel with long waves, but with a time lag of from 1/2 to 2 days.

There is also a tendency for the period of long waves to decrease with the increase in height. This is probably because meteorological disturbances tend more toward exciting the swell and the short period end of the long wave spectrum than the long period end of the long wave spectrum. The time lag seems merely to be due to the difference in propagation velocity of various waves.

Efforts have been made to identify the nature of these long waves, by installing portable long wave recorders at places 10～20 km. distant from Enoshima, but no decisive result has been obtained. They will probably be either edge waves or seiches inherent to the continental shelf along the Pacific side of Honshu, because we could seldom observe long waves of periods greater than 10 min. at Hachijo Island which stands on a deep ocean floor.

In ending this chapter, the writers wish to express their hearty thanks to Yoji Takahasi, for his devotion to the IGY long wave observations. The writers are also grateful to Dr. W. G. Van Dorn through the courtesy of whom we were able to use the long wave recorders during the IGY period.

---

16. 江の島津波観測所における IGY 期間中の観測

地震研究所 高橋龍太郎 平能金太郎 相田勇 羽鳥徳太郎 清水静子

宮城県女川町の沖合 15 km にある離れ島，江の島で津波の観測を始めたのは，1941 年のことであつた．しかし不幸にして台風の際の激浪のため施設を破壊され，観測は翌 42 年に中止されてしまつた．しかし 1954 年に小規模の観測を復活した．その後 1957 年地球観測年にあたり，わが国における長波観測点に選ばれ，観測計器も充実された．IGY 期間中より現在まで同所で観測を行つている計器は，a) 震研Ⅲ型津波計 b) Van Dorn 型長波計，c) 波浪計，d) 微気圧計，e) その他気象観測計器類である．これらの計器の特性曲線は第 7 図に示してある．

江の島における長波の記録は，平常でも 10～70 分の周期にわたる，海面の実振巾 3 cm 以下程度の波動が見られる．しかし 1958 年 9 月 27 日の狩野川台風，その他の強い低気圧が附近を通過した際は顕著な長波の発達が見られた．又 1958 年 11 月 7 日には，エトロフ島附近の地震による津波を観測した．その記録は第 9 図に示してある．

江の島において，種々な周期の長波が，常に現われるということは，江の島が本州東岸に沿つた陸棚の上に位置していることによると思われる．今この長波の消長と種々な気象的要素との関係を

見るため，江の島で観測した結果を，IGY 期間中の各月毎にまとめて図示したものが第 10～27 図である．これによつて次のようなことがわかつた．長波の振巾は低気圧或いは前線が江の島附近を通過すると大きくなる，殊に台風の通過の際は顕著であり，長波の発達は風浪の発達より 1/2～1日早い．又長波の振巾が増大すると周期が短くなる傾向がある．

なお現地の観測は，高橋湯治氏が種々な困難な事情を克服して，熱心に遂行され，この期間中欠測無しという好成績を挙げられた．ここに特記して謝意を表する次第である．

地震研究所彙報
第39号 (1961) 523-535頁

17. 津波スペクトルの研究

1. ウェーブアナライザーの製作
2. 江の島津波観測所で観測された津波及び常時長波の周期分析
3. 日本各地で観測されたチリ津波の周期分析

地震研究所 高橋龍太郎
相田勇

(昭和36年2月28日発表——昭和36年6月30日受理)

§1. ウェーブアナライザーの製作

津波波形のスペクトル的研究を行うにあたつて，そのフーリェスペクトルを求める方法は種々考えられる．大別して機械的計算機或は電子計算機を使用して数値的に求める方法と，アナログ方式で直ちにスペクトルを図示させる方法とがある．吾々が津波波形の分析を行おうとする場合，後者の方法は精度等の点で劣る所があるにしても，非常に手軽な便利さがある．電気音響関係では，古くから種々の波形分析器が作られているが，吾々がそのまま使用するには，多くは機械的記録器で記録された津波波形を電気量に変換するとか，音響に比して極めて低周波数の津波の，タイムスケールの変換を行うとか，適当な考慮が必要である．

海の波の分析器として作られた物は古くは Dr. M.J. TUCKER によるもの[1]，最近の国内のものとしては，気象研究所降旗常雄氏によるもの[2] 等がある．吾々も数年前，建物の地震時のレスポンスを記録させる，レスポンスアナライザー[3] を製作したが，これに使用したいわゆる記録変換装置を利用して，方式としては Dr. TUCKER のものと同様なウェーブアナライザーを試作した．その後これを使用して見た経験から，改良を行い，昨年 Fig. 1 写真に示すような器械を完成し，これによつて先ず色々な津波の記録の分析を行つて見ることにした．

この器械は前述の記録変換装置と，アナライザー本体とより成つている．長波計，検潮儀等で得られた記録は，適当な方法で潮汐を取り除いて書直し，記録変換装置のドラムに巻付ける．これと同軸に 35 mm フィルムを装填したドラムがあり，これ等を共に極めて

1) M.J. TUCKER, "A Frequency Analyser used in the Study of Ocean Waves", *Nature* **158** (1946), 329.

2) 西田道典・降旗常雄 「スペクトラム計算機 NERIAC-1-F について」電気通信学会雑誌 **42** (1959), 1045.

3) R. TAKAHASI, "A Response Computer. Preliminary Report", *Proceedings of the 3rd Japan NCTAM* (1953), 373.

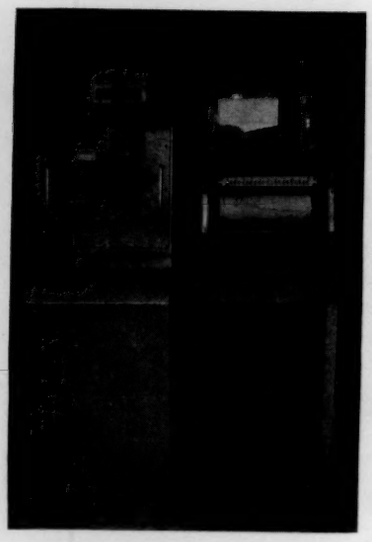

Fig. 1. Wave Analyser.

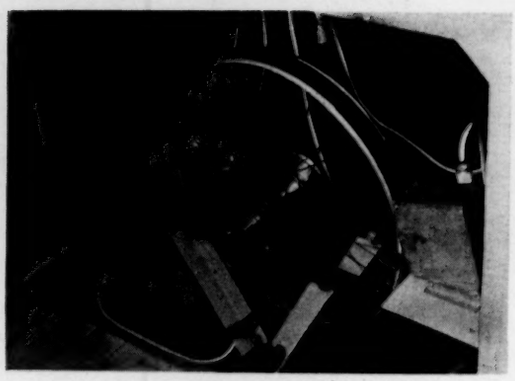

Fig. 2. The mechanism of the film-wheel.

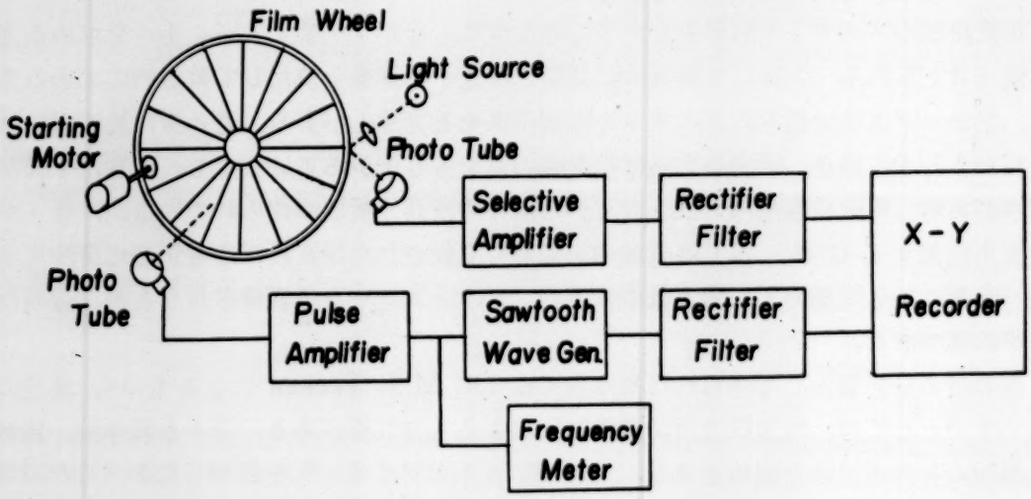

Fig. 3. Block diagram of the wave analyser.

ゆつくりと回転しながら，ドラム上の記録を手で追跡すると，フィルム上に黒白のトーキー録音に似た記録が得られる．これまでが第1段であつて，このフィルム記録を次にアナライザーにかける．アナライザー本体の構成は Fig. 3 に示す．フィルム車輪は，その円周に沿つて鉛の板を巻付けて，慣性を大きくしてあり，その外側にニッケルクローム鍍金の輪がはめてあつて，これが鏡となつている．この鏡面上にフィルム記録を巻付けて，回転させるのであるが，このフィルム面上に直線フィラメントの電球のイメージを投写する．そしてフィルムの記録を透して，鏡面からの反射を光電管で受け，解析する記録に比例した電流変化として取り出すようになつている．光電管の電流は並列 T 型回路を負帰還回路に持つた選択増巾器で増巾し，更に整流沪波されて，X-Y 軸レコーダーの Y 軸に入る．若しフィルム車輪の回転数を種々に変えるならば，フィルム車輪に巻き付けた記

録のタイムスケールを種々に変えることになり，一つの選択周波数を持つた選択増巾器で，種々な周期の成分を取り出すことが出来る．吾々の場合，フィルム車輪は先ず起動電動機で最高速まで回転をあげ，クラッチで電動機を切離すと，車輪の慣性が大きいので車は序々に減速して行く．この減速期間を利用して，各周期成分を取り出すようにしている．これでスペクトルの Y 軸は得られるが，X 軸に解析周期をとらねばならない．これはフィルム車輪の回転数に関係した量であるので，この車輪のスポークを利用して，光源からの光をこのスポークで切り，光電管にパルス電流を流すようにする．このパルスの数は回転数に比例するから，これを電圧変化に直して，X-Y 軸レコーダーの X 軸に入れればよいわけである．この方法は種々考えられるけれども，ここでは鋸歯状波を作つてそれを整流する方法を取つた．

これで吾々は，先ず車輪にフィルムを巻付け，起動電動機のスイッチを入れて車輪を回転させ，最高速に達した所でスイッチを切り，X-Y 軸レコーダーの入力スイッチを入れれば，車輪が減速して行く間に，自動的にスペクトルが得られることになつた．この間の所要時間は約 20 分である．なおフィルム車輪及びそれに附属した機構の写真は Fig. 2 に示してある．

この器械の性能の大要は次の通りである．

フィルム車輪円周	143.3 cm		フィルム車輪回転数	402～40 r.p.m.
選択増巾器周波数	F_0	240～ 及び 120～ 切替		
同　選択度	Q	34　33		
解析範囲	F_0	240～ の時	フィルム記録上の波長	4～40 mm
	F_0	120～ の時	同	8～80 mm

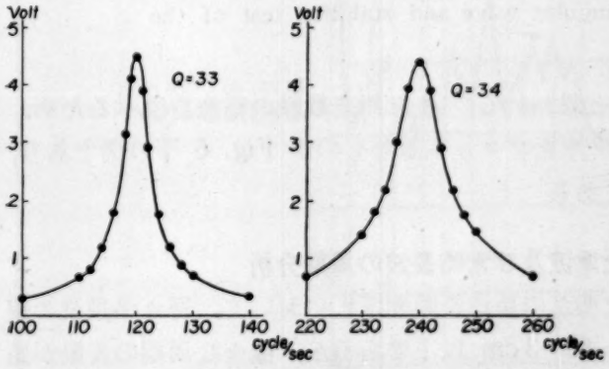

Fig. 4. Frequency characteristics of the selective amplifier.

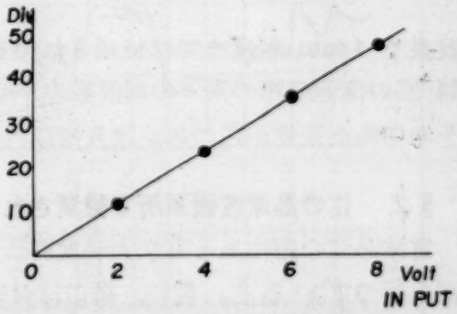

Fig. 5. Linearity of the rectifier.

選択増巾器の特性は Fig. 4 に示してある通りであり，また整流沪波回路の直線性は Fig. 5 に示すようである．

また周期のはつきりした矩形波を解析して見て，理論値と比較すると Fig. 6 上の図のようになる．これは波長 79.6 mm の矩形波の第 3 高調波以上の各高調波のスペクトルが得られているが，高次の高調波でやや誤差が大きくなつて来ているが，フィルム記録上の

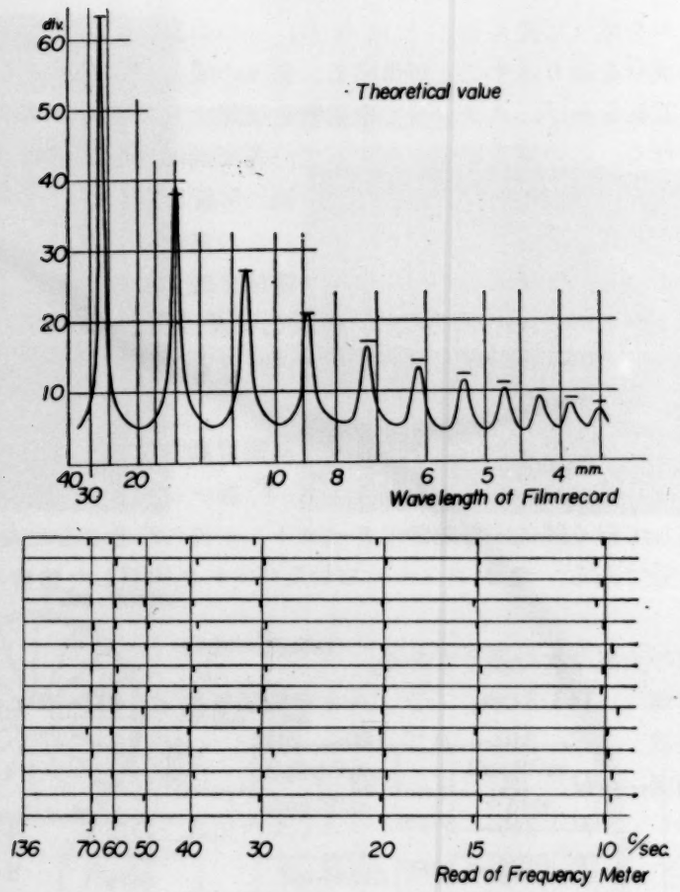

Fig. 6. Spectrum of a rectangular wave and stability test of the frequency axis.

波長で 4 mm 程度までは実用され得ると思われる．また周波数軸の精度を検べるため，14 回の測定の際の夫々の周波数のバラツキをプロットしたものが Fig. 6 下の図であり，予め定めた目盛からのズレは5％以内にある．

§ 2. 江の島津波観測所で観測された津波及び常時長波の周期分析

宮城県江の島にある東京大学地震研究所江の島津波観測所[4] において，吾々が長波の観測を行つてゐると，常に，振巾はせいぜい 3 cm 以下であるが，種々な周期の波動が認められる．この常時あらわれる長波の周期分析をまず行なつた．そのスペクトルは Fig. 7 に示される．これは 1960 年 10 月 12 日 12 時より 10 時間づつ5期間をとり，その各々を解析したものである．この観測は Van Dorn 型長波計で行なつたものであり，その特性の補正をほどこしてある．この結果を見ると，比較的よく似ているものと，あまり似ていないものとがあるが，スペクトルの山はそれぞれに共通した周期があるように見え

4) 地震研究所彙報 **39** (1961), 491.

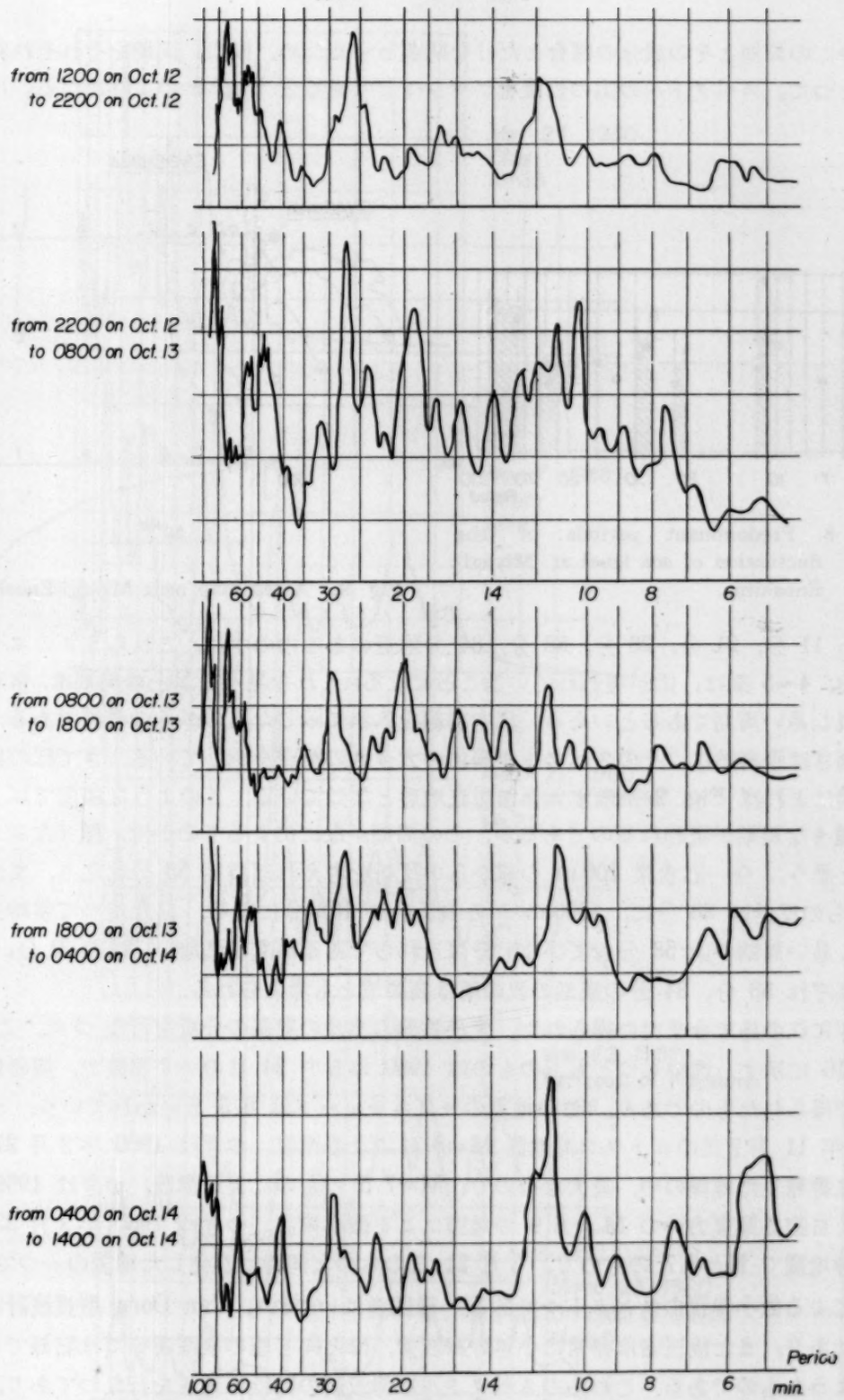

Fig. 7. Spectra of long waves observed at Miyagi-Enoshima on Oct. 12-14, 1960.

る．今この周期とその成分の割合とだけを問題とするため，振巾，周期をそれぞれ対数目盛にとつて，スペクトルの山の位置をプロットして見ると Fig. 8 のようになる。

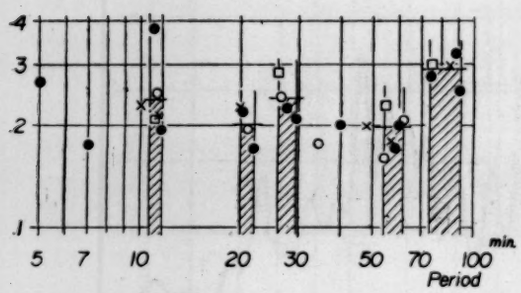

Fig. 8. Predominant periods of the fluctuation of sea level at Miyagi-Enoshima.

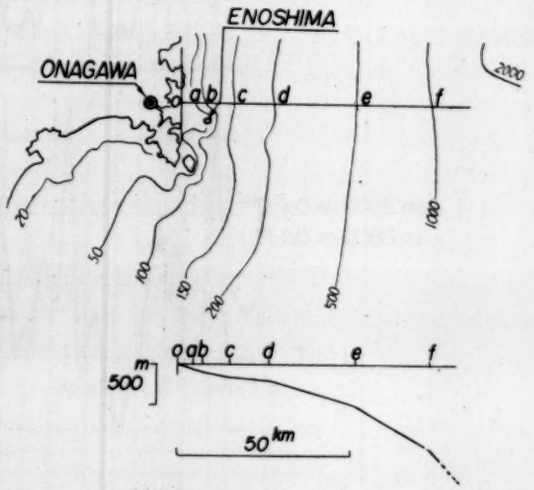

Fig. 9. A sea map near Miyagi-Enoshima.

即ち 11 分，21 分，28 分，58 分，84 分附近のある巾の中に，これら 5 ケのスペクトルの中，4～5 回は，山が現われていることになる，これを見ると以上の周期は，常時長波の出現し易い周期であるといえる．図中斜線を入れて示したものがその帯域である．またこの高さは平均的に，そのスペクトル振巾の大きさの割合を示している．さて江の島附近の海図によれば Fig. 9 に示すような海底地形となつている．このような場所で以上のような種々な周期が現われるのであるが，この周期がなににによるものかは，種々な考え方があると思う．今一応水深 200 m の線からの反射を考えれば周期 58 分になり，また 500 m からの反射は 86 分に，1000 m からの反射は 102 分になる．したがつて常時長波の出現し易い周期の中 58 分および 86 分はこれらであるかもしれない．また 21 分，28 分はそれぞれ 58 分，84 分の周期の波の第 3 高調波とも考えられる．

つぎに江の島で今までに得られた，大小数箇の津波の記録の分析を行なつた．これを Fig. 10 に示す．図中もつとも上のものは 1960 年 5 月 24 日のチリ津波で，震研Ⅲ型津波計で得られたものであり，この地震のマグニチュードは 8.5 といわれている．つぎは 1958 年 11 月 7 日のエトロフ沖地震 M=8.1 による津波，つぎは 1960 年 3 月 21 日三陸沖に群発した地震の中，最大なもので，M=7.5 のものによる津波，つぎは 1959 年 1 月 22 日福島県東方沖の M = 6.9 の地震による微小津波，つぎは 1960 年 3 月 23 日の三陸沖地震で M=6.7 のもので，3 月 21 日のものと同時に群発した地震の一つであり，それによる微小津波のスペクトルである．後四者はいづれも Van Dorn 型長波計による記録であり，また後三者は非常に小さい津波で，ほとんど他の検潮所等では記録できなかつたようなものである．これらのスペクトルは津波計の特性の補正を行なつてあり，解析した記録は前二者は 20 時間，後三者は数時間乃至 10 時間である．なおスペクトルは振

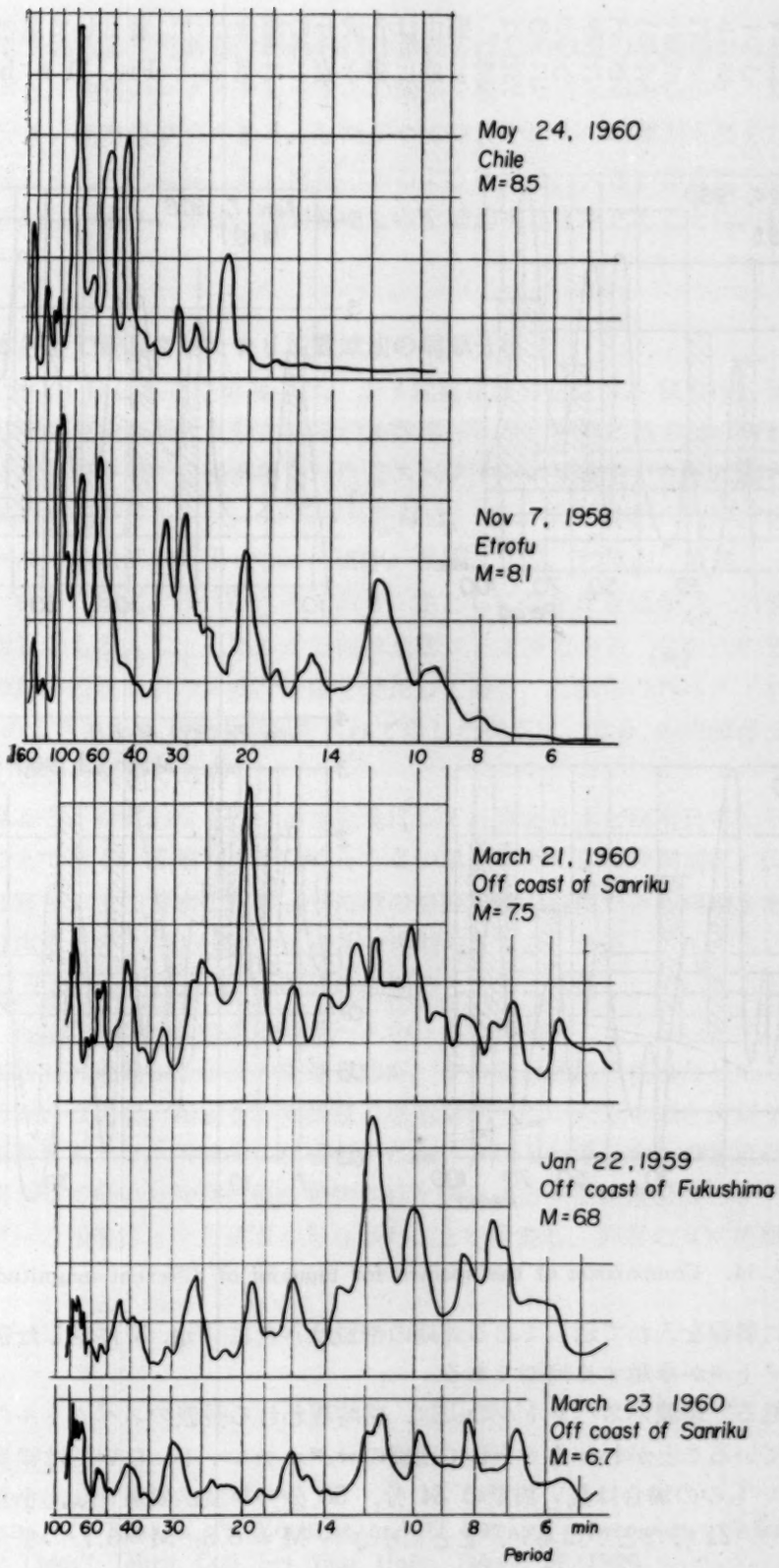

Fig. 10. Spectra of various tsunamis observed of Miyagi-Enoshima.

巾を任意スケールにとつてあるので，振巾は各成分の割合だけに着目して頂きたい．これをもう少しはつきりさせるために対数目盛に書き直して見ると Fig. 11 a, b, c, d のようになる．

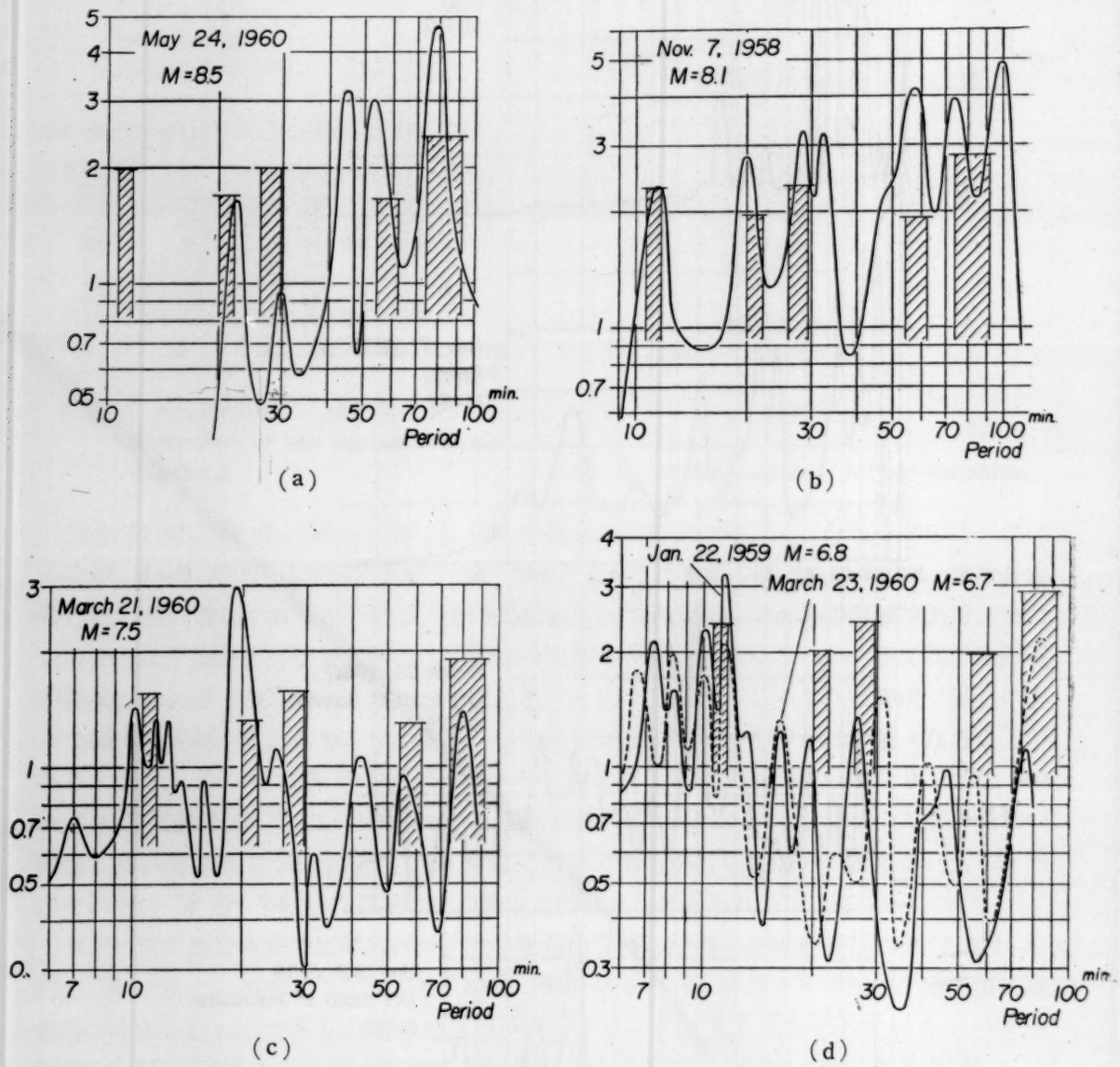

Fig. 11. Comparison of the spectra for tsunami of different magnitudes.

それぞれに斜線を入れて示してある周期の帯域はさきに Fig. 8 に示した常時現われる長波のスペクトルが卓越する周期である．

こうして見ると津波のスペクトルの山は，常時現われる長波のスペクトルの山にかなりよく一致していることがわかる．そして地震のマグニチュード，ひいては津波の規模によつて，大きいものの場合は長い周期の 84 分，58 分の帯域が出易いし，小さい場合は短周期の 28 分，21 分などが出易い．ことに小さい M＝6.8，M＝6.7 の場合は 11 分の

周期がよくでているようである．われわれは津波のはじめの波の半周期から想像される浪源域の大きさと，地震のマグニチュードとの関係を検べたことがあるが[5]．地震のマグニチュードが大きい程浪源域が大きく，したがつて津波そのものの周期も長くなる．したがつて常時長波にそれぞれ卓越し易い周期のあるような場合，大きい津波程その中の長い周期のものを励起し，小さい津波は短周期のものを励起すると考えることは，自然のことであると思う．

§3. 日本各地で観測されたチリ地震津波の周期分析

1960 年5月 26 日日本各地を襲つた，チリ地震津波の記録は，気象庁，国土地理院等を始めとする関係各検潮所で良好な記録が多数得られた．非常に遠方から伝わつてきた津波であり，日本全国各地で記録が得られた点スペクトルの比較を行なうに適当であるので，この記録の解析を行なつた．解析した記録は，北より，網走，八戸，宮古，江の島(宮城)，那珂湊，久里浜，岡田(大島)，清水，鳥羽，下津，和歌山，高知，土佐清水，宇和島，油津，枕崎，富江，の 17 ケ所であり，主として気象庁管理のフース型検潮儀の記録で，他の所管のものも二，三あるが器械は全部フース型である．なお江の島は §2 で述べた本所江の島津波観測所の津波計記録を使用してある．これらのスペクトルを図示すると Fig. 12 のようになる．図中斜線を入れて示した周期は，本多，寺田両博士によつて計算された湾の静振の周期である[6]．

これらを見ると，特徴的なことは清水を境にして，東北日本と西南日本とやや形が異なつて見えることである．各地とも少なくとも2つ以上のたくさんの周期に，山を持つていて，たとえば宮古，土佐清水などのように湾の静振周期で説明できる周期もある．しかしながら東北日本のものは 60～80 分位の長い周期のところに共通して，大きい山が現われており，西南日本のものは，40～50 分の周期のところに共通した山があるように見ることができる．もしこれが，これだけのデータからくる偶然のことでないとすれば，東北日本と西南日本とで，来襲した津波の周期分布が，その通過経路の相違などによつて異なつていたか，あるいは陸棚，海嶺その他長波の卓越周期ともいえるものを決定する要素が，東北日本と西南日本とで，系統的に相違があるということかを示すものと思われる．

最後に使用させて頂いた検潮記録を提供された関係の方々に謝意を表します．また実際にアナライザーの操作は，今泉啓君が行なつたことを附記し，同君の労に感謝の意を表します．

5) 地震研究所談話会 (昭和 35 年1月).
6) K. HONDA, T. TERADA, Y. YOSHIDA and D. ISITANI, "Secondary Undulations of Oceanic Tides", Journ. Coll. Sci. Imp. Univ. Tokyo, **24** (1908).

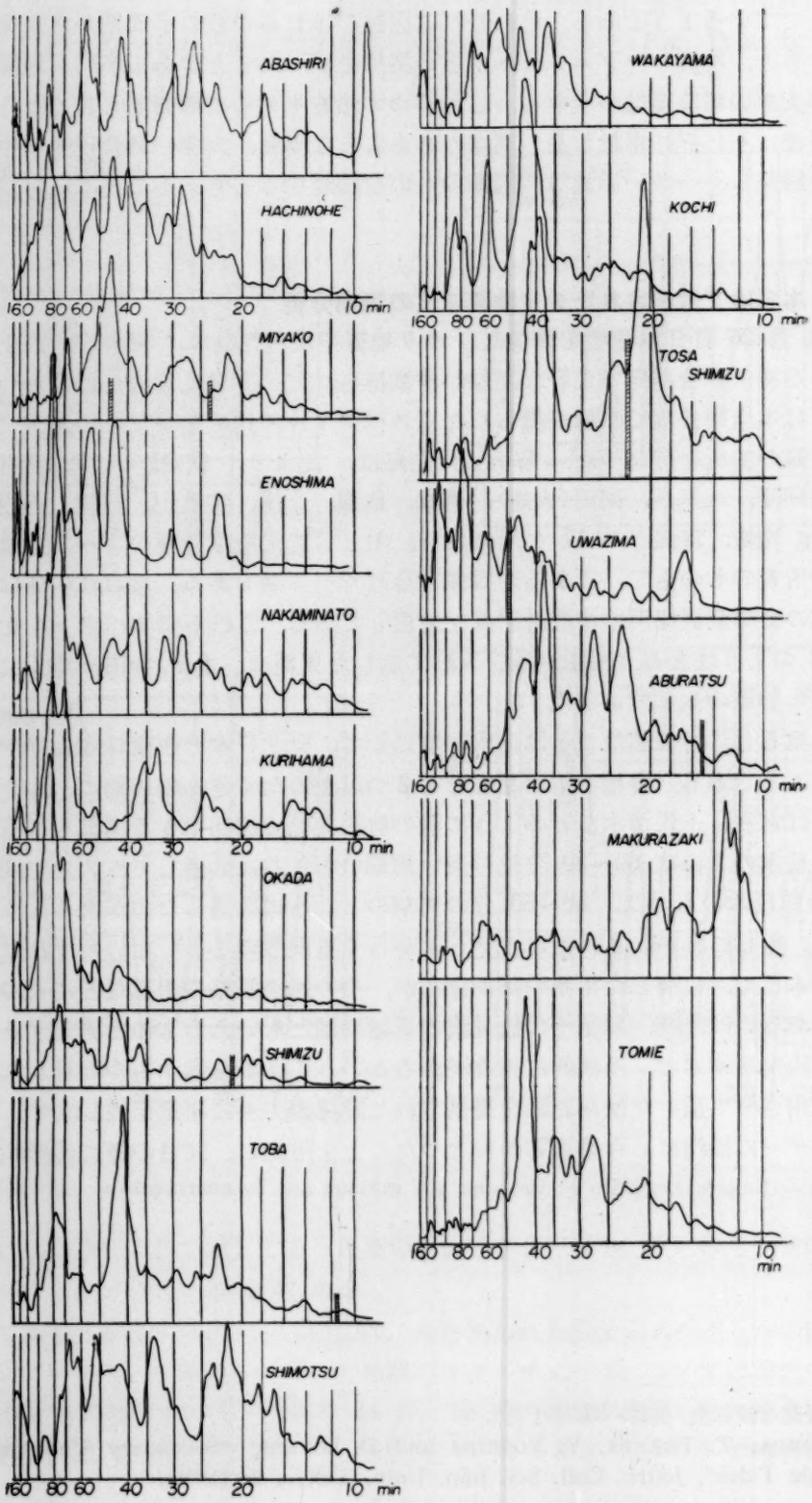

Fig. 12. Spectra of Chilean tsunami observed at Japanese stations.

17. *Studies on the Spectrum of Tsunami.*

By Ryutaro TAKAHASI and Isamu AIDA,

Earthquake Research Institute.

Part 1. Design and Construction of a Wave Analyser.

Several years ago we constructed a wave analyser which is similar in principle with that written by Dr. M.J. Tucker. According to experience gained in the use of this prototype instrument, several modifications were made, and finally the instrument was improved as shown in Fig. 1.

The present analyser is composed of a record transcriber and the analyser proper. A wave record to be analysed is firstly copied on 35 mm film in a similar way to an area-type talkie sound truck. This record film is wound on an inertia wheel as shown in Fig. 2, which has a mirror surface on the periphery. A light beam is thrown on to this wheel and reflected to a photo-cell head by the mirror surface under the record film. The light beam is modulated in this way, when the film wheel rotates.

The output of the photocell is fed to a selective amplifier and then to a filter and rectifier and finally to the Y-axis of a X-Y recorder. So, if the film wheel is rotated at different speeds, different harmonic components of the record will be taken out.

In the present analyser, the film wheel is speeded up first by a small motor and then it is allowed to slow down very gradually by itself. The rotation speed is taken out by the interruption of another light beam thrown to another photo-cell by the spokes of the film wheel. The number of pulses thus obtained is counted by the combination of a pulse amplifier, a saw-tooth wave generator, a filter and a rectifier. The out-put of the rectifier, which is a function of the rotation speed of the film wheel, is fed to the X-axis of the X-Y recorder. We can thus obtain the spectrum of a wave record. The schematic diagram of the analyser is given in Fig. 3.

The characteristic data of the present analyser is as follows:

Peripheral length of the film wheel: 143.3 cm

Rotation speed of the film wheel: 402–40 r.p.m.

Frequency of the selective amplifier F_0: 240 cycles and 120 cycles.

Q-value of the selective amplifier: 34 and 33

Range of analysis:

Wave lengths betw. 4～40 mm on the record film in case $F_0=240$

Wave lengths betw. 8～80 mm on the record film in case $F_0=120$

Part 2. Spectral analysis of Tsunamis and Long Waves observed at the Miyagi-Enoshima Tsunami Observatory.

At the Miyagi-Enoshima Tsunami Observatory, which is attached to the Earthquake Research Institute, long period sea level changes, ranging from 5 min. to more than 100 min. are observed all the time, although the amplitude of these oscillations seldom exceeds 3 cm.

The spectra of these long waves which appear incessantly were first studied. Examples of such spectra are shown in Fig. 7. The spectra correspond respectively to five successive time-intervals of 10 hour length, beginning at 12 h, Oct. 12, 1960. The record of the Van Dorn long wave recorder was used, and results of the analysis are corrected by the sensitivity curve of the Van Dorn instrument. To pay the closest

attention to the predominating frequency, and to their relative intensities, we plotted the positions and heights of the remarkable peaks of the spectra in logarithmic scales as shown in Fig. 8.

By this Figure we can see that in almost all spectra, peaks fall within narrow bands arround 11 min., 21 min., 28 min., 58 min. and 84 min. respectively. This shows that there are several fixed predominant periods in the continual fluctuation of the sea level observed at Miyagi-Enoshima. Their relative intensities are to been seen by the relative height of the peaks plotted in Fig. 8.

To explane the nature of these predominant oscillations we calculated the period of seiche on the continental shelf off Miyagi-Enoshima. The sea bottom topography is shown in Fig. 9. Slight changes are noticeable in the bottom slope at 200 m and 500 m. If a part of long wave energy is reflected at the 200 m depth line, the period of the resulting seiche will be 58 min., while if the wave energy is reflected at the 500 m depth line, seiches of the period of 86 min. will result. These seiches may be the origin of the continual fluctuation at Miyagi-Enoshima. The fluctuation with the periods of 21 min. and 28 min. may be respectively the third harmonics of the seiches cited above.

Secondly we made the analysis of records of tsunamis of different magnitudes that were felt at Miyagi-Enoshima. Results of the analysis are shown in Fig. 10. In the Figure, the uppermost curve is the spectrum of the Chilean Tsunami of 1960. The magnitude of the Chilean earthquake that caused this tsunami has been estimated as 8.5. Other curves are spectra of tsunamis caused respectively (from top to bottom) by the Etorof Earthquake (M=8.1) of Nov. 1958, the Sanriku Earthquake (M=7.5) of March 1960, the Earthquake (M=6.8) off the coast of Fukushima Prefecture, and the other Sanriku Earthquake (M=6.7) of March 1960. Since the ordinate of each spectrum is of an arbitrary scale, we should notice that only the shapes of the spectra are significant. So we plotted these spectra again in a logarithmic scale as shown in Fig. 11a~11d.

Comparing these Figures with Fig. 8, we can find that the peaks in the spectra of tsunami coincide pretty well with the peaks in the spectra of sea level fluctuation at ordinary times; that the predominating peaks fall in the bands of periods of 84 min. and 58 min. when the magnitude of the earthquake and accordingly the magnitude of the tsunami is large, while the peaks of the shorter period of 28 min. and 21 min. are liable to appear when the magnitude of the earthquake is small. Especially when M was as small as 6.8 or 6.7, the shortest period of 11 min. appeared most intensely.

Two years ago, we found that the larger the magnitude of an earthquake, the larger is the size of the origin area of the accompanying tsunami, as estimated from the period of the main part of the tsunami. Accordingly, if there are several dominating periods in the spectrum at ordinary times, it is very natural that large earthquakes will excite the longer part of the ordinary time spectrum and small earthquakes the shorter part of the spectrum.

Part 3. The spectra of tide-gauge records of the Chilean tsunami as obtained at different stations along the Japanese Coast.

In the case of the Chilean tsunami of May 24, 1960, tide-gauge records were obtained at almost all tide-stations along the Pacific Coast of Japan. We made a spectrum analysis of records obtained at 17 stations well distributed from Hokkaido to Kyushu. The tide-gauges at these stations are mostly of the same type. In Fig. 12, the spectra of these records are shown side by side.

It is remarkable that the features of tsunami spectra for NE Japan are different from that for SW Japan. In the former region, spectra seem to have a common large peak in the interval 60~80 min., while in the latter region, spectra seem to show a common peak in the interval 40~50 min. This difference in the spectrum features for the two regions might be attributed to the difference in the paths of propagation or to the difference in the directions of emission of wave energy at the origin. The difference might also be considered to show some systematic difference in the near-shore topographies of the two regions such as trench, continental slope or ridge which can effect the change of shape of the spectrum.

地震研究所彙報
第39号(1961)537—547頁

18. 長岡地震による地盤変動

地震研究所　岡　田　　惇

(昭和36年5月23日発表—昭和36年6月30日受理)

1. まえがき

1961年(昭和36年)2月2日3時29分長岡市内信濃川左岸周辺に発生した地震は，いわゆる局部的な強震で，震央附近は震度5～6を示した．震央の位置はFig. 1およびFig. 2に示す通りで気象庁発表によれば37°27′N，138°49′E震源の深さは約10 kmである．Magnitude (Gutenberg—Richter)は5.0，震央附近半径2～4 kmの地域の農村家屋は強震によつて甚大な被害を生じた[1)2)]．不幸にも現地は日本有数の豪雪地域で，地震発生当時は近年にない大積雪と重なり，地盤の変動あるいは地表面における変化は全く観測できなかつた．したがつて雪解けをまつて1961年5月中旬震央附近の一等水準路線について検測を行ない，地震前国土地理院（旧地理調査所）によつて数回改測された結果[3)]と比較し，昭和2年10月27日発生したほぼ同じ地域の同じ程度の関原地震前後における水準点の垂直変動についても比較した．その結果及び融雪後になつて観測された地表面のfractureなどについて報告する．

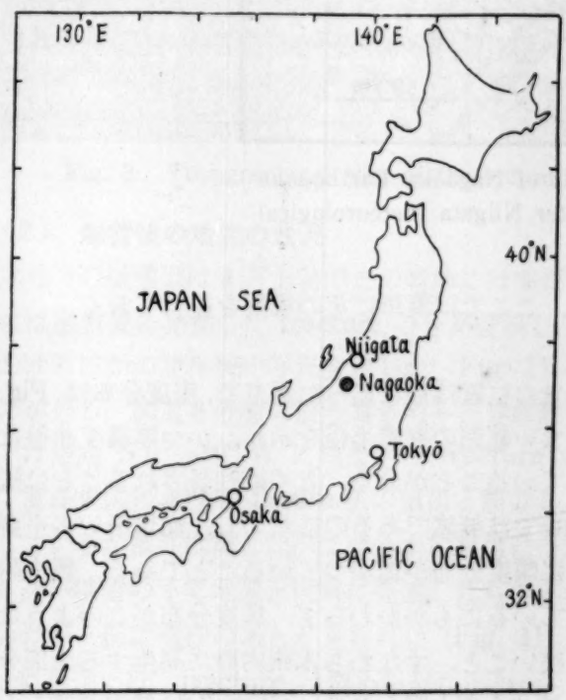

Fig. 1. Location map of Nagaoka Earthquake (1961. 2. 2).

2. 長岡地震の概要

本地震については地震直後に地震研究所河角広教授[4)]，大沢胖助教授[5)]および柴野睦郎技官らによつて一般調査ならびに構造物の被害に関する詳細な報告がなされ，また地震計測は気象庁

1) 気象庁新潟気象台　長岡地震調査概報　1961年2月.
2) 新潟県　長岡地震の状況　昭和36年2月25日調査.
3) 国土地理院　新潟地方地盤調査一，二等水準点成果表　1960年7月.
4) 地震研究所談話会　昭和36年2月28日.
5) 地震研究所談話会　昭和36年3月28日.

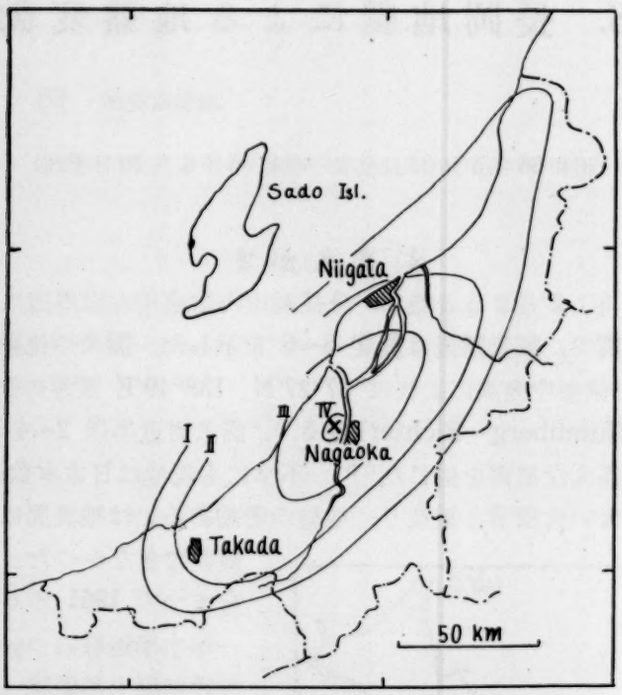

Fig. 2. Isoseismal map of Nagaoka Earthquake Feb. 2nd, 1961 (after Niigata Meteorological observatory).

新潟気象台の調査報告[6] が発表されている．ここでは簡単にその概要を述べておく．

（1） 震央および震度分布

新潟気象台長岡地震調査報告によれば震央の位置は前に述べた通りで，震度分布は Fig. 2 に示した．Fig. 2 によれば限られたせまい範囲の有感半径を示し，かつ等震度曲線は北東より南西にのびる長細い楕円形をなしていることが分る．とくに注目されることは近接した南東部山岳地帯 (Tertiary crop out) では無感であるのにたいし，海岸沿いの平野および丘陵地帯 (Alluvium, Delluvium) に震度分布が拡がつていることである．震央附近では震度 5～6 を示し大きな被害を生じているにもかかわらず，震度分布がこのような拡がりを示していることは，震源が非常に浅いこと，すなわち本州内陸に発生する大部分の浅発性の破壊的地震が示す共通の性質を持つものと思われる． Fig. 3 は被害の著しかつた震央附近の震度分布と地形を示したものである．震央附近の地変は積雪のため観測されなかつたが積雪上の crack が古正寺町附近で幾条か認められたことが報告されている．

6) 気象庁新潟気象台 *loc. cit.* 1)

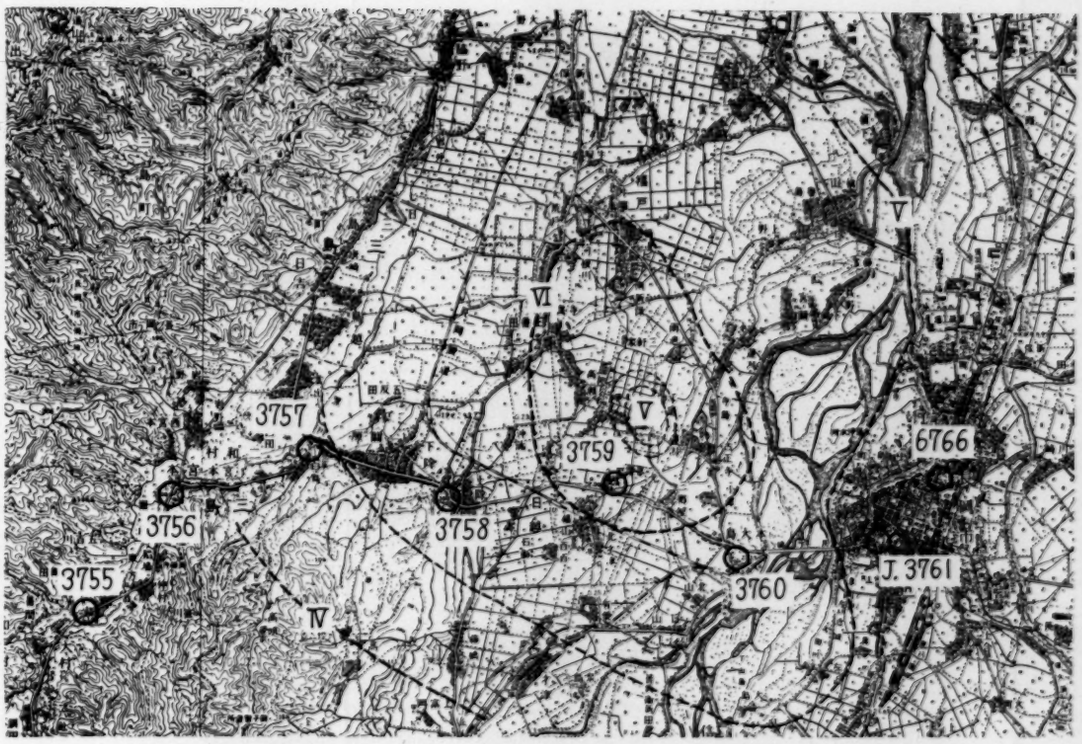

Fig. 3. Topographical map of the epicentral area showing isoseismal lines.

(2) 融雪後の地変の状況

本地方の融雪期は4月上旬でこの時季には田畑を覆つた積雪は全く消えてしまう．Fig. 4 には融雪後に発見した fracture の分布を示し，Figs. 8～11 には当時の様子と5月中旬における田畑の耕作後の写真を示した．Fig. 11 には白い噴砂がかすかに地表に残つているのが分る．国道8号線に沿う喜多町―三津郷屋町間には走向 N60°―70°E，古正寺町北西では走向 N 0°―10° W に幾条かの fracture が主なものである[7]，Figs. 8～10 を見ると丁度泥火山における fissure 状の噴出と類似し，福井地震の場合における噴砂と全く類似しているが福井地震と比べてはるかに規模は小さいようである．これらの fracture は2m近い積雪の下で地震と同時に発生したものと考えられる．5月中旬にはすでに耕されていたが一部に噴砂のあとが見られた (Fig. 11)．前節で述べた地震時における積雪上の crack の下には，fracture は認められなかつた．

3. 地形および地質

長岡市周辺の地勢は信濃川本流が中央背陵山脈より発して北流しながら越後平野に入る附近で東西約 6 km の巾を有する沖積層および洪積層でその厚さはそれぞれ 80～100 m といわれている．この下は新第三期の互層からなり第三期の基盤に達する．新第三期に

7) 新潟気象台，長岡気象通報所々長小黒技官調査による．

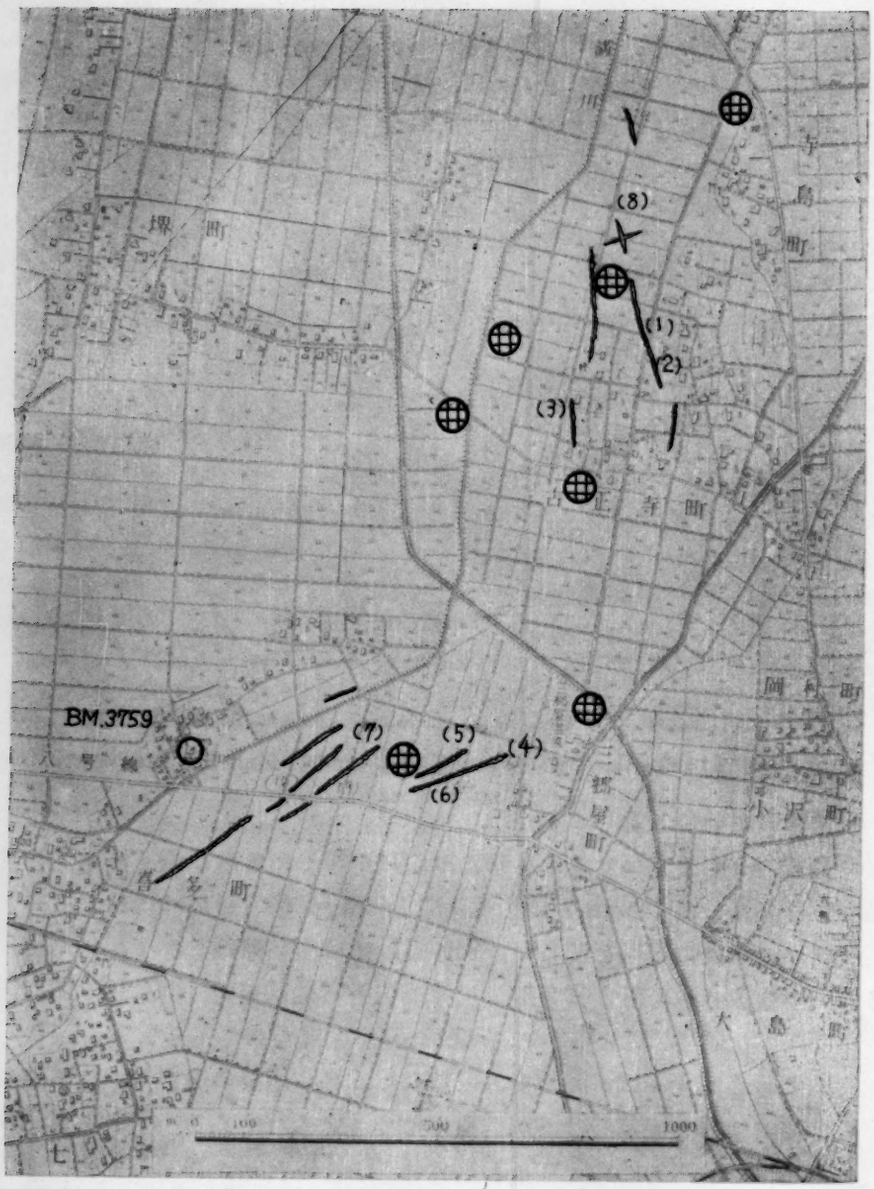

Fig. 4. Fracture zones. (after Nagaoka Weather Reporting Station)

は構造性ガスを含む推谷層，寺泊層が地表より約 1000 m 内外にあつて，この地域は近年構造性ガスの採取が盛んに行われ近代工業都市として発展しつつある．したがつて地質構造も良く調査されているものと思われる． Fig. 5 にはこの地域の地質構造を概観するために地質図の概要を示した．震央附近と推定される沖積層の下部には新第三期の魚沼層，灰爪層，西山層，推谷層，寺泊層が夫々互層し，推谷層より構造性ガスが採取されることからこの附近沖積層下にも背斜構造が認められる．昭和2年 10 月 27 日発生した関原地

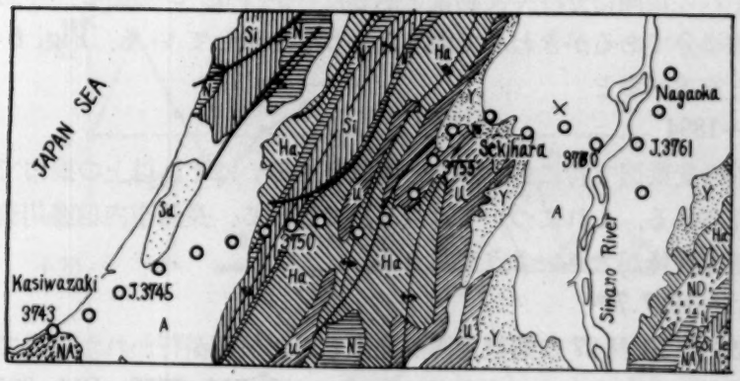

A	Alluvial	Quaternary
Sd	Sand hill	
Y	Yasirota formation	
U	Uonuma bed	Pliocene
Ha	Haizume formation	
ND	Quartz andesite	
N	Nisiyama formation	
Si	Siiya formation	Miocene
Te	Teradomari formation	

Fig. 5. Geological map (after Niigata Prefecture) and levelling route from Kasiwazaki City to Nagaoka City.

震[8] の震央はやや今回の震央に比べて西に偏し，地質図で見られる関原町附近にある背斜軸附近と考えられる．浅発性の地震がこのような地質構造の下で 10 km 以内の浅い所に発生していることは，興味あることで始めにも述べたように，過去の大町地震，関原地震，今市地震，二つ井地震，白石地震なども同型の内陸性の小型破壊地震であると考えられる．

4. 水準点の垂直変動

(1) 震央附近の変動

地震発生から約3ヵ月後の昭和 36 年5月 14 日より 21 日までの間，Fig. 3 に示すような一等水準路線に沿つて検測を行つた．すなわち長岡市 (BM. No. 6766)—宮本町 (BM. No. 3755) まで約 14 km の route について水準点の変動を調べた．使用器械は Zeiss Opton Precise Automatic Level[9] および plane parallel with micrometer と invar staff を用いた．検測の結果は Table 1 および 2 に示してある．この route は過去5回改測が行われていて，関原地震前後における短い期間にも再測があつて良く調べられた所である．前の測定結果と今回の測定を，BM. No. 3749 (中通) を不動として比較し，そ

8) C. TSUBOI, "Investigation on the Deformation of the Earth Crust Found by Precise Geodetic Means" *Japanese Journal of Astronomy and Geophysics*, **10** (1932), 109.

9) 岡田　惇「紀伊半島南端部附近の地殻変動について」地震研究所彙報 **38** (1960), 115.

の結果をそれぞれの期間に分けて変動量を示したのが Fig. 6 である．今回の測定はこの route のうち約半分であるがきわめて顕著なようすを示している．Fig. 6 の変動図から気のついたことを述べると

(a) 1927.7—1894

関原地震以前の変動図で特に目立つことは数粁あるいはそれ以上の振巾で明瞭な上昇あるいは沈降が見られる．これについては（2）で述べる．長岡市内信濃川流域沖積層の最も厚くなる附近で沈降が大きいように見える．

(b) 1927.11—1927.7[10]

1927（昭和2年）10月27日関原地震が発生し直に検測が行われた結果で震央附近の二つの水準点が隆起を示している．変動量は約 2 cm で BM. 3757, BM. 3758 号附近が極大となり両側はほとんど変化がない．この地震の Magnitude は 5.2 である．

(c) 1930～1927.7

1930 年度における広範囲にわたる検測の結果と 1927.7 とを比べたものである．すなわち関原地震の隆起がそのまま残つていてほとんど変化が見られない．

(d) 1955～1930

この長期間の変動図であるが，故障点が多く 1955 年度に新らしく復旧したため旧の測定値との詳しい比較ができない．ただ BM. 3755 より東寄りが関原町附近まで上昇している．

(e) 1958～1955

国土地理院による新潟地方地盤沈下調査の一部として行われたもので約3年間の変動は BM. 3755 を頂点に全く対称的に傾動している．これは興味ある現象で特に 8～9 mm の沈降が B.M. 3759 において認められる．

(f) 1961.5—1958

今回の長岡地震による変動の結果で (e) に示した BM. 3759 の沈降部が相対的に約 5 cm の上昇をした．BM. 3759 は震央地域に最も近い所に位置し Fig. 4 に示したような fracture zone にも近接していることから，震央附近にほぼ同程度あるいはそれ以上の隆起が行なわれたと推定される．上昇地域の範囲は限られていて震央より 2～3 km より遠くには及ばないようである．

以上の観点からそれぞれの期間を綜合して考へると BM. 3755 より西方の小さい起伏は地震活動とは直接関係しているようには見えない．なぜならば BM. 3749 ～ BM. 3755 間の相対変動量は微少で関原および長岡地震に関係する地域の変動ははるかに大きくて判別することができる．

（2） 柏崎—長岡間における垂直変動

Fig. 7 は 1894 年の測量に refer した 1927.7, 1930, 1955, 1958 年の結果を BM. 3742

10) C. TSUBOI, *loc. cit.* 8)

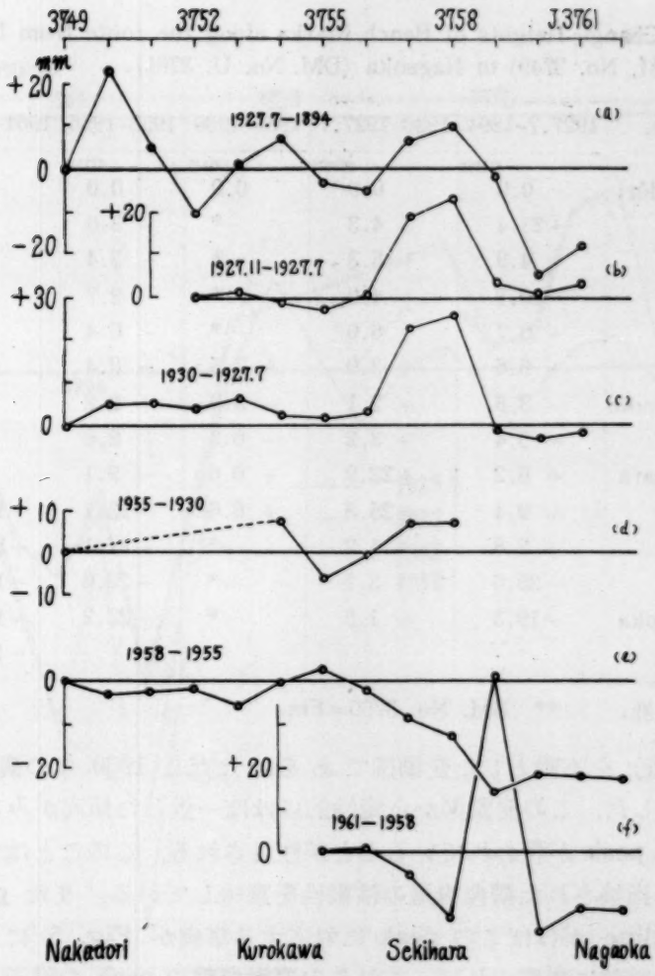

Fig. 6. Change of heights of bench marks in the neighbourhood of Sekihara and Nagaoka earthquake.

Table 1. Results of the Levelling Survey

BM. No.	Loc.	1955*	1958*	1961
		m	m	**
3755	Miyamoto	41,9811	41,9297	41,9297
3756		33,6551	33,5989	33,5996
3757	Sekihara	29,0299	28,9672	28,9607
3758		37,3920	37,3253	37,3102
3759	Kita	22,3154	22,2347	22,2744
3760		23,0264	22,9502	22,9316
J 3761	Nagaoka	21,4049	21,3281	21,3152
6766		——	20,5048	20,4912

* GSI の成果より　　** 1958 の結果を不動と仮定

Table 2. Change Heights of Bench Marks along the route from Nakadôri (BM. No. 3749) to Nagaoka (DM. No. U. 3761).

BM. No.	Loc.	1927.7–1894	1930–1927.7	1955–1930	1958–1955	1961–1958	Remark
		mm	mm	mm	mm	mm	
3749	Nakadôri	0.0	0.0	0.0	0.0		Assum.
3750		+23.4	+ 4.3	—*	− 3.6		
3751		+ 4.9	+ 5.3	—*	− 3.4		
3752		−10.1	+ 4.0	—*	− 2.7		
3753		+ 0.7	+ 6.0	—*	− 6.4		
3754		+ 6.5	+ 3.0	+ 7.5	− 0.4		
3755	Miyamoto	− 3.8	+ 2.1	− 5.9	+ 2.2	0.0**	
3756		− 5.4	+ 3.2	− 0.3	− 2.6	+ 0.7	
3757	Sekihara	+ 6.2	+22.9	+ 6.6	− 9.1	− 6.5	
3758		+ 9.4	+25.8	+ 6.6	−13.1	−15.1	
3759	Kita	− 2.8	− 1.2	—*	−27.1	+39.7	
3760		−25.6	− 3.1	—*	−22.6	−18.7	
J. 3761	Nagaoka	−19.5	− 1.5	—*	−23.2	−12.9	
6766						−13.6	

* 1955 移転改埋. ** BM. No. 3755=Fix.

(柏崎西方鯨波附近) を不動とした変動図である. ただし 1930 年の観測は柏崎市 BM. J. 3745 に refer した. この変動図から定性的にほぼ一致した傾向がみられる. すなわちある一定の波長で peak が現われていることが注目される. このことはすでに山崎, 大塚両博士[11]によつて指摘された褶曲構造の活動性を意味している. また geology の詳しい知識からも anticline がほぼこの peak に対応する事実が Fig. 5 によつても証明される. また一方地形学的に考察すれば, これらの変動曲線の peak の附近には日本海々岸に平行に走る mountain ridge にも対応し, 長岡地震の震央附近にも, 南方来迎寺附近で沖積層に没する ridge の延長を考えることができる.

活動褶曲については秋田県米代川流域, 山形県小国川流域, 新潟県小千谷市周辺で更に細かく Bench Mark を設置して研究を進めているので変動の様子はもつと短い波長で分ることと思う[12][13].

5. 結果の考察

昭和 8 年 9 月 21 日能登地震による変動, 大町地震 (1918.11.11)[14], 関原地震 (1927.

11) 大塚弥之助 地質構造とその研究 昭和 27 年.
12) 「活動褶曲に関する研究の概要」 地震研究所 1956 年 1 月.
13) 宮村摂三・岡田 惇 「米代川にそう一部水準路線の測量(第 3 報)」—1955 年 10 月 19 日二ツ井地震にともなう水準変動—地震研究所彙報 **34** (1956).
14) 大森房吉 「大正 7 年信州大町地方激震調査報告 (第二回)」「松本糸魚川ならびに糸魚川輪島間地盤垂直変動」震災予防調査会報告第 98 号.

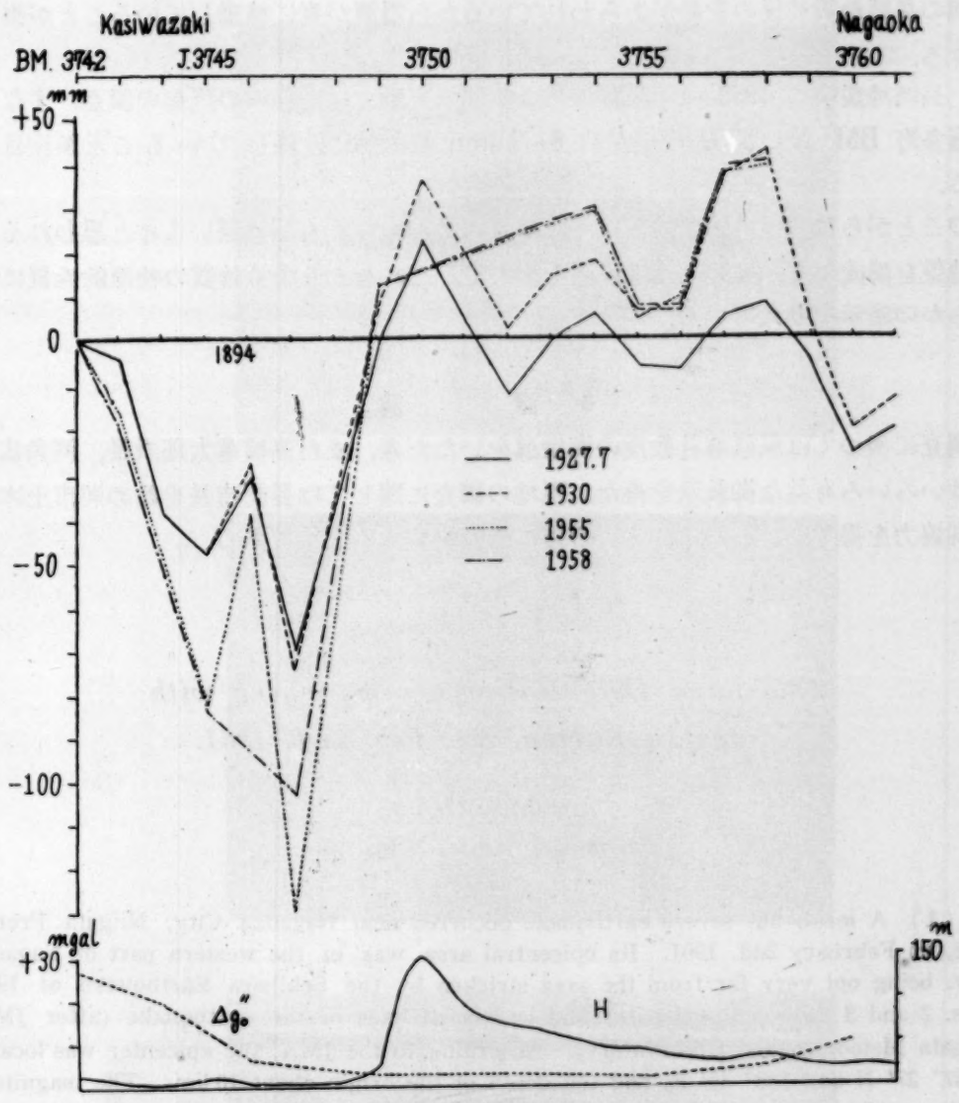

Fig. 7. Vertical displacement of Bench Marks along the route from Kasiwazaki City to Nagaoka City.

10.27)[15]，今市地震 (1949.12.26)[16]いずれも同様の隆起変動を生じた局部的な，いわゆる内陸型の小型破壊地震と考えられ，これらの地震は発生した場所の地理的分布には規則性はないが発生の機構には共通したものが，本調査の垂直変動の調査結果を加へて更に強く感じられる．

長岡地震による水準点の垂直変位から

1) 1927 年関原地震前後の水準点の垂直変動の peak より約 2～3 km 東にずれて今

15) C. TSUBOI, *loc. cit.* 8)

16) 地理調査所「一等水準点検測成果集録」第1巻 昭和 30 年.

回の長岡地震前後の変動があらわれているから震源が東に移動していることが推定できる.

2) 長岡地震前の 1958—1955 年の約3年間の変動では，今回の隆起の頂点，すなわち喜多町 BM. No. 3759 附近が約 8～9 mm 相対的に沈降していることが注目される.

以上のことがらは震源の物理的性状と，地質構造の上で最も関係深いことと思われる．同様に地殻を構成する，換言すれば震源を含めて，これをとりまく物質の物理的性質について何らかの暗示を与えている.

6. 謝 辞

本調査に当つては萩原尊礼教授の御指導をいただき，また高橋竜太郎所長，河角広教授からはいろいろ有益な御教示を得た．現地の調査に関しては長岡市長を始め同市土木課諸氏の御協力を得た．ここにそれぞれの方に謝意を表する次第である.

18. Land Deformation accompanying with Nagaoka Earthquake, Feb. 2nd, 1961.

By Atusi OKADA,
Earthquake Research Institute.

(1) A local, but severe earthquake occurred near Nagaoka City, Niigata Prefecture, on February 2nd, 1961. Its epicentral area was in the western part of Nagaoka City, being not very far from the area stricken by the Sekihara Earthquake of 1927. Figs. 2 and 3 show the epicenter and isoseismal lines of the earthquake (after JMA, Niigata Meteorological Observatory). According to the JMA, the epicenter was located at 37° 27′ N and 138° 49′ E, and the depth of the origin about 10 km. The magnitude of the earthquake was 5.0. (Gutenberg—Richter)

Damage was sustained in a small area within about 2—4 km radius in the vicinity of the epicenter. As the stricken district was deeply covered with snow, any topographical change such as earthquake fault and fracture in the ground could not be found there at that time. In order to determine the crustal movement, if any, of the epicentral area, the writer carried out in May, 1961, a 1st order precise levelling resurvey along the route in the area. (Fig. 3)

This report presents the results of the levelling resurvey and shows the vertical change of the ground in the past sixty years by comparing the results with old data given by the GSI. It refers to the active folds mentioned before as being revealed in the level change along the route from Nagaoka to Kasiwazaki.

(2) According to Prof. H. Kawasumi and others, who inspected the stricken area immediatly after the earthquake, the earthquake shocks were felt in an area only about 50 km in radius, in Niigata Prefecture and mainly in the Quaternary terrane near the

(1)

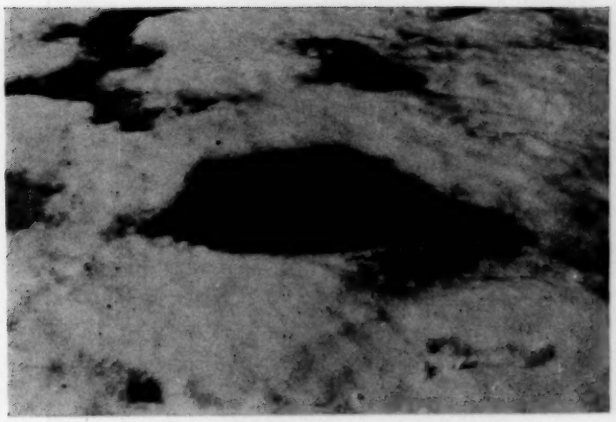

(2)

(3)

Fig. 8. Fractures, location showed in Fig. 4 (Photo by Mr. Koguro).

（震研彙報 第三十九号 図版 岡田）

(4)

(5)

(6)

Fig. 9. Fractures, location showed in Fig. 4 (Photo by Mr. Koguro).

(震研彙報 第三十九号 図版 岡田)

(7)

(8)

Fig. 10. Fractures, location showed in Fig. 4 (Photo by Mr. Koguro)

(9)

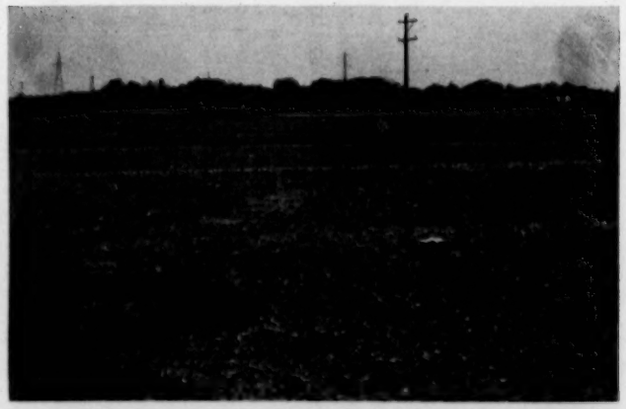

(10)

Fig. 11. View of fractured area on May 18th.

shore of the Japan Sea, and they were not felt in the eastern mountainous area bounded by the Tertiary zone. Thus the isoseismal lines described ellipsoidal form with the major axis in a NE-SW direction. In spite of the relative narrowness of the affected area, the earthquake near its epicenter was 5—6 in intensity, the sudden attenuation of the isoseismal distribution being perphaps due to the shallow depth of the earthquake origin as is usual in most cases of the inland destructive earthquakes of Japan. Intensity distribution in the epicentral area is shown in Fig. 3. About two months after the earthquake, when the ground of the stricken area had been completely exposed to view after the thaw, we found many fractures in the ground as in Fig. 4 and Figs. 8—11. On Highway No. 8, between Kita-town and Mitugoya-town, the general strike of the fractures was N 60°—70° E, in Kosyôji-town it was about N 0°—10° W. Some of these fractures were attended by small cones and spouts formed of sand and mud, just like mud volcanoes. These cones and spouts showed that they had been formed by spouting of mud and sand with the water from underground water layers about 5—20 meters beneath, at the time of the earthquake.

(3) The route along which the writer carried out the levelling resurvey in May 14th—21th, is about 14 km distance from Nagaoka to Miyamoto (BM. No. 3755—6766). The levelling of this route was carried out at six previous times by GSI that is in 1894, 1927.7, 1927.11, 1930, 1955, and 1958. Fig. 6 shows the vertical displacement of the bench marks during successive time intervals the BM. No. 3749 being assumed to be fixed. Of the remarkable features shown in the diagrams, the following may be mentioned.

1) The vertical change in height of the bench marks along the route from No. 3749 to No. 6766 during the period 1958—1955, shows a general subsidence to the east. The BM. No. 3759 shows a little extra depression (8—9 mm) than other bench marks.
2) In the period in which the present earthquake occurred, the general subsidence was still going on, but remarkable uplift took place at the BM. No. 3759, possibly in conversion with the earthquake.
3) The BM. No. 3759 is closest in distance to the presumed epicenter, and the upheaved area is considered to be about 2—3 km in radius.

Vertical displacement of the bench marks from Kasiwazaki to Nagaoka is shown in Fig. 7. The curves in the figure are drawn using the survey in 1894 as a comparative base and the BM. No. 3742 as fixed. It is remarkable that the displacement took place in the same way and with an undulation of almost constant wave length in the successive periods.

地震研究所彙報
第39号 (1991) 549-559頁

19. 昭和36年2月2日長岡地震の家屋被害について

地震研究所　大沢　胖
東京大学工学部建築学教室　山本正勝

(昭和36年3月28日および4月25日発表——昭和36年6月30日受理)

1. 緒　言

昭和 36 年2月2日午前3時 39 分，長岡市西部におこつた地震は，同地域にかなり大きな被害をもたらし，全壊家屋259戸，死傷者 35 名におよんだ．

筆者らは，東京大学工学部建築学教室の大学院学生9名の援助をえて，2月 13 日より約1週間にわたり，主として家屋の被害調査を行なつた．たまたま長岡地区は大雪のあつた後で震害地の積雪は 2m に近く，さらに調査期間中はおおむね雪が降りつづくという悪条件下であつたが，長岡市役所よりいろいろ便宜をはかつて頂いたおかげで，無事調査を行なうことができた．

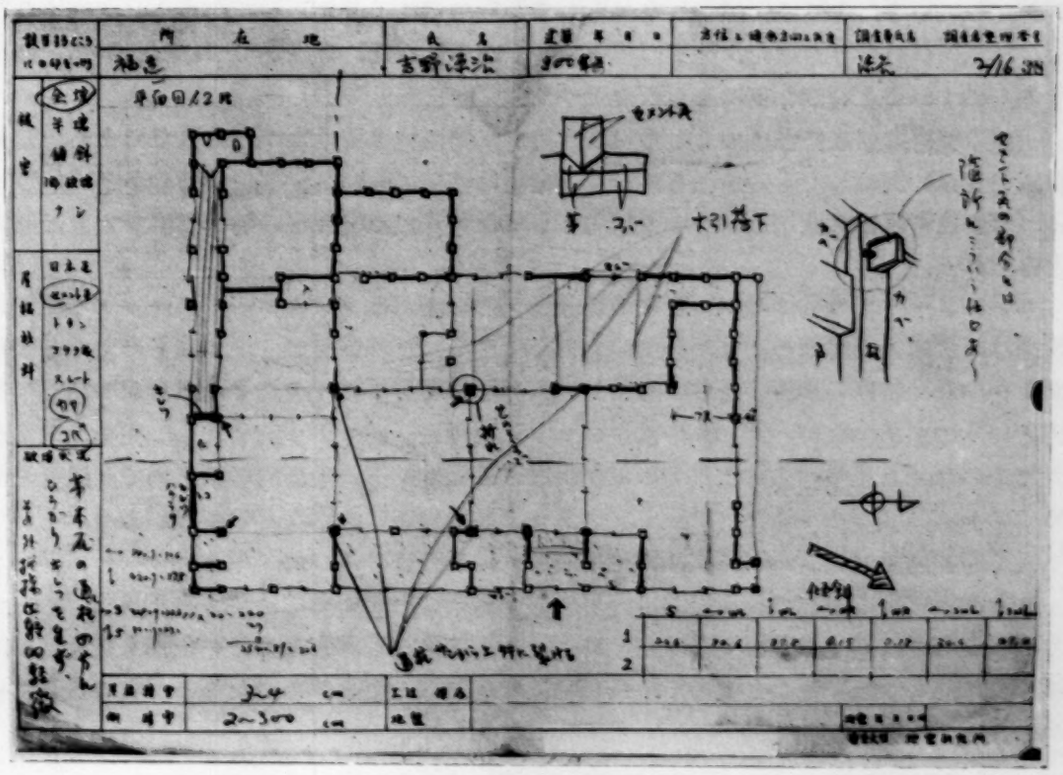

第1図　家屋震害調査票

調査のおもな対象は，被害のもつともはげしかつた6つの町（古正寺・寺宝・王番田・福道・南新保・高瀬）の住家で，その大部分（306戸中207戸）について戸別調査を行なつた．その要領は，第1図に示す所定の調査票に，被害状況，平面図，主要柱・梁の寸法，壁の配置，積雪状況などを書きこむこととした．

ここには，長岡地震における建物被害の概要，およびこの調査票を集計して得られた，住家の被害詳細，被害と壁率・建築年代・積雪との関係，推定作用震度などについて報告する．

2. 建物被害の概況

第1表に主として家屋被害の概要を，また第2図に住家の被害分布図を示す．これらの数字は長岡市役所より発表されたものである．図に見るように，被害が大きかつたのは長岡市西部信濃川沿いの直径約3kmの地域で，南新保・高瀬・古正寺・寺宝の各町では，全壊率50%以上という大被害をうけている．

この地域は長岡市内といつてもいわゆる市街地ではなく，住家は農家が大部分である．したがつて木造建物がほとんど大多数で，鉄筋コンクリート造などほかの種類の構造物はきわめてわずかであつた．

木造建物のうち住家の被害で致命的なのは2階の倒壊したもので，そのため多くの死傷者をだしている．1階は大傾斜しながらもまわりの雪によりかかつてかろうじて倒壊をまぬがれた例がかなりあつた．従来の震害報告にあるような，1階がつぶれて2階がそのまま地上にすわるといつた例はみられなかつた．

土蔵の被害は住家ほど詳しくしらべてないが，特に大きくはなかつたようである．農業倉庫で完全に倒壊したものがあるが，この建物は住家に較べて屋根に積雪の多かつたこと，倉庫内の米俵が壁に崩れかかり横力として作用したことなどの特殊事情が大きな原因とみられる．

コンクリートブロック造および腰の部分を大谷石またはコンクリートブロックで積んだ構造は，倉庫・納屋などに使われているのが若干あつた程度だが，いずれもほとんど被害がなかつた．住家の被害のもつとも著しい高瀬町にあるブロック造2階建倉庫で全く無被害というのがあつたが，20cmの重量ブロックを用い，がりようをまわし，完全な耐震設計施工の建物と見受けられた．そのほかかなり激震地に近い大島町の某工場で，鉄骨造倉庫のブレースのボルト切断，鉄筋コンクリート架台のひびわれなどの被害があり，そのすぐ近くの鉄筋コンクリート壁式4階建アパートは無被害であつた．

なお被害状況で特色のあるのは，各町により家屋の倒壊または傾斜方向が異なつており，福道町では南，寺宝町・高瀬町では東，古正寺町では西となつていずれも被災地のほぼ中心に向かつていることである．長野地震でも同様の現象があつたことが報告されている[1]．

---

1) 金井 清「昭和16年7月15日長野地震の家屋被害に就て」地震研究所彙報 **19** (1941), 647.

第1表　町別震災被害状況

町名	総世帯数	住家						非住家			死者	傷者
		総戸数	全壊	半壊	小壊	被害戸数	全壊率(%)	全壊	半壊	小壊		
古正寺町	56	53	28	25	0	53	53	1	0	0	1	12
寺宝町	28	27	14	13	0	27	52	2	1	2	0	8
王番田町	79	79	20	33	26	79	25	7	4	7	0	4
寺島町	18	15	5	10	0	15	33	0	0	0	0	0
福道町	89	88	42	43	3	88	48	5	0	0	4	3
南新保町	13	12	8	4	0	12	67	2	0	1	0	0
堺町	82	—	19	51	10	80	23	15	5	0	0	0
宝地町	42	—	10	25	6	41	24	4	11	0	0	1
福戸町	22	—	3	19	0	22	14	1	2	2	0	0
雨池町	35	35	7	14	4	25	28	0	0	0	0	0
高瀬町	48	47	28	19	0	47	60	0	0	0	0	0
喜多町	70	—	1	56	13	70	1	2	0	2	0	1
河根川町	63	62	5	21	36	62	8	0	0	0	0	0
蓮潟町	64	—	14	40	5	59	22	0	0	0	0	0
その他	—	—	16	95	494	1289	—	0	5	3	0	1
計	—	—	220	465	804	1489	—	39	28	17	5	30

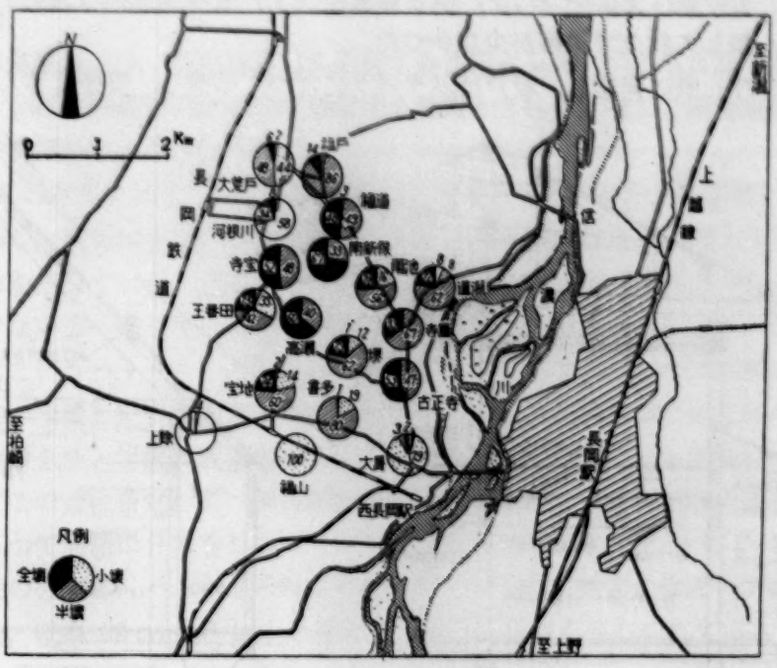

第2図　住家被害分布図

3.　住家被害の詳細

住家の構造と耐震性

この地方の住家はおおむね木造2階建で，屋根ふき材により，瓦ぶき（セメント瓦または日本瓦）かやぶきその他とわかれるが，過半数は瓦ぶき，ついでかやぶきが多い．第3図に瓦ぶきとかやぶきの骨組詳細図，第4図に1階標準平面図を示す．間取りはどの家も大同小異で標準平面とあまりかわらない．2階は4間×6間またはそれに近い大きさのものが大部分で，特に間仕切りをせず物置または納屋に使用しているといつた家が多かつた．

耐震的な面からこの構造をみると，まず1階は寄付・茶ノ間・座敷などの間仕切りがすべて戸障子の類で，それらを取り払えばすぐ大広間ができるようになつており，力になる壁の類が少なくかつ偏在している．これは2階も同様である．また多雪地域のせいで小屋材が太く屋根部分が重くなつている．さらに筋かいを用いた家がほとんどみられなかつた．これらの悪条件が地震の被害を大きくしたものと思われる．

被害詳細

被害の詳細は，写真（第 9—20 図）にもみられるように，

柱　　2階床上または1階差し下で折れるかさけるかしている．

梁　　柱との接合部で大入れ部分がはずれ，ほぞが折れたものが多い．

壁　　ひどいものは，くずれ落ちまたははらく，軽いものは，水平（仕上げてない壁）または斜め（仕上げてある壁）方向にひびわれを生じている．

筋かい　　その数は少なかつたが，ぬき程度のうすいものは折れた例が多かつた．

小屋組　　概して健全で被害が少なかつた．

戸障子　　ひし形に変形し，板戸はバラバラになつて四散し，障子はさんが折れたりし

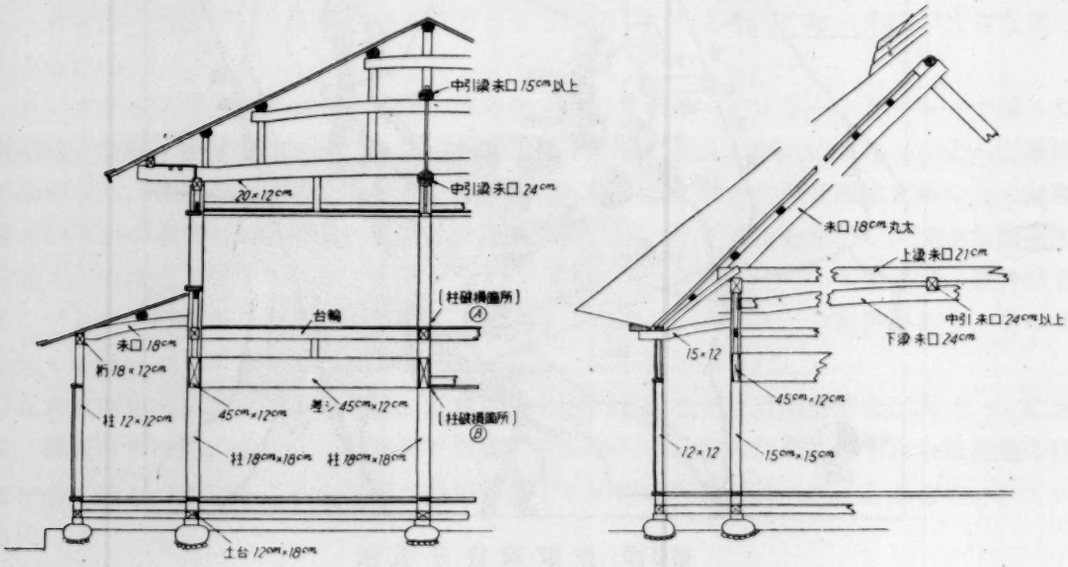

第3図　標準骨組詳細図

た.

このような各部材の被害のほかに，建物の接合部，古い家に増築したときのつなぎ目，下屋部分のつけねというようなところで，梁がぬけ出る，壁と柱の間が大きく口をあく，不同沈下で一方の柱が下がる，といつた被害が自立つた.

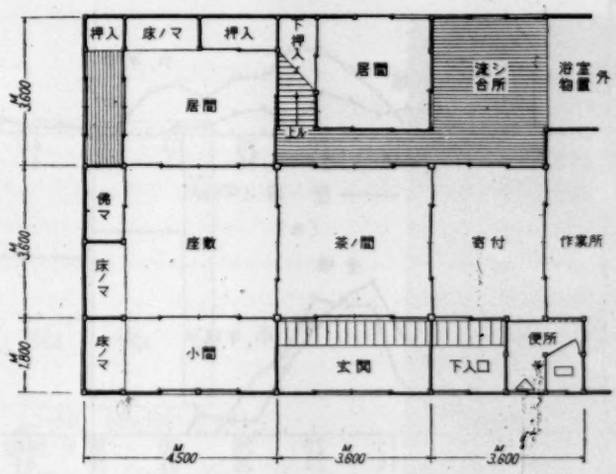

第4図　1階標準平面図

4.　壁率・建築年代・積雪と被害の関係

壁率と被害

ふつうの木造家屋では，壁は地震力に抵抗する骨組としてもつとも重要なものであり，壁の多い少ないがその建物の耐震力を推定する目安とされる．そこで調査家屋について，壁率と震害との関係をしらべてみた.

第5図にその結果を示す．この図の横軸は，壁率＝(壁の全長)/(床面積) を (cm/m²) の単位で表わし，縦軸は家屋の戸数をとつており，黒丸は全壊家屋，白丸は半壊または小壊家屋の分布を示している．この図でみると，全壊家屋の分布がそれ以外のものに較べてやや壁率の少ない方へ寄つているが，両者の差はごくわずかである．壁率いくら以下のものが全壊したというハッキリした結果はみられない．これは，ひとつは家屋の大部分が2階建であつて，全壊といつても2階が倒壊して1階が被害僅少だつた例もあり，1，2階にわけた場合の全壊・半壊の区別が必らずしも明りようでないことも影響している.

そこで特にこの点に留意して，調査の比較的よく行届いている古正寺町について，2階部分だけをとつて同様の分布をしらべてみると，第6図のようになつている．この場合は，全壊家屋の分布は，ハッキリそれ以外のものとわかれて壁率の少ない方によつている．すなわち，壁率 20 cm/m² 以上の壁のある家は，全壊をまぬがれていることがわかる.

もつとも，この地方の家屋では，柱せいが 15 cm，18 cm といつた太い柱を通し柱とし

て用いており，この柱にも相当の耐震力があると認められるので，壁だけでその家の耐震力をきめることはできない．この点については，あとで，推定震度の項でふれることにする．

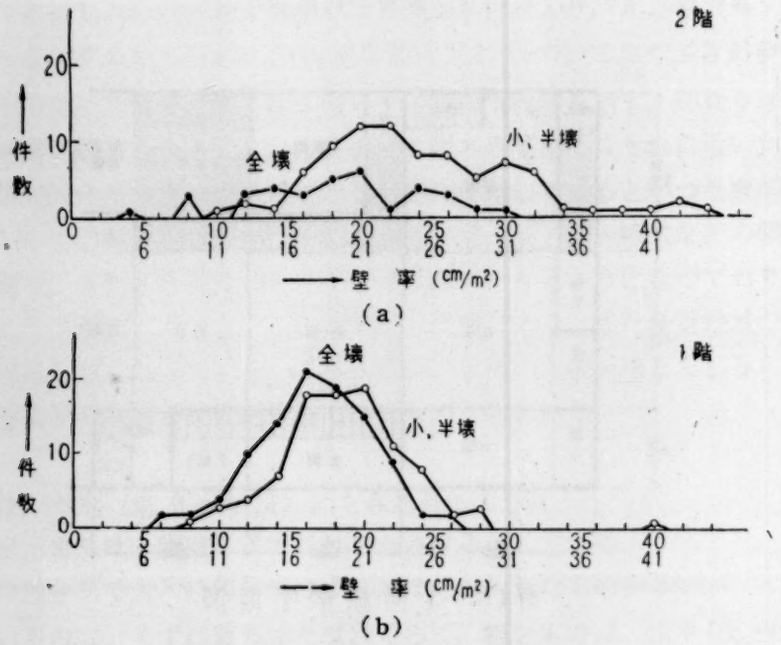

第5図 壁率と震害Ⅰ（全調査家屋）

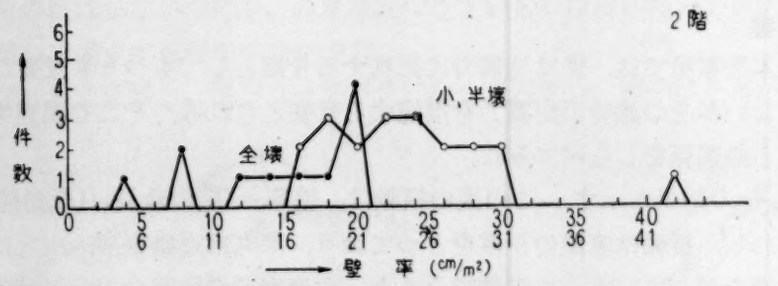

第6図 壁率と震害Ⅱ（古正寺町2階）

建築年代と被害

被害調査当初の印象では，新築後間もない家があちらこちらで大被害をうけており，古い家の方がかえつて丈夫なように感ぜられた．そこで調査の対象となつた207戸の家屋について，建築年代と震害の関係をしらべたところ，第7図のようになつた．図の縦軸は全壊率を百分率で表わしたもので，横に左から，新築後 20 年以内，20～50 年，50～100 年．100 年以上と4段階にわけて建築年代との関係を示した．

この図でみると，最初の印象に反して，全体として年代の古いものほど全壊率が多くなつていることがわかる．これは当然のことといえるが，一方 20 年以内の家（といつても 10 年以内のものが多い）が 40%に近い全壊率を示していることは，大部分が建築基準法

制定後の建物であることと考え合わせると，いかに地震動が激しかつたとはいえ，はなはだ残念な事実である．実際これらの大被害をうけた新築家屋は，いずれも筋かいのない，耐震的考慮にかけたものであつた．

一方基準法の規定通り十分に筋かいを用いた家がほとんど無被害であつた例が堺町にみられた．

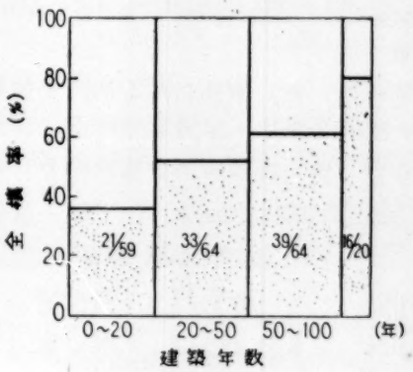

第7図　建築年代と被害

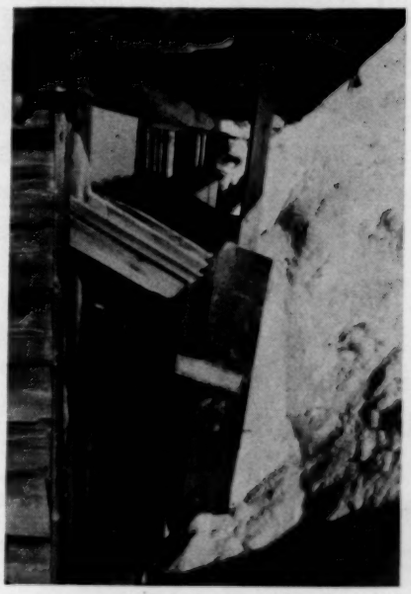

第8図　住宅の側面が積雪でおさえられ，1階の倒壊を防いでいる状況（寺宝町）

積雪と被害

長岡地方は昨年暮の豪雪で雪害をうけた地域であり，地震のおこつたとき長岡市内の積雪量は 171 cm（長岡気象通報所調べ）になつていた．当初この雪が建物の屋根荷重を増加させ，震害をひどくしたのではないかと考えられた．実際しらべてみると，被災地の住家はほとんど例外なく屋根の雪おろしをしており，被災時の屋根の積雪量は多くて 30 cm 位ということがわかつた．これは重量にすると屋根荷重の 20～30% 程度となり，確かに屋根を重くはしているが致命的な要素と考えるほどの量ではない．むしろ屋根からおろした雪が家のまわりを 2～3 m の高さにつみ重ねられ，1階の倒壊を防いだ功積の方が大きいとも考えられる．（第8図参照）

したがつて住家の間では，積雪量の差による被害程度の差は問題にならなかつた．一方非住家では，雪おろしが十分行なわれていないため 70～80 cm の積雪があつてそのため倒壊したと思われる例も 2，3 あつた．

5.　家屋作用震度の推定

建物の破壊状況からその建物に作用した地震力を推定することは必らずしも容易でない．地震が動的作用である上に，建物の骨組が複雑で耐力の性状がわかりにくいからであ

る.

今回の被害調査の結果から作用地震力を推定するのにもかなりの困難を感じたが，一応つぎのような取り扱いによつて，家屋作用震度の形で求めてみた.

まず調査家屋のうちから下記の条件に合う9軒をえらび，それぞれについて屋根重量（W）および2階水平耐力（F）を求め，その比（$k=F/W$）をとつて耐震度を算出した．9軒のなかには倒壊したものも小被害のものも含むので，それらの値から家屋作用震度を推定する．具体的にはつぎのようにして行なつた.

1. 対象とした家屋

（i） 昭和 22 年以降建築の比較的新らしい家屋

（ii） 激震地にある2階建家屋（例外1戸～堆肥小屋）で，倒壊したもの，大傾斜したもの，被害の僅少なものを含む.

2. 作用震度算定要領

（i） 屋根部分（小壁を含む）の重量算出（W）

（ii） 2階水平方向の耐力算出（F）

(iii) $k=F/W$ により家屋2階部分の耐震度算出

3. 重 量 概 算

屋根材料，積雪量によりそれぞれ下表のような単位荷重（2階床面積当り）を定め，これに2階床面積を乗じて算出する.

屋根材料	積雪量 (cm)	単位重量 (kg/m²)
セメント瓦	0～10	200
セメント瓦	10～20	220
セメント瓦	20～30	250
日 本 瓦	20～30	280

4. 骨 組 耐 力

壁，柱に関する従来の実験結果[2)3)]を参照して下のように各単位骨組の水平耐力を定め，各建物につきこれら個々の骨組の耐力を集計した.

壁　長さ 1 m につき　120 kg

筋かい入り壁　同上

通し柱　21 cm 角1本につき　1700 kg

〃　18 cm 角　〃　950

〃　15 cm 角　〃　460

〃　12 cm 角　〃　180

(たとえば 18 cm 角柱の耐力はつぎのようにして算出した.

仕口部分正味断面　12.6 cm×15 cm

2) 竹山謙三郎「荷重と外力・木構造」共立全書　昭和 26 年.

3) 久田俊彦「木造建物の耐力計算法一案」建築技術 No. 47　昭和 30 年4月.

断面係数　$Z = 0.6 \times \dfrac{12.6 \times 15^2}{6} = 284\ (\mathrm{cm}^3)$

ここに 0.6 は断面欠損による強度低減率

杉材の曲げ強度　$f_b = 600\ \mathrm{kg/cm}^2$ を用いて，

許容曲げ耐力　$M = Z \cdot f_b = 284 \times 600 = 170 \times 10^3\ (\mathrm{kg \cdot cm})$

2階柱頭ピン柱脚連続の条件より 2階の水平剪断耐力 R は，支点間距離 180 cm を仮定して

$$R = \frac{170 \times 10^3}{180} = 950\ \mathrm{kg})$$

5. 算　定　例

福道町　金内勘蔵氏宅，木造2階建セメント瓦ぶき，昭和 35 年建築，

被害　2階南南東へ大傾斜，通し柱6本折れる．

重量　$W = 71.4\ (\mathrm{m}^2) \times 250\ (\mathrm{kg/m}^2) = 17.9\ (\mathrm{t})$

耐力　（2階 N-S 方向）

壁全長	11.7 m	$120 \times 11.7 = 1.4$
通し柱，	15 cm 角4本	$460 \times 4 = 1.84$
	12 cm 角2本	$180 \times 2 = 0.36$
		3.60 (t)

耐震度　$k = \dfrac{3.60}{17.9} = 0.20$

以上のようにして算定した結果を第2表に示す．これでみると，倒壊または大傾斜した家屋の耐震度は 0.14～0.28（平均 0.22），小被害のものは 0.34～0.37（平均 0.36）となつていて，被害の状況がハッキリ耐震度で説明でき，大体 0.3 前後が，倒壊または大傾斜と小被害のさかい，したがつてこの場合の作用震度と推定される．

第2表　被害家屋耐震度

所在地	床面積 (m²)	屋根重量 W (ton)	水平耐力 F (ton)	耐震度 $k=F/W$	被害程度 2階(1階)	壁率 (cm/m²)	備考
寺宝町 A	78	15.5	5.75	0.37	小（小）	13	
〃 B	49	12.2	1.72	*0.14*	倒壊(大)	9	
〃 C	80	19.9	5.59	*0.28*	倒壊(大)	7	
高瀬町 A	24	5.5	1.26	*0.23*	大		堆肥小屋方杖付1階建
福道町 A	72	17.9	3.60	*0.20*	大（小）	8	
南新保町 A	68	15.0	5.11	0.34	小（小）	14	
古正寺町 A	65	18.2	3.71	*0.20*	倒壊(小)	8	
〃 B	95	23.7	5.60	*0.24*	倒壊(小)	5	
〃 C	72	14.2	5.20	0.37	小（小）		壁筋かい入

もちろん，計算上の重量および骨組耐力は，実際のものと幾分ちがうことが考えられるし，また計算例も決して多くないので，なお検討の余地はあるが，一応の推定値として求めたものである．

6. 結

長岡地震の家屋被害について調査した結果を総合するとつぎのようになる．

1. 家屋の著しい被害をうけたのは，直径 3 km 位の範囲に限られている．
2. 震害地の住家の大部分は，耐震上つぎのような欠点をもつている．
   (i) 大部屋式で壁が少なくかつ偏在している．
   (ii) 屋根部分が重い．
   (iii) 筋かい，方杖，ひうちなど耐震上必要な斜材を用いていない．
3. 住家の壁率と被害の関係は，全体としてはハッキリした傾向がつかみにくいが，古正寺町の例について綿密に整理したものでは，壁率 20 cm/m² のあたりが境界となり，これより壁の少ないものは大部分全壊，多いものは半壊または小壊という結果がでている．
4. 建築年代と被害の関係は，古い家と新らしい家で，全壊率に大きな差はないが，傾向としては古い家ほど全壊率が大きくなつている．
5. 屋根面の積雪の影響は，ふつうの住家ではちようど雪おろし後で積雪量がわずかであつたため，明りようにはあらわれていない．
6. 調査家屋のうち 9 軒について算出した水平耐震度から家屋作用震度（水平方向）の推定値として約 0.3g を得た．

今回の調査にあたつて，長岡市の内山市長はじめ市役所の方々に多大の御援助を頂き，震害写真を提供して頂いた．また長岡市大工職組合の方々に被害地家屋構造に関する資料を提供して頂いた．ここに厚く御礼申しあげます．またこの調査および整理を手伝つて頂いた東京大学工学部建築学科大学院学生，山根昭，宮武恒男．吉田靖，上杉啓，洪忠憙，塩野谷健治郎，柴田明徳，渋谷盛和，広沢雅也の諸氏に感謝致します．

おわりにこの報告の作成上種々御指示を仰いだ河角広教授，原稿を閲読して頂いた金井清助教授に厚く謝意を表します．

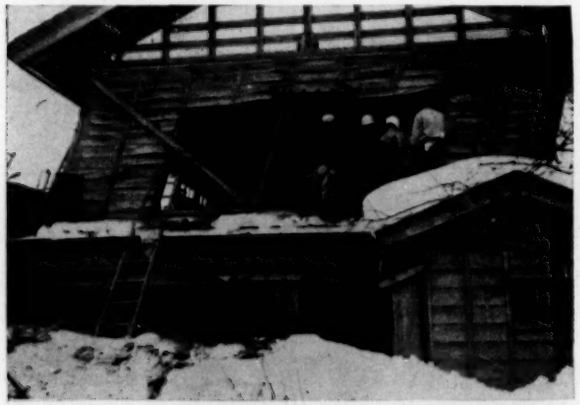

第 9 図

典形的な被害例で2階が大傾斜しているが1階はほとんど傾いていない（古正寺町）

第 10 図

死者4名を出した家，主屋部分は1階，2階共倒壊，付属した作業場(写真右端)は残つている(福道町)

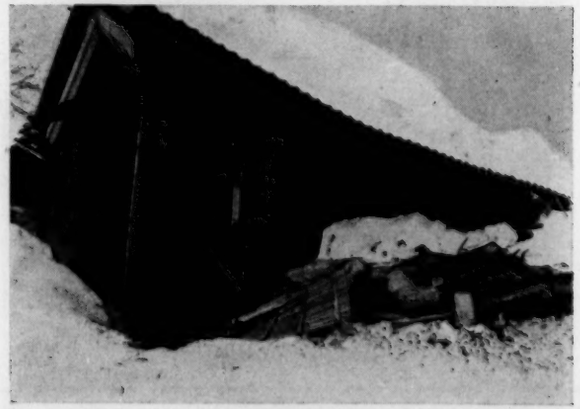

第 11 図

米俵を積んだ農業倉庫の被害状況，方杖付き木造骨組が倒壊，屋根の積雪は住家より多い(寺宝町)

第 12 図

土蔵の被害例（王番田町）

第 13 図
激震地にありながら無被害だつたコンクリートブロック造倉庫（高瀬町）

第 14 図
大傾斜した家の 1 階内部（寺宝町）その 1

第 15 図
大傾斜した家の 1 階内部（寺宝町）その 2

第 16 図
1 階柱の被害状況（福道町）

（震研彙報 第三十九号 図版 大沢・山本）

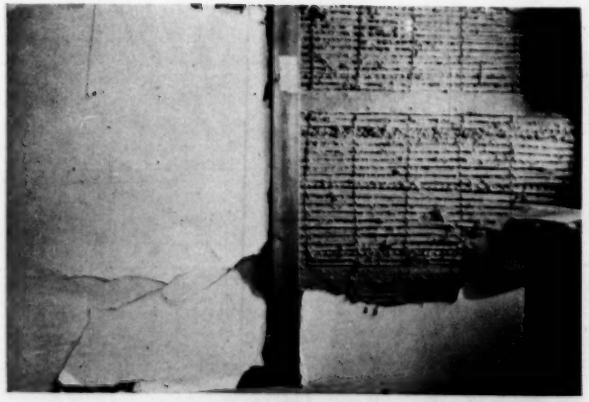

第 17 図
壁の被害状況（仕上げた壁）

第 18 図
壁の被害状況（仕上げない壁）

（震研彙報　第三十九号　図版　大沢・山本）

第 19 図
障子の被害状況（寺宝町）

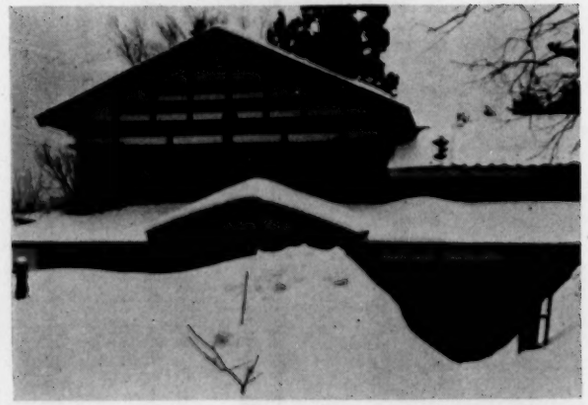

第 20 図
激震地にあつて比較的被害の少なかつた家．震動の激しかつた方向に壁が数多く配置されていた（福道町）

19. *On the Damage to Buildings during the Nagaoka Earthquake of February 2, 1961.*

By Yutaka OSAWA,
Earthquake Research Institute

and Masakatsu YAMAMOTO,
Department of Architecture, Faculty of Engineering,
University of Tokyo.

A strong earthquake occurred in the western part of Nagaoka City, Niigata Prefecture, at 3:39 a.m. on February 2, 1961. It was reported that 5 persons were killed and 259 houses were seriously damaged.

This report describes mainly the damage to dwelling-houses in the Nagaoka district where the writers investigated about two hundred houses which were either seriously or slightly damaged.

The results of the investigation are summarized as follows:

1. The region in which the houses were seriously damaged, is only within 3 km in diameter, and is underlain by an aluvium layer.

2. The dwelling-houses in this region betrayed their weak points such as (i) insufficient wall to resist horizontal forces, (ii) heavy roof, (iii) lack of bracing and other diagonal members.

3. At Koshōji-machi in Nagaoka City the houses with wall ratio (ratio of wall length to floor area) of more than 20 cm/m² were slightly damaged, while most of houses with wall ratio of less than 20 cm/m² were seriously damaged.

4. According to the statistical investigation of 207 houses, 80% of the houses which are more than 100 years old were damaged, while only about 40% of the houses less than 20 years old were damaged.

5. The maximum horizontal acceleration on the roof of dwelling-houses during the earthquake is estimated to be about 0.3 g.

地震研究所彙報
第39号 (1961) 561-577頁

20. 1961年2月27日日向灘地震に伴なつた津波について

地震研究所 高橋龍太郎
羽鳥徳太郎

(昭和36年3月28日発表——昭和36年6月30日受理)

§1. 緒　　言

1961年2月27日03時10分59.1秒日向灘に起きた地震に伴ない日向灘および四国西南岸地域に，軽微な津波があつた．

地震のマグニチュードは7.2，震央は宮城地方気象台の発表によると31°.7 N, 131°.7 E, 深さ17 kmということである．

過去日向灘に生じた地震で，震度IV以上のものは1662年以来14あり，この地震に伴つた津波は1941年11月19日，宮崎，大分両県四国の西南部海岸に全振巾1mの津波があつたことが記録されている[1]．

筆者らはこの津波の概要を調査するため，各測候所，国土地理院，海上保安庁および各県土木部より検潮記録の提供を賜わり，集収した資料および，筆者らが観測している大島・八丈島の津波計記録をもとに，今回の津波の波高，伝播時間および浪源について報告する．

§2. 津波の波高および初動到達時刻

今回の津波の高さは浪源附近の海岸において1m以下であり，このため津波による直接の被害はない模様である．したがつて現地踏査による津波の痕跡から，津波の高さを測定することは困難であるので，各地の検潮記録から津波の初動，振巾および周期を読み取つた．

従来津波の高さは測定地附近における東京湾中等潮位面 (T.P.) および平均海水面を基準として定義されているが，ここで筆者らのいう津波の波高は，上記の理由から，検潮儀で計測された全振巾（山から次の谷または谷から次の山までの高さの差）の最大を指すのであることを，おことわりしておく．

各地の津波波高および到達時刻を Table 1 および Fig. 1 に示す．

津波の伝播範囲は西南部では，奄美大島，名瀬で明瞭に計測されており，東北部では布良の記録が，湾の副振動と重なつているが，やや明らかに津波の初動と思われるところが周期がのび津波を検出できる．つぎに大島泉津の津波計記録では検出不能である．また八

1) 昭和36年2月27日日向灘地震調査報告　昭和36年異常気象報告　第1号　宮崎地方気象台．

Table 1. The Tsunami of Feb. 27, 1961, as recorded on tide gauges
(All times are J.S.T.)

Wave originated at earthquake epicenter off the coast of Hiuga
(31°.7 N, 131°.7 E) at 03 11 Feb. 27, 1961.

No.	Tide Station	Time of Arrival	Up or Down	Time of Max. Amplitude	Max. Amplitude H	Period T
1	Naze	04h23m	+	04h52m	13 cm	20 min
2	Nishino-omote	04 00	+	06 00	25	
3	Makurazaki	04 27	+	05 32	13	16
4	Namimi	03 30	+	04 20	12	
5	Suzureishi	03 30	+	04 18	12	
6	Aburatsu	03 14	+	03 51	45	22
7	Miyazaki	03 35	+	03 42	12	
8	Hosojima	03 22	+	05 22	78	20
9	Hosojima, New Harbour	03 25	+	05 55	124	
10	Tōkai	03 35	+	03 42	13	18
11	Hebizaki	04 00	+	05 10	10	19
12	Yawatahama	04 25	+	06 30	28	22
13	Uwajima	04 12	+	06 53	18	22
14	Hosogi	03 58	+	04 55	17	20
15	Mishō	04 08	+	07 16	70	30
16	Tosa-Shimizu	03 42	+	04 12	96	22
17	Tosa-Shimoda	03 55	+	04 47	10	20
18	Urado	04 08	+	06 08	20	18
19	Kōchi	04 15	+	06 05	17	20
20	Kushimoto	03 46	+	05 25	36	23
21	Aburatsubo	05 36	+	07 56	6	16
22	Mera	05 32	+	13 25	35	22
23	Hachijo I.	05 10	?	?	3	?

丈島八重根の長波計記録ではやや不明瞭であるが初動を認められた．したがつて今回の津波は東南海，南海地震の津波同様，日本東北地方には減衰，発散して影響をおよぼさなかつたように思われる．

つぎに津波の初動は各地点とも例外なく，押しで始まつているので津波の発生機構から浪源附近において，海底隆起の現象があつたのであろうと思われるが，この変動は今後の海底測量であるいは明らかにされるかも知れない．

一般に津波の波高分布は浪源よりの距離による減衰，浪源より伝達される経路に影響されるエネルギーの配分の仕方，湾形の影響および，津波の周期と湾セイシュの共振による影響などが考えられる．

今回の津波で浪源周辺の波高分布をみると，非常に湾の共振の影響をうけたように思わ

Fig. 1. Distribution of Wave Heights (cm) and Arrival time (JST) of the Hiuganada tsunami of 1961.

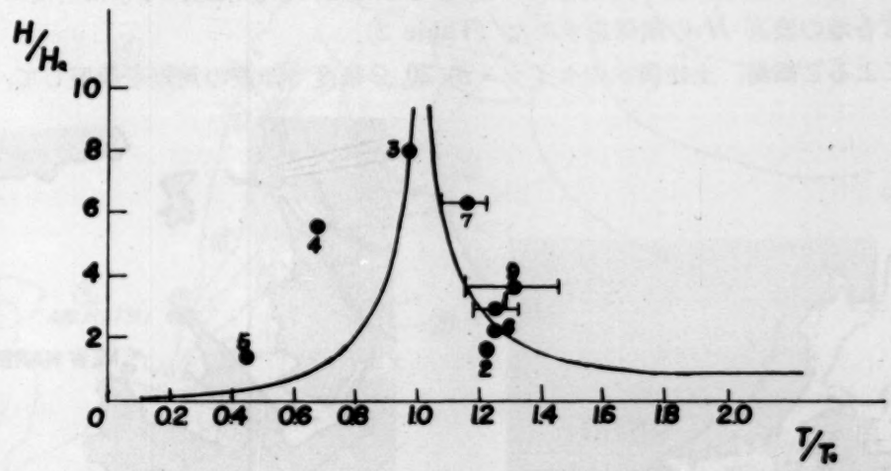

Fig. 2. Relation between the proper period T_0 of seiche in a bay and the wave height H in that bay.

れる (Fig.2)。本多・寺田[2]により観測および計算から各湾のセイシュ T_0 が調べられて

2) K. HONDA, T. TERADA, Y. YOSHIDA, and D. ISITANI, "Secondary Undulations of Oceanic Tides", *Journ. Coll.Sci. Imperial Univ. Tokyo, Japan*, **24** (1903~06).

Table 2. Response of the tsunami at Various stations: Periods of seiches and heights of the tsunami.

T: The mean periods of the tsunami estimated to be 22 min.
H_0: The maximum wave height at Miyazaki.

No.	Tide Station	Seiches T_0	T/T_0	Wave Height of Tsunami H	H/H_0
		min		cm	
1	Kushimoto	16.5~18.6	1.33~1.18	36	3.0
2	Urado	18	1.22	20	1.7
3	Tosa-Shimizu	(22.8)	0.97	96	8.0
4	Mishō	34.1	0.65	70	5.8
5	Uwajima	(49.8)	0.44	18	1.5
6	Yawatahama	(17.6)	1.25	28	2.3
7	Hosojima	17.8~20.3	1.23~1.08	78	6.5
8	Miyazaki			12	1.0
9	Aburatsu	15.0~19.0	1.46~1.15	45	3.8

いる．第2表において（ ）内は同氏の計算値。

御荘の周期も同様に $T_0=4l/\sqrt{gh}$ の公式で求めたものであるが，検潮記録において津波前にセイシュと思われる周期 35 分の振動が観測される．浦戸の周期も検潮記録からの読み取値を掲げた．

各検潮記録の第1波と第2波内の時間を周期とすると各地域平均して 22 分が観測される．したがつて今回の津波の周期を $T=22$ 分として T/T_0 を求め，つぎに宮崎の波高 H_0 に対する各地の波高 H の関係を求めた（Table 2）．

これによると細島，土佐清水のセイシュが 20 分程度で津波の周期と共振して，他点よ

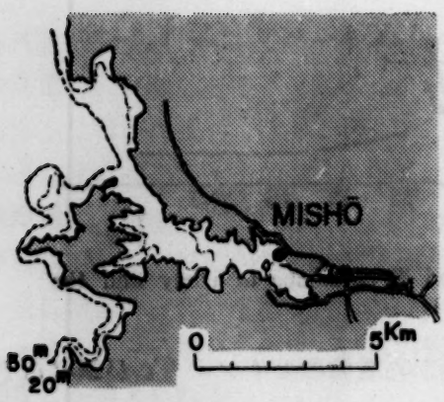

Fig. 3. The topography of Misho Bay.

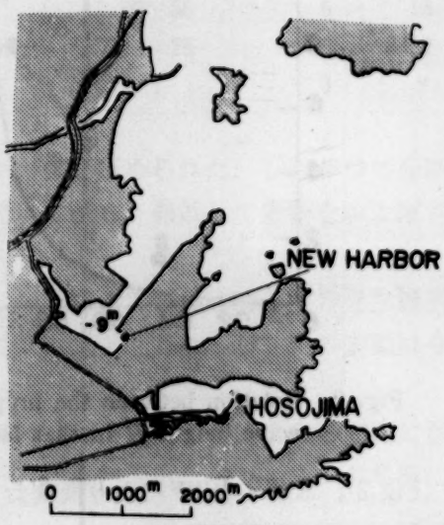

Fig. 4. The topography arround the Hosojima tide-station.

りも波高が高くなつたものと見られることは注目に価いする.

御荘の値がこの共振曲線より外れ，波高が高かつたのは△型湾のため，湾奥において水位が盛上つたためであろう (Fig. 3).

細島の検潮記録は2ケ所で観測されたもので，国土地理院管理のものは部落に面した旧細島港に位置し，その北部に宮崎県にて管理せる新港のものがある (Fig. 4).

3. 浪　源　域

浦戸，土佐清水，宇和島，細島，油津および西之表の各点から波の伝播速度を $\sqrt{gh}$ として津波の逆伝播図を画いて，浪源域を求めた (Fig. 5).

等時線は1分ごとに画いたが，Fig. 5 にははん雑を防ぐため5分ごとの波面が画かれている.

この図によると浪源域は日向灘に沿つて南北に延びた細長い楕円となり，長径は約 80 km である.

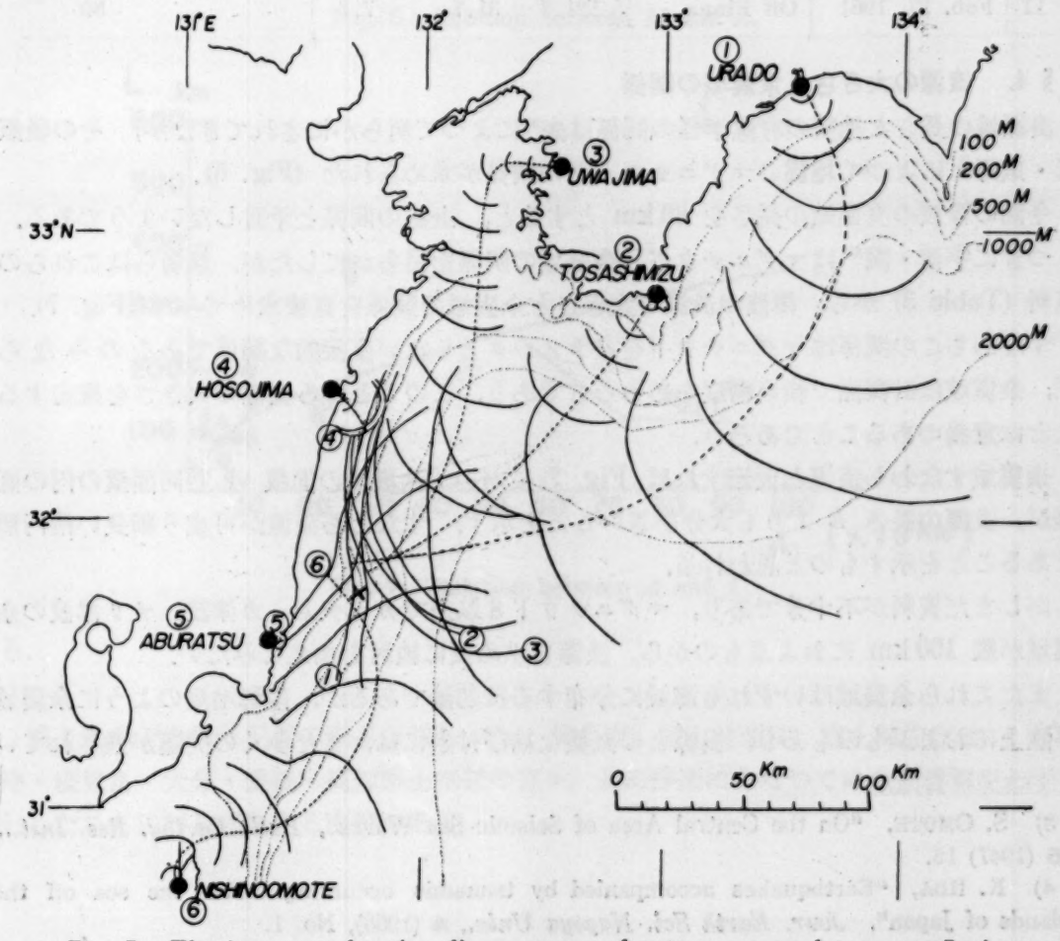

Fig. 5. The inverse refraction diagram wave fronts correspond to every 5 min.

Table 3

No.	Date	Location	Epicenter		M	A (10^3 km^2)	Linear dimension of central area L km
			λ (°E)	φ (°N)			
1	Mar. 9, 1931	Off Hachinohe	141.9	40.6	7.3	5.6	50
2	Mar. 3, 1933	Off Sanriku	144.7	39.1	8.5	87	600
3	Oct. 13, 1935	Off Miyako	143.3	40.4	7.1	2.9	100
4	Nov. 3, 1936	Off Kinkazan	142.0	38.4	7.5	5.3	90
5	May 23, 1938	Off Shioyasaki	141.45	36.7	7.4	8.2	90
6	Nov. 5, 1938	Off Fukushima	141.65	37.1	7.7	10	120
7	May 1, 1939	Oga Peninsula	139°49′	39°57′	6.9	0.52	40
8	Dec. 7, 1944	Tōnankai	136.2	35.7	7.9	10	200
9	Dec. 21, 1946	Nankaido	135.6	33.0	8.2	27	350
10	Mar. 4, 1952	Tokachi	143°52′	42°09′	8.1	22	120
11	Feb. 27, 1961	Off Fiuga	131.7	31.7	7.2		80

§ 4. 浪源の大きさと余震域の関係

浪源域の長さと地震の有感半径の関係は表[3]によつて明らかにされてきたが，その後飯田・広野[4]によつて地震のマグニチウドとの関係が求められた (Fig. 6).

今回の津波の浪源域の長さを 80 km とすると，上記の関係と矛盾しないようである.

つぎに宇津・関[5]はマグニチウドと余震域の関係を明らかにしたが，筆者らはこれらの資料 (Table 3) から，津波の浪源の大きさと全震域の関係を直接求めてみた (Fig. 7).

すなわちこの関係はマグニチウドをパラメータとしない直接的な関係であるのみならず，余震域は計測面で相当精度もあることであり，このことから浪源の大きさを推定することは意義のあることであろう.

余震域すなわち浪源と仮定すれば Fig. 7 において余震域の面積 A と同面積の円の直径が，浪源の長さ L よりも大分小さいことを示す. すなわち浪源が可成り細長い楕円形であることを示すものと思われる.

しかしまだ資料が不十分であり，マグニチウド 8 以上でカムチャッカ津波，チリ津波の余震域が数 100 km におよぶものから，浪源を求め更に検討を加えてみたい.

またこれら余震域はいずれも海域に分布するは勿論であるが，南海地震のように余震域が陸上におよぶものもあり，浪源との直接な結び付きには，まだ多くの問題が残されてい

3) S. OMOTE, "On the Central Area of Seismic Sea Waves", *Bull. Earthq. Res. Inst.*, **25** (1947) 15.

4) K. IIDA, "Earthquakes accompanied by tsunamis occurring under the sea off the Islands of Japan". *Jour. Earth Sci. Nagoya Univ.*, **4** (1956), No. 1.

5) 宇津徳治・関　彰「余震区域の面積と本震のエネルギーとの関係」地震，ii, **7** (1955), No. 4.

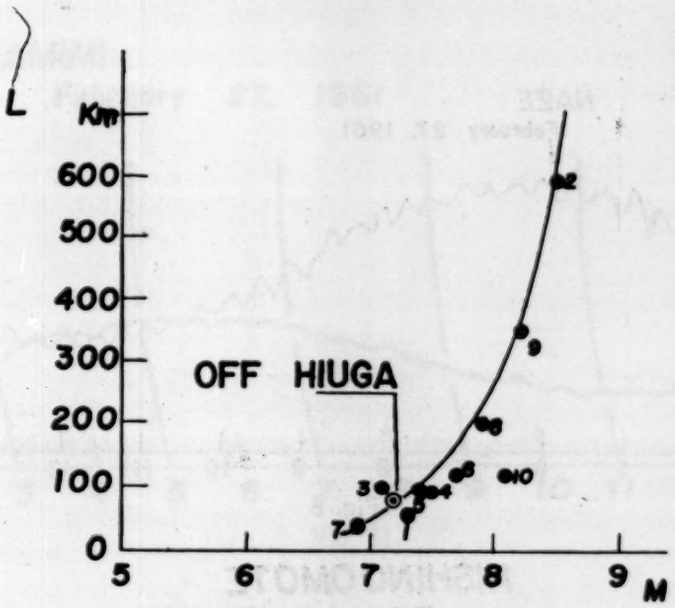

Fig. 6. Relation between M and L.

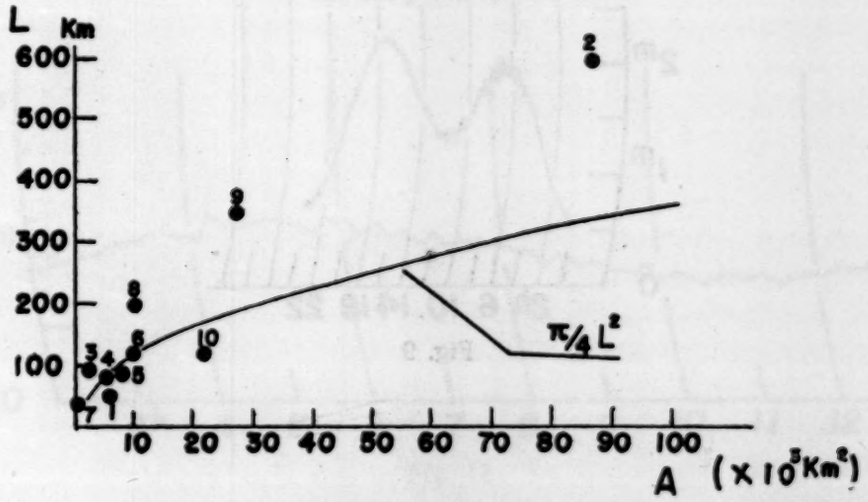

Fig. 7. Relation between A and L.

る.

終りにのぞみ検潮記録の御提供賜わつた，気象庁，国土地理院，海上保安庁および宮崎・鹿児島・大分・愛媛・高知県土木部の方々，並に作図にあたつては今泉啓君をわずらわしたことに対し感謝する次第である.

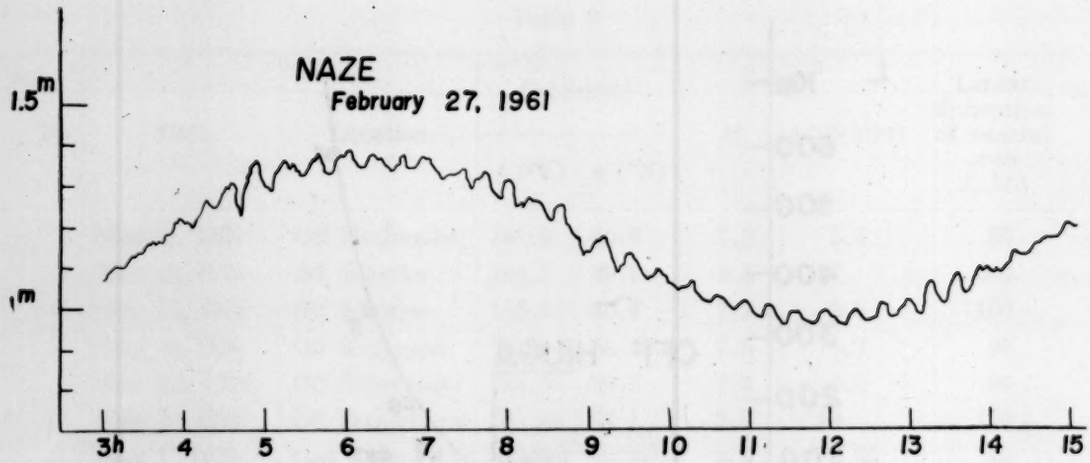

Fig. 8

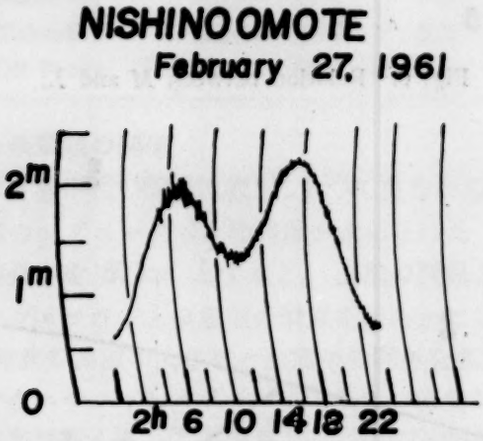

Fig. 9

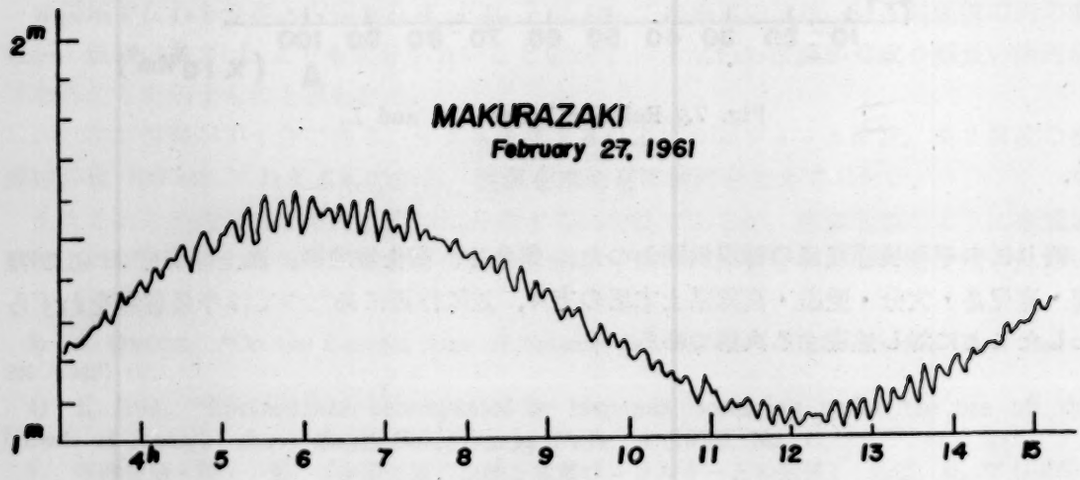

Fig. 10

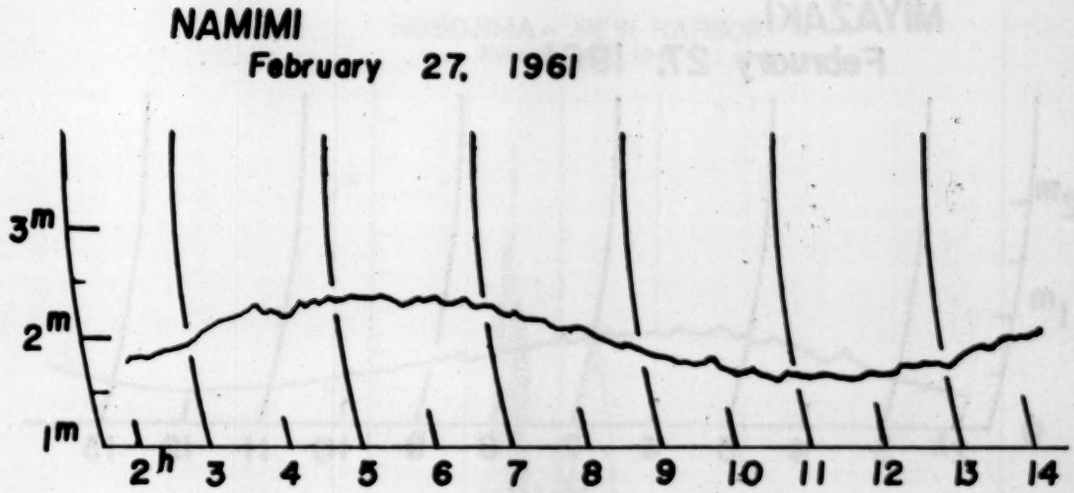

Fig. 11

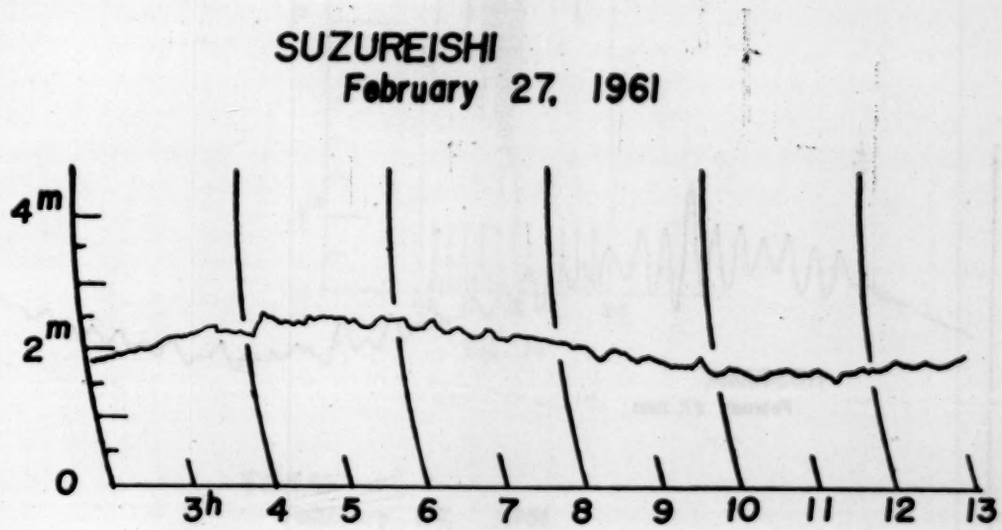

Fig. 12

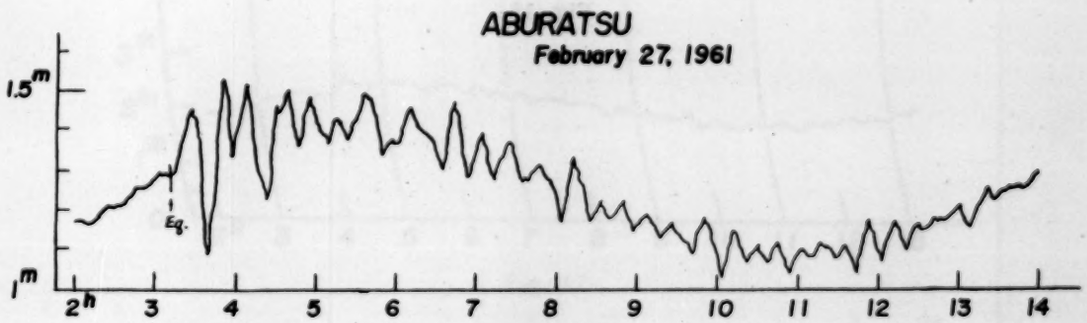

Fig. 13

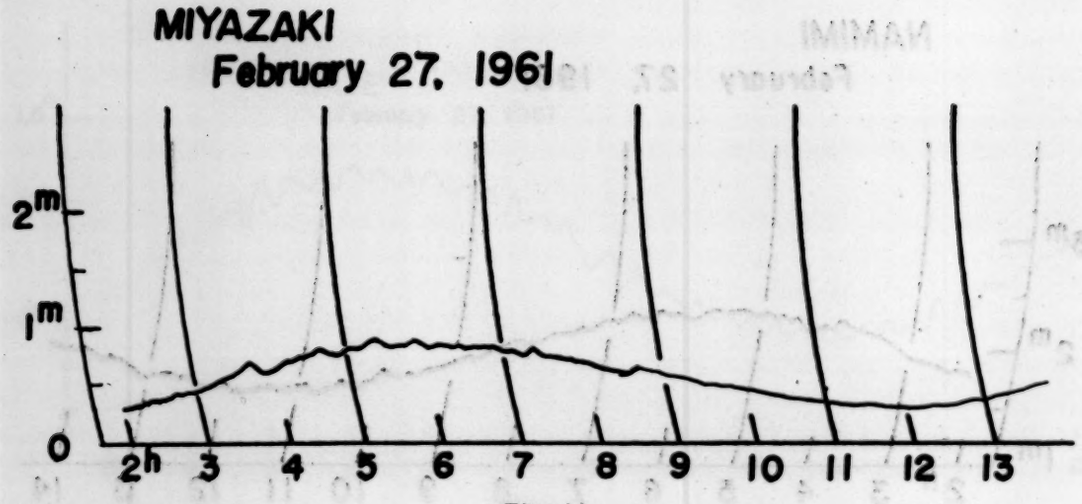
MIYAZAKI
February 27, 1961
2m
1m
0
2h
3
4
5
6
7
8
9
10
11
12
13

Fig. 14

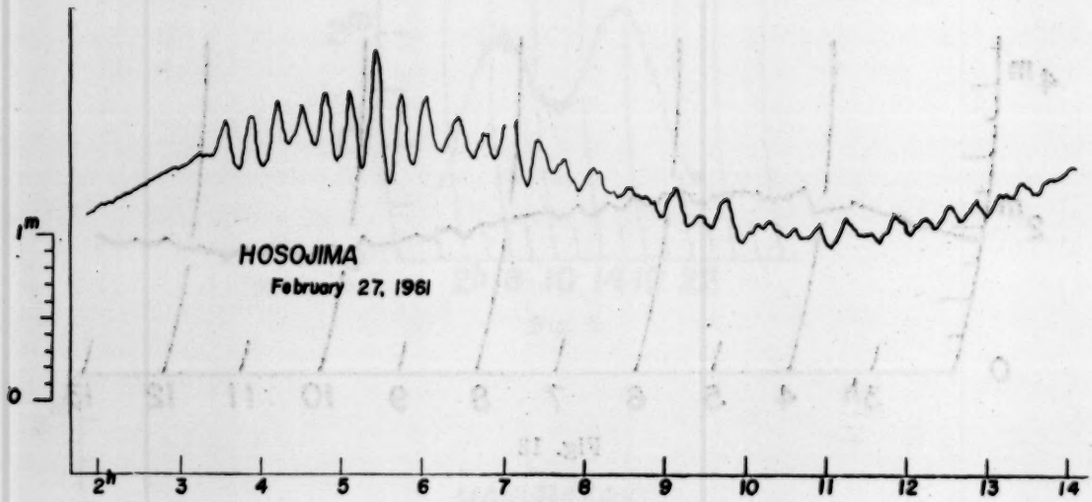
1m
0
HOSOJIMA
February 27, 1961
2h
3
4
5
6
7
8
9
10
11
12
13
14

Fig. 15

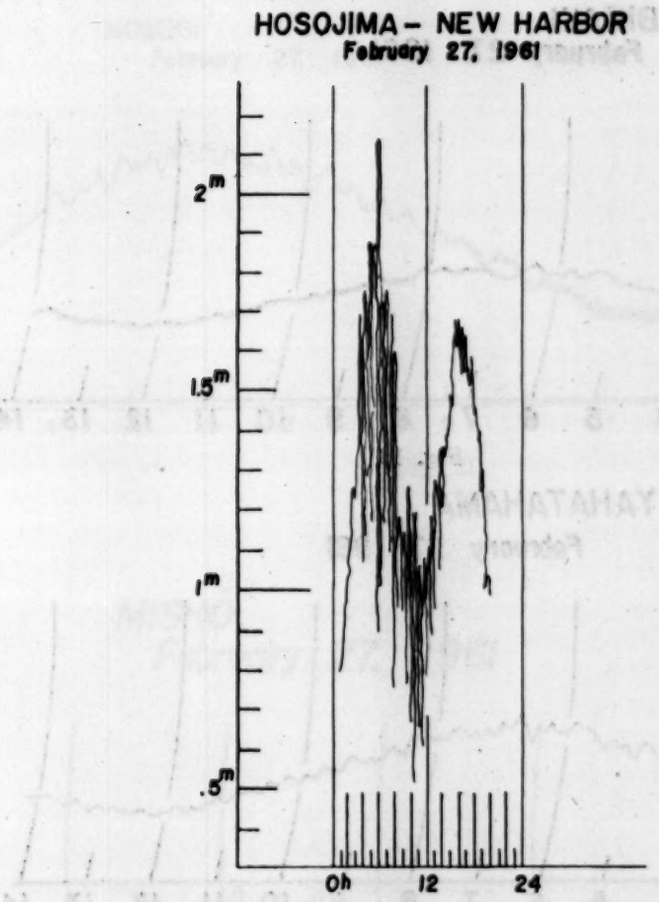
HOSOJIMA – NEW HARBOR
February 27, 1961
2m
1.5m
1m
.5m
0h
12
24

Fig. 16

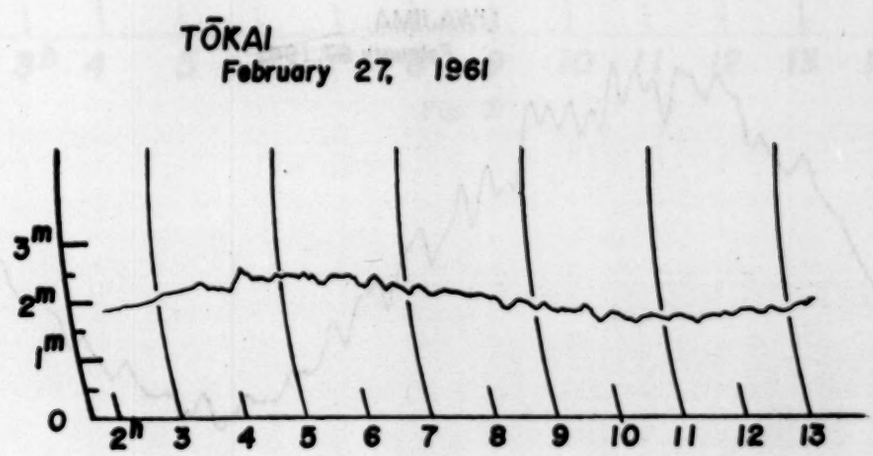
TŌKAI
February 27, 1961
3m
2m
1m
0
2h
3
4
5
6
7
8
9
10
11
12
13

Fig. 17

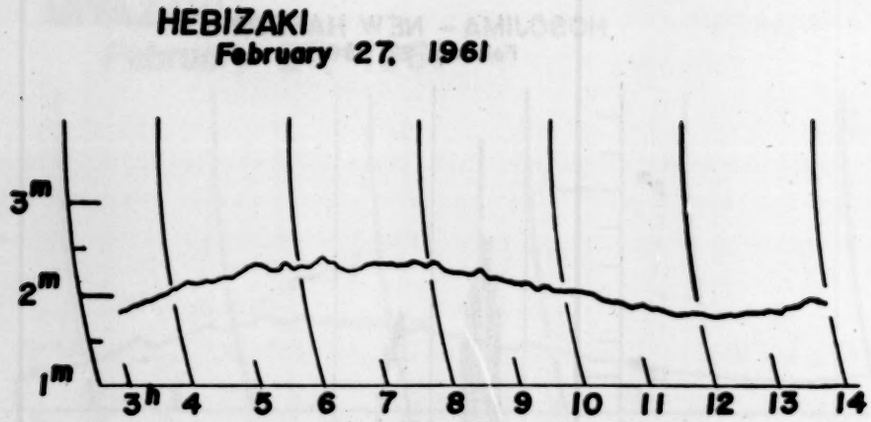

Fig. 18

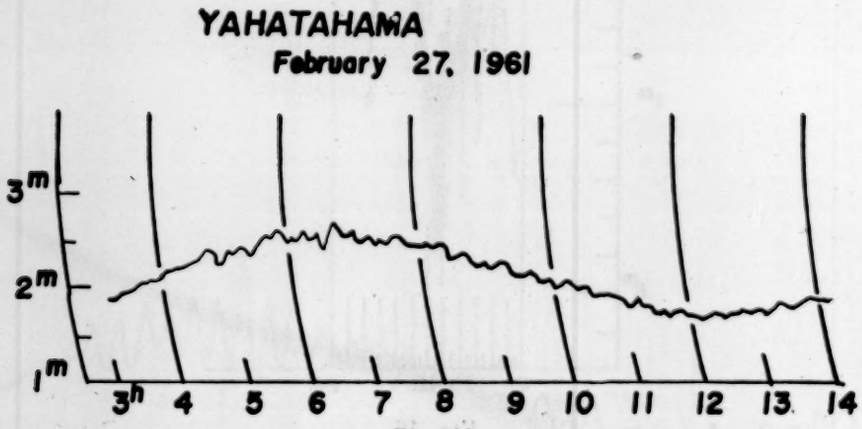

Fig. 19

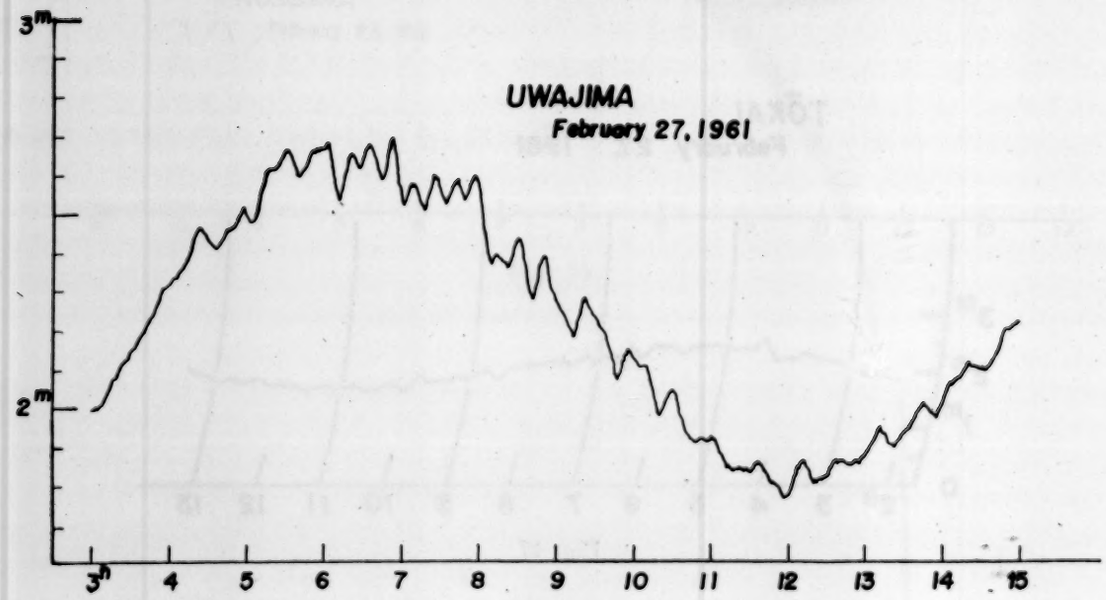

Fig. 20

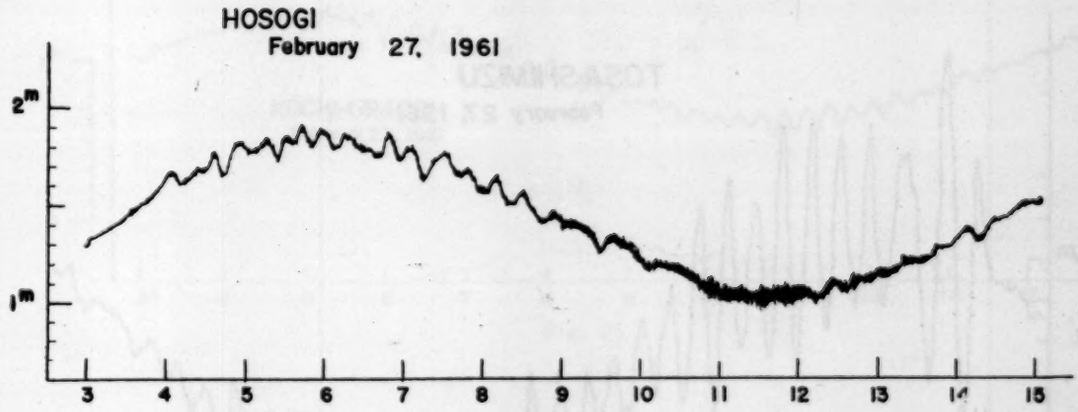
HOSOGI
February 27, 1961
2m
1m
3
4
5
6
7
8
9
10
11
12
13
14
15

Fig. 21

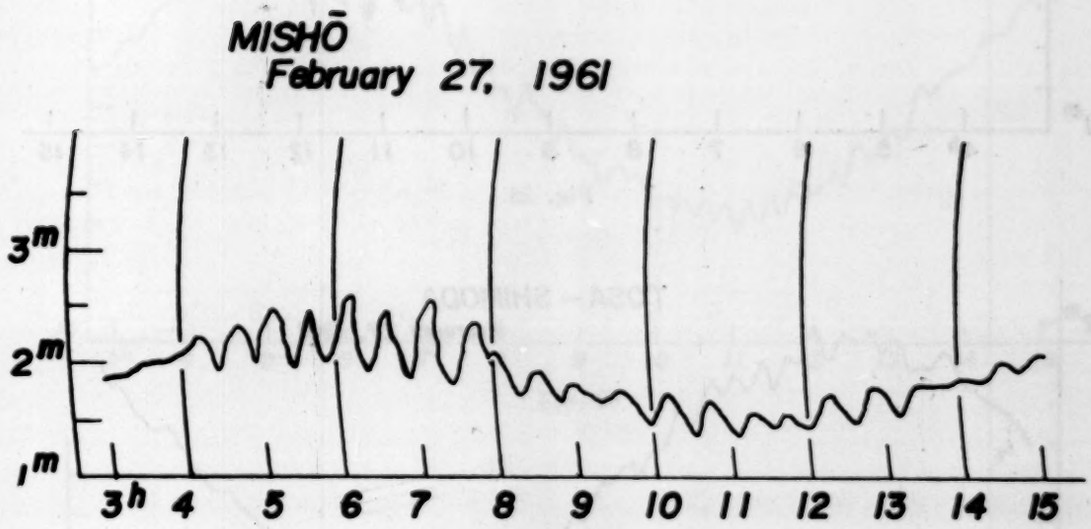
MISHŌ
February 27, 1961
3m
2m
1m
3h
4
5
6
7
8
9
10
11
12
13
14
15

Fig. 22

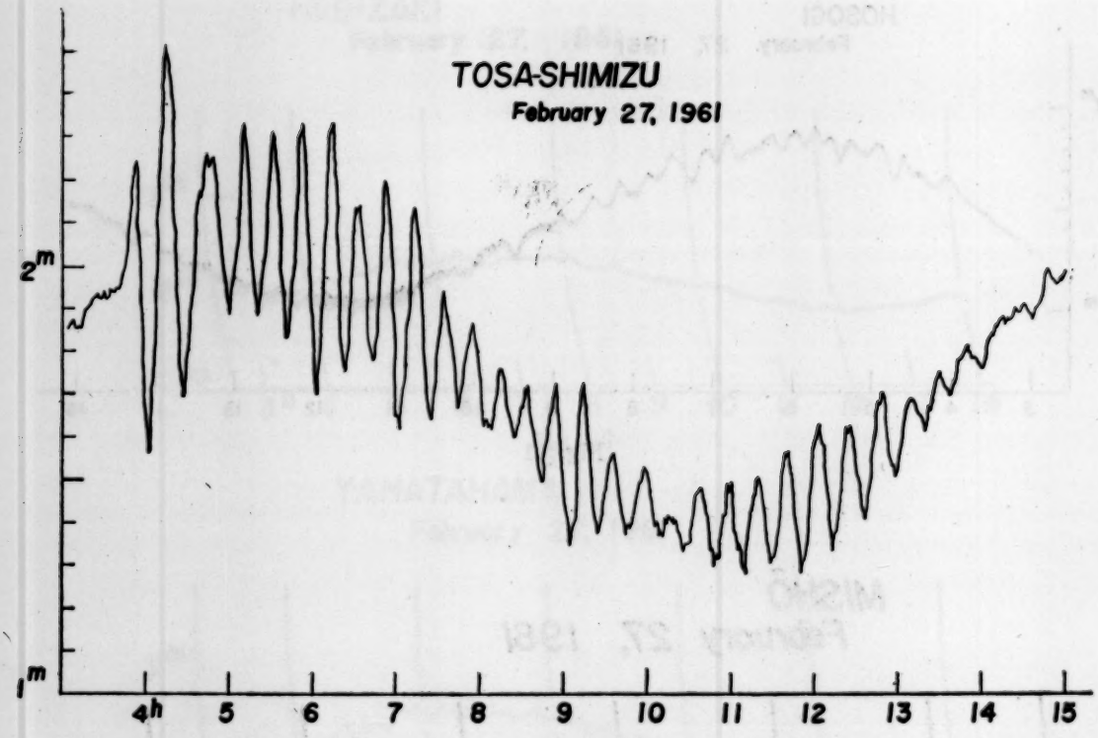
TOSA-SHIMIZU
February 27, 1961
2m
1m
4h
5
6
7
8
9
10
11
12
13
14
15

Fig. 23

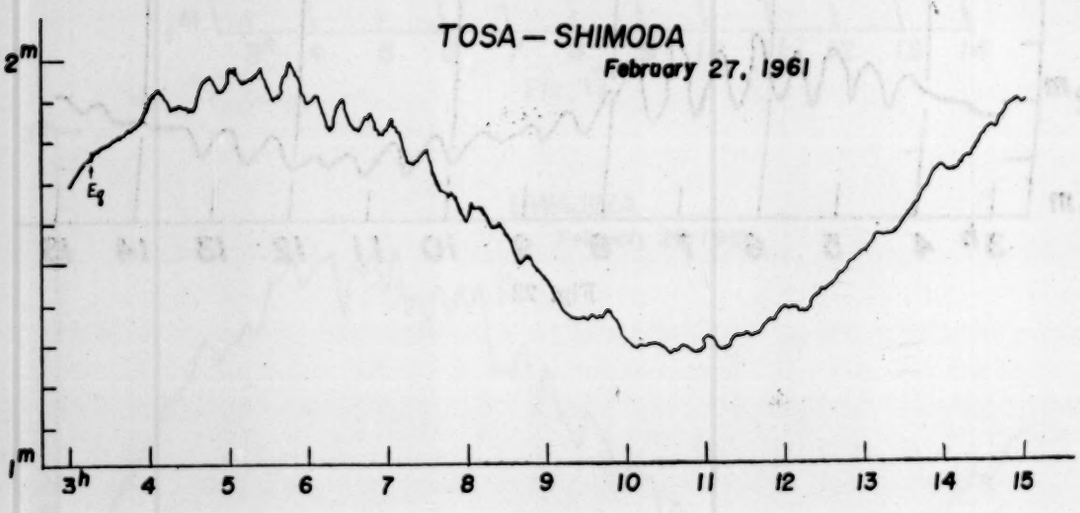
TOSA — SHIMODA
February 27, 1961
2m
1m
Eq
3h
4
5
6
7
8
9
10
11
12
13
14
15

Fig. 24

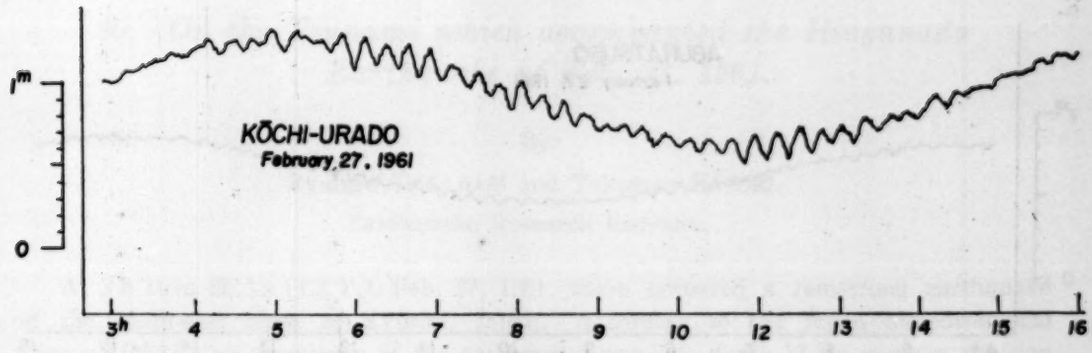

Fig. 25

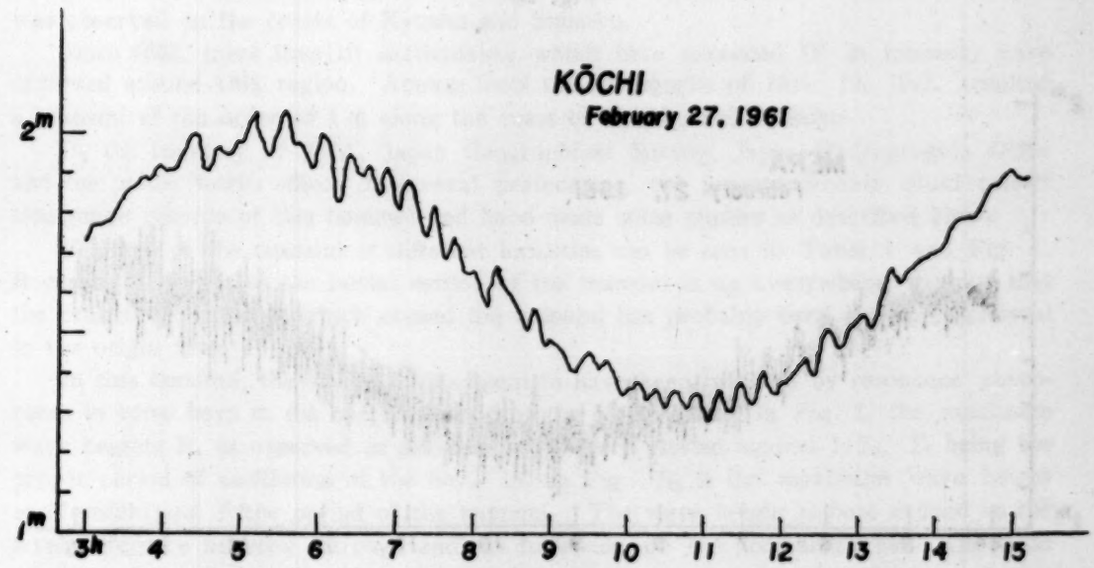

Fig. 26

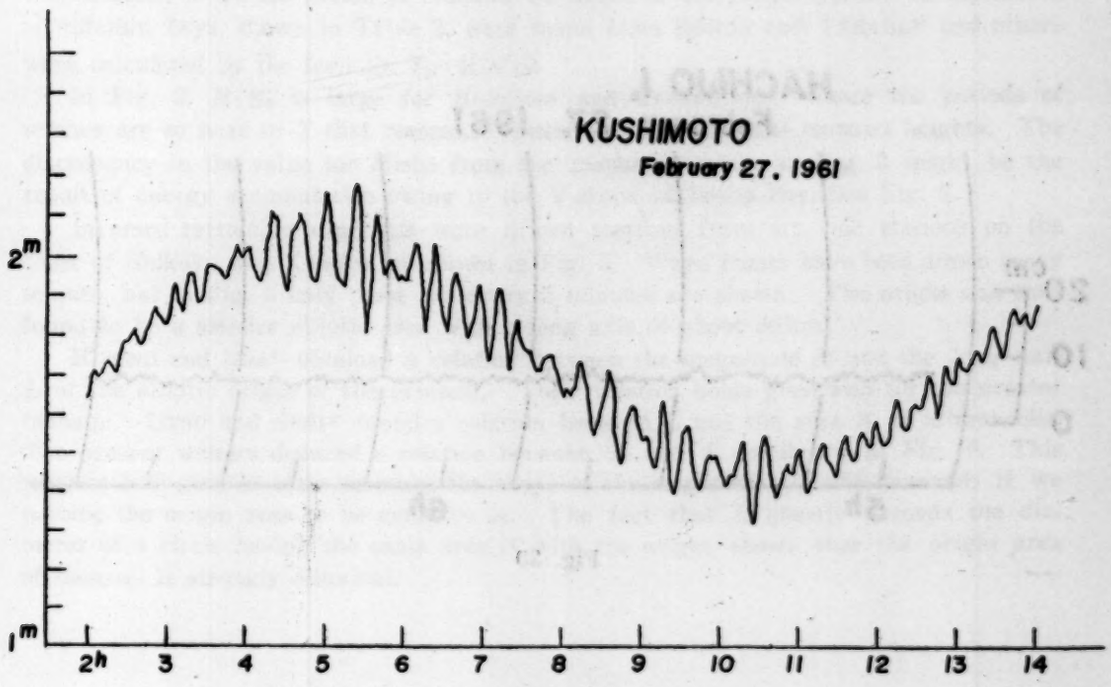

Fig. 27

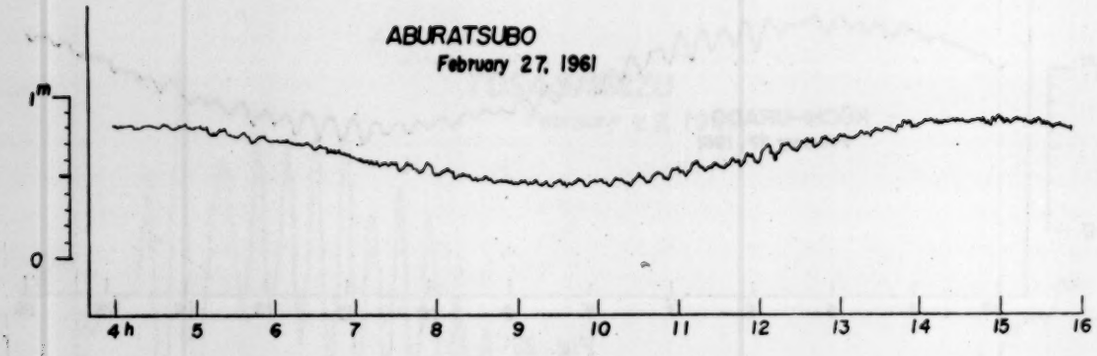

Fig. 28

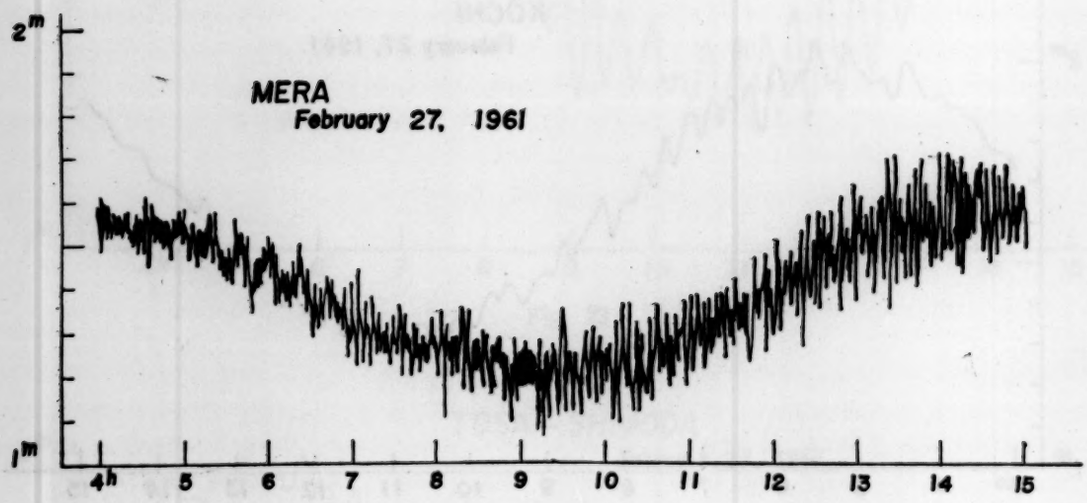

Fig. 29

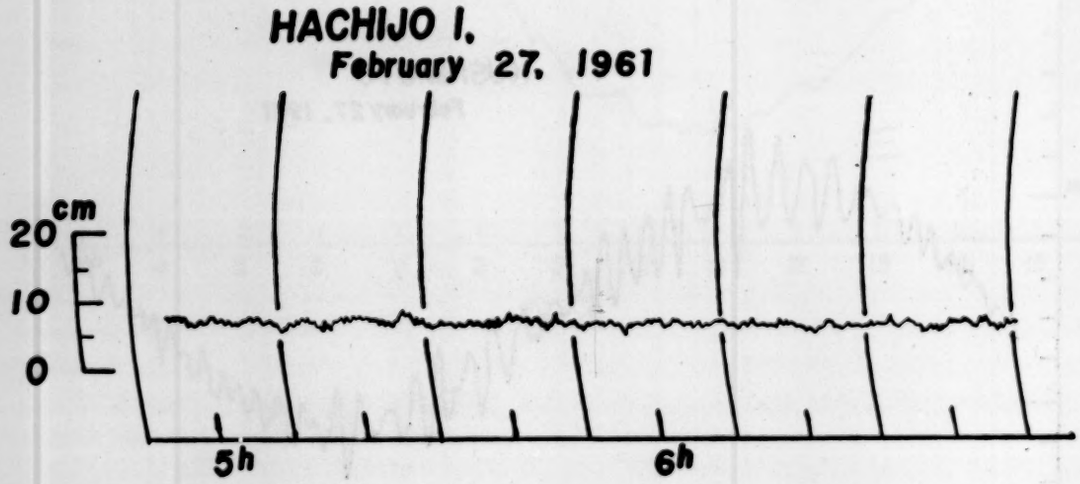

Fig. 30

20. *On the Tsunami which accompanied the Hiuganada Earthquake of Feb. 27, 1961.*

By

Ryutaro TAKAHASI and Tokutaro HATORI,

Earthquake Research Institute.

At 3 h 10 m 59.1 s (J.S.T.), Feb. 27, 1961, there occurred a remstrong earthquake off the south-east coast of Kyushu, Japan. According to the Japan Meteorological Agency (JMA), the magnitude of the earthquake was 7.2, depth 17 km and the position of the epicenter 31°. 7 N, 131°. 7 E. Accompanying this earthquake, a moderate tsunami was observed on the coasts of Kyushu and Shikoku.

Since 1662, more than 10 earthquakes which here exceeded IV in intensity have occurred around this region. Among them the earthquake of Nov. 19, 1941, resulted a tsunami of the order of 1 m along the coast of Kyushu and Shikoku.

By the courtesy of JMA, Japan Geographical Survey, Japan Hydrographic Office and the public works offices of several prefectures, the present writers could collect tide-gauge records of this tsunami and have made some studies as described blow.

Features of the tsunami at different localities can be seen in Table 1 and Fig. 1. It can be noticed that the initial motion of the tsunami is *up* everywhere, showing that the crustal deformation which caused the tsunami has probably been a simple upheaval in the origin area.

In this tsunami, the wave heights seem to have been modified by resonance phenomena in some bays in the neighbourhood of the origin area. In Fig. 2, the maximum wave heights H, as observed in different bays, were plotted against $1/T_0$, T_0 being the proper period of oscillation of the bay. In the Fig. H_0 is the maximum wave height at Miyazaki and T the period of the tsunami. The wave height is here defined as the level difference between a trough and the following or the preceding crest. The mean of the periods of tsunami waves at various localities was found to be 22 min. and this was assumed to be the period of tsunami T. Some of the proper periods of oscillation at different bays, shown in Table 2, were taken from HONDA and TERADA[2] and others were calculated by the formula $T_0=4l/\sqrt{gh}$

In Fig. 2, H/H_0 is large for Hosojima and Tosashimizu, where the periods of seiches are so near to T that resonance must have amplified the tsunami heights. The discrepancy in the value for Misho from the resonance curve in Fig. 2 might be the result of energy accumulation owing to the V-shape of Misho Bay. See Fig. 3.

Inversed refraction diagrams were drawn starting from six tide stations on the coast of Shikoku and Kyushu, as shown in Fig. 5. Wave fronts have been drawn every minute, but in Fig. 5 only those for every 5 minutes are shown. The origin was thus found to be a slender elliptic area with a long axis of about 80 km.

HIRONO and IIDA[4] obtained a relation between the magnitude M and the long axis L of the elliptic origin of the tsunami. Their relation holds good also for the present tsunami. UTSU and SEKI[5] found a relation between L and the area A of aftershocks. The present writers deduced a relation between A and L as shown in Fig. 7. This relation will give in some measure the shape of the origin area of the tsunami, if we assume the origin area to be equal to A. The fact that L greatly exceeds the diameter of a circle having the same area A with the origin, shows that the origin area of tsunami is strongly elliptical.

CORRIGENDUM

In the Bulletin of the Earthquake Research Institute, Vol. 39, Part 2, June, 1961;

Page	Line		Read
291	E5	Hotako	Hotaka
299	E5	Hotoka	Hotaka
325	10	in these observation.	in these observations.
327	20	derived the from	derived from the
330	2	Δ'	Δ'_0
330	10	$<\Delta<$	$<\Delta'_0<$
334	25	estimated two	estimated
338	8	Western profile.	Western profiles.
341	27	in the two the layers	in the two layers
348	29	structres	structures

正　　誤

地震研究所彙報　第 39 号　第 2 冊　昭和 36 年 6 月で

頁	行	誤	正
291	E5	Hotako	Hotaka
299	E5	Hotoka	Hotaka
325	10	in these observation.	in these observations.
327	20	derived the from	derived from the
330	2	Δ'	Δ_0'
330	10	$<\Delta<$	$<\Delta_0'<$
334	25	estimated two	estimated
338	8	Western profile.	Western profiles.
341	27	in the two the layers	in the two layers
348	29	structres	structures

に訂正して下さい

昭和36年12月10日 印刷
昭和36年12月15日 発行

東京都文京区本富士町一番地
東京大学構内
編纂兼発行者 東京大学地震研究所

東京都新宿区山吹町一八四番地
印刷者 笠井康頼

東京都新宿区山吹町一八四番地
印刷所 株式会社 国際文献印刷社

売捌所
東京都中央区日本橋通二丁目六番地
丸善株式会社

Sold by Maruzen Co., Ltd., Nihonbashi-dôri, Chûô-ku, Tôkyô.
Price of this copy: 650 Yen. (Postage exclusive.)